

INFLUENCE OF GROUND MOTION SCALING METHODS ON SEISMIC
RESPONSE OF HIGHWAY BRIDGES

A THESIS SUBMITTED TO
THE GRADUATE SCHOOL OF NATURAL AND APPLIED SCIENCES
OF
MIDDLE EAST TECHNICAL UNIVERSITY

BY
MERVE GÖZÜTOK GÜNDÜZ

IN PARTIAL FULFILLMENT OF THE REQUIREMENTS
FOR
THE DEGREE OF MASTER OF SCIENCE
IN
EARTHQUAKE STUDIES

August 2022

Approval of the thesis:

**INFLUENCE OF GROUND MOTION SCALING METHODS ON SEISMIC
RESPONSE OF HIGHWAY BRIDGES**

submitted by **MERVE GÖZÜTOK GÜNDÜZ** in partial fulfillment of the requirements for the degree of **Master of Science** in Choose an item., **Middle East Technical University** by,

Prof. Dr. Halil Kalıpçılar
Dean, Graduate School of **Natural and Applied Sciences**

Prof. Dr. Ayşegül Askan Gündoğan
Head of the Department, **Earthquake Studies**

Prof. Dr. Ahmet Yakut
Supervisor, **Earthquake Studies, METU**

Assoc. Prof. Dr. Mustafa Tolga Yılmaz
Co-Supervisor, **Engineering Sciences, METU**

Examining Committee Members:

Prof. Dr. Ayşegül Askan Gündoğan
Earthquake Studies, METU

Prof. Dr. Ahmet Yakut
Earthquake Studies, METU

Assoc. Prof. Dr. Mustafa Tolga Yılmaz
Engineering Sciences, METU

Prof. Dr. Alp Caner
Earthquake Studies, METU

Assoc. Prof. Dr. Özkan Kale
Civil Engineering., TED University

Date: 29.08.2022

I hereby declare that all information in this document has been obtained and presented in accordance with academic rules and ethical conduct. I also declare that, as required by these rules and conduct, I have fully cited and referenced all material and results that are not original to this work.

Name Last name : Merve Gözütok Gündüz

Signature :

ABSTRACT

INFLUENCE OF GROUND MOTION SCALING METHODS ON SEISMIC RESPONSE OF HIGHWAY BRIDGES

Gündüz Gözütok, Merve
Master of Science, Earthquake Studies
Supervisor: Prof. Dr. Ahmet Yakut
Co-Supervisor: Assoc. Prof. Dr. Mustafa Tolga Yılmaz

August 2022, 307 pages

Seismic behavior of bridges is a vital issue for all earthquake prone countries. Accurate seismic analysis of bridges is important because bridges are one of the most important transportation networks in Türkiye which is an earthquake prone country located on three main fault lines as Northern Anatolia Fault, East Anatolia Fault and West Anatolia Fault. In engineering practice in Türkiye there are three main specifications which are AASHTO LRFD Design Specifications for Bridge Design, Eurocodes and Turkish Earthquake Specification for Bridges. Those have different seismic design criteria having different design response spectrum curves and time history analysis criteria. Time history criteria include selection of ground motion records, number of ground motions to be employed, scaling criteria etc. Also, there are different types of scaling methods and there is no strict rule of which one to choose. In this thesis three scaling methods are compared employing the three bridge design specification criteria for three different highway bridges having different fundamental periods.

Keywords: Time history analysis, ground motion selection, seismic analysis of bridges, scaling methods

ÖZ

KARAYOLU KÖPRÜLERİNİN SİSMİK TEPKİLERİNE YER HAREKETİ ÖLÇEKLENDİRME METODLARININ ETKİSİ

Gündüz Gözütok, Merve
Yüksek Lisans, Deprem Çalışmaları
Tez Yöneticisi: Prof. Dr. Ahmet Yakut
Ortak Tez Yöneticisi: Doç. Dr. Mustafa Tolga Yılmaz

Ağustos 2022, 307 sayfa

Deprem bölgesinde bulunan ülkeler için köprülerin sismik davranışları hayati bir konudur. Kuzey Anadolu Fay Hattı, Doğu Anadolu Fay Hattı, Batı Anadolu Fay Hattı gibi üç önemli fay hattı üzerinde bulunan ve ana ulaşım ağlarından biri köprüler olan Türkiye gibi bir ülke için sismik analizlerinin doğru yapılması çok önemlidir. Günümüzde mühendislerin kullandığı üç ana köprü tasarımı yönetmeliği vardır: AASHTO LRFD Köprü Tasarım Şartnamesi, Eurocode Şartnameleri ve Köprüler için Türkiye Deprem Yönetmeliği. Bu üç yönetmelik farklı tasarım spektrumu ve zaman-tanım alanı analizi kriterlerine sahiptir. Zaman-tanım alanı analizi kriterleri yer hareketi seçimi, seçilen yer hareketi sayısı ve ölçeklendirme kriterlerini içermektedir. Ek olarak, ölçeklendirme konusunda çok farklı yöntemler bulunmaktadır ve hiç bir yönetmelik hangi metodun kullanılacağını belirten kesin bir kurala sahip değildir. Bu tezde üç ölçeklendirme metodu üç farklı yönetmeliğin zaman-tanım alanı analizi kriterini göre farklı temel periyotlarına sahip üç karayolu köprüsü için kıyaslanacaktır.

Anahtar Kelimeler: Zaman-tanım alanı analizi, yer hareketi seçimi, köprülerin sismik analizi, ölçeklendirme yöntemleri

To my family..

ACKNOWLEDGMENTS

I would like to thank my supervisor Prof. Dr. Ahmet Yakut for his endless support and encouragement with his guidance from beginning to the end of this study. It was a relief that to know that he was always there for me. I would like to declare my thanks to Assoc. Prof. Dr. Mustafa Tolga Yılmaz for his valuable help with his wide experience.

I also would like to declare my gratitude to committee members Prof. Dr. Ayşegül Askan Gündoğan, Prof. Dr. Alp Caner and Assoc. Prof. Dr. Özkan Kale for their precious time, contributions and suggestions for this study.

I'm grateful to my colleagues Doğuşcan Kardeş and Ozan Orhan, and my boss Mehmet Kozluca for their supports, tolerance and enlightening knowledge.

My deepest thanks to my mother Esra Gözütok and my father Mehmet Ali Gözütok who always believe in me and support me to be a successful and an independent woman, and my sister İrem Gözütok for being not only a sister but my best friend.

I'm very grateful to my husband Özer Gündüz for his moral support and knowledge to guide me when I lost my way.

TABLE OF CONTENTS

ABSTRACT.....	vii
ÖZ.....	viii
ACKNOWLEDGMENTS	x
TABLE OF CONTENTS.....	xi
LIST OF TABLES	xiv
LIST OF FIGURES	xxv
LIST OF ABBREVIATIONS.....	xlvi
LIST OF SYMBOLS	xlvi
1 INTRODUCTION	1
2 LITERATURE REVIEW	3
2.1 Time History Requirements in Current Codes	4
2.2 Selection of Ground Motion Records in Previous Studies.....	5
2.3 Scaling Methods Used in Previous Studies.....	6
3 LINEAR TIME HISTORY ANALYSIS OF HIGHWAY BRIDGES	9
3.1 Selection and Description of Bridges.....	9
3.1.1 V03 Bridge.....	10
3.1.2 V08 Bridge.....	13
3.1.3 V14 Bridge.....	16

3.2	Earthquake Hazard Analysis for Bridges.....	20
3.3	Bridge Analysis Models.....	22
3.3.1	Superstructure.....	24
3.3.2	Substructure.....	25
3.4	Design Target Spectra of the Bridge Design Specifications.....	29
3.5	Selection and Scaling of Ground Motion Records	36
3.5.1	Selection of Ground Motion Records.....	36
3.5.2	Scaling Methods of Selected Ground Motion Records	39
4	COMPARISON OF THE SEISMIC DEMAND PARAMETERS	
	FOR DIFFERENT SCALING METHODS AND SCALING CRITERIA.....	51
4.1	Comparison of Results for V03 Bridge	57
4.1.1	Comparison of Results for Scaling Method-1	65
4.1.2	Comparison of Results for Scaling Method-2.....	75
4.1.3	Comparison of Results for Scaling Method-3.....	85
4.1.4	Summary of the Comparison Results	95
4.2	Comparison of Results for V08 Bridge	112
4.2.1	Comparison of Results for Scaling Method-1	120
4.2.2	Comparison of Results for Scaling Method-2.....	130
4.2.3	Comparison of Results for Scaling Method-3	140
4.2.4	Summary of the Comparison Results	150
4.3	Comparison of Results for V14 Bridge	166
4.3.1	Comparison of Results for Scaling Method-1	174

4.3.2	Comparison of Results for Scaling Method-2	181
4.3.3	Comparison of Results for Scaling Method-3	188
4.3.4	Summary of the Comparison Results	194
5	CONCLUSIONS AND FUTURE WORK.....	207
	REFERENCES	211
A.	Accelerograms of Selected Earthquakes	213
B.	Response Spectra of Unscaled and Scaled Time Histories	227

LIST OF TABLES

TABLES

Table 3.1 Summary of selected bridges	19
Table 3.2 PGA, S_s and S_1 values for 475 years return period	21
Table 3.3 Selected earthquake ground motions from PEER Database	37
Table 3.4 Scale factors of bridge V14 (T=0.73 s) for ground motion set “SET-1”	42
Table 3.5 Scale factors of bridge V14 (T=0.73 s) for ground motion set “SET-2”	43
Table 3.6 Scale factors of bridge V14 (T=0.73 s) for ground motion set “SET-3”	44
Table 3.7 Scale factors of bridge V08 (T=1.00 s) for ground motion set “SET-1”	45
Table 3.8 Scale factors of bridge V08 (T=1.00 s) for ground motion set “SET-2”	46
Table 3.9 Scale factors of bridge V08 (T=1.00 s) for ground motion set “SET-3”	47
Table 3.10 Scale factors of bridge V03 (T=1.29 s) for ground motion set “SET1”	48
Table 3.11 Scale factors of bridge V03 (T=1.29 s) for ground motion set “SET2”	49
Table 3.12 Scale factors of bridge V03 (T=1.29 s) for ground motion set “SET3”	50
Table 4.1 Modal load participation ratios of V14 Bridge	51
Table 4.2 Modal participating mass ratios for the first 15 modes of V14 Bridge...	52
Table 4.3 Modal load participation ratios of V08 Bridge	52
Table 4.4 Modal participating mass ratios for the first 15 modes of V08 Bridge...	53
Table 4.5 Modal load participation ratios of V03 Bridge	53
Table 4.6 Modal participating mass ratios for the first 15 modes of V03 Bridge...	54
Table 4.7 Maximum spectral acceleration (S_a) values (g).....	57
Table 4.8 Spectral acceleration (S_a) values at T=1.29 sec. (g).....	58
Table 4.9 The maximum M_y values of pier P7 for M1 (kN.m).....	66
Table 4.10 Specification-wise percentage differences of M_y values of pier P7 for M1.....	67

Table 4.11 Ground motion set-wise percentage differences of M_y values of pier P7 for M1	67
Table 4.12 The maximum M_x values of pier P7 for M1 (kN.m)	67
Table 4.13 Specification-wise percentage differences of M_x values of pier P7 for M1	68
Table 4.14 Ground motion set-wise percentage differences of M_x values of pier P7 for M1	68
Table 4.15 The maximum u_y values of pier P7 for M1 (m).....	68
Table 4.16 Specification-wise percentage differences of u_y values of pier P7 for M1	69
Table 4.17 Ground motion set-wise percentage differences of u_y values of pier P7 for M1	69
Table 4.18 The maximum u_x values of pier P7 for M1 (m).....	69
Table 4.19 Specification-wise percentage differences of u_x values of pier P7 for M1	70
Table 4.20 Ground motion set-wise percentage differences of u_x values of pier P7 for M1	70
Table 4.21 Ground motion set-wise percentage differences of M_y values of all pier columns for M1	71
Table 4.22 Ground motion set-wise percentage differences of M_x values of all pier columns for M1	72
Table 4.23 Ground motion set-wise percentage differences of u_y values of all pier columns for M1	73
Table 4.24 Ground motion set-wise percentage differences of u_x values of all pier columns for M1	74
Table 4.25 The maximum M_y values of pier P7 for M2 (kN.m)	76

Table 4.26 Specification-wise percentage differences of M_y values of pier P7 for M2.....	77
Table 4.27 Ground motion set-wise percentage differences of M_y values of pier P7 for M2.....	77
Table 4.28 The maximum M_x values of pier P7 for M2 (kN.m).....	77
Table 4.29 Specification-wise percentage differences of M_x values of pier P7 for M2.....	78
Table 4.30 Ground motion set-wise percentage differences of M_x values of pier P7 for M2.....	78
Table 4.31 The maximum u_y values of pier P7 for M2 (m)	78
Table 4.32 Specification-wise percentage differences of u_y values of pier P7 for M2	79
Table 4.33 Ground motion set-wise percentage differences of u_y values of pier P7 for M2.....	79
Table 4.34 The maximum u_x values of pier P7 for M2 (m)	79
Table 4.35 Specification-wise percentage differences of u_x values of pier P7 for M2	80
Table 4.36 Ground motion set-wise percentage differences of u_x values of pier P7 for M2.....	80
Table 4.37 Ground motion set-wise percentage differences of M_y values of all pier columns for M2	81
Table 4.38 Ground motion set-wise percentage differences of M_x values of all pier columns for M2	82
Table 4.39 Ground motion set-wise percentage differences of u_y values of all pier columns for M2	83
Table 4.40 Ground motion set-wise percentage differences of u_x values of all pier columns for M2	84

Table 4.41 The maximum M_y values of pier P7 for M3 (kN.m)	86
Table 4.42 Specification-wise percentage differences of M_y values of pier P7 for M3	87
Table 4.43 Ground motion set-wise percentage differences of M_y values of pier P7 for M3	87
Table 4.44 The maximum M_x values of pier P7 for M3 (kN.m)	88
Table 4.45 Specification-wise percentage differences of M_x values of pier P7 for M3	88
Table 4.46 Ground motion set-wise percentage differences of M_x values of pier P7 for M3	88
Table 4.47 The maximum u_y values of pier P7 for M3 (m).....	89
Table 4.48 Specification-wise percentage differences of u_y values of pier P7 for M3	89
Table 4.49 Ground motion set-wise percentage differences of u_y values of pier P7 for M3	89
Table 4.50 The maximum u_x values of pier P7 for M3 (m).....	90
Table 4.51 Specification-wise percentage differences of u_x values of pier P7 for M3	90
Table 4.52 Ground motion set-wise percentage differences of u_x values of pier P7 for M3	90
Table 4.53 Ground motion set-wise percentage differences of M_y values of all pier columns for M3	91
Table 4.54 Ground motion set-wise percentage differences of M_x values of all pier columns for M3	92
Table 4.55 Ground motion set-wise percentage differences of u_y values of all pier columns for M3	93

Table 4.56 Ground motion set-wise percentage differences of u_x values of all pier columns for M3	94
Table 4.57 AASHTO LRFD method-wise differences for SET-1	98
Table 4.58 AASHTO LRFD method-wise differences for SET-2	99
Table 4.59 AASHTO LRFD method-wise differences for SET-3	100
Table 4.60 EN-8 method-wise differences for SET-1	103
Table 4.61 EN-8 method-wise differences for SET-2	104
Table 4.62 EN-8 method-wise differences for SET-3	105
Table 4.63 TDY 2020 method-wise differences for SET-1	108
Table 4.64 TDY 2020 method-wise differences for SET-2	109
Table 4.65 TDY 2020 method-wise differences for SET-3	110
Table 4.66 Maximum spectral acceleration (S_a) values (g).....	112
Table 4.67 Spectral acceleration (S_a) values at $T=1.00$ sec. (g).....	113
Table 4.68 The maximum M_y values of pier P3 for M1 (kN.m).....	121
Table 4.69 Specification-wise percentage differences of M_y values of pier P3 for M1.....	122
Table 4.70 Ground motion set-wise percentage differences of M_y values of pier P3 for M1	122
Table 4.71 The maximum M_x values of pier P3 for M1 (kN.m).....	123
Table 4.72 Specification-wise percentage differences of M_x values of pier P3 for M1.....	123
Table 4.73 Ground motion set-wise percentage differences of M_x values of pier P3 for M1	123
Table 4.74 The maximum u_y values of pier P3 for M1 (m)	124
Table 4.75 Specification-wise percentage differences of u_y values of pier P3 for M1	124

Table 4.76 Ground motion set-wise percentage differences of u_y values of pier P3 for M1	124
Table 4.77 The maximum u_x values of pier P3 for M1 (m).....	125
Table 4.78 Specification-wise percentage differences of u_x values of pier P3 for M1	125
Table 4.79 Ground motion set-wise percentage differences of u_x values of pier P3 for M1	125
Table 4.80 Ground motion set-wise percentage differences of M_y values of all pier columns for M1.....	126
Table 4.81 Ground motion set-wise percentage differences of M_x values of all pier columns for M1.....	127
Table 4.82 Ground motion set-wise percentage differences of u_y values of all pier columns for M1.....	128
Table 4.83 Ground motion set-wise percentage differences of u_x values of all pier columns for M1.....	129
Table 4.84 The maximum M_y values of pier P3 for M2 (kN.m)	131
Table 4.85 Specification-wise percentage differences of M_y values of pier P3 for M2.....	132
Table 4.86 Ground motion set-wise percentage differences of M_y values of pier P3 for M2	132
Table 4.87 The maximum M_x values of pier P3 for M2 (kN.m)	132
Table 4.88 Specification-wise percentage differences of M_x values of pier P3 for M2.....	133
Table 4.89 Ground motion set-wise percentage differences of M_x values of pier P3 for M2	133
Table 4.90 The maximum u_y values of pier P3 for M2 (m).....	133

Table 4.91 Specification-wise percentage differences of u_y values of pier P3 for M2	134
Table 4.92 Ground motion set-wise percentage differences of u_y values of pier P3 for M2.....	134
Table 4.93 The maximum u_x values of pier P3 for M2 (m)	134
Table 4.94 Specification-wise percentage differences of u_x values of pier P3 for M2	135
Table 4.95 Ground motion set-wise percentage differences of u_x values of pier P3 for M2.....	135
Table 4.96 Ground motion set-wise percentage differences of M_y values of all pier columns for M2	136
Table 4.97 Ground motion set-wise percentage differences of M_x values of all pier columns for M2	137
Table 4.98 Ground motion set-wise percentage differences of u_y values of all pier columns for M2	138
Table 4.99 Ground motion set-wise percentage differences of u_x values of all pier columns for M2	139
Table 4.100 The maximum M_y values of pier P3 for M3 (kN.m).....	141
Table 4.101 Specification-wise percentage differences of M_y values of pier P3 for M3.....	142
Table 4.102 Ground motion set-wise percentage differences of M_y values of pier P3 for M3.....	142
Table 4.103 The maximum M_x values of pier P3 for M3 (kN.m).....	142
Table 4.104 Specification-wise percentage differences of M_x values of pier P3 for M3.....	143
Table 4.105 Ground motion set-wise percentage differences of M_x values of pier P3 for M3.....	143

Table 4.106 The maximum u_y values of pier P3 for M3 (m).....	143
Table 4.107 Specification-wise percentage differences of u_y values of pier P3 for M3	144
Table 4.108 Ground motion set-wise percentage differences of u_y values of pier P3 for M3	144
Table 4.109 The maximum u_x values of pier P3 for M3 (m).....	144
Table 4.110 Specification-wise percentage differences of u_x values of pier P3 for M3	145
Table 4.111 Ground motion set-wise percentage differences of u_x values of pier P3 for M3	145
Table 4.112 Ground motion set-wise percentage differences of M_y values of all pier columns for M3.....	146
Table 4.113 Ground motion set-wise percentage differences of M_x values of all pier columns for M3.....	147
Table 4.114 Ground motion set-wise percentage differences of u_y values of all pier columns for M3.....	148
Table 4.115 Ground motion set-wise percentage differences of u_x values of all pier columns for M3.....	149
Table 4.116 AASHTO LRFD method-wise differences for SET-1.....	153
Table 4.117 AASHTO LRFD method-wise differences for SET-2.....	154
Table 4.118 AASHTO LRFD method-wise differences for SET-3.....	155
Table 4.119 EN-8 method-wise differences for SET-1	158
Table 4.120 EN-8 method-wise differences for SET-2	159
Table 4.121 EN-8 method-wise differences for SET-3	160
Table 4.122 TDY 2020 method-wise differences for SET-1.....	163
Table 4.123 TDY 2020 method-wise differences for SET-2.....	164
Table 4.124 TDY 2020 method-wise differences for SET-3.....	165

Table 4.125 Maximum spectral acceleration (S_a) values (g).....	166
Table 4.126 Spectral acceleration (S_a) values at $T=0.73$ sec. (g).....	167
Table 4.127 The maximum M_y values of pier P2 for M1 (kN.m).....	175
Table 4.128 Specification-wise percentage differences of M_y values of pier P2 for M1.....	176
Table 4.129 The maximum M_x values of pier P2 for M1 (kN.m).....	176
Table 4.130 Specification-wise percentage differences of M_x values of pier P2 for M1.....	176
Table 4.131 The maximum u_y values of pier P2 for M1 (m)	177
Table 4.132 Specification-wise percentage differences of u_y values of pier P2 for M1.....	177
Table 4.133 The maximum u_x values of pier P2 for M1 (m)	177
Table 4.134 Specification-wise percentage differences of u_x values of pier P2 for M1.....	178
Table 4.135 Ground motion set-wise percentage differences of M_y values of all pier columns for M1	178
Table 4.136 Ground motion set-wise percentage differences of M_x values of all pier columns for M1	179
Table 4.137 Ground motion set-wise percentage differences of u_y values of all pier columns for M1	179
Table 4.138 Ground motion set-wise percentage differences of u_x values of all pier columns for M1	180
Table 4.139 The maximum M_y values of pier P2 for M2 (kN.m).....	182
Table 4.140 Specification-wise percentage differences of M_y values of pier P2 for M2.....	182
Table 4.141 The maximum M_x values of pier P2 for M2 (kN.m).....	183

Table 4.142 Specification-wise percentage differences of M_x values of pier P2 for M2	183
Table 4.143 The maximum u_y values of pier P2 for M2 (m).....	183
Table 4.144 Specification-wise percentage differences of u_y values of pier P2 for M2	184
Table 4.145 The maximum u_x values of pier P2 for M2 (m).....	184
Table 4.146 Specification-wise percentage differences of u_x values of pier P2 for M2	185
Table 4.147 Ground motion set-wise percentage differences of M_y values of all pier columns for M2.....	185
Table 4.148 Ground motion set-wise percentage differences of M_x values of all pier columns for M2.....	186
Table 4.149 Ground motion set-wise percentage differences of u_y values of all pier columns for M2.....	186
Table 4.150 Ground motion set-wise percentage differences of u_x values of all pier columns for M2.....	187
Table 4.151 The maximum M_y values of pier P2 for M3 (kN.m)	189
Table 4.152 Specification-wise percentage differences of M_y values of pier P2 for M3	189
Table 4.153 The maximum M_x values of pier P2 for M3 (kN.m)	190
Table 4.154 Specification-wise percentage differences of M_x values of pier P2 for M3	190
Table 4.155 The maximum u_y values of pier P2 for M3 (m).....	190
Table 4.156 Specification-wise percentage differences of u_y values of pier P2 for M3	191
Table 4.157 The maximum u_x values of pier P2 for M3 (m).....	191

Table 4.158 Specification-wise percentage differences of u_x values of pier P2 for M3.....	192
Table 4.159 Ground motion set-wise percentage differences of M_y values of all pier columns for M3	192
Table 4.160 Ground motion set-wise percentage differences of M_x values of all pier columns for M3	193
Table 4.161 Ground motion set-wise percentage differences of u_y values of all pier columns for M3	193
Table 4.162 Ground motion set-wise percentage differences of u_x values of all pier columns for M3	194
Table 4.163 AASHTO LRFD method-wise differences for SET-1	197
Table 4.164 AASHTO LRFD method-wise differences for SET-2	197
Table 4.165 AASHTO LRFD method-wise differences for SET-3	198
Table 4.166 EN-8 method-wise differences for SET-1	200
Table 4.167 EN-8 method-wise differences for SET-2.....	201
Table 4.168 EN-8 method-wise differences for SET-3.....	201
Table 4.169 TDY 2020 method-wise differences for SET-1	204
Table 4.170 TDY 2020 method-wise differences for SET-2	204
Table 4.171 TDY 2020 method-wise differences for SET-3	205

LIST OF FIGURES

FIGURES

Figure 3.1. Plan view of V03 Bridge	10
Figure 3.2. Longitudinal profile of V03 Bridge.....	10
Figure 3.3. Profile view of pier axis P1 to show the pier cap details.....	11
Figure 3.4. Cross section of the superstructure.....	11
Figure 3.5. Cross section of the beam.....	12
Figure 3.6. Cross section of the column	12
Figure 3.7. Plan view of V08 Bridge	13
Figure 3.8. Longitudinal profile of V08 Bridge.....	13
Figure 3.9. Profile view of pier axis P1 to show the pier cap details.....	14
Figure 3.10. Cross section of the superstructure.....	14
Figure 3.11. Cross section of the beam.....	15
Figure 3.12. Cross section of the column	15
Figure 3.13. Plan view of V14 Bridge	16
Figure 3.14. Longitudinal profile of V14 Bridge.....	16
Figure 3.15. Profile view of pier axis P1 to show the pier cap details.....	17
Figure 3.16. Cross section of the superstructure.....	17
Figure 3.17. Cross section of the beam.....	18
Figure 3.18. Cross section of the column	18
Figure 3.19. Tectonic map of the Marmara Region.....	20
Figure 3.20. Representation of bridge elements	22
Figure 3.21. Analysis model of V03 Bridge	23
Figure 3.22. Analysis model of V08 Bridge	23
Figure 3.23. Analysis model of V14 Bridge	23
Figure 3.24. view of V14 Bridge (similar in V03 and V08 Bridges)	24
Figure 3.25. Properties of h=200 cm I-beam	24

Figure 3.26. Deck-beam, beam-cap beam, cap beam-column connections and links for elastomeric bearings	25
Figure 3.27. Geometrical properties of columns of V03 Bridge	26
Figure 3.28. Geometrical properties of columns of V08 Bridge	27
Figure 3.29. Geometrical properties of columns of V14 Bridge	28
Figure 3.30. AASHTO LRFD design spectrum curve	29
Figure 3.31. Eurocode-8 design spectrum curve	30
Figure 3.32. TDY 2020 design spectrum curve	31
Figure 3.33. Site class definitions in AASHTO LRFD (2012)	31
Figure 3.34. Site class definitions in Eurocode-8 (2003)	32
Figure 3.35. Site class definitions in TDY (2020).....	32
Figure 3.36. AASHTO LRFD design spectrum for V03 Bridge ($S_a(g)$ - $T(s)$)	33
Figure 3.37. Eurocode-8 design spectrum for V03 Bridge ($S_a(g)$ - $T(s)$).....	33
Figure 3.38. TDY (2020) design spectrum for V03 Bridge ($S_a(g)$ - $T(s)$).....	33
Figure 3.39. AASHTO LRFD design spectrum for V08 Bridge ($S_a(g)$ - $T(s)$)	34
Figure 3.40. Eurocode-8 design spectrum for V08 Bridge ($S_a(g)$ - $T(s)$).....	34
Figure 3.41. TDY (2020) design spectrum for V08 Bridge ($S_a(g)$ - $T(s)$).....	34
Figure 3.42. AASHTO LRFD design spectrum for V14 Bridge ($S_a(g)$ - $T(s)$)	35
Figure 3.43. Eurocode-8 design spectrum for V14 Bridge ($S_a(g)$ - $T(s)$).....	35
Figure 3.44. TDY (2020) design spectrum for V14 Bridge ($S_a(g)$ - $T(s)$).....	35
Figure 3.45. Ground motion sets to be used in analyses	38
Figure 3.46. AASHTO LRFD design spectrum and response spectrum of unscaled time histories for ground motion SET-1 of V03 Bridge.....	40
Figure 3.47. AASHTO LRFD design spectrum and response spectrum of scaled time histories with the scaling method M1 for ground motion SET-1 of V03 Bridge	41
Figure 4.1 Unscaled accelerogram for Basso Tirreno earthquake	55

Figure 4.2. Scaled accelerogram for Basso Tirreno earthquake	55
Figure 4.3. An example of time history function definition	56
Figure 4.4. Scaled mean spectra for M1,M2 and M3 and AASHTO LRFD design response spectrum for SET-1	59
Figure 4.5. Scaled mean spectra for M1,M2 and M3 and EN 8 design response spectrum for SET-1	59
Figure 4.6. Scaled mean spectra for M1,M2 and M3 and TDY design response spectrum for SET-1	60
Figure 4.7. Scaled mean spectra for M1,M2 and M3 and AASHTO LRFD design response spectrum for SET-2.....	60
Figure 4.8. Scaled mean spectra for M1,M2 and M3 and EN 8 design response spectrum for SET-2.....	61
Figure 4.9. Scaled mean spectra for M1,M2 and M3 and TDY design response spectrum for SET-2.....	61
Figure 4.10. Scaled mean spectra for M1,M2 and M3 and AASHTO LRFD design response spectrum for SET-3.....	62
Figure 4.11. Scaled mean spectra for M1,M2 and M3 and EN 8 design response spectrum for SET-3.....	62
Figure 4.12. Scaled mean spectra for M1,M2 and M3 and TDY design response spectrum for SET-3.....	63
Figure 4.13. M_y values of all of the pier columns for three scaling methods applied according to AASHTO LRFD (kN.m).....	96
Figure 4.14. M_x values of all of the pier columns for three scaling methods applied according to AASHTO LRFD (kN.m).....	97
Figure 4.15. M_y values of all of the pier columns for three scaling methods applied according to EN-8 (kN.m)	101

Figure 4.16. M_x values of all of the pier columns for three scaling methods applied according to EN-8 (kN.m)	102
Figure 4.17. M_y values of all of the pier columns for three scaling methods applied according to TDY 2020 (kN.m)	106
Figure 4.18. M_x values of all of the pier columns for three scaling methods applied according to TDY 2020 (kN.m)	107
Figure 4.19. Scaled mean spectra for M1,M2 and M3 and AASHTO LRFD design response spectrum for SET-1	114
Figure 4.20. Scaled mean spectra for M1,M2 and M3 and EN 8 design response spectrum for SET-1	114
Figure 4.21. Scaled mean spectra for M1,M2 and M3 and TDY design response spectrum for SET-1	115
Figure 4.22. Scaled mean spectra for M1,M2 and M3 and AASHTO LRFD design response spectrum for SET-2	115
Figure 4.23. Scaled mean spectra for M1,M2 and M3 and EN 8 design response spectrum for SET-2	116
Figure 4.24. Scaled mean spectra for M1,M2 and M3 and TDY design response spectrum for SET-2	116
Figure 4.25. Scaled mean spectra for M1,M2 and M3 and AASHTO LRFD design response spectrum for SET-3	117
Figure 4.26. Scaled mean spectra for M1,M2 and M3 and EN 8 design response spectrum for SET-3	117
Figure 4.27. Scaled mean spectra for M1,M2 and M3 and TDY design response spectrum for SET-3	118
Figure 4.28. M_y values of all of the pier columns for three scaling methods applied according to AASHTO LRFD (kN.m)	151

Figure 4.29. M_x values of all of the pier columns for three scaling methods applied according to AASHTO LRFD (kN.m).....	152
Figure 4.30. M_y values of all of the pier columns for three scaling methods applied according to EN-8 (kN.m)	156
Figure 4.31. M_x values of all of the pier columns for three scaling methods applied according to EN-8 (kN.m)	157
Figure 4.32. M_y values of all of the pier columns for three scaling methods applied according to TDY 2020 (kN.m).....	161
Figure 4.33. M_x values of all of the pier columns for three scaling methods applied according to TDY 2020 (kN.m).....	162
Figure 4.34. Scaled mean spectra for M1,M2 and M3 and AASHTO LRFD design response spectrum for SET-1	168
Figure 4.35. Scaled mean spectra for M1,M2 and M3 and EN 8 design response spectrum for SET-1	168
Figure 4.36. Scaled mean spectra for M1,M2 and M3 and TDY design response spectrum for SET-1	169
Figure 4.37. Scaled mean spectra for M1,M2 and M3 and AASHTO LRFD design response spectrum for SET-2.....	169
Figure 4.38. Scaled mean spectra for M1,M2 and M3 and EN 8 design response spectrum for SET-2.....	170
Figure 4.39. Scaled mean spectra for M1,M2 and M3 and TDY design response spectrum for SET-2.....	170
Figure 4.40. Scaled mean spectra for M1,M2 and M3 and AASHTO LRFD design response spectrum for SET-3	171
Figure 4.41. Scaled mean spectra for M1,M2 and M3 and EN 8 design response spectrum for SET-3	171

Figure 4.42. Scaled mean spectra for M1,M2 and M3 and TDY design response spectrum for SET-3	172
Figure 4.43. M_y values of all of the pier columns for three scaling methods applied according to AASHTO LRFD (kN.m)	195
Figure 4.44. M_x values of all of the pier columns for three scaling methods applied according to AASHTO LRFD (kN.m)	196
Figure 4.45. M_y values of all of the pier columns for three scaling methods applied according to EN-8 (kN.m)	199
Figure 4.46. M_x values of all of the pier columns for three scaling methods applied according to EN-8 (kN.m)	199
Figure 4.47. M_y values of all of the pier columns for three scaling methods applied according to TDY 2020 (kN.m)	202
Figure 4.48. M_x values of all of the pier columns for three scaling methods applied according to TDY 2020 (kN.m)	203
Figure A.1. Accelerogram of Basso Tirreno earthquake in x-direction (SET-1) ..	213
Figure A.2. Accelerogram of Basso Tirreno earthquake in y-direction (SET-1) ..	213
Figure A.3. Accelerogram of Chi Chi_2871 earthquake in x-direction (SET-1) ..	213
Figure A.4. Accelerogram of Chi Chi_2871 earthquake in y-direction (SET-1) ..	214
Figure A.5. Accelerogram of Hector earthquake in x-direction (SET-1)	214
Figure A.6. Accelerogram of Hector earthquake in y-direction (SET-1)	214
Figure A.7. Accelerogram of Kocaeli_1165 earthquake in x-direction (SET-1) ..	215
Figure A.8. Accelerogram of Kocaeli_1165 earthquake in y-direction (SET-1) ..	215
Figure A.9. Accelerogram of Manjil Abbar earthquake in x-direction (SET-1) ..	215
Figure A.10. Accelerogram of Manjil Abbar earthquake in y-direction (SET-1) ..	216
Figure A.11. Accelerogram of Sirtka earthquake in x-direction (SET-1)	216
Figure A.12. Accelerogram of Sirtka earthquake in y-direction (SET-1)	216
Figure A.13. Accelerogram of Tottori-3 earthquake in x-direction (SET-1)	217

Figure A.14. Accelerogram of Tottori-3 earthquake in y-direction (SET-1).....	217
Figure A.15. Accelerogram of Chi Chi_2712 earthquake in x-direction (SET-2)	217
Figure A.16. Accelerogram of Chi Chi_2712 earthquake in y-direction (SET-2)	218
Figure A.17. Accelerogram of Darfield earthquake in x-direction (SET-2).....	218
Figure A.18. Accelerogram of Darfield earthquake in y-direction (SET-2).....	218
Figure A.19. Accelerogram of Irpiana285 earthquake in x-direction (SET-2).....	219
Figure A.20. Accelerogram of Irpiana285 earthquake in y-direction (SET-2).....	219
Figure A.21. Accelerogram of Kobe earthquake in x-direction (SET-2)	219
Figure A.22. Accelerogram of Kobe earthquake in y-direction (SET-2)	220
Figure A.23. Accelerogram of Kocaeli_1161 earthquake in x-direction (SET-2)	220
Figure A.24. Accelerogram of Kocaeli_1161 earthquake in y-direction (SET-2)	220
Figure A.25. Accelerogram of Morgan Hill-2 earthquake in x-direction (SET-2)	221
Figure A.26. Accelerogram of Morgan Hill-2 earthquake in y-direction (SET-2)	221
Figure A.27. Accelerogram of Tottori-2 earthquake in x-direction (SET-2).....	221
Figure A.28. Accelerogram of Tottori-2 earthquake in y-direction (SET-2).....	222
Figure A.29. Accelerogram of Basso Tirreno earthquake in x-direction (SET-3)	222
Figure A.30. Accelerogram of Basso Tirreno earthquake in y-direction (SET-3)	222
Figure A.31. Accelerogram of Chi Chi_2742 earthquake in x-direction (SET-3)	223
Figure A.32. Accelerogram of Chi Chi_2742 earthquake in y-direction (SET-3)	223
Figure A.33. Accelerogram of Düzce_1618 earthquake in x-direction (SET-3)..	223
Figure A.34. Accelerogram of Düzce_1618 earthquake in y-direction (SET-3)..	224
Figure A.35. Accelerogram of Kobe earthquake in x-direction (SET-3)	224
Figure A.36. Accelerogram of Kobe earthquake in y-direction (SET-3)	224
Figure A.37. Accelerogram of Manjil Abbar earthquake in x-direction (SET-3)	225
Figure A.38. Accelerogram of Manjil Abbar earthquake in y-direction (SET-3)	225
Figure A.39. Accelerogram of Tottori-2 earthquake in x-direction (SET-3).....	225
Figure A.40. Accelerogram of Tottori-2 earthquake in y-direction (SET-3).....	226

Figure A.41. Accelerogram of Tottori-3 earthquake in x-direction (SET-3)	226
Figure A.42. Accelerogram of Tottori-3 earthquake in y-direction (SET-3)	226
Figure B.1. AASHTO LRFD design spectrum and response spectrum of unscaled time histories for ground motion SET-1 and scaling method M1 of V03 Bridge	227
Figure B.2. AASHTO LRFD design spectrum and response spectrum of scaled time histories for ground motion SET-1 and scaling method M1 of V03 Bridge	227
Figure B.3. EN-8 design spectrum and response spectrum of unscaled time histories for ground motion SET-1 and scaling method M1 of V03 Bridge	228
Figure B.4. EN-8 design spectrum and response spectrum of scaled time histories for ground motion SET-1 and scaling method M1 of V03 Bridge	228
Figure B.5. TDY 2020 design spectrum and response spectrum of unscaled time histories for ground motion SET-1 and scaling method M1 of V03 Bridge	229
Figure B.6. TDY 2020 design spectrum and response spectrum of scaled time histories for ground motion SET-1 and scaling method M1 of V03 Bridge	229
Figure B.7. AASHTO LRFD design spectrum and response spectrum of unscaled time histories for ground motion SET-2 and scaling method M1 of V03 Bridge	230
Figure B.8. AASHTO LRFD design spectrum and response spectrum of scaled time histories for ground motion SET-2 and scaling method M1 of V03 Bridge	230
Figure B.9. EN-8 design spectrum and response spectrum of unscaled time histories for ground motion SET-2 and scaling method M1 of V03 Bridge	231
Figure B.10. EN-8 design spectrum and response spectrum of scaled time histories for ground motion SET-2 and scaling method M1 of V03 Bridge	231
Figure B.11. TDY 2020 design spectrum and response spectrum of unscaled time histories for ground motion SET-2 and scaling method M1 of V03 Bridge	232
Figure B.12. TDY 2020 design spectrum and response spectrum of scaled time histories for ground motion SET-2 and scaling method M1 of V03 Bridge	232

Figure B.13. AASHTO LRFD design spectrum and response spectrum of unscaled time histories for ground motion SET-3 and scaling method M1 of V03 Bridge	233
Figure B.14. AASHTO LRFD design spectrum and response spectrum of scaled time histories for ground motion SET-3 and scaling method M1 of V03 Bridge	233
Figure B.15. EN-8 design spectrum and response spectrum of unscaled time histories for ground motion SET-3 and scaling method M1 of V03 Bridge	234
Figure B.16. EN-8 design spectrum and response spectrum of scaled time histories for ground motion SET-3 and scaling method M1 of V03 Bridge	234
Figure B.17. TDY 2020 design spectrum and response spectrum of unscaled time histories for ground motion SET-3 and scaling method M1 of V03 Bridge	235
Figure B.18. TDY 2020 design spectrum and response spectrum of scaled time histories for ground motion SET-3 and scaling method M1 of V03 Bridge	235
Figure B.19. AASHTO LRFD design spectrum and response spectrum of unscaled time histories for ground motion SET-1 and scaling method M2 of V03 Bridge	236
Figure B.20. AASHTO LRFD design spectrum and response spectrum of scaled time histories for ground motion SET-1 and scaling method M2 of V03 Bridge	236
Figure B.21. EN-8 design spectrum and response spectrum of unscaled time histories for ground motion SET-1 and scaling method M2 of V03 Bridge	237
Figure B.22. EN-8 design spectrum and response spectrum of scaled time histories for ground motion SET-1 and scaling method M2 of V03 Bridge	237
Figure B.23. TDY 2020 design spectrum and response spectrum of unscaled time histories for ground motion SET-1 and scaling method M2 of V03 Bridge	238
Figure B.24. TDY 2020 design spectrum and response spectrum of scaled time histories for ground motion SET-1 and scaling method M2 of V03 Bridge	238
Figure B.25. AASHTO LRFD design spectrum and response spectrum of unscaled time histories for ground motion SET-2 and scaling method M2 of V03 Bridge	239

Figure B.26. AASHTO LRFD design spectrum and response spectrum of scaled time histories for ground motion SET-2 and scaling method M2 of V03 Bridge. 239

Figure B.27. EN-8 design spectrum and response spectrum of unscaled time histories for ground motion SET-2 and scaling method M2 of V03 Bridge 240

Figure B.28. EN-8 design spectrum and response spectrum of scaled time histories for ground motion SET-2 and scaling method M2 of V03 Bridge..... 240

Figure B.29. TDY 2020 design spectrum and response spectrum of unscaled time histories for ground motion SET-2 and scaling method M2 of V03 Bridge 241

Figure B.30. TDY 2020 design spectrum and response spectrum of scaled time histories for ground motion SET-2 and scaling method M2 of V03 Bridge 241

Figure B.31. AASHTO LRFD design spectrum and response spectrum of unscaled time histories for ground motion SET-3 and scaling method M2 of V03 Bridge. 242

Figure B.32. AASHTO LRFD design spectrum and response spectrum of scaled time histories for ground motion SET-3 and scaling method M2 of V03 Bridge. 242

Figure B.33. EN-8 design spectrum and response spectrum of unscaled time histories for ground motion SET-3 and scaling method M2 of V03 Bridge 243

Figure B.34. EN-8 design spectrum and response spectrum of scaled time histories for ground motion SET-3 and scaling method M2 of V03 Bridge..... 243

Figure B.35. TDY 2020 design spectrum and response spectrum of unscaled time histories for ground motion SET-3 and scaling method M2 of V03 Bridge 244

Figure B.36. TDY 2020 design spectrum and response spectrum of scaled time histories for ground motion SET-3 and scaling method M2 of V03 Bridge 244

Figure B.37. AASHTO LRFD design spectrum and response spectrum of unscaled time histories for ground motion SET-1 and scaling method M3 of V03 Bridge. 245

Figure B.38. AASHTO LRFD design spectrum and response spectrum of scaled time histories for ground motion SET-1 and scaling method M3 of V03 Bridge. 245

Figure B.39. EN-8 design spectrum and response spectrum of unscaled time histories for ground motion SET-1 and scaling method M3 of V03 Bridge	246
Figure B.40. EN-8 design spectrum and response spectrum of scaled time histories for ground motion SET-1 and scaling method M3 of V03 Bridge	246
Figure B.41. TDY 2020 design spectrum and response spectrum of unscaled time histories for ground motion SET-1 and scaling method M3 of V03 Bridge	247
Figure B.42. TDY 2020 design spectrum and response spectrum of scaled time histories for ground motion SET-1 and scaling method M3 of V03 Bridge	247
Figure B.43. AASHTO LRFD design spectrum and response spectrum of unscaled time histories for ground motion SET-2 and scaling method M3 of V03 Bridge	248
Figure B.44. AASHTO LRFD design spectrum and response spectrum of scaled time histories for ground motion SET-2 and scaling method M3 of V03 Bridge	248
Figure B.45. EN-8 design spectrum and response spectrum of unscaled time histories for ground motion SET-2 and scaling method M3 of V03 Bridge	249
Figure B.46. EN-8 design spectrum and response spectrum of scaled time histories for ground motion SET-2 and scaling method M3 of V03 Bridge	249
Figure B.47. TDY 2020 design spectrum and response spectrum of unscaled time histories for ground motion SET-2 and scaling method M3 of V03 Bridge	250
Figure B.48. TDY 2020 design spectrum and response spectrum of scaled time histories for ground motion SET-2 and scaling method M3 of V03 Bridge	250
Figure B.49. AASHTO LRFD design spectrum and response spectrum of unscaled time histories for ground motion SET-3 and scaling method M3 of V03 Bridge	251
Figure B.50. AASHTO LRFD design spectrum and response spectrum of scaled time histories for ground motion SET-3 and scaling method M3 of V03 Bridge	251
Figure B.51. EN-8 design spectrum and response spectrum of unscaled time histories for ground motion SET-3 and scaling method M3 of V03 Bridge	252

Figure B.52. EN-8 design spectrum and response spectrum of scaled time histories for ground motion SET-3 and scaling method M3 of V03 Bridge..... 252

Figure B.53. TDY 2020 design spectrum and response spectrum of unscaled time histories for ground motion SET-3 and scaling method M3 of V03 Bridge 253

Figure B.54. TDY 2020 design spectrum and response spectrum of scaled time histories for ground motion SET-3 and scaling method M3 of V03 Bridge 253

Figure B.55. AASHTO LRFD design spectrum and response spectrum of unscaled time histories for ground motion SET-1 and scaling method M1 of V08 Bridge. 254

Figure B.56. AASHTO LRFD design spectrum and response spectrum of scaled time histories for ground motion SET-1 and scaling method M1 of V08 Bridge. 254

Figure B.57. EN-8 design spectrum and response spectrum of unscaled time histories for ground motion SET-1 and scaling method M1 of V08 Bridge 255

Figure B.58. EN-8 design spectrum and response spectrum of scaled time histories for ground motion SET-1 and scaling method M1 of V08 Bridge..... 255

Figure B.59. TDY 2020 design spectrum and response spectrum of unscaled time histories for ground motion SET-1 and scaling method M1 of V08 Bridge 256

Figure B.60. TDY 2020 design spectrum and response spectrum of scaled time histories for ground motion SET-1 and scaling method M1 of V08 Bridge 256

Figure B.61. AASHTO LRFD design spectrum and response spectrum of unscaled time histories for ground motion SET-2 and scaling method M1 of V08 Bridge. 257

Figure B.62. AASHTO LRFD design spectrum and response spectrum of scaled time histories for ground motion SET-2 and scaling method M1 of V08 Bridge. 257

Figure B.63. EN-8 design spectrum and response spectrum of unscaled time histories for ground motion SET-2 and scaling method M1 of V08 Bridge 258

Figure B.64. EN-8 design spectrum and response spectrum of scaled time histories for ground motion SET-2 and scaling method M1 of V08 Bridge..... 258

Figure B.65. TDY 2020 design spectrum and response spectrum of unscaled time histories for ground motion SET-2 and scaling method M1 of V08 Bridge	259
Figure B.66. TDY 2020 design spectrum and response spectrum of scaled time histories for ground motion SET-2 and scaling method M1 of V08 Bridge	259
Figure B.67. AASHTO LRFD design spectrum and response spectrum of unscaled time histories for ground motion SET-3 and scaling method M1 of V08 Bridge	260
Figure B.68. AASHTO LRFD design spectrum and response spectrum of scaled time histories for ground motion SET-3 and scaling method M1 of V08 Bridge	260
Figure B.69. EN-8 design spectrum and response spectrum of unscaled time histories for ground motion SET-3 and scaling method M1 of V08 Bridge	261
Figure B.70. EN-8 design spectrum and response spectrum of scaled time histories for ground motion SET-3 and scaling method M1 of V08 Bridge	261
Figure B.71. TDY 2020 design spectrum and response spectrum of unscaled time histories for ground motion SET-3 and scaling method M1 of V08 Bridge	262
Figure B.72. TDY 2020 design spectrum and response spectrum of scaled time histories for ground motion SET-3 and scaling method M1 of V08 Bridge	262
Figure B.73. AASHTO LRFD design spectrum and response spectrum of unscaled time histories for ground motion SET-1 and scaling method M2 of V08 Bridge	263
Figure B.74. AASHTO LRFD design spectrum and response spectrum of scaled time histories for ground motion SET-1 and scaling method M2 of V08 Bridge	263
Figure B.75. EN-8 design spectrum and response spectrum of unscaled time histories for ground motion SET-1 and scaling method M2 of V08 Bridge	264
Figure B.76. EN-8 design spectrum and response spectrum of scaled time histories for ground motion SET-1 and scaling method M2 of V08 Bridge	264
Figure B.77. TDY 2020 design spectrum and response spectrum of unscaled time histories for ground motion SET-1 and scaling method M2 of V08 Bridge	265

Figure B.78. TDY 2020 design spectrum and response spectrum of scaled time histories for ground motion SET-1 and scaling method M2 of V08 Bridge 265

Figure B.79. AASHTO LRFD design spectrum and response spectrum of unscaled time histories for ground motion SET-2 and scaling method M2 of V08 Bridge. 266

Figure B.80. AASHTO LRFD design spectrum and response spectrum of scaled time histories for ground motion SET-2 and scaling method M2 of V08 Bridge. 266

Figure B.81. EN-8 design spectrum and response spectrum of unscaled time histories for ground motion SET-2 and scaling method M2 of V08 Bridge 267

Figure B.82. EN-8 design spectrum and response spectrum of scaled time histories for ground motion SET-2 and scaling method M2 of V08 Bridge..... 267

Figure B.83. TDY 2020 design spectrum and response spectrum of unscaled time histories for ground motion SET-2 and scaling method M2 of V08 Bridge 268

Figure B.84. TDY 2020 design spectrum and response spectrum of scaled time histories for ground motion SET-2 and scaling method M2 of V08 Bridge 268

Figure B.85. AASHTO LRFD design spectrum and response spectrum of unscaled time histories for ground motion SET-3 and scaling method M2 of V08 Bridge. 269

Figure B.86. AASHTO LRFD design spectrum and response spectrum of scaled time histories for ground motion SET-3 and scaling method M2 of V08 Bridge. 269

Figure B.87. EN-8 design spectrum and response spectrum of unscaled time histories for ground motion SET-3 and scaling method M2 of V08 Bridge 270

Figure B.88. EN-8 design spectrum and response spectrum of scaled time histories for ground motion SET-3 and scaling method M2 of V08 Bridge..... 270

Figure B.89. TDY 2020 design spectrum and response spectrum of unscaled time histories for ground motion SET-3 and scaling method M2 of V08 Bridge 271

Figure B.90. TDY 2020 design spectrum and response spectrum of scaled time histories for ground motion SET-3 and scaling method M2 of V08 Bridge 271

Figure B.91. AASHTO LRFD design spectrum and response spectrum of unscaled time histories for ground motion SET-1 and scaling method M3 of V08 Bridge	272
Figure B.92. AASHTO LRFD design spectrum and response spectrum of scaled time histories for ground motion SET-1 and scaling method M3 of V08 Bridge	272
Figure B.93. EN-8 design spectrum and response spectrum of unscaled time histories for ground motion SET-1 and scaling method M3 of V08 Bridge	273
Figure B.94. EN-8 design spectrum and response spectrum of scaled time histories for ground motion SET-1 and scaling method M3 of V08 Bridge	273
Figure B.95. TDY 2020 design spectrum and response spectrum of unscaled time histories for ground motion SET-1 and scaling method M3 of V08 Bridge	274
Figure B.96. TDY 2020 design spectrum and response spectrum of scaled time histories for ground motion SET-1 and scaling method M3 of V08 Bridge	274
Figure B.97. AASHTO LRFD design spectrum and response spectrum of unscaled time histories for ground motion SET-2 and scaling method M3 of V08 Bridge	275
Figure B.98. AASHTO LRFD design spectrum and response spectrum of scaled time histories for ground motion SET-2 and scaling method M3 of V08 Bridge	275
Figure B.99. EN-8 design spectrum and response spectrum of unscaled time histories for ground motion SET-2 and scaling method M3 of V03 Bridge	276
Figure B.100. EN-8 design spectrum and response spectrum of scaled time histories for ground motion SET-2 and scaling method M3 of V03 Bridge	276
Figure B.101. TDY 2020 design spectrum and response spectrum of unscaled time histories for ground motion SET-2 and scaling method M3 of V03 Bridge	277
Figure B.102. TDY 2020 design spectrum and response spectrum of scaled time histories for ground motion SET-2 and scaling method M3 of V08 Bridge	277
Figure B.103. AASHTO LRFD design spectrum and response spectrum of unscaled time histories for ground motion SET-3 and scaling method M3 of V08 Bridge	278

Figure B.104. AASHTO LRFD design spectrum and response spectrum of scaled time histories for ground motion SET-3 and scaling method M3 of V08 Bridge	278
Figure B.105. EN-8 design spectrum and response spectrum of unscaled time histories for ground motion SET-3 and scaling method M3 of V03 Bridge	279
Figure B.106. EN-8 design spectrum and response spectrum of scaled time histories for ground motion SET-3 and scaling method M3 of V03 Bridge	279
Figure B.107. TDY 2020 design spectrum and response spectrum of unscaled time histories for ground motion SET-3 and scaling method M3 of V03 Bridge	280
Figure B.108. TDY 2020 design spectrum and response spectrum of scaled time histories for ground motion SET-3 and scaling method M3 of V03 Bridge	280
Figure B.109. AASHTO LRFD design spectrum and response spectrum of unscaled time histories for ground motion SET-1 and scaling method M1 of V14 Bridge	281
Figure B.110. AASHTO LRFD design spectrum and response spectrum of scaled time histories for ground motion SET-1 and scaling method M1 of V14 Bridge	281
Figure B.111. EN-8 design spectrum and response spectrum of unscaled time histories for ground motion SET-1 and scaling method M1 of V14 Bridge	282
Figure B.112. EN-8 design spectrum and response spectrum of scaled time histories for ground motion SET-1 and scaling method M1 of V14 Bridge	282
Figure B.113. TDY 2020 design spectrum and response spectrum of unscaled time histories for ground motion SET-1 and scaling method M1 of V14 Bridge	283
Figure B.114. TDY 2020 design spectrum and response spectrum of scaled time histories for ground motion SET-1 and scaling method M1 of V14 Bridge	283
Figure B.115. AASHTO LRFD design spectrum and response spectrum of unscaled time histories for ground motion SET-2 and scaling method M1 of V14 Bridge	284

Figure B.116. AASHTO LRFD design spectrum and response spectrum of scaled time histories for ground motion SET-2 and scaling method M1 of V14 Bridge	284
Figure B.117. EN-8 design spectrum and response spectrum of unscaled time histories for ground motion SET-2 and scaling method M1 of V14 Bridge	285
Figure B.118. EN-8 design spectrum and response spectrum of scaled time histories for ground motion SET-2 and scaling method M1 of V14 Bridge	285
Figure B.119. TDY 2020 design spectrum and response spectrum of unscaled time histories for ground motion SET-2 and scaling method M1 of V14 Bridge	286
Figure B.120. TDY 2020 design spectrum and response spectrum of scaled time histories for ground motion SET-2 and scaling method M1 of V14 Bridge	286
Figure B.121. AASHTO LRFD design spectrum and response spectrum of unscaled time histories for ground motion SET-3 and scaling method M1 of V14 Bridge	287
Figure B.122. AASHTO LRFD design spectrum and response spectrum of scaled time histories for ground motion SET-3 and scaling method M1 of V14 Bridge	287
Figure B.123. EN-8 design spectrum and response spectrum of unscaled time histories for ground motion SET-3 and scaling method M1 of V14 Bridge	288
Figure B.124. EN-8 design spectrum and response spectrum of scaled time histories for ground motion SET-3 and scaling method M1 of V14 Bridge	288
Figure B.125. TDY 2020 design spectrum and response spectrum of unscaled time histories for ground motion SET-3 and scaling method M1 of V14 Bridge	289
Figure B.126. TDY 2020 design spectrum and response spectrum of scaled time histories for ground motion SET-3 and scaling method M1 of V14 Bridge	289
Figure B.127. AASHTO LRFD design spectrum and response spectrum of unscaled time histories for ground motion SET-1 and scaling method M2 of V14 Bridge	290

Figure B.128. AASHTO LRFD design spectrum and response spectrum of scaled time histories for ground motion SET-1 and scaling method M2 of V14 Bridge	290
Figure B.129. EN-8 design spectrum and response spectrum of unscaled time histories for ground motion SET-1 and scaling method M2 of V14 Bridge	291
Figure B.130. EN-8 design spectrum and response spectrum of scaled time histories for ground motion SET-1 and scaling method M2 of V14 Bridge	291
Figure B.131. TDY 2020 design spectrum and response spectrum of unscaled time histories for ground motion SET-1 and scaling method M2 of V14 Bridge	292
Figure B.132. TDY 2020 design spectrum and response spectrum of scaled time histories for ground motion SET-1 and scaling method M2 of V14 Bridge	292
Figure B.133. AASHTO LRFD design spectrum and response spectrum of unscaled time histories for ground motion SET-2 and scaling method M2 of V14 Bridge	293
Figure B.134. AASHTO LRFD design spectrum and response spectrum of scaled time histories for ground motion SET-2 and scaling method M2 of V14 Bridge	293
Figure B.135. EN-8 design spectrum and response spectrum of unscaled time histories for ground motion SET-2 and scaling method M2 of V14 Bridge	294
Figure B.136. EN-8 design spectrum and response spectrum of scaled time histories for ground motion SET-2 and scaling method M2 of V14 Bridge	294
Figure B.137. TDY 2020 design spectrum and response spectrum of unscaled time histories for ground motion SET-2 and scaling method M2 of V14 Bridge	295
Figure B.138. TDY 2020 design spectrum and response spectrum of scaled time histories for ground motion SET-2 and scaling method M2 of V14 Bridge	295
Figure B.139. AASHTO LRFD design spectrum and response spectrum of unscaled time histories for ground motion SET-3 and scaling method M2 of V14 Bridge	296

Figure B.140. AASHTO LRFD design spectrum and response spectrum of scaled time histories for ground motion SET-3 and scaling method M2 of V14 Bridge	296
Figure B.141. EN-8 design spectrum and response spectrum of unscaled time histories for ground motion SET-3 and scaling method M2 of V14 Bridge	297
Figure B.142. EN-8 design spectrum and response spectrum of scaled time histories for ground motion SET-3 and scaling method M2 of V14 Bridge	297
Figure B.143. TDY 2020 design spectrum and response spectrum of unscaled time histories for ground motion SET-3 and scaling method M2 of V14 Bridge	298
Figure B.144. TDY 2020 design spectrum and response spectrum of scaled time histories for ground motion SET-3 and scaling method M2 of V14 Bridge	298
Figure B.145. AASHTO LRFD design spectrum and response spectrum of unscaled time histories for ground motion SET-1 and scaling method M3 of V14 Bridge	299
Figure B.146. AASHTO LRFD design spectrum and response spectrum of scaled time histories for ground motion SET-1 and scaling method M3 of V14 Bridge	299
Figure B.147. EN-8 design spectrum and response spectrum of unscaled time histories for ground motion SET-1 and scaling method M3 of V14 Bridge	300
Figure B.148. EN-8 design spectrum and response spectrum of scaled time histories for ground motion SET-1 and scaling method M3 of V14 Bridge	300
Figure B.149. TDY 2020 design spectrum and response spectrum of unscaled time histories for ground motion SET-1 and scaling method M3 of V14 Bridge	301
Figure B.150. TDY 2020 design spectrum and response spectrum of scaled time histories for ground motion SET-1 and scaling method M3 of V14 Bridge	301
Figure B.151. AASHTO LRFD design spectrum and response spectrum of unscaled time histories for ground motion SET-2 and scaling method M3 of V14 Bridge	302

Figure B.152. AASHTO LRFD design spectrum and response spectrum of scaled time histories for ground motion SET-2 and scaling method M3 of V14 Bridge	302
Figure B.153. EN-8 design spectrum and response spectrum of unscaled time histories for ground motion SET-2 and scaling method M3 of V14 Bridge	303
Figure B.154. EN-8 design spectrum and response spectrum of scaled time histories for ground motion SET-2 and scaling method M3 of V14 Bridge	303
Figure B.155. TDY 2020 design spectrum and response spectrum of unscaled time histories for ground motion SET-2 and scaling method M3 of V14 Bridge	304
Figure B.156. TDY 2020 design spectrum and response spectrum of scaled time histories for ground motion SET-2 and scaling method M3 of V14 Bridge	304
Figure B.157. AASHTO LRFD design spectrum and response spectrum of unscaled time histories for ground motion SET-3 and scaling method M3 of V14 Bridge	305
Figure B.158. AASHTO LRFD design spectrum and response spectrum of scaled time histories for ground motion SET-3 and scaling method M3 of V14 Bridge	305
Figure B.159. EN-8 design spectrum and response spectrum of unscaled time histories for ground motion SET-3 and scaling method M3 of V14 Bridge	306
Figure B.160. EN-8 design spectrum and response spectrum of scaled time histories for ground motion SET-3 and scaling method M3 of V14 Bridge	306
Figure B.161. TDY 2020 design spectrum and response spectrum of unscaled time histories for ground motion SET-3 and scaling method M3 of V14 Bridge	307
Figure B.162. TDY 2020 design spectrum and response spectrum of scaled time histories for ground motion SET-3 and scaling method M3 of V14 Bridge	307

LIST OF ABBREVIATIONS

AASHTO LRFD = American Association of State Highway and Transportation
Officials Load and Resistance Factor Design

EN-8 = Eurocode-8

M1 = Scaling Method 1

M2= Scaling Method 2

M3= Scaling Method 3

NEHRP = National Earthquake Hazards Reduction Program

PGA = Peak Ground Acceleration

PGV = Peak Ground Velocity

PEER = Pacific Earthquake Engineering Research

TDY = Turkish Earthquake Code

SRSS = Square Root of the Sum of the Squares

SS = Strike Slip Fault

SSE = Sum of Square Errors

LIST OF SYMBOLS

S_a = Spectral Acceleration

S_s = Spectral Acceleration Coefficient at Period 1.0 sec

S_1 = Spectral Acceleration Coefficient at Period 0.2 sec

T_n = Fundamental Period

M3- M_x or M_x = Moment in the Longitudinal Direction

M2- M_y or M_y = Moment in the Transverse Direction

u_x = Displacement in the Longitudinal Direction

u_y = Displacement in the Transverse Direction

V_{s30} = Average Shear Wave Velocity to the Depth of 30 meters

CHAPTER 1

INTRODUCTION

Seismic design of bridges is an important issue for earthquake countries like Turkiye. In such countries, bridge elements are typically designed considering the seismic effects of the region. Seismic forces generally govern the design of pier columns, pier foundations and piles, cap beams and shear keys. In the scope of this study three types of highway bridges having different fundamental periods ($T_n < 1, T_n = 1, T_n > 1$) are selected in Istanbul which is laid on the Northern Anatolia Fault. Bridges which are namely V03, V08 and V14 have fundamental periods of 1.29s, 1.00s and 0.73s respectively and are examined through time history ground motion sets.

There are different types of dynamic analysis methods to comprehend the seismic behavior and to evaluate the seismic demand parameters of bridges. Response spectrum analysis, linear and nonlinear time history analysis and push-over analysis are the most commonly known seismic analysis methods. Linear time history analysis is performed for this study.

There are also different specifications written and adopted from worldwide. In engineering practice of Turkiye, AASHTO LRFD (2012), Eurocode-8 and Turkish Earthquake Code for Bridges (2020) are the most commonly used specifications.

In the scope of this study these three bridge design specifications are used for comparison purposes. Each specification has different time history analysis requirements as scaling criteria, considered period range etc. and parameters of design response spectrum curves.

Also, there are different types of scaling methods and there is no strict rule of which one to choose. For the accurate seismic design of the bridges the most appropriate method should be chosen considering the ground motion parameters, soil parameters and the bridge's modal properties. Three scaling methods are used in the scope of this study. The first method (M1) is to scale the ground motion records with one factor according to the mean spectrum of selected earthquakes. The second method (M2) is to scale each ground motion record separately according to the mean spectrum of selected earthquakes without setting any upper limits. The third method (M3) is same as the second method but the scale factors' upper limit are assigned as 2.

These methods will be compared using SAP2000 software, and the seismic demand parameters like moments and displacements in the longitudinal and transverse directions. First, the methods are compared within each other for the selected bridges. Then the specifications are compared in between each other. And finally, scaling methods and specification criteria are considered and compared together.

CHAPTER 2

LITERATURE REVIEW

Since the last decade, because the seismic design of structures in the earthquake prone cities is the most important step of the design, researches about the time history analysis and the scaling of the ground motions become significantly wide. In the design codes, time history requirements and the key parameters of ground motion selection are explicitly specified. However for the scaling methods, there is no detailed explanation. Thus, there are several researches on the scaling topic including the scaling methods, intensity measures and the ground motion selection parameters. In most of the researches, it can be seen that scaling methods, ground motion sets and code provisions are compared among themselves. A research including all of them to see the effect of code provisions, ground motion sets and scaling methods as a whole like used in a design procedure is needed. Due to limited research related directly to the topic, the most common and relevant code requirements, ground motion selections used in previous studies and studies related to scaling are briefly discussed here.

2.1 Time History Requirements in Current Codes

Selection of time history records is defined in detail in seismic design specifications.

In this study, three different specifications namely AASHTO LRFD (2012), Eurocode-8 and Turkish Earthquake Code for Bridges (2020) are used for comparison purposes. Each specification has distinctive time history analysis requirements as scaling criteria, considered period range etc. and parameters of design response spectrum curves.

All of the specifications mentioned above suggest that at least three response-spectrum-compatible time histories should be used for each component. If three time histories are used, then the design actions shall be according to the maximum of the three time histories. If a minimum of seven time histories for each direction are used, then design actions shall be taken as the mean response of the time histories. Each component of the time histories should be scaled with the same scale factor in the specified time interval.

For each time history having two horizontal components, the GeoMean spectrum should be considered according to the AASHTO LRFD (2012), while the SRSS spectrum should be considered for the Eurocode-8 and Turkish Earthquake Code for Bridges (2020).

In *AASHTO LRFD (2012)*, it is stated that mean response spectrum of the selected time histories should not be less than the design response spectrum in the interval of $0.5T - 2T$ (T is the natural period of the structure).

Eurocode-8 (2003) and Turkish Earthquake Code for Bridges (2020) have approximately the same scaling criteria. However, because they have different design response spectrum curves, they should be considered separately in the analysis process. It is stated that response spectrum of the selected time histories

should be scaled so that their mean spectrum is not less than the 1.3 times the design response spectrum in the interval of $0.2T - 1.5T$.

2.2 Selection of Ground Motion Records in Previous Studies

There are many ground motion selection criteria like fault mechanism, shear wave velocity under 30 m, magnitudes, rupture distance etc. Manolis et al. (2010) states that the most common parameters of a seismic event are the earthquake magnitude (M) and rupture distance (R). However, to consider and choose only these parameters as ground motion selection criteria were observed as leading to unstable results in the structural response. Manolis et al. (2010) also states that although the rupture distance is an inadequate parameter of structural response, especially both parameters are commonly used in practice by structural engineers.

Cornell and Iervolino (2010) conducted a study to understand the dependence of structural response on M and R parameters. In this study accelerograms are chosen in two categories. First category is composed of six sets of ten accelerograms with large magnitudes and small distances. Second category is composed of arbitrary sets of ten ground motion records without any limitations. At the end of the study, results show that the carefully selected sets of accelerograms are not superior to the arbitrary ones in case of the structural response. This study shows that the most common parameters to select ground motion records in the engineer practice which are magnitude and rupture distance are considerable.

On the other hand, O'Donnell et al. (2017) conducted a study by selecting ground motion records in the same manner, in other words considering only the magnitude and rupture distance to compare the three scaling methods. Study results show that the scaling methods and criteria are the most important things to achieve stable seismic demand results besides the selection criteria.

Besides, the number of the ground motion records and the forming of the ground motions set are important issues. In the bridge specifications AASHTO LRFD (2012), Eurocode-8 (2003) and TDY (2020), it is stated that seven earthquake ground motion records should be selected if the mean response of those seven earthquakes will be used in the design. However if the maximum response will be used, then three ground motion records are sufficient. O'Donnell et al. (2017) states that seven ground-motions are sufficient to achieve correct analysis results. In addition, a comparative study conducted by Chopra and Kalkan (2010), three sets of seven earthquakes were selected. They compared the scaling methods and the selected sets on low-, mid- and high-rise buildings and bridges. Results showed variation between the selected ground motion sets.

2.3 Scaling Methods Used in Previous Studies

There are considerable amount of scaling methods in practice. Bridge design specifications classified the methods into two that can be named as spectral matching and fundamental period scaling to a target spectrum. Spectral matching is to get the response spectrum of accelerograms to be compatible with the selected target spectrum (Lancieri et al. (2018)). In other words, spectral matching is to fit the response spectrum of accelerograms to a target spectrum by changing the nature of the accelerograms. On the other hand, fundamental period scaling to a target spectrum, is to amplify the accelerograms to be not less than or to be greater than the target spectrum in the related time period (based on fundamental periods of the structures) as specified in the provisions.

The fundamental period scaling to a target spectrum method is branched off different methods like scaling according to a single factor, scaling by attaining an upper limit, scaling the ground motions by separate factor, scaling according to the maximum incremental velocity etc. However, in the provisions, there are no detailed

explanation of the scaling methods. Thus, a proper scaling method to meet the demands of the structure should be selected.

O'Donnell et al. (2017) conducted a study to compare the four scaling methods which are scaled according to ASCE 7 (2010), scaled to the median linear-elastic spectral acceleration at the fundamental period of the structures ($S_a(T_1)$ method), scaled to the median MIV (maximum incremental velocity) and scaled based on the modal pushover-based scaling, respectively.

Results show that the $S_a(T_1)$ method is less efficient and the less accurate for the structures having higher fundamental periods and responding mostly in the nonlinear range. "Maximum Incremental Velocity" method is the only method that does not depend on the properties of structure. MIV which can be defined as the maximum area under the accelerogram of a ground motion record was found by Kurama and Farrow (2003) for nonlinear structures.

In addition to scaling methods, selection of the intensity measure, in other words intensity-based assessment, is the other important parameter for the ground motion scaling. In practice, the mostly used intensity measure is the PGA (peak ground acceleration). However, Liang and Mosalam (2017) states that the PGV (peak ground velocity) is an appropriate intensity measure that correlates well with the nonlinear peak response.

CHAPTER 3

LINEAR TIME HISTORY ANALYSIS OF HIGHWAY BRIDGES

3.1 Selection and Description of Bridges

In the scope of this study, three types of highway bridges having different fundamental periods ($T_n < 1, T_n = 1, T_n > 1$) are selected. The reason of selecting bridges as $T_n < 1, T_n = 1, T_n > 1$ is because in AASHTO LRFD Section 3.10.32, structures are classified as in short-period range if $T_n < 1$ and as in long-period range if $T_n > 1$. On the other hand, $T_n = 1$ can be thought as a transition zone between the short- and long-period structures. Bridges which are namely V03, V08 and V14 have fundamental periods of 1.29s, 1.00s and 0.73s respectively. These bridges are selected for examining the time history ground motion sets in different period ranges. The bridges that are part of the Northern Marmara Motorway Project located in Istanbul. Istanbul is especially chosen for this study because of two main reasons. Firstly, Istanbul is laid on the North Anatolian Fault. Thus, there are large scale of ground motion records to be studied on. Secondly, in the scope of the Northern Marmara Motorway Project, an Earthquake Hazard Analysis is provided by Boğaziçi University Kandilli Observatory and Earthquake Research Institute. Thanks to this study, seismic design parameters are available such as peak ground acceleration (PGA) and essential seismic coefficients (S_s, S_1 etc.) for different return periods, and also soil types according to NEHRP soil classifications.

Superstructure of all of the bridges consists of composite prestressed I-beam. Column types, column dimensions and heights, number of spans, span lengths and superstructure widths are different for each bridge. Elastomeric bearings (400x500x110 cm) are located under each beam to connect the superstructure to the substructure. Bridges are classified as straight precast I girder bridge type.

3.1.1 V03 Bridge

V03 is located on the Istanbul-Edirne State Highway between Km:40+395.000 and Km:40+420.000. Plan view and longitudinal profile views are given in Figure 3.1 to Figure 3.3 below.

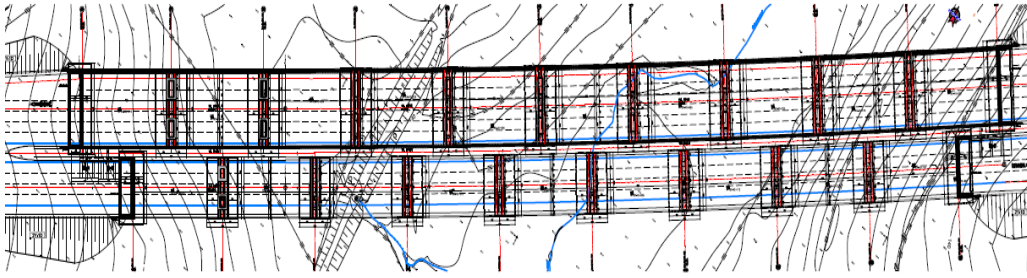


Figure 3.1. Plan view of V03 Bridge

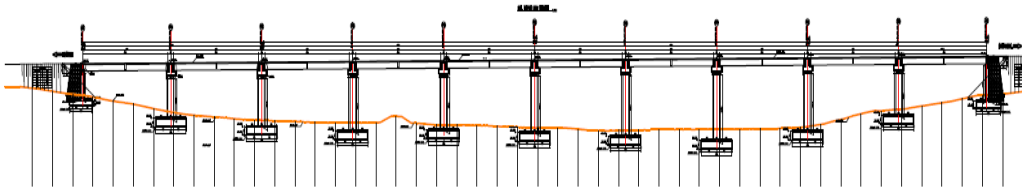


Figure 3.2. Longitudinal profile of V03 Bridge

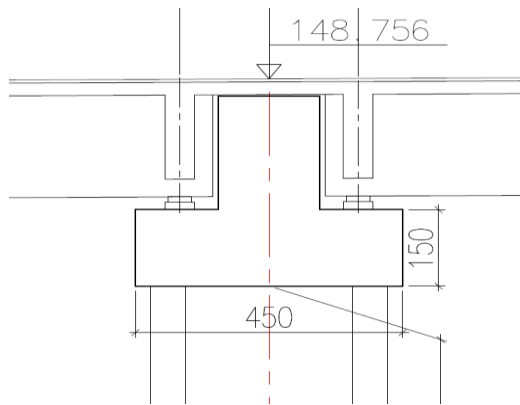


Figure 3.3. Profile view of pier axis P1 to show the pier cap details

Total length of the bridge is 447 m designed as 10 spans with 42 m length for per span. Superstructure width is 28 m and composed of 14 prestressed I-beams. Beam height is 200 cm and slab thickness is 25 cm. Each pier has two box section columns with a dimension of 7x4 m. Maximum column height for this bridge is 21.4 m. Cross sections of superstructure, prestressed beam and column are given in Figure 3.4 to Figure 3.6 below.

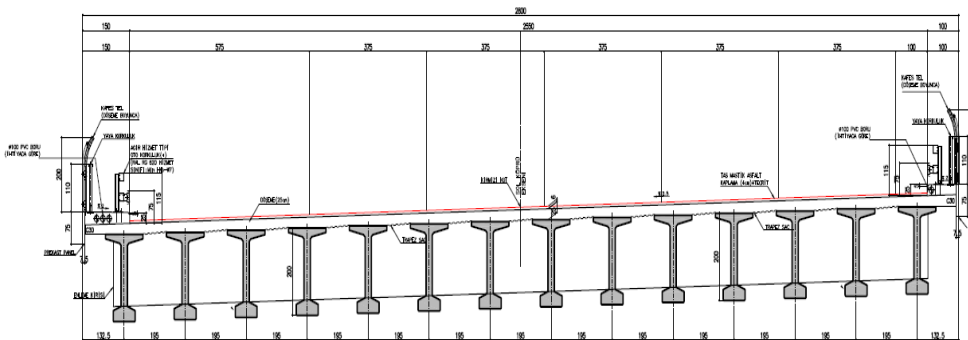


Figure 3.4. Cross section of the superstructure

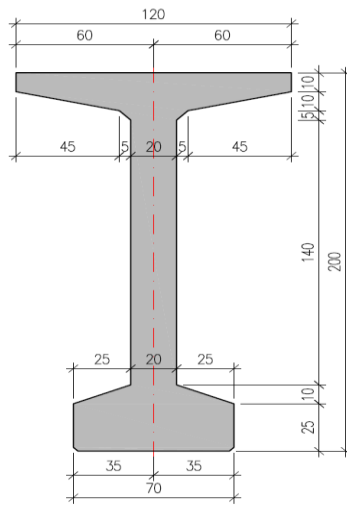


Figure 3.5. Cross section of the beam

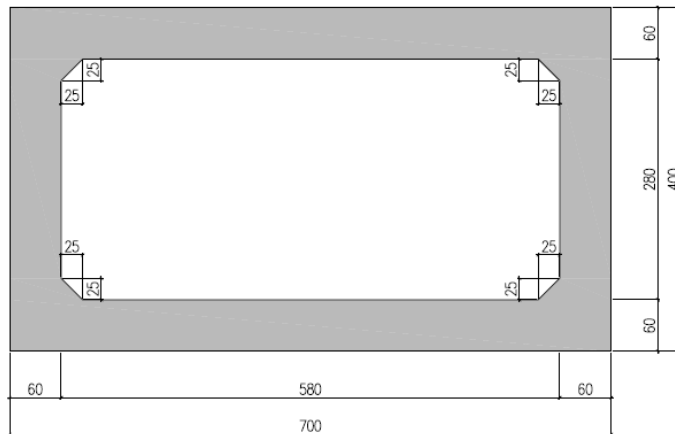


Figure 3.6. Cross section of the column

3.1.2 V08 Bridge

V08 is located on the Istanbul-Edirne State Highway between Km:70+884.849 and Km:71+169.849. Plan view and longitudinal profile views are given in Figure 3.7 to Figure 3.9 below.

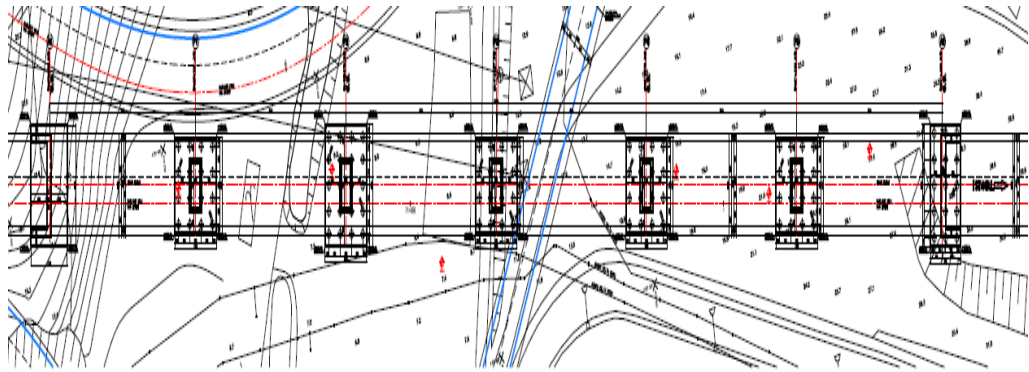


Figure 3.7. Plan view of V08 Bridge

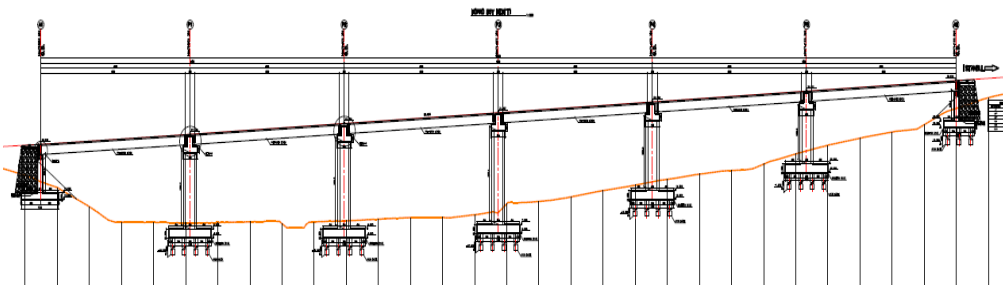


Figure 3.8. Longitudinal profile of V08 Bridge

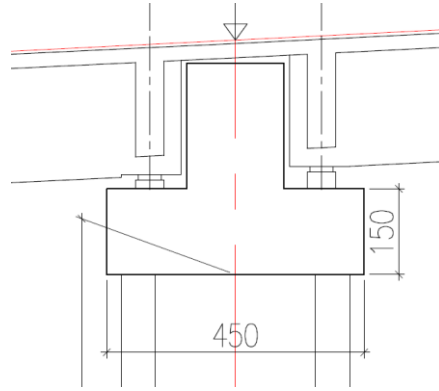


Figure 3.9. Profile view of pier axis P1 to show the pier cap details

Total length of the bridge is 285 m designed as 6 spans with 45 m length for per span. Superstructure width is 14 m and composed of 11 prestressed I-beams. Beam height is 200 cm and slab thickness is 25 cm. Each pier has a box section column with a dimension of 7.5x4 m. Maximum column height for this bridge is 20.7 m. Cross sections of superstructure, prestressed beam and column are given in Figure 3.10 to Figure 3.12 below.

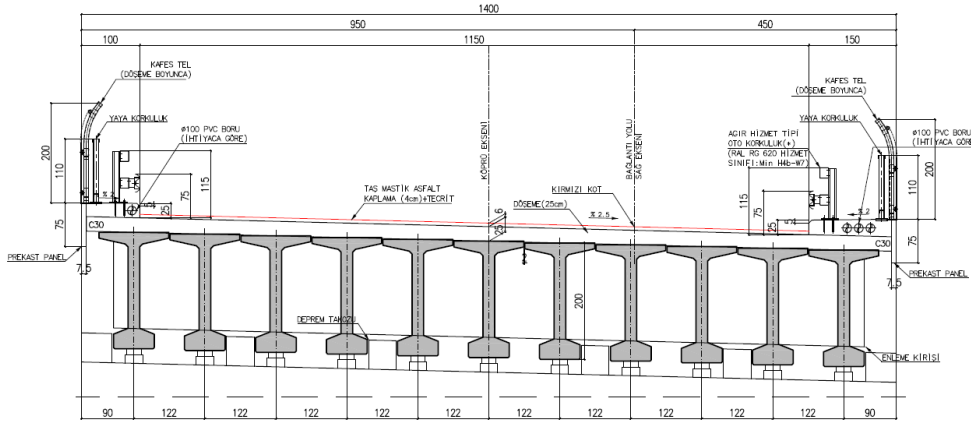


Figure 3.10. Cross section of the superstructure

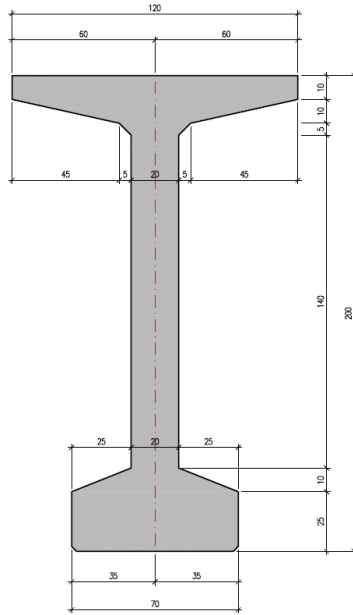


Figure 3.11. Cross section of the beam

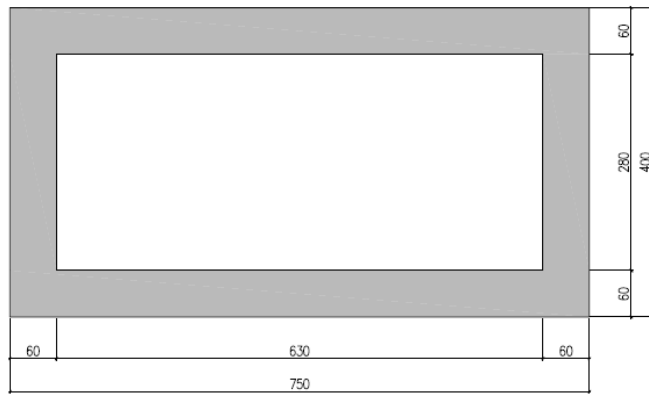


Figure 3.12. Cross section of the column

3.1.3 V14 Bridge

V14 is located on the Istanbul-Edirne State Highway between Km:63+971.000 and Km:64+103.000. Plan view and longitudinal profile views are given in Figure 3.13 to Figure 3.15 below.

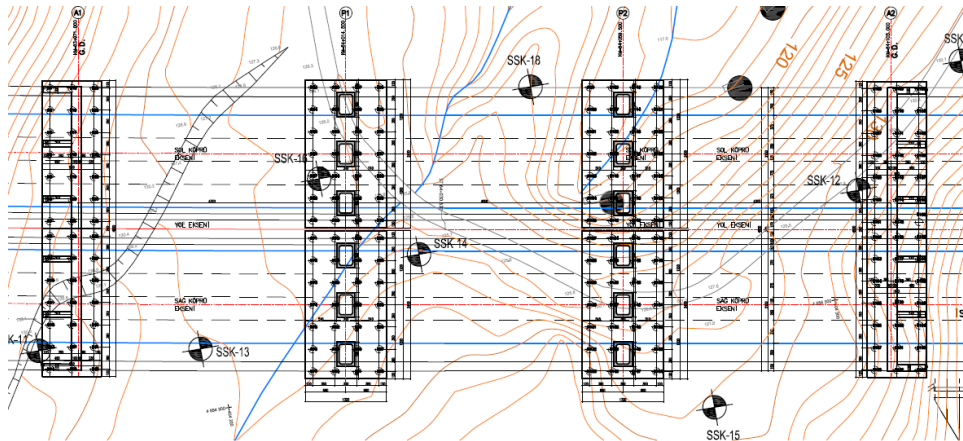


Figure 3.13. Plan view of V14 Bridge

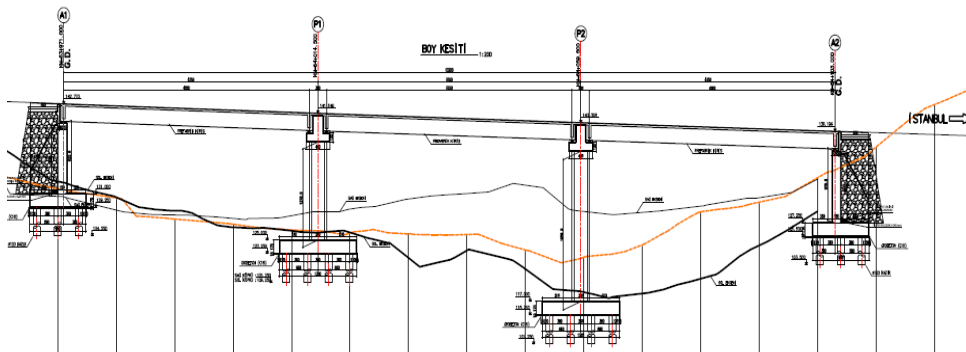


Figure 3.14. Longitudinal profile of V14 Bridge

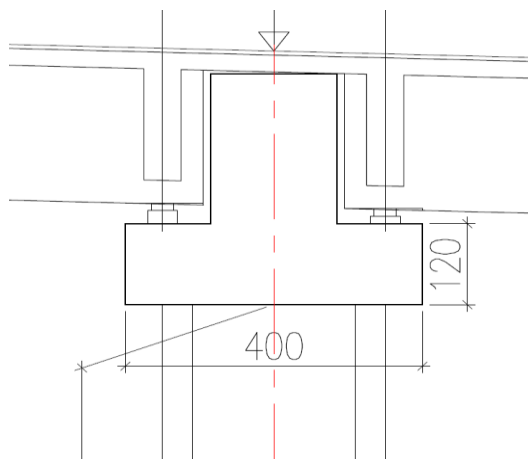


Figure 3.15. Profile view of pier axis P1 to show the pier cap details

Total length of the bridge is 132 m designed as 3 spans with 42 m length per span. Superstructure width is 21.5 m and composed of 17 prestressed I-beams. Beam height is 200 cm and slab thickness is 25 cm. Each pier has three box section columns with a dimension of 4x3 m. Maximum column height for this bridge is 19.6 m. Cross sections of superstructure, prestressed beam and column are given in Figure 3.16 to Figure 3.18 below.

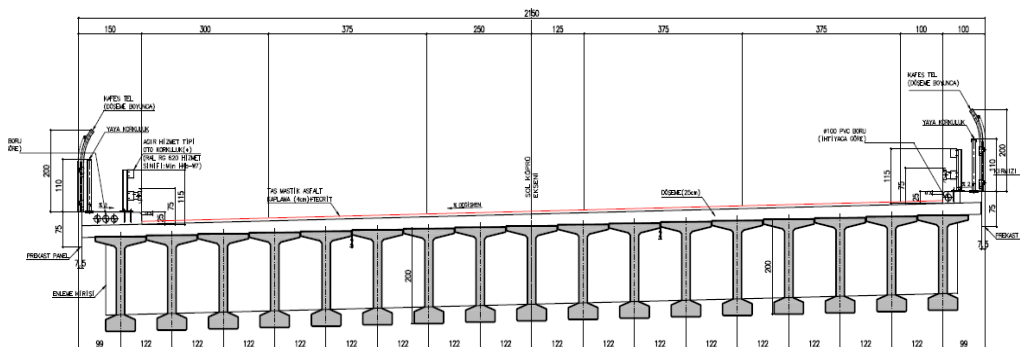


Figure 3.16. Cross section of the superstructure

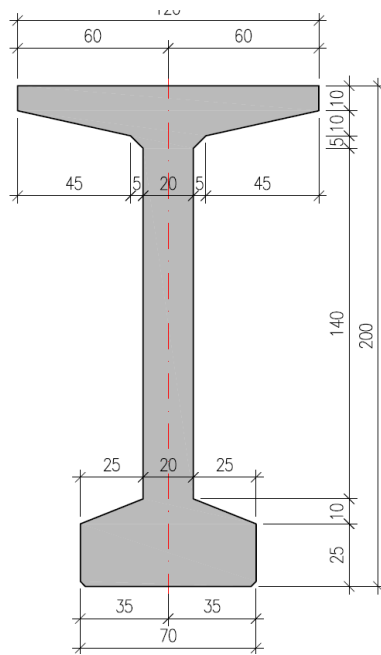


Figure 3.17. Cross section of the beam

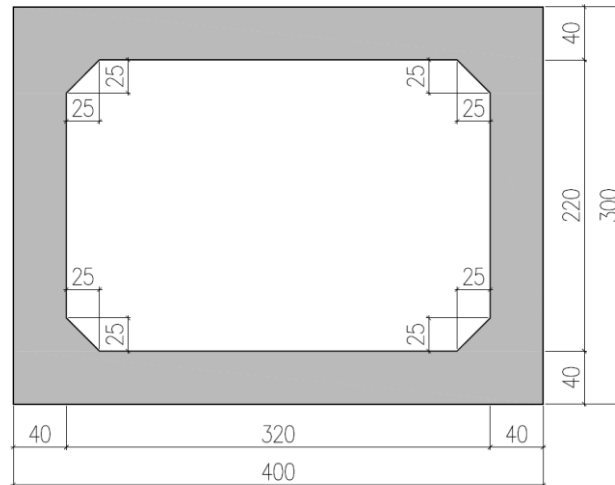


Figure 3.18. Cross section of the column

The general properties of selected bridges are summarized in Table 3.1.

Table 3.1 Summary of selected bridges

Bridge	Number of Spans	Span Length (m)	Total Length (m)	Superstructure Width (m)	Column Dimensions (m)	Max.Column Height (m)	Tn (Longitudinal Direction) (s)	Tn (Transverse Direction) (s)
V03	10	42	447	28	7x4	21.4	0.73	0.57
V08	6	45	285	14	7.5x4	20.7	1.00	0.95
V14	3	42	132	21.5	4x3	19.6	1.29	0.94

3.2 Earthquake Hazard Analysis for Bridges

In the scope of the Northern Marmara Motorway Project, an Earthquake Hazard Analysis is provided by Boğaziçi University Kandilli Observatory and Earthquake Research Institute (2017).

In the Marmara Region's tectonic structure, active faults and basins of the western side of the Northern Anatolian Fault are effective. Tectonic map of the Marmara Region can be seen in Figure 3.19. This fault is 1200 km long right strike slip fault separating the Anatolian block from the Eurasia plate. In this region, five earthquakes occurred with surface wave magnitudes greater than 7.0 ($M_s \geq 7.0$) in the 20th century.

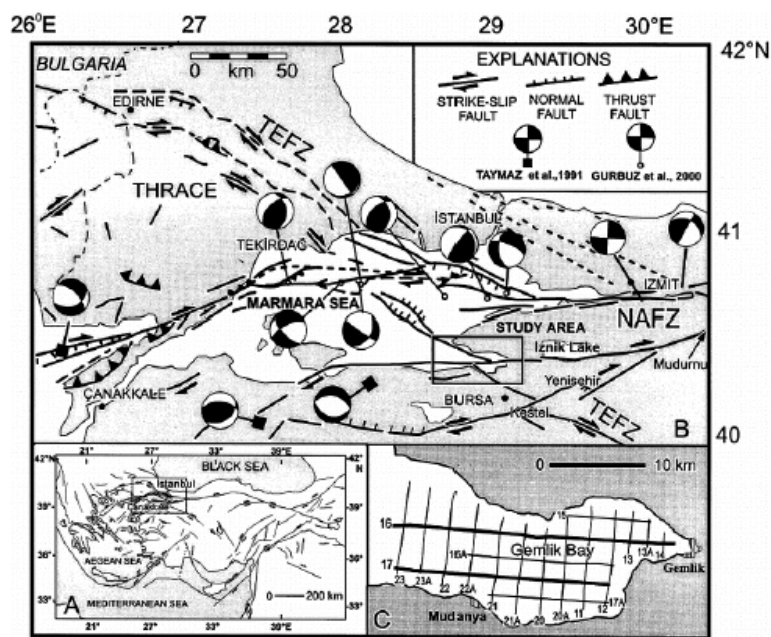


Figure 3.19. Tectonic map of the Marmara Region

In the report done by Boğaziçi Kandilli Observatory and Earthquake Research Institute, a probabilistic earthquake hazard analysis has been conducted with the help of neotectonic structure, earthquake formations and modelling, seismic source regions and their characteristics, ground motion prediction equations and the probabilistic model employed. Hazard analysis was conducted to obtain the values of peak ground acceleration (PGA), peak ground velocity (PGV), spectral accelerations (S_s and S_1) with %5 damping ratio for 72,475,100 and 2475 years return periods. These parameters are obtained for the $V_{s30}=760$ m/s, in other words NEHRP B/C boundary. In this study 475-year return period values are used.

According to the results of the conducted Earthquake Hazard Analysis PGA, S_s and S_1 values for the selected bridges are listed in Table 3.2 below:

Table 3.2 PGA, S_s and S_1 values for 475 years return period

	<i>PGA (g)</i>	<i>S_s</i>	<i>S₁</i>
V03	0.270	0.652	0.230
V08	0.337	0.821	0.277
V14	0.518	1.280	0.443

3.3 Bridge Analysis Models

V03, V08 and V14 Bridges are modeled using a structural analysis program which is SAP2000 V19.2.1 (Computers & Structures Inc., 2017) by CSI. The models consist of superstructure, substructure and supports (Figure 3.20). I-beams and bridge deck are the main elements of the superstructure while cap beams, columns, pier foundations and abutments are the main elements of the substructure. Bearings and the shear keys are parts of the supports. The 3-D models of each bridge are shown in Figures 3.21, 3.22 and 3.23.

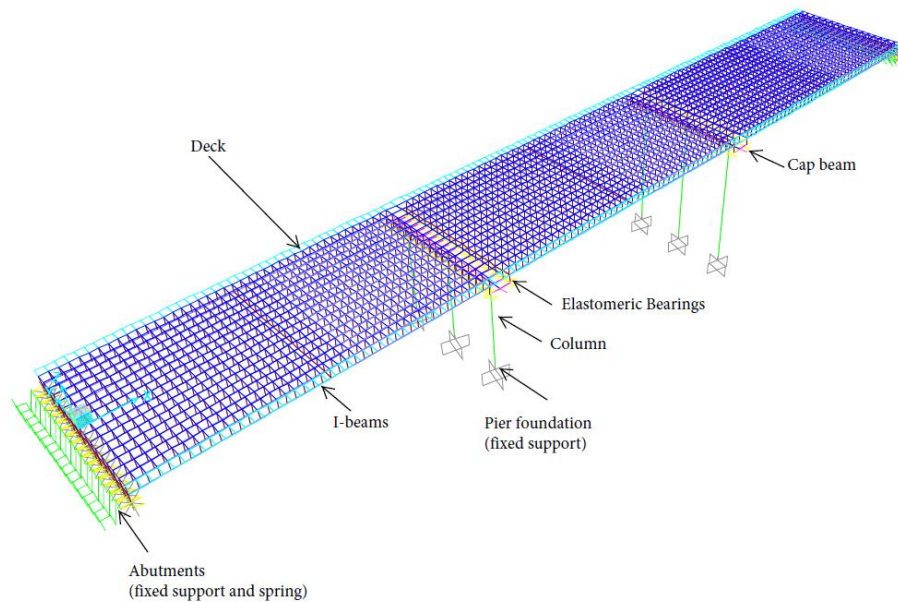


Figure 3.20. Representation of bridge elements

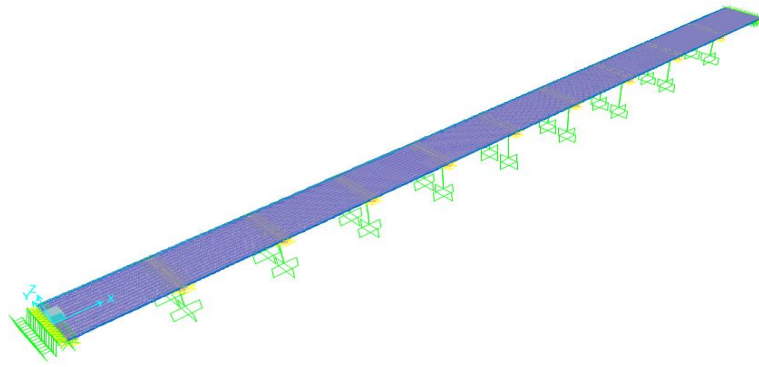


Figure 3.21. Analysis model of V03 Bridge

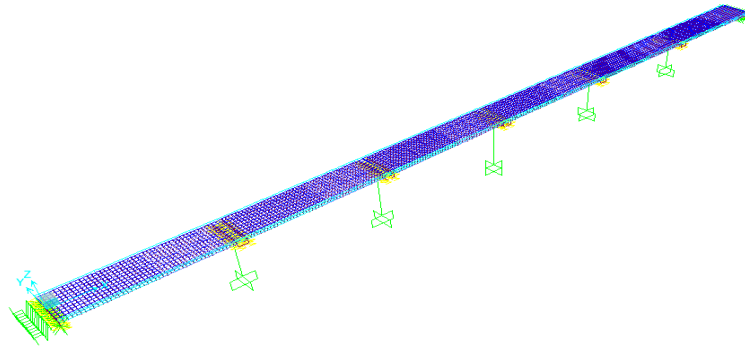


Figure 3.22. Analysis model of V08 Bridge

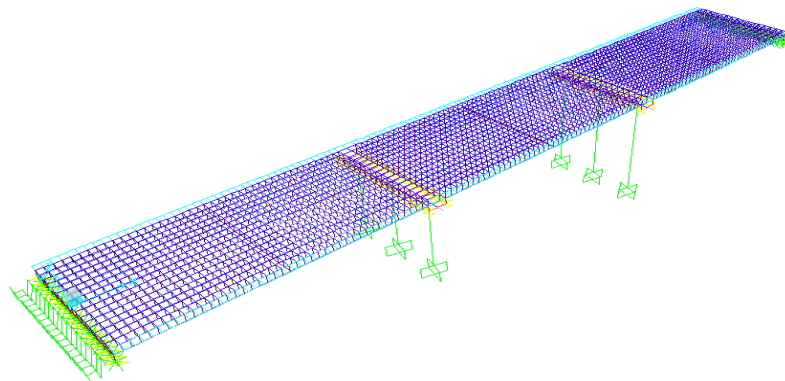


Figure 3.23. Analysis model of V14 Bridge

3.3.1 Superstructure

Bridge deck is modeled using shell elements while I-girders are modeled using frame elements (Figure 3.24 and 3.25). To connect and to represent the composite characteristic of the superstructure, shell elements of the deck and frame elements of the beams are linked with massless rigid frames.

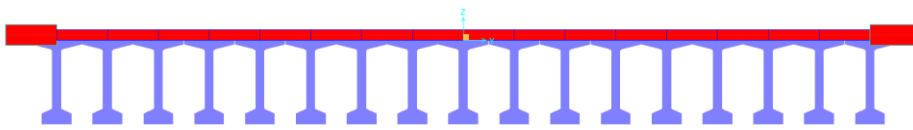


Figure 3.24. view of V14 Bridge (similar in V03 and V08 Bridges)

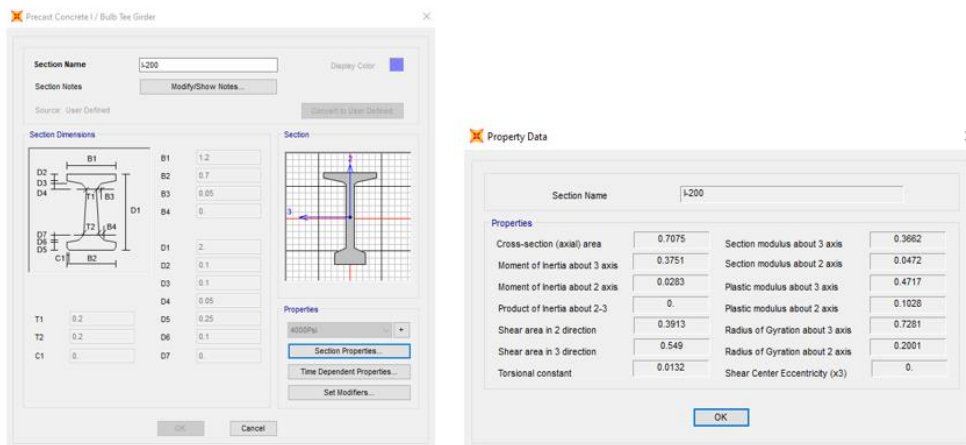


Figure 3.25. Properties of h=200 cm I-beam

3.3.2 Substructure

Like superstructure configuration, frame elements of beams and cap beams are connected with the rigid frames. Columns are directly connected through the cap beams. Geometrical properties of columns are shown in Figure 3.27, 3.28 and 3.29 for the selected bridges. Elastomeric bearings are represented with the link elements between the I-beams and the cap beam (Figure 3.26).

In this study seismic demands of abutments and pier foundations are not considered. Thus, pier foundations are modeled as fixed supports. On the other hand, abutments are represented with supports and springs. Abutment supports are released in translation for longitudinal direction (u_1) by assigning equivalent spring coefficients while fixed in translation and rotation for other directions (u_2, u_3, r_1, r_2, r_3).

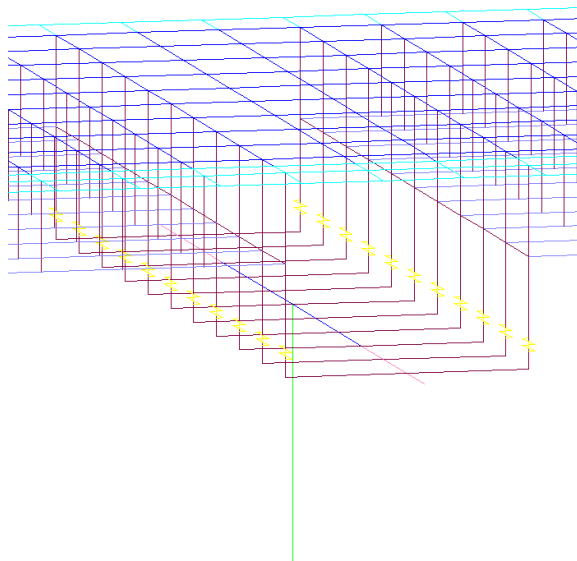


Figure 3.26. Deck-beam, beam-cap beam, cap beam-column connections and links for elastomeric bearings

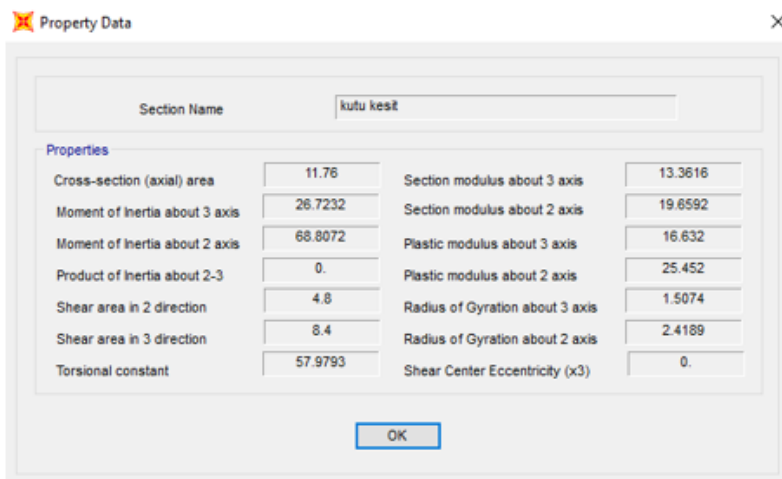
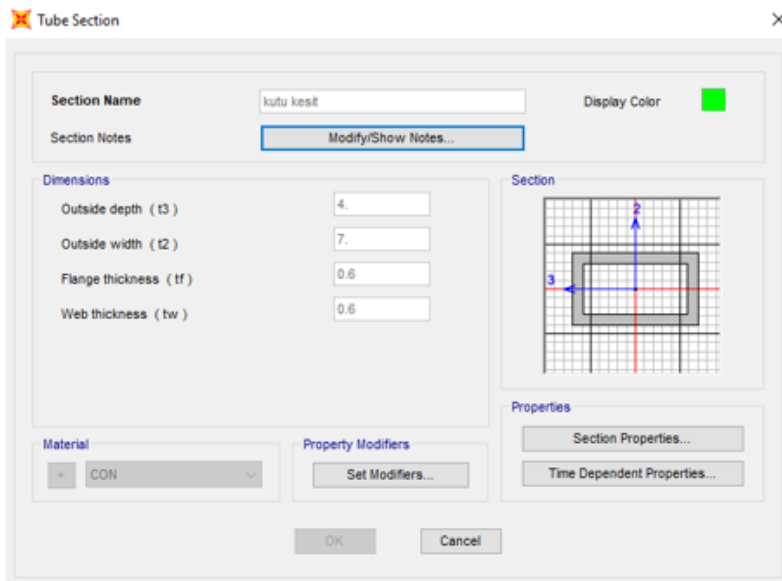


Figure 3.27. Geometrical properties of columns of V03 Bridge

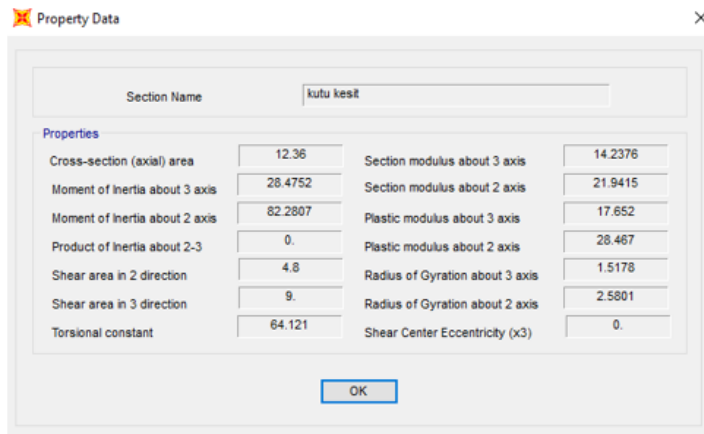
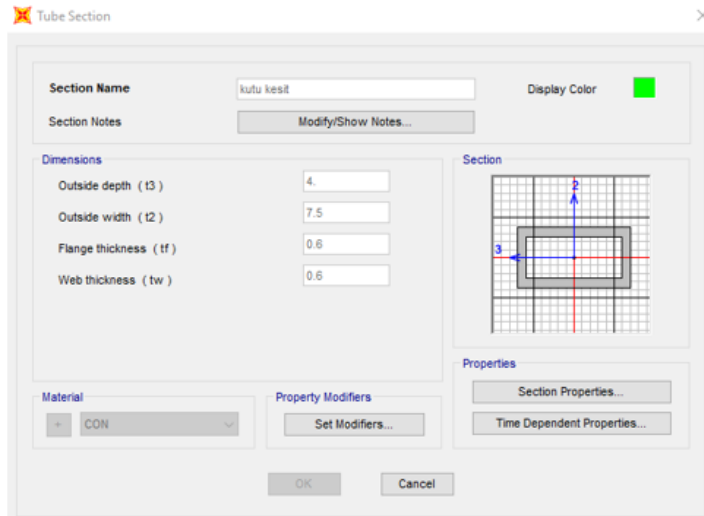


Figure 3.28. Geometrical properties of columns of V08 Bridge

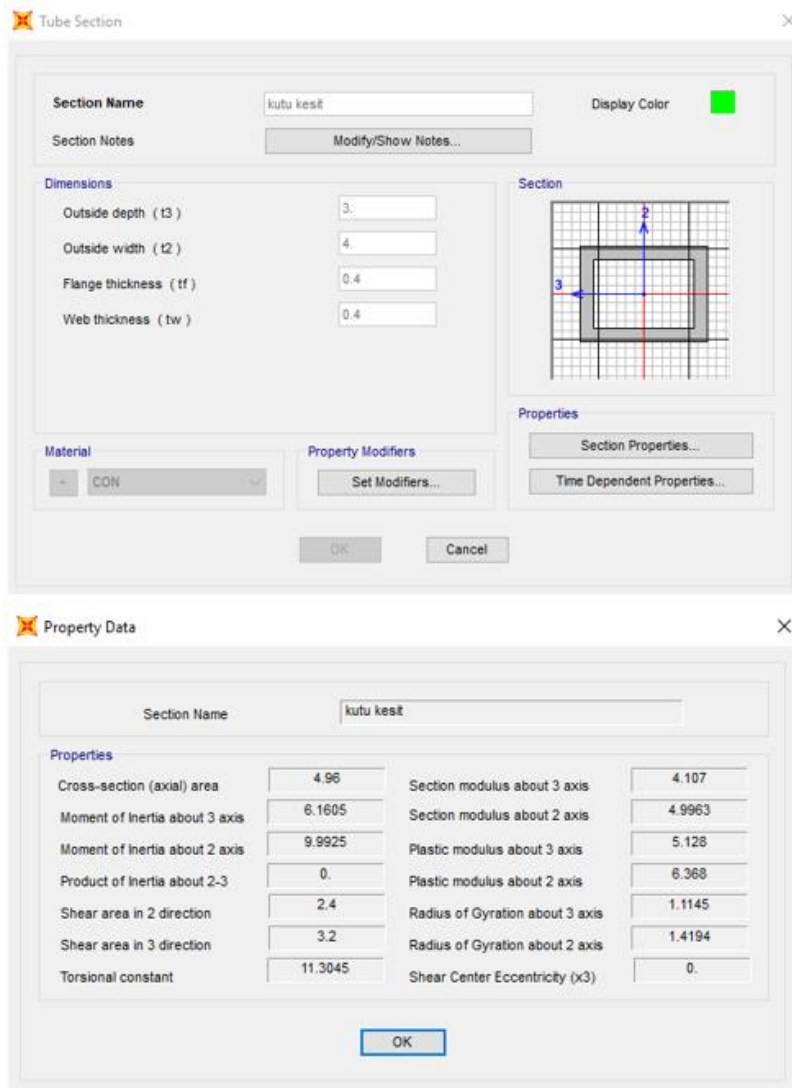


Figure 3.29. Geometrical properties of columns of V14 Bridge

3.4 Design Target Spectra of the Bridge Design Specifications

In the Earthquake Hazard Analysis is provided by Boğaziçi University Kandilli Observatory and Earthquake Research Institute, PGA, S_s and S_1 values for each bridge are provided as shown in Table 3.2 in Section 3.2.

Design spectra of AASHTO LRFD (2012), Eurocode-8 (2003) and TDY (2020) are constituted for each of the three bridges. Formulations for the design spectra according to each code are demonstrated in the Figures 30-32. Soil type is taken as NEHRP B/C boundary which corresponds to type B for AASHTO LRFD classification, type A for Eurocode-8 classification and type B for TDY classification as shown in the Figures 33-35.

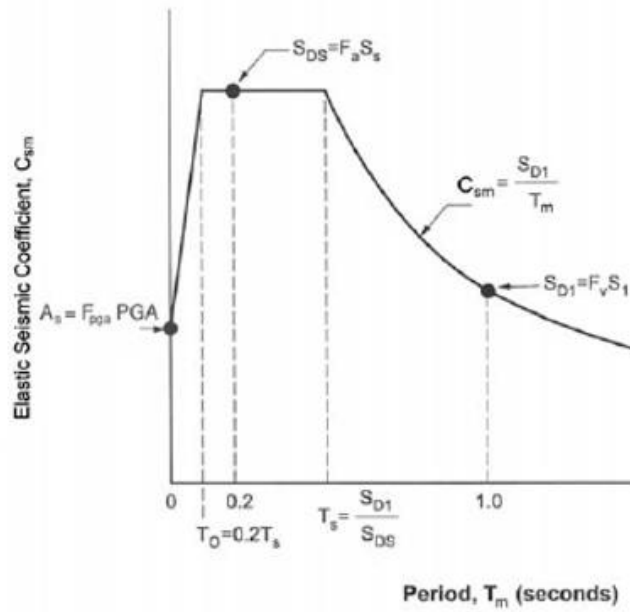
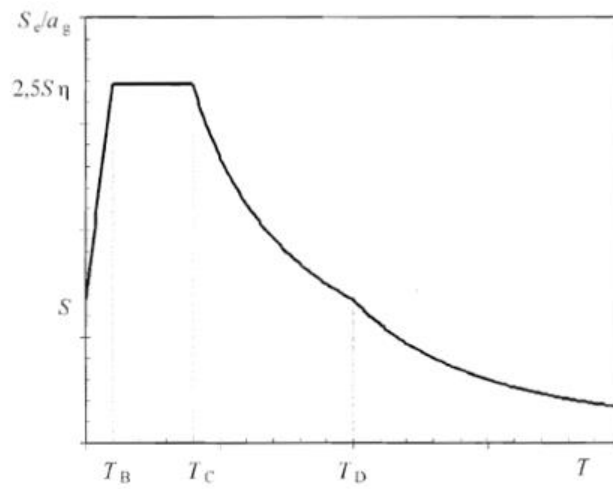


Figure 3.30. AASHTO LRFD design spectrum curve

According to AASHTO LRFD (2012) Section 3.10.4.2 Equation 3.10.4.2-1, for periods less than or equal to T_0 , the seismic coefficient C_{sm} is calculated as:

$$C_{sm} = A_s + (S_{ds} - A_s) * (T_m/T_0)$$



$$0 \leq T \leq T_B : S_c(T) = a_g \cdot S \cdot \left[1 + \frac{T}{T_B} \cdot (\eta \cdot 2,5 - 1) \right]$$

$$T_B \leq T \leq T_C : S_c(T) = a_g \cdot S \cdot \eta \cdot 2,5$$

$$T_C \leq T \leq T_D : S_c(T) = a_g \cdot S \cdot \eta \cdot 2,5 \left[\frac{T_C}{T} \right]$$

$$T_D \leq T \leq 4s : S_c(T) = a_g \cdot S \cdot \eta \cdot 2,5 \left[\frac{T_C T_D}{T^2} \right]$$

Figure 3.31. Eurocode-8 design spectrum curve

$$\begin{aligned}
S_{ac}(T) &= \left(0.4 + 0.6 \frac{T}{T_A}\right) S_{DS} & (0 \leq T \leq T_A) \\
S_{ac}(T) &= S_{DS} & (T_A \leq T \leq T_B) \\
S_{ac}(T) &= \frac{S_{D1}}{T} & (T_B \leq T \leq T_L) \\
S_{ac}(T) &= \frac{S_{D1} T_L}{T^2} & (T_L \leq T)
\end{aligned}$$

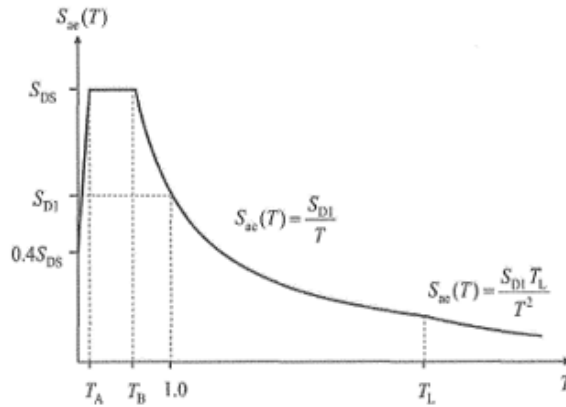


Figure 3.32. TDY 2020 design spectrum curve

Site Class	Soil Type and Profile
A	Hard rock with measured shear wave velocity, $\bar{v}_s > 5,000$ ft/s
B	Rock with $2,500$ ft/sec $< \bar{v}_s < 5,000$ ft/s
C	Very dense soil and soil rock with $1,200$ ft/sec $< \bar{v}_s < 2,500$ ft/s, or with either $\bar{N} > 50$ blows/ft, or $\bar{\epsilon}_u > 2.0$ ksf
D	Stiff soil with 600 ft/s $< \bar{v}_s < 1,200$ ft/s, or with either $15 < \bar{N} < 50$ blows/ft, or $1.0 < \bar{\epsilon}_u < 2.0$ ksf
E	Soil profile with $\bar{v}_s < 600$ ft/s or with either $\bar{N} < 15$ blows/ft or $\bar{\epsilon}_u < 1.0$ ksf, or any profile with more than 10 ft of soft clay defined as soil with $PI > 20$, $w > 40$ percent and $\bar{\epsilon}_u < 0.5$ ksf
F	Soils requiring site-specific evaluations, such as: <ul style="list-style-type: none"> • Peats or highly organic clays ($H > 10$ ft of peat or highly organic clay where H = thickness of soil) • Very high plasticity clays ($H > 25$ ft with $PI > 75$) • Very thick soft/medium stiff clays ($H > 120$ ft)

Figure 3.33. Site class definitions in AASHTO LRFD (2012)

Ground type	Description of stratigraphic profile	Parameters		
		$v_{s,30}$ (m/s)	N_{SPT} (blows/30cm)	c_u (kPa)
A	Rock or other rock-like geological formation, including at most 5 m of weaker material at the surface.	> 800	—	—
B	Deposits of very dense sand, gravel, or very stiff clay, at least several tens of metres in thickness, characterised by a gradual increase of mechanical properties with depth.	360 – 800	> 50	> 250
C	Deep deposits of dense or medium-dense sand, gravel or stiff clay with thickness from several tens to many hundreds of metres.	180 – 360	15 - 50	70 - 250
D	Deposits of loose-to-medium cohesionless soil (with or without some soft cohesive layers), or of predominantly soft-to-firm cohesive soil.	< 180	< 15	< 70
E	A soil profile consisting of a surface alluvium layer with v_s values of type C or D and thickness varying between about 5 m and 20 m, underlain by stiffer material with $v_s > 800$ m/s.			
S_1	Deposits consisting, or containing a layer at least 10 m thick, of soft clays/silts with a high plasticity index ($PI > 40$) and high water content	< 100 (indicative)	—	10 - 20
S_2	Deposits of liquefiable soils, of sensitive clays, or any other soil profile not included in types A – E or S_1 .			

Figure 3.34. Site class definitions in Eurocode-8 (2003)

Yerel Zemin Sınıfı	Zemin Cinsi	Üst 30 metrede ortalama		
		$(V_s)_{30}$ [m/s]	$(N_{60})_{30}$ [darbe/30 cm]	$(C_u)_{30}$ [kPa]
ZA	Sağlam, sert kayalar	> 1500	-	-
ZB	Az ayrışmış, orta sağlam kayalar	760 - 1500	-	-
ZC	Çok sıkı kum, çakıl ve sert kil tabakaları veya ayrışmış, çok çatlaklı zayıf kayalar	360 - 760	> 50	> 250
ZD	Orta sıkı - sıkı kum, çakıl veya çok katı kil tabakaları	180 - 360	15 - 50	70 - 250
ZE	Gevşek kum, çakıl veya yumuşak - katı kil tabakaları veya $PI > 20$ ve $w > \% 40$ koşullarını sağlayan toplamda 3 metreden daha kalın yumuşak kil tabakası ($C_u < 25$ kPa) içeren profiller	< 180	< 15	< 70
ZF	Sahaya özel araştırma ve değerlendirme gerektiren zeminler : 1) Deprem etkisi altında çökme ve potansiyel göçme riskine sahip zeminler (sıvılaştırılabilir zeminler, yüksek derecede hassas killler, göçebilir zayıf çimentolu zeminler vb.), 2) Toplam kalınlığı 3 metreden fazla turba ve/veya organik içeriği yüksek killler, 3) Toplam kalınlığı 8 metreden fazla olan yüksek plastisiteli ($PI > 50$) killler , 4) Çok kalın (> 35 m) yumuşak veya orta katı killler.			

Figure 3.35. Site class definitions in TDY (2020)

Design spectra for each bridge are demonstrated in the figures below.

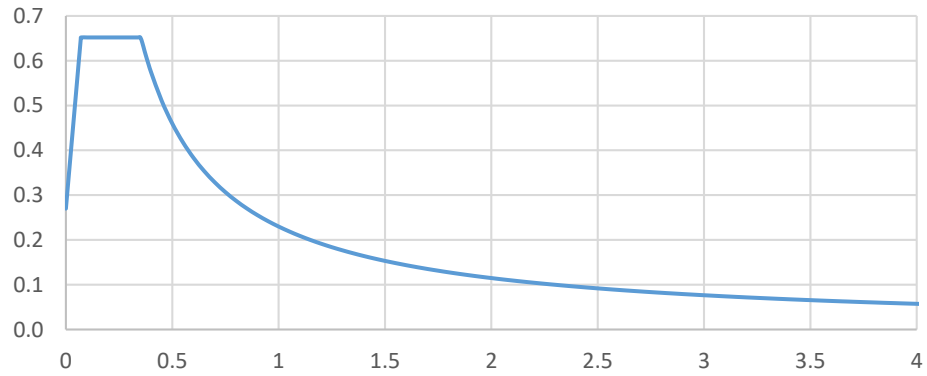


Figure 3.36. AASHTO LRFD design spectrum for V03 Bridge ($S_a(g)$ - $T(s)$)

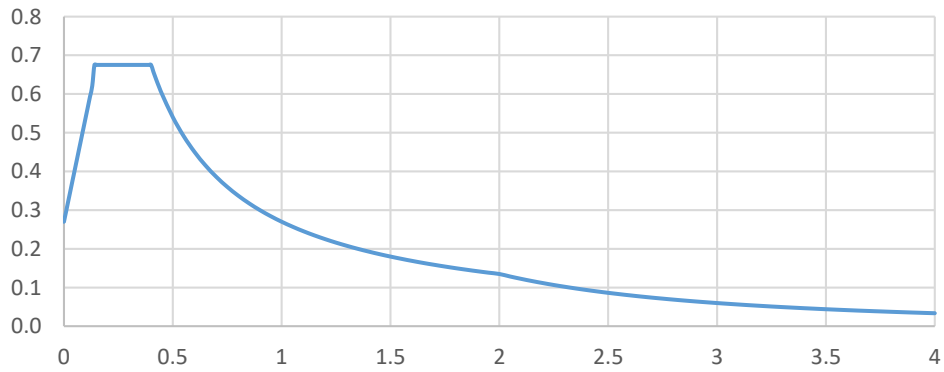


Figure 3.37. Eurocode-8 design spectrum for V03 Bridge ($S_a(g)$ - $T(s)$)

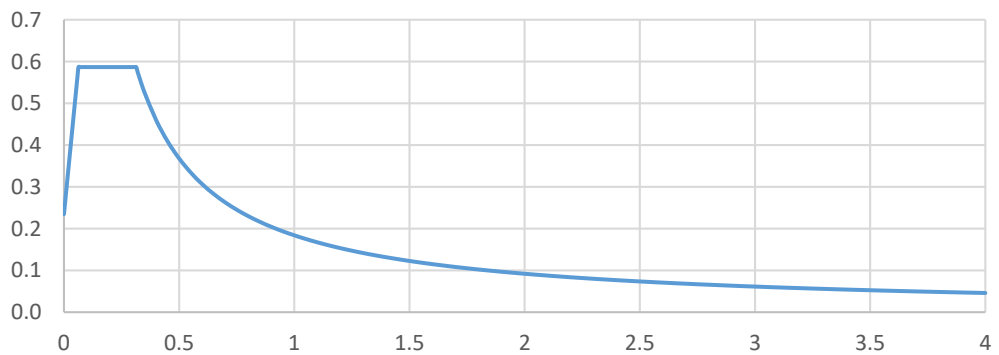


Figure 3.38. TDY (2020) design spectrum for V03 Bridge ($S_a(g)$ - $T(s)$)

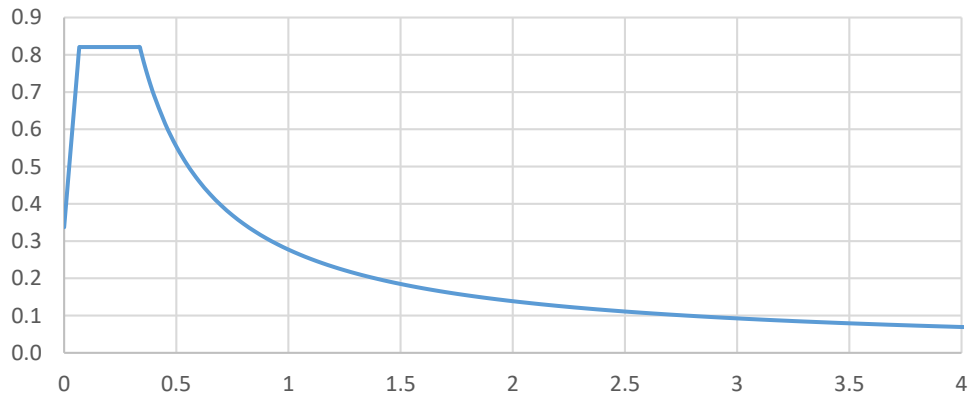


Figure 3.39. AASHTO LRFD design spectrum for V08 Bridge ($S_a(g)$ - $T(s)$)

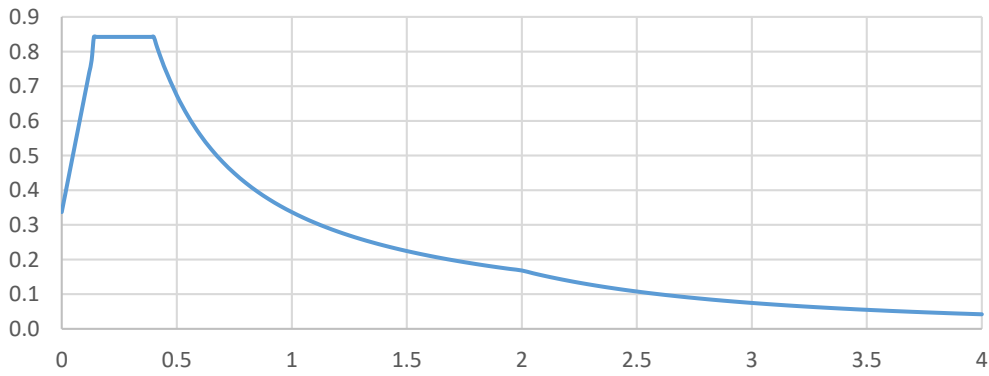


Figure 3.40. Eurocode-8 design spectrum for V08 Bridge ($S_a(g)$ - $T(s)$)

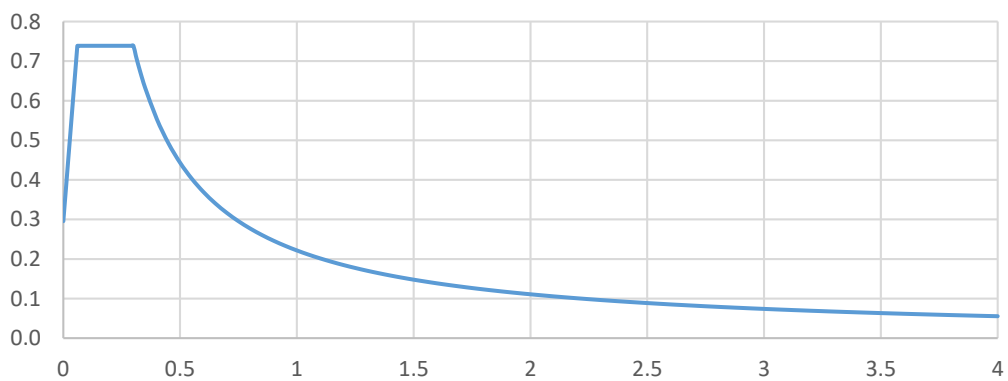


Figure 3.41. TDY (2020) design spectrum for V08 Bridge ($S_a(g)$ - $T(s)$)

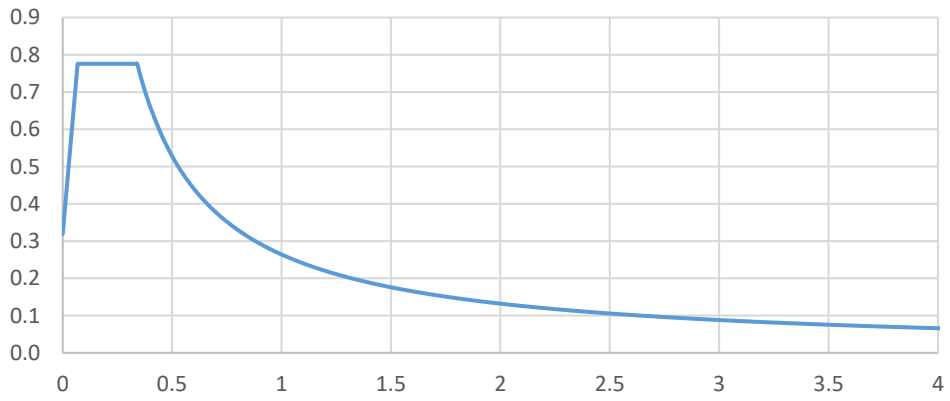


Figure 3.42. AASHTO LRFD design spectrum for V14 Bridge ($S_a(g)$ - $T(s)$)

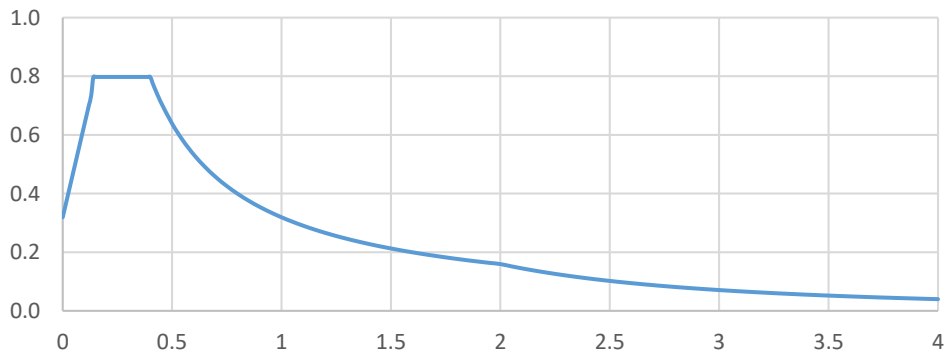


Figure 3.43. Eurocode-8 design spectrum for V14 Bridge ($S_a(g)$ - $T(s)$)

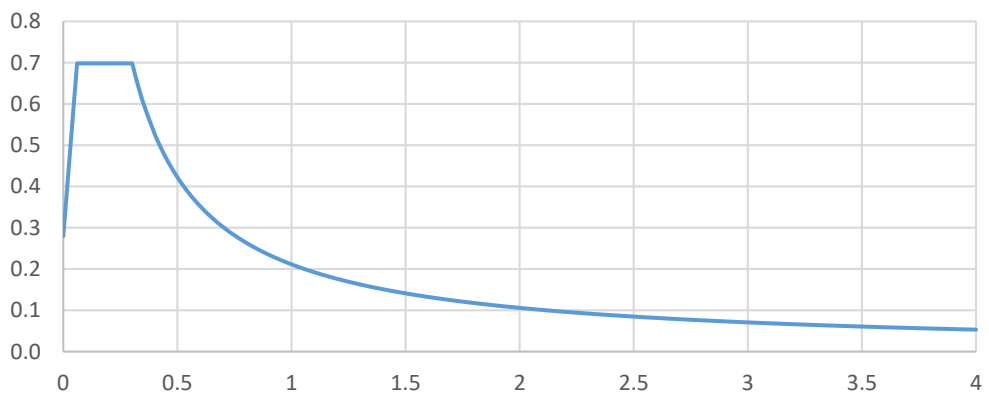


Figure 3.44. TDY (2020) design spectrum for V14 Bridge ($S_a(g)$ - $T(s)$)

3.5 Selection and Scaling of Ground Motion Records

3.5.1 Selection of Ground Motion Records

Strong ground motion records to be used in this study are obtained from PEER NGA-West Database (Yang, Moehle, &Stojadinovic, 2009). In total sixteen earthquake records are selected. Design codes referred in this study (AASHTO LRFD (2012), Eurocode-8 (2005) and Turkish Earthquake Code for Bridges (2020)) suggest that ground motion selection should be done by considering the consistency of:

- Type of faulting
- Magnitudes
- Station to site distance
- Local site conditions

Since the bridges are in Istanbul near the Northern Anatolian Fault having a fault mechanism of strike slip, records are selected as strike slip fault type. In addition, to be used in the future studies for different soil types, shear wave velocity below 30 km is chosen as $600 \text{ m/s} \leq V_{s30} \leq 850 \text{ m/s}$ which corresponds to the engineering rock. Selected ground motion records can be seen in Table 3.3. In summary, ground motion selection limitations are listed below:

- Accelerograms are unscaled,
- Fault mechanism is strike slip,
- Magnitude range is $6 \leq M_w \leq 8$,
- Rupture distance range is $5 \text{ km} \leq R_{rup} \leq 40 \text{ km}$ and
- Average shear wave velocity to the depth of 30 meters V_{s30} range is $600 \text{ m/s} \leq V_{s30} \leq 850 \text{ m/s}$

Table 3.3 Selected earthquake ground motions from PEER Database

Event	Year	Station	Magnitude	Mechanism	Rjb(km)	Rrup (km)	Vs30 (m/s)
Morgan Hill	1984	Gilroy Array #6	6.19	Strike Slip	9.85	9.87	663.31
Kobe, Japan	1995	Nishi-Akashi	6.9	Strike Slip	7.08	7.08	609
Kocaeli, Turkey	1999	Gebze	7.51	Strike Slip	7.57	10.92	792
Kocaeli, Turkey	1999	Izmit	7.51	Strike Slip	3.62	7.21	811
Duzce, Turkey	1999	Lamont 531	7.14	Strike Slip	8.03	8.03	638.39
Sitka, Alaska	1972	Sitka Observatory	7.68	Strike Slip	34.61	34.61	649.67
Manjil, Iran	1990	Abbar	7.37	Strike Slip	12.55	12.55	723.95
Hector Mine	1999	Hector	7.13	Strike Slip	10.35	11.66	726
Chi-Chi, Taiwan-04	1999	CHY042	6.2	Strike Slip	34.1	34.13	665.2
Chi-Chi, Taiwan-04	1999	CHY086	6.2	Strike Slip	33.63	33.66	665.2
Chi-Chi, Taiwan-04	1999	TCU084	6.2	Strike Slip	26.83	27.13	665.2
Tottori, Japan	2000	OKYH14	6.61	Strike Slip	26.51	26.51	709.86
Tottori, Japan	2000	SMN015	6.61	Strike Slip	9.1	9.12	616.55
Basso Tirreno, Italy	1978	Naso	6	Strike Slip	17.15	19.59	620.56
Darfield, New Zealand	2010	LPCC	7	Strike Slip	25.21	25.67	649.67
Irpinia, Italy-01	1980	Bagnoli Irpinio	6.9	SS+Normal	8.14	8.18	649.67

PEER Database provides ground motion data for both horizontal and vertical components. In this study, only the horizontal components are considered. 5% damped response spectra for each component of selected time histories are obtained by using SeismoSignal Software. After that, these spectra for the related earthquake data are combined with using either SRSS or GeoMean according to the specification concerned.

These spectra of time histories are grouped as SET-1, SET-2 and SET-3 as can be seen in Figure 3.45. Each set has seven ground motion records. In some cases, for a certain earthquake, ground motions recorded from different stations are selected to be used in different ground motion sets.

SET-1				
Earthquake	Max PGA (g)	Magnitude	Fault Type	Vs30 (m/s)
Basso Tirreno	0.640	6.0	SS	620.56
Manjil Abbar	2.530	7.37	SS	723.95
Sitka	0.350	7.68	SS	649.67
Hector	1.480	7.13	SS	726
Tottori 3	1.020	6.61	SS	616.55
Chi Chi 2871	0.240	6.2	SS	665.2
Kocaeli 1165	1.220	7.51	SS	811

SET-2				
Earthquake	Max PGA (g)	Magnitude	Fault Type	Vs30 (m/s)
Morgan Hill-2	1.380	6.19	SS	663.31
Kobe	2.680	6.9	SS	609
Irpiana285	0.590	6.9	SS+Normal	649.67
Tottori-2	1.760	6.61	SS	709.86
Darfield	1.190	7.0	SS	649.67
Kocaeli 1161	0.699	7.51	SS	792
Chi Chi 2712	0.414	6.2	SS	665.2

SET-3				
Earthquake	Max PGA (g)	Magnitude	Fault Type	Vs30 (m/s)
Manjil Abbar	2.530	7.37	SS	723.95
Chi Chi 2742	0.750	6.2	SS	665.2
Düzce 1618	0.810	7.14	SS	638.4
Tottori-2	1.760	6.61	SS	709.86
Basso Tirreno	0.640	6.0	SS	620.56
Tottori 3	1.020	6.61	SS	616.55
Kobe	2.680	6.9	SS	609

Figure 3.45. Ground motion sets to be used in analyses

3.5.2 Scaling Methods of Selected Ground Motion Records

Three scaling methods are used in the scope of this study. First method (Method-1 or M1) is to scale the ground motion records with a single factor according to the mean spectrum of selected earthquakes. Second method (Method-2 or M2) is to scale each ground motion record separately according to the mean spectrum of selected earthquakes without setting any upper limits. Third method (Method-3 or M3) is the same as the second method but the scale factors' upper limit is assigned as 2.

According to the *AASHTO LRFD (2012)*, mean response spectrum of the selected time histories should be scaled in the interval of $0.5T - 2T$, and according to the *Eurocode-8 and Turkish Earthquake Code for Bridges (2020)* scaling should be in the range of $0.2T - 1.5T$ (T is the natural period of the structure).

So for the selected bridges V03, V08 and V14 whose fundamental periods are 1.29s, 1.00s and 0.73s respectively time history records are scaled in the specified period range of specifications, as listed below:

According to the *AASHTO LRFD (2012)*;

- V03 Bridge's period range is 0.65-2.60 sec.
- V08 Bridge's period range is 0.50-2.00 sec.
- V14 Bridge's period range is 0.40-1.45 sec.

According to the *Eurocode-8 and Turkish Earthquake Code for Bridges (2020)*;

- V03 Bridge's period range is 0.25-1.95 sec.
- V08 Bridge's period range is 0.20-1.50 sec.
- V14 Bridge's period range is 0.15-1.10 sec.

Scaling of ground motion records is an iterative procedure which is mainly focused on minimizing the sum of squares errors (SSE) between the related code target spectrum and the spectrum of the ground motions. Firstly, for each ground motion's spectrum square errors are calculated. Then the sum of square errors is obtained by adding the calculated square errors of the selected seven earthquakes from each ground motion sets (as mentioned in 3.4.1). This iterative procedure continues until the mean spectrum minus the code-based target spectrum greater than or equal to zero and the sum of square errors minimizes in the related period range. To illustrate, response spectra of unscaled and scaled time histories for ground motion SET-1 of V03 according to AASHTO LRFD design spectrum are shown in Figure 3.46 and 3.47. Response spectra of unscaled and scaled time histories for each bridge, specification, scaling method and ground motion sets are in the Appendix B.

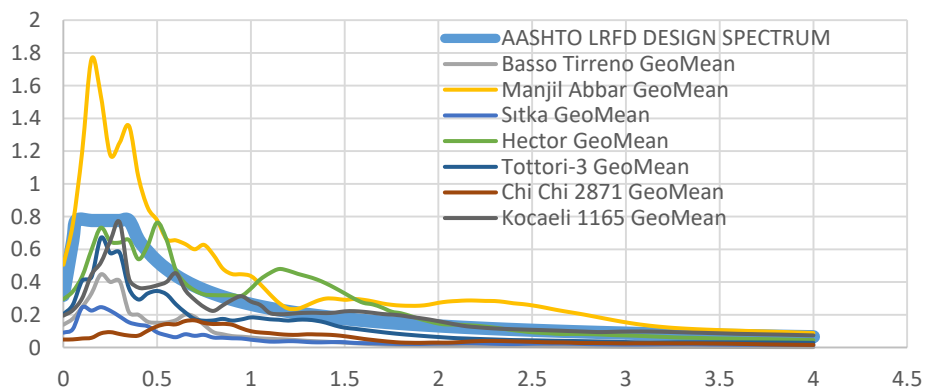


Figure 3.46. AASHTO LRFD design spectrum and response spectrum of unscaled time histories for ground motion SET-1 of V03 Bridge

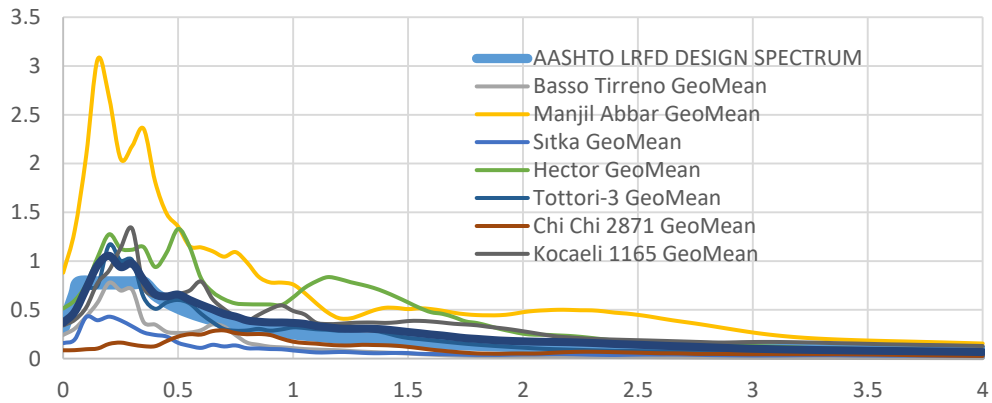


Figure 3.47. AASHTO LRFD design spectrum and response spectrum of scaled time histories with the scaling method M1 for ground motion SET-1 of V03 Bridge

Scaling factors according to these methods are calculated for the constituted three ground motion sets (SET-1,SET-2,SET-3) and the selected three highway bridges having different fundamental periods ($T_n < 1, T_n = 1, T_n > 1$) by employing the design spectra of three bridge design specifications (AASHTO LRFD (2012), Eurocode-8 (2005) and Turkish Earthquake Code for Bridges (2020)). In this way, each specification itself is compared for bridges having different periods using different scale methods. The computed scaling factors are summarize in Tables 3.4-3.12.

In addition, to compare only the specification based scaling criteria for those three methods, the factors are calculated using the same design spectrum for two specifications. Because TDY 2020 and Eurocode-8 have the same scaling criteria, these two codes are compared with the AASHTO LRFD (2012) using its design spectrum.

Table 3.4 Scale factors of bridge V14 (T=0.73 s) for ground motion set “SET-1”

SET-1		Method-1	Method-2	Method-3
BASSO TIREENO	AASHTO LRFD 2012	1.74	4.07	2.00
	EUROCODE 8	1.86	3.37	2.00
	TDY 2020	1.23	2.28	2.00
MANJIL	AASHTO LRFD 2012	1.74	0.89	1.63
	EUROCODE 8	1.86	0.92	1.64
	TDY 2020	1.23	0.60	0.75
SITKA	AASHTO LRFD 2012	1.74	7.24	2.00
	EUROCODE 8	1.86	6.45	2.00
	TDY 2020	1.23	4.28	2.00
HECTOR	AASHTO LRFD 2012	1.74	0.91	1.44
	EUROCODE 8	1.86	1.39	2.00
	TDY 2020	1.23	0.89	1.11
TOTTORI-3	AASHTO LRFD 2012	1.74	2.07	2.00
	EUROCODE 8	1.86	2.14	2.00
	TDY 2020	1.23	1.45	1.75
CHI CHI_2871	AASHTO LRFD 2012	1.74	3.20	2.00
	EUROCODE 8	1.86	5.05	2.00
	TDY 2020	1.23	3.27	2.00
KOCAELI_1165	AASHTO LRFD 2012	1.74	1.46	2.00
	EUROCODE 8	1.86	1.82	2.00
	TDY 2020	1.23	1.22	1.48

Table 3.5 Scale factors of bridge V14 (T=0.73 s) for ground motion set “SET-2”

SET-2		Method-1	Method-2	Method-3
MORGAN_HILL-2	AASHTO LRFD 2012	1.49	1.33	1.68
	EUROCODE 8	1.79	1.33	2.00
	TDY 2020	1.35	1.23	1.28
KOBE	AASHTO LRFD 2012	1.49	0.67	0.96
	EUROCODE 8	1.79	0.81	1.37
	TDY 2020	1.35	0.65	0.67
IRPIANA285	AASHTO LRFD 2012	1.49	1.44	1.84
	EUROCODE 8	1.79	2.66	2.00
	TDY 2020	1.35	1.87	1.92
TOTTORI-2	AASHTO LRFD 2012	1.49	4.87	2.00
	EUROCODE 8	1.79	1.60	2.00
	TDY 2020	1.35	1.53	1.58
DARFIELD	AASHTO LRFD 2012	1.49	2.11	2.00
	EUROCODE 8	1.79	2.10	2.00
	TDY 2020	1.35	1.63	1.69
KOCAELI_1161	AASHTO LRFD 2012	1.49	1.95	2.00
	EUROCODE 8	1.79	2.59	2.00
	TDY 2020	1.35	1.92	2.00
CHI CHI_2712	AASHTO LRFD 2012	1.49	2.92	2.00
	EUROCODE 8	1.79	4.08	2.00
	TDY 2020	1.35	2.85	2.00

Table 3.6 Scale factors of bridge V14 (T=0.73 s) for ground motion set “SET-3”

SET-3		Method-1	Method-2	Method-3
MANJIL	AASHTO LRFD 2012	1.75	0.85	1.95
	EUROCODE 8	1.59	0.90	1.38
	TDY 2020	1.05	0.88	0.88
KOBE	AASHTO LRFD 2012	1.75	0.53	1.05
	EUROCODE 8	1.59	0.71	1.00
	TDY 2020	1.05	0.81	0.81
CHI CHI_2742	AASHTO LRFD 2012	1.75	1.53	2.00
	EUROCODE 8	1.59	2.46	2.00
	TDY 2020	1.05	1.23	1.23
TOTTORI-2	AASHTO LRFD 2012	1.75	5.11	2.00
	EUROCODE 8	1.59	1.78	2.00
	TDY 2020	1.05	1.18	1.18
TOTTORI-3	AASHTO LRFD 2012	1.75	2.50	2.00
	EUROCODE 8	1.59	2.57	2.00
	TDY 2020	1.05	1.39	1.39
BASSO TIREENO	AASHTO LRFD 2012	1.75	3.94	2.00
	EUROCODE 8	1.59	3.01	2.00
	TDY 2020	1.05	1.20	1.20
DUZCE_1618	AASHTO LRFD 2012	1.75	2.23	2.00
	EUROCODE 8	1.59	2.59	2.00
	TDY 2020	1.05	1.27	1.27

Table 3.7 Scale factors of bridge V08 (T=1.00 s) for ground motion set “SET-1”

SET-1		Method-1	Method-2	Method-3
BASSO TIREENO	AASHTO LRFD 2012	1.54	3.33	2.00
	EUROCODE 8	1.97	3.67	2.00
	TDY 2020	1.29	2.47	2.00
MANJIL	AASHTO LRFD 2012	1.54	0.82	1.30
	EUROCODE 8	1.97	1.06	1.91
	TDY 2020	1.29	0.69	0.90
SITKA	AASHTO LRFD 2012	1.54	6.84	2.00
	EUROCODE 8	1.97	7.35	2.00
	TDY 2020	1.29	4.82	2.00
HECTOR	AASHTO LRFD 2012	1.54	0.84	1.15
	EUROCODE 8	1.97	1.28	2.00
	TDY 2020	1.29	0.82	1.84
TOTTORI-3	AASHTO LRFD 2012	1.54	1.91	2.00
	EUROCODE 8	1.97	2.20	2.00
	TDY 2020	1.29	1.48	1.75
CHI CHI_2871	AASHTO LRFD 2012	1.54	3.11	2.00
	EUROCODE 8	1.97	4.87	2.00
	TDY 2020	1.29	3.16	2.00
KOCAELI_1165	AASHTO LRFD 2012	1.54	1.36	1.75
	EUROCODE 8	1.97	1.84	2.00
	TDY 2020	1.29	1.22	1.53

Table 3.8 Scale factors of bridge V08 (T=1.00 s) for ground motion set “SET-2”

SET-2		Method-1	Method-2	Method-3
MORGAN_HILL-2	AASHTO LRFD 2012	1.63	1.18	1.35
	EUROCODE 8	1.89	1.30	2.00
	TDY 2020	1.42	1.04	1.30
KOBE	AASHTO LRFD 2012	1.63	0.64	0.81
	EUROCODE 8	1.89	0.82	1.67
	TDY 2020	1.42	0.62	0.72
IRPIANA285	AASHTO LRFD 2012	1.63	1.44	1.97
	EUROCODE 8	1.89	2.10	2.00
	TDY 2020	1.42	1.48	1.57
TOTTORI-2	AASHTO LRFD 2012	1.63	4.57	2.00
	EUROCODE 8	1.89	3.71	2.00
	TDY 2020	1.42	3.10	2.00
DARFIELD	AASHTO LRFD 2012	1.63	1.88	2.00
	EUROCODE 8	1.89	2.35	2.00
	TDY 2020	1.42	1.77	2.00
KOCAELI_1161	AASHTO LRFD 2012	1.63	1.85	2.00
	EUROCODE 8	1.89	2.57	2.00
	TDY 2020	1.42	1.88	2.00
CHI CHI_2712	AASHTO LRFD 2012	1.63	2.72	2.00
	EUROCODE 8	1.89	4.09	2.00
	TDY 2020	1.42	2.90	2.00

Table 3.9 Scale factors of bridge V08 (T=1.00 s) for ground motion set “SET-3”

SET-3		Method-1	Method-2	Method-3
MANJIL	AASHTO LRFD 2012	1.84	1.13	1.99
	EUROCODE 8	1.96	0.98	2.00
	TDY 2020	1.29	0.65	0.73
KOBE	AASHTO LRFD 2012	1.84	0.72	1.35
	EUROCODE 8	1.96	0.73	1.81
	TDY 2020	1.29	0.49	0.54
CHI CHI_2742	AASHTO LRFD 2012	1.84	1.56	2.00
	EUROCODE 8	1.96	2.38	2.00
	TDY 2020	1.29	1.53	1.71
TOTTORI-2	AASHTO LRFD 2012	1.84	5.56	2.00
	EUROCODE 8	1.96	4.48	2.00
	TDY 2020	1.29	2.93	2.00
TOTTORI-3	AASHTO LRFD 2012	1.84	2.49	2.00
	EUROCODE 8	1.96	2.81	2.00
	TDY 2020	1.29	1.79	2.00
BASSO TIREENO	AASHTO LRFD 2012	1.84	3.76	2.00
	EUROCODE 8	1.96	3.32	2.00
	TDY 2020	1.29	2.31	2.00
DUZCE_1618	AASHTO LRFD 2012	1.84	2.67	2.00
	EUROCODE 8	1.96	2.55	2.00
	TDY 2020	1.29	1.72	1.91

Table 3.10 Scale factors of bridge V03 (T=1.29 s) for ground motion set “SET1”

SET-1		Method-1	Method-2	Method-3
BASSO TIREENO	AASHTO LRFD 2012	1.28	2.87	2.00
	EUROCODE 8	1.58	3.17	2.00
	TDY 2020	1.07	2.19	2.00
MANJIL	AASHTO LRFD 2012	1.28	0.65	0.90
	EUROCODE 8	1.58	0.83	1.28
	TDY 2020	1.07	0.56	0.71
SITKA	AASHTO LRFD 2012	1.28	5.57	2.00
	EUROCODE 8	1.58	6.29	2.00
	TDY 2020	1.07	4.27	2.00
HECTOR	AASHTO LRFD 2012	1.28	0.72	0.90
	EUROCODE 8	1.58	0.94	1.36
	TDY 2020	1.07	0.63	0.77
TOTTORI-3	AASHTO LRFD 2012	1.28	1.71	2.00
	EUROCODE 8	1.58	1.86	2.00
	TDY 2020	1.07	1.28	1.56
CHI CHI_2871	AASHTO LRFD 2012	1.28	2.48	2.00
	EUROCODE 8	1.58	3.65	2.00
	TDY 2020	1.07	2.47	2.00
KOCAELI_1165	AASHTO LRFD 2012	1.28	1.13	1.30
	EUROCODE 8	1.58	1.35	1.91
	TDY 2020	1.07	0.93	1.12

Table 3.11 Scale factors of bridge V03 (T=1.29 s) for ground motion set “SET2”

SET-2		Method-1	Method-2	Method-3
MORGAN_HILL-2	AASHTO LRFD 2012	1.38	0.87	0.93
	EUROCODE 8	1.51	0.82	1.04
	TDY 2020	1.18	0.61	0.63
KOBE	AASHTO LRFD 2012	1.38	0.63	0.74
	EUROCODE 8	1.51	0.82	1.19
	TDY 2020	1.18	0.64	0.69
IRPIANA285	AASHTO LRFD 2012	1.38	0.97	1.15
	EUROCODE 8	1.51	0.99	1.21
	TDY 2020	1.18	0.73	0.75
TOTTORI-2	AASHTO LRFD 2012	1.38	3.73	2.00
	EUROCODE 8	1.51	3.71	2.00
	TDY 2020	1.18	2.87	2.00
DARFIELD	AASHTO LRFD 2012	1.38	1.68	1.95
	EUROCODE 8	1.51	2.33	2.00
	TDY 2020	1.18	1.86	1.99
KOCAELI_1161	AASHTO LRFD 2012	1.38	1.65	2.00
	EUROCODE 8	1.51	1.88	2.00
	TDY 2020	1.18	1.47	1.56
CHI CHI_2712	AASHTO LRFD 2012	1.38	2.71	2.00
	EUROCODE 8	1.51	2.67	2.00
	TDY 2020	1.18	2.06	2.00

Table 3.12 Scale factors of bridge V03 (T=1.29 s) for ground motion set “SET3”

SET-3		Method-1	Method-2	Method-3
MANJIL	AASHTO LRFD 2012	1.53	0.80	1.09
	EUROCODE 8	1.57	0.97	1.34
	TDY 2020	1.07	0.65	0.68
KOBE	AASHTO LRFD 2012	1.53	0.70	1.07
	EUROCODE 8	1.57	0.60	0.89
	TDY 2020	1.07	0.41	0.43
CHI CHI_2742	AASHTO LRFD 2012	1.53	1.44	2.00
	EUROCODE 8	1.57	1.78	2.00
	TDY 2020	1.07	1.21	1.26
TOTTORI-2	AASHTO LRFD 2012	1.53	4.44	2.00
	EUROCODE 8	1.57	3.75	2.00
	TDY 2020	1.07	2.56	2.00
TOTTORI-3	AASHTO LRFD 2012	1.53	2.10	2.00
	EUROCODE 8	1.57	2.07	2.00
	TDY 2020	1.07	1.41	1.50
BASSO TIREENO	AASHTO LRFD 2012	1.53	3.17	2.00
	EUROCODE 8	1.57	2.49	2.00
	TDY 2020	1.07	1.81	1.88
DUZCE_1618	AASHTO LRFD 2012	1.53	2.78	2.00
	EUROCODE 8	1.57	1.86	2.00
	TDY 2020	1.07	1.32	1.37

CHAPTER 4

COMPARISON OF THE SEISMIC DEMAND PARAMETERS FOR DIFFERENT SCALING METHODS AND SCALING CRITERIA

Comparison of the scaling methods and criteria per bridge specification is carried on for pier columns. The maximum moments and column tip displacements in transverse and longitudinal directions are compared. For this purpose 108 analysis models are generated. Modal properties of the three bridges are given in the Tables 1-6 as SAP2000 outputs. For each case, mean value of seismic demands of the seven ground motions are obtained and results are compared according to these mean values.

Table 4.1 Modal load participation ratios of V14 Bridge

OutputCase	ItemType	Item	Static	Dynamic
Text	Text	Text	Percent	Percent
MODAL	Acceleration	UX	100.00	99.98
MODAL	Acceleration	UY	100.00	99.94
MODAL	Acceleration	UZ	99.87	80.00

Table 4.2 Modal participating mass ratios for the first 15 modes of V14 Bridge

OutputCase	StepType	StepNum	Period	UX	UY	UZ
Text	Text	Unitless	Sec	Unitless	Unitless	Unitless
MODAL	Mode	1	0.729	9.59E-01	4.53E-17	5.01E-05
MODAL	Mode	2	0.572	7.13E-17	7.33E-01	4.30E-17
MODAL	Mode	3	0.516	8.42E-06	2.80E-17	7.84E-02
MODAL	Mode	4	0.515	3.64E-17	3.27E-03	1.30E-17
MODAL	Mode	5	0.514	1.78E-17	1.49E-02	2.97E-17
MODAL	Mode	6	0.506	7.80E-04	1.07E-16	5.88E-02
MODAL	Mode	7	0.505	4.40E-04	1.62E-17	5.10E-01
MODAL	Mode	8	0.479	5.45E-17	1.21E-01	8.15E-17
MODAL	Mode	9	0.425	1.81E-18	5.72E-03	2.54E-17
MODAL	Mode	10	0.402	3.22E-07	1.57E-16	6.91E-03
MODAL	Mode	11	0.398	1.33E-05	1.03E-17	3.33E-07
MODAL	Mode	12	0.398	8.32E-07	5.23E-17	3.55E-03
MODAL	Mode	13	0.293	2.99E-03	1.56E-17	3.10E-04
MODAL	Mode	14	0.270	3.32E-16	1.09E-03	5.37E-16
MODAL	Mode	15	0.269	2.85E-16	1.25E-03	2.20E-14

Table 4.3 Modal load participation ratios of V08 Bridge

OutputCase	ItemType	Item	Static	Dynamic
Text	Text	Text	Percent	Percent
MODAL	Acceleration	UX	100.00	100.00
MODAL	Acceleration	UY	100.00	98.25
MODAL	Acceleration	UZ	99.87	73.11

Table 4.4 Modal participating mass ratios for the first 15 modes of V08 Bridge

OutputCase	StepType	StepNum	Period	UX	UY	UZ
Text	Text	Unitless	Sec	Unitless	Unitless	Unitless
MODAL	Mode	1	1.001	4.95E-01	6.92E-08	7.90E-06
MODAL	Mode	2	0.945	2.36E-06	4.38E-01	2.01E-05
MODAL	Mode	3	0.891	1.29E-01	3.00E-04	7.80E-04
MODAL	Mode	4	0.884	6.70E-04	5.79E-02	5.35E-07
MODAL	Mode	5	0.861	9.60E-04	2.12E-01	2.47E-05
MODAL	Mode	6	0.852	2.24E-01	8.10E-04	7.50E-04
MODAL	Mode	7	0.757	3.38E-06	1.11E-03	8.90E-08
MODAL	Mode	8	0.672	1.96E-06	3.40E-04	2.42E-01
MODAL	Mode	9	0.666	3.50E-04	1.60E-04	1.17E-01
MODAL	Mode	10	0.666	4.30E-04	1.30E-04	1.17E-01
MODAL	Mode	11	0.658	4.60E-04	9.19E-07	5.46E-06
MODAL	Mode	12	0.655	8.01E-08	7.47E-03	1.62E-02
MODAL	Mode	13	0.646	4.49E-06	4.90E-04	1.30E-04
MODAL	Mode	14	0.645	8.07E-07	4.13E-03	2.76E-03
MODAL	Mode	15	0.629	3.17E-06	1.40E-04	5.76E-06

Table 4.5 Modal load participation ratios of V03 Bridge

OutputCase	ItemType	Item	Static	Dynamic
Text	Text	Text	Percent	Percent
MODAL	Acceleration	UX	100.00	100.00
MODAL	Acceleration	UY	100.00	99.28
MODAL	Acceleration	UZ	99.78	64.76

Table 4.6 Modal participating mass ratios for the first 15 modes of V03 Bridge

OutputCase	StepType	StepNum	Period	UX	UY	UZ
Text	Text	Unitless	Sec	Unitless	Unitless	Unitless
MODAL	Mode	1	1.290	3.92E-01	6.10E-10	3.14E-07
MODAL	Mode	2	1.249	1.45E-01	3.37E-10	1.17E-06
MODAL	Mode	3	1.209	1.03E-01	2.08E-08	3.56E-05
MODAL	Mode	4	1.202	9.10E-02	2.00E-08	3.93E-05
MODAL	Mode	5	0.940	2.01E-09	3.75E-01	1.17E-06
MODAL	Mode	6	0.932	3.53E-10	7.30E-02	2.44E-07
MODAL	Mode	7	0.883	2.08E-08	1.14E-01	3.30E-07
MODAL	Mode	8	0.880	3.24E-08	1.00E-01	2.98E-07
MODAL	Mode	9	0.835	7.59E-09	1.06E-03	1.07E-09
MODAL	Mode	10	0.824	6.91E-07	2.40E-04	1.63E-09
MODAL	Mode	11	0.691	2.01E-07	6.71E-03	2.17E-06
MODAL	Mode	12	0.690	1.93E-07	6.09E-03	2.29E-06
MODAL	Mode	13	0.652	6.86E-10	1.56E-03	1.27E-02
MODAL	Mode	14	0.651	1.26E-10	4.63E-06	2.23E-05
MODAL	Mode	15	0.644	2.58E-08	3.71E-05	3.24E-01

After the scaling process, horizontal components of time history accelerograms are scaled with the calculated scaling factors and defined as time history functions in SAP2000 (Computers & Structures Inc.,2017) as can be seen from Figure 4.1 to Figure 4.3 as an example for Basso Tirreno earthquake. In the analysis models, time history functions are named with x and y suffixes corresponding to longitudinal and transverse directions respectively. Horizontal components of the unscaled accelerograms of the selected ground motion records are demonstrated in Appendix A.

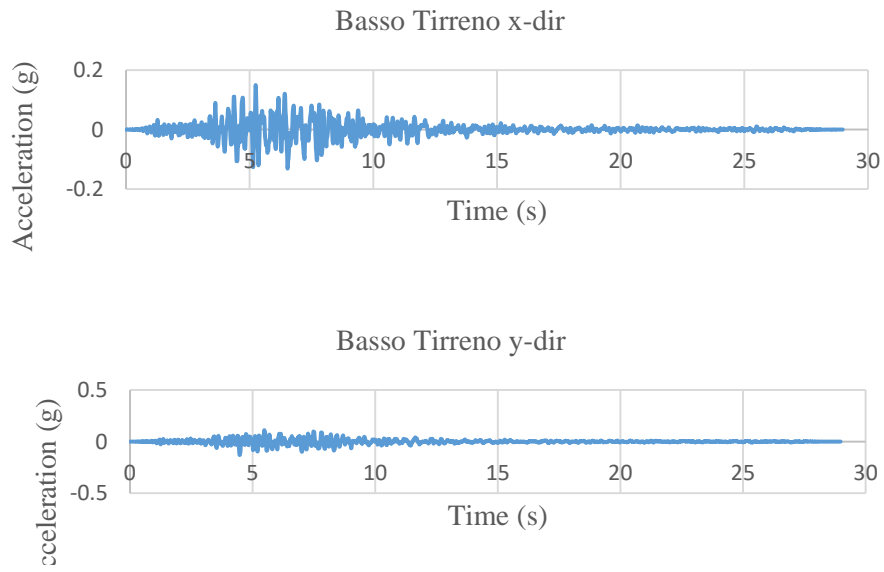


Figure 4.1 Unscaled accelerogram for Basso Tirreno earthquake

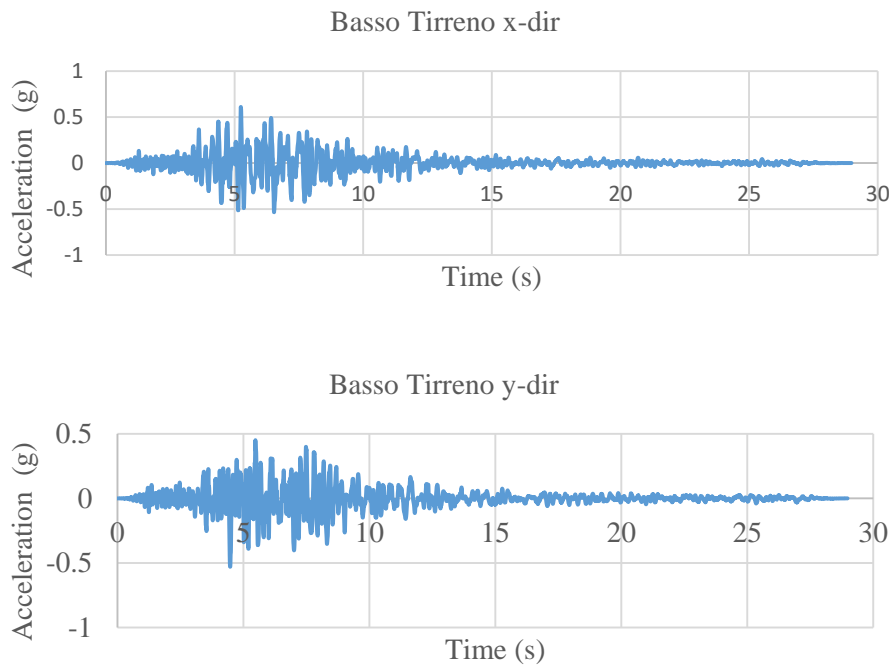


Figure 4.2. Scaled accelerogram for Basso Tirreno earthquake

To account for matching the horizontal directions of ground motions and the horizontal directions of bridge layouts, accelerograms are defined twice by changing the principal directions. These load cases are named by 1 and 2 suffixes. For instance for Basso Tirreno earthquake, Basso Tirreno-1 load case is composed of Basso Tirreno-x function assigned for the bridge longitudinal direction and Basso Tirreno-y function assigned for the bridge transverse direction. Likewise, Basso Tirreno-2 load case is composed of Basso Tirreno-x function assigned for the bridge transverse direction and Basso Tirreno-y function assigned for the bridge longitudinal direction.

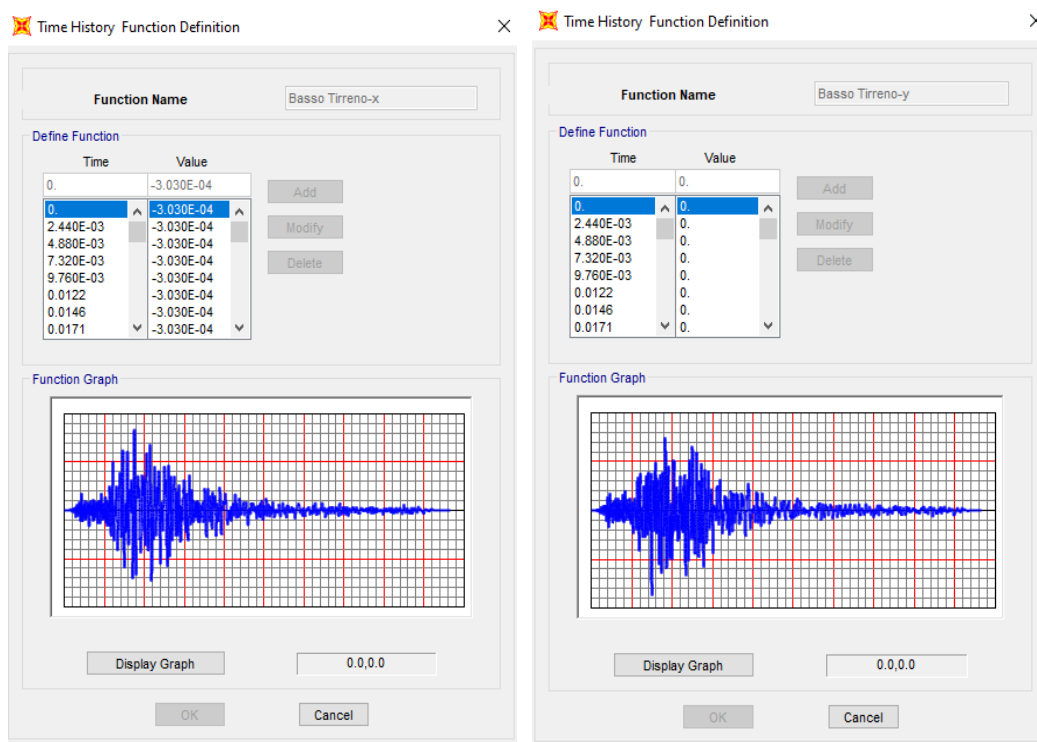


Figure 4.3. An example of time history function definition

4.1 Comparison of Results for V03 Bridge

Before the comparison of the analysis results, first the maximum spectral acceleration values of the mean spectra of the selected set of earthquakes are compared. Mean spectra of the ground motion sets scaled according to three scaling methods (M1, M2 and M3) are shown in Figures 4.4-4.12 per specification. Maximum spectral acceleration values of mean response spectrum of the scaled time histories change both according to specifications and methods. For TDY 2020 design spectrum, maximum S_a resulted in Method-2 conducted on ground motion set SET-2 as 1.42g, while for AASHTO LRFD and EN-8 design spectra, maximum S_a resulted in Method-2 conducted on ground motion set SET-3 as 1.32g and 1.91g, respectively (Table 4.7).

Table 4.7 Maximum spectral acceleration (S_a) values (g)

	AASHTO LRFD			EN-8			TDY		
	M1	M2	M3	M1	M2	M3	M1	M2	M3
SET-1	0.774	0.874	0.801	1.386	1.491	1.429	0.945	1.018	1.008
SET-2	0.860	1.032	0.868	1.371	1.835	1.444	1.068	1.423	1.242
SET-3	1.069	1.322	1.037	1.613	1.911	1.635	1.099	1.310	1.204

Spectral acceleration values at $T=1.29$ sec. (fundamental period of V03) of mean response spectrum of the scaled time histories have different pattern than the maximum values (Table 4.8). For both AASHTO LRFD and TDY design spectrum, the maximum value occurs for Method-1. However, while for AASHTO LRFD SET-1 governs, for TDY SET-2 governs. For EN-8 maximum value occurs for Method-3 on SET-1.

Table 4.8 Spectral acceleration (S_a) values at $T=1.29$ sec. (g)

	AASHTO LRFD			EN-8			TDY		
	M1	M2	M3	M1	M2	M3	M1	M2	M3
SET-1	0.225	0.217	0.221	0.401	0.383	0.408	0.273	0.261	0.275
SET-2	0.218	0.203	0.208	0.378	0.347	0.354	0.295	0.267	0.264
SET-3	0.190	0.200	0.188	0.286	0.279	0.283	0.195	0.191	0.191

The maximum acceleration values (Table 4.7) regardless of the scaling methods in time interval 0-4 seconds based on the selected ground motion sets are sorted as follows per specification:

For AASHTO LRFD: SET-3 > SET-2 > SET-1

For EN-8: SET-3 > SET-2 > SET-1

For TDY 2020: SET-2 > SET-3 > SET-1

To sum up, in time interval 0-4 seconds, Method-2 resulted in the maximum spectral acceleration values for all the three sets and the specifications. However, at the fundamental period of the bridge, Method-1 and Method-3 give the maximum S_a values.

In overall, EN-8 response spectrum scaling and Method-2 give the maximum acceleration values.

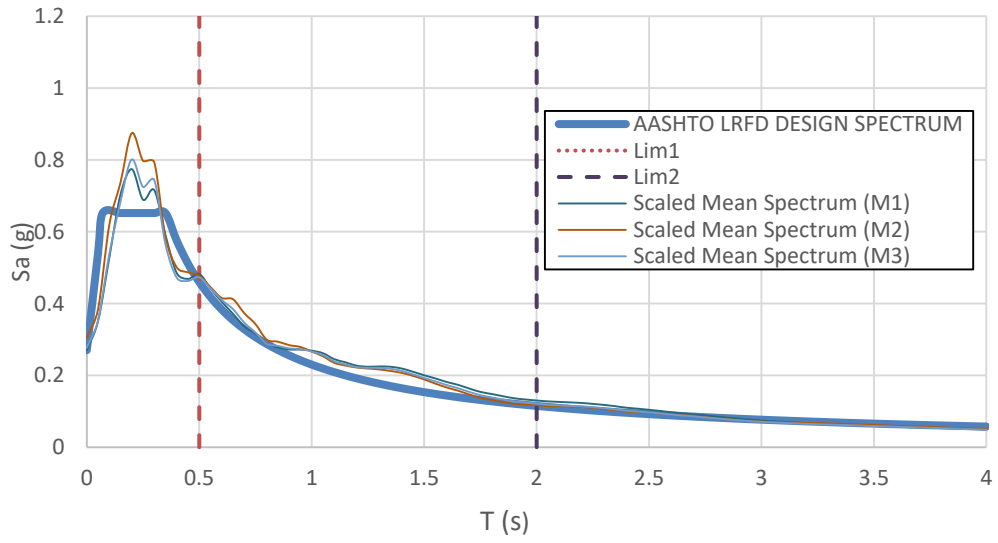


Figure 4.4. Scaled mean spectra for M1,M2 and M3 and AASHTO LRFD design response spectrum for SET-1

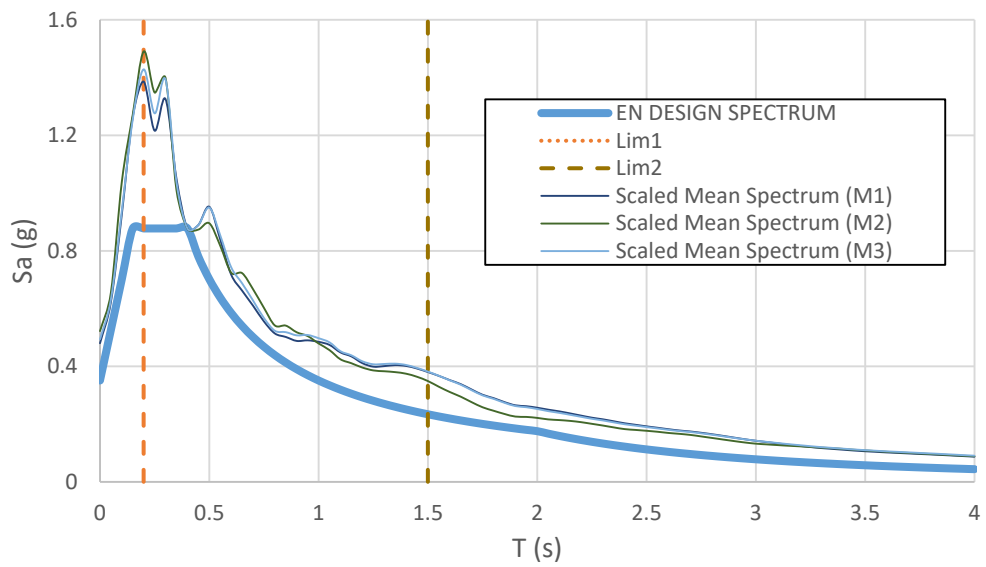


Figure 4.5. Scaled mean spectra for M1,M2 and M3 and EN 8 design response spectrum for SET-1

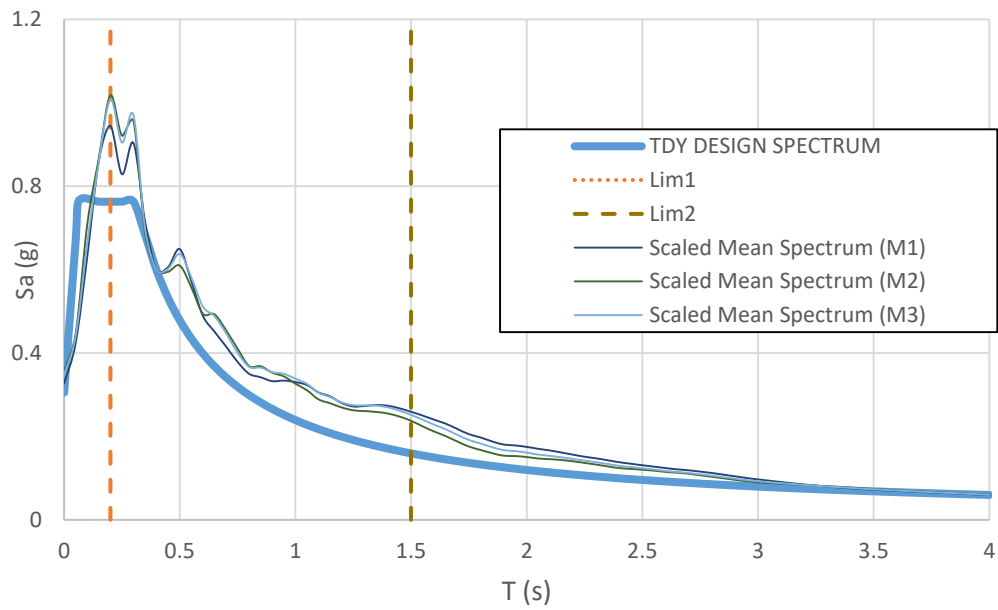


Figure 4.6. Scaled mean spectra for M1,M2 and M3 and TDY design response spectrum for SET-1

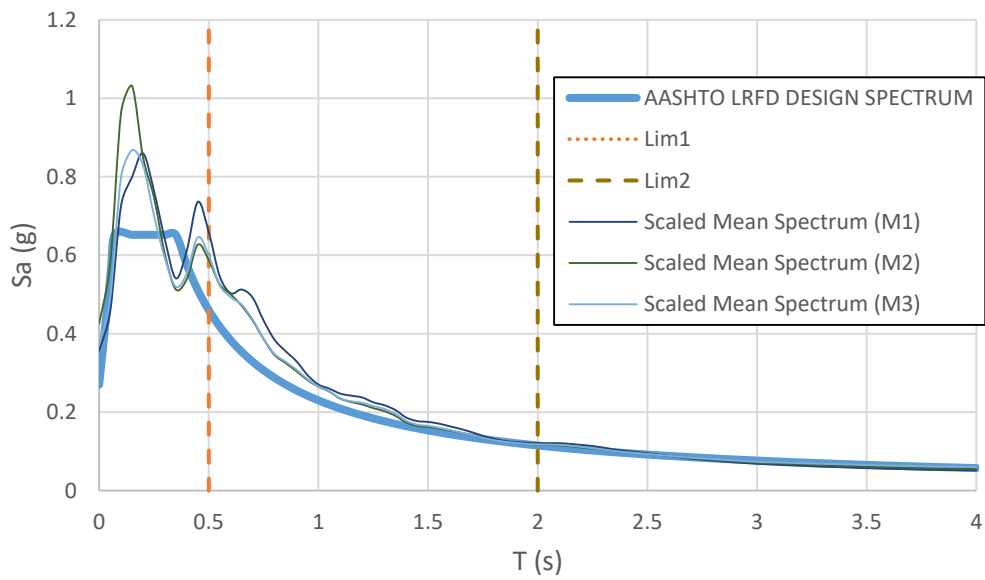


Figure 4.7. Scaled mean spectra for M1,M2 and M3 and AASHTO LRFD design response spectrum for SET-2

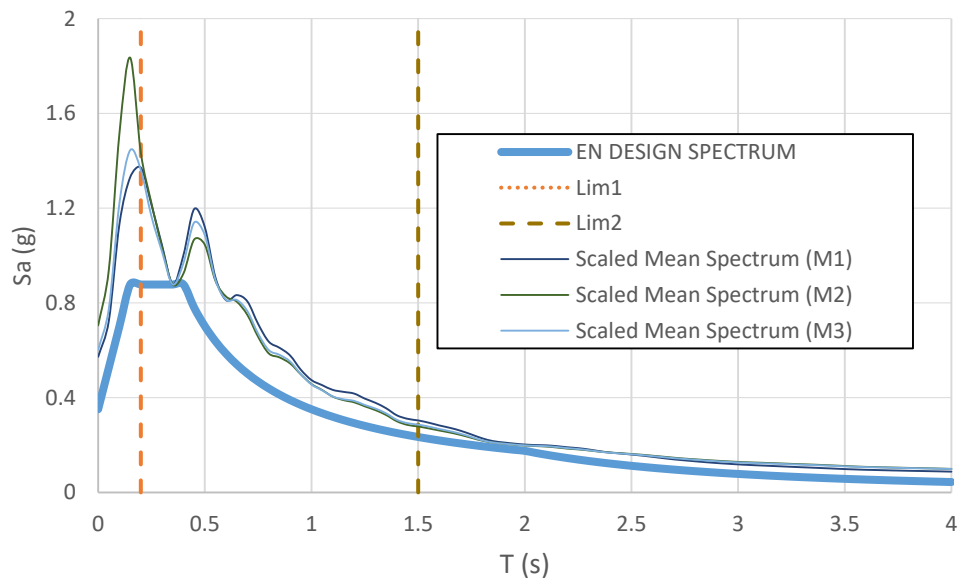


Figure 4.8. Scaled mean spectra for M1,M2 and M3 and EN 8 design response spectrum for SET-2

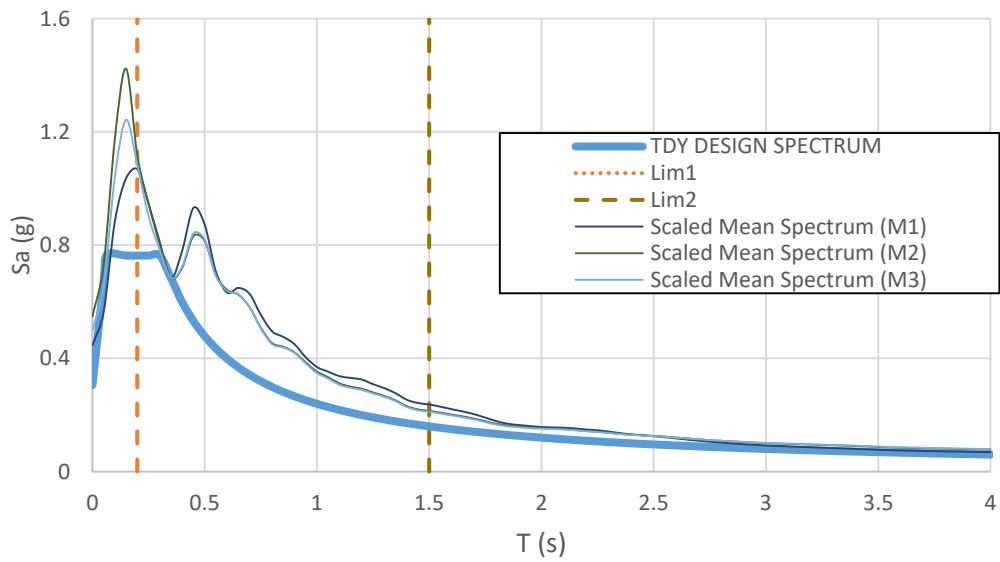


Figure 4.9. Scaled mean spectra for M1,M2 and M3 and TDY design response spectrum for SET-2

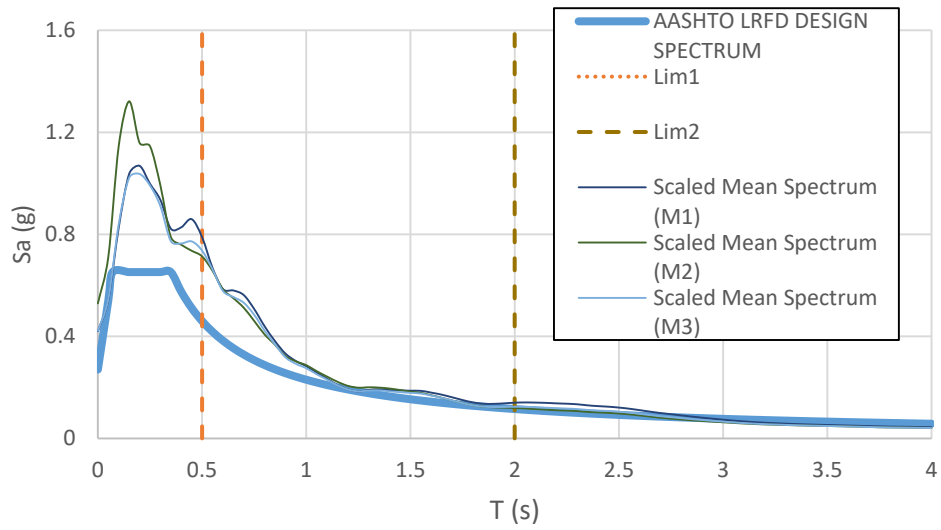


Figure 4.10. Scaled mean spectra for M1,M2 and M3 and AASHTO LRFD design response spectrum for SET-3

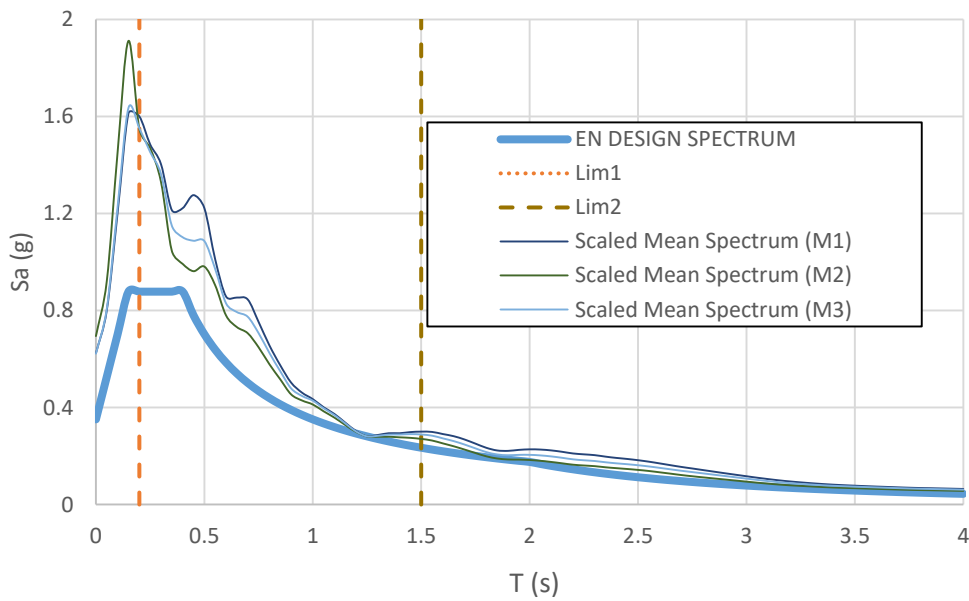


Figure 4.11. Scaled mean spectra for M1,M2 and M3 and EN 8 design response spectrum for SET-3

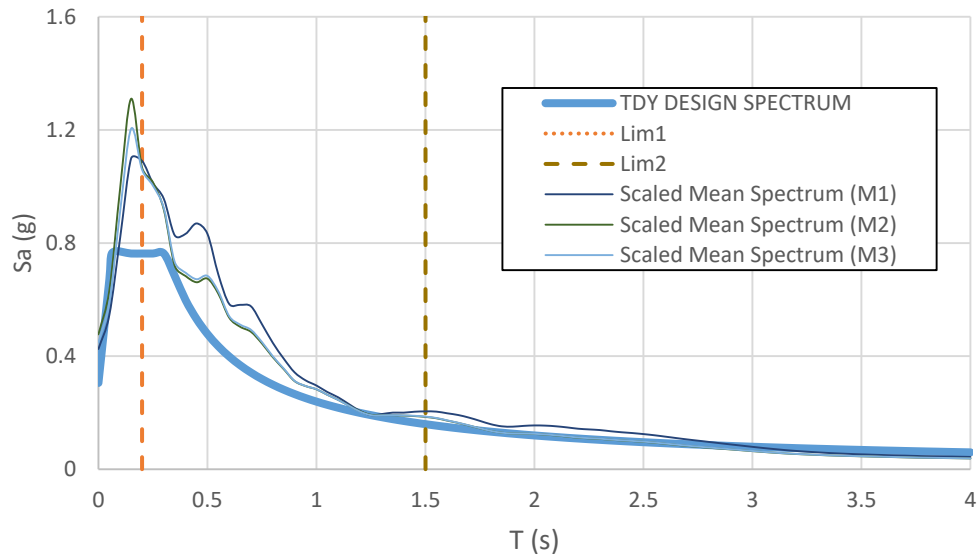


Figure 4.12. Scaled mean spectra for M1,M2 and M3 and TDY design response spectrum for SET-3

Comparison of the analysis results is made both for ground motion set-wise and bridge specification-wise and given in detail in the subsections 4.1.1 to 4.1.4 per scaling method. Although the seismic demand parameters M_x - M_y and u_x - u_y are taken as mean values of seven scaled earthquake ground motions, the results seem to be not strictly dependent on the ratio of the mean spectrum S_a values. For example, as shown in Table 4.8, AASHTO LRFD spectral acceleration values are sorted larger to smaller as SET-1 > SET-2 > SET-3 at $t=1.29$ sec for all of the three scaling methods. On the contrary, moment and displacement values are sorted as SET-3 > SET-2 > SET-1 in transverse direction (M_y), and as SET-2 > SET-3 > SET-1 in longitudinal direction (M_x). For EN-8 and TDY 2020 this comparison is likewise but sorting of sets differs.

This result can be explained with the diversity of the predominant periods of the earthquakes. V03 Bridge has 9 piers and when the seismic demand parameters are compared, it can be seen that dominant earthquakes are different for each pier column. To illustrate, while Sitka earthquake gives the maximum moment and displacement values for pier P2, Tottori earthquake governs for pier P7 in the same analysis with the same set of ground motions.

The change in the mean maximum moment values of the columns for the three bridge specifications is summarized for each scaling methods. Because the specification-wise percentage differences between the three ground motion sets are approximately the same for each pier column, the results are tabulated according to P7 for demonstration in the next subsections 4.1.1, 4.1.2 and 4.1.3. However, ground motion set-wise percentage differences considerably vary for each pier column.

4.1.1 Comparison of Results for Scaling Method-1

In Method-1, while the maximum M_x and M_y values of SET-1 and SET-3 occurs in pier P7, maximum M_y of SET-2 occurs in P2 and maximum M_x of SET-2 occurs in P7.

Sorting of maximum M_y values:

For AASHTO LRFD: SET-3 > SET-2 > SET-1 (88810 > 83817 > 75157) (kN.m)

For EN-8: SET-1 > SET-2 > SET-3 (92641 > 91835 > 91175) (kN.m)

For TDY 2020: SET-2 > SET-1 > SET-3 (71524 > 63133 > 62134) (kN.m)

Sorting of maximum M_x values:

For AASHTO LRFD: SET-2 > SET-3 > SET-1 (99057 > 98761 > 81595) (kN.m)

For EN-8: SET-2 > SET-3 > SET-1 (108533 > 101392 > 100576) (kN.m)

For TDY 2020: SET-2 > SET-3 > SET-1 (84529 > 69096 > 68541) (kN.m)

In Method-1, the maximum u_x and u_y values of SET-1, SET-2 and SET-3 occurs in pier P7 unlike the moment values.

Sorting of maximum u_y values:

For AASHTO LRFD: SET-3 > SET-1 > SET-2 (1.03 > 0.87 > 0.82) cm

For EN-8: SET-1 > SET-3 > SET-2 (1.08 > 1.06 > 0.89) cm

For TDY 2020: SET-1 > SET-3 > SET-2 (0.73 > 0.72 > 0.70) cm

Sorting of maximum u_x values:

For AASHTO LRFD: SET-2 > SET-3 > SET-1 (3.65 > 3.64 > 3.01) cm

For EN-8: SET-2 > SET-3 > SET-1 (4.00 > 3.73 > 3.70) cm

For TDY 2020: SET-2 > SET-3 > SET-1 (3.11 > 2.55 > 2.52) cm

Moment and displacement values are not very close to each other as it can be seen from the given results. When the results are sorted, it can be seen that specifications point to different sets as critical and there is a considerable amount of difference between both M_x, M_y and u_x, u_y values. In addition, sorting of the values is different between the values of moment and displacement. Besides, the lowest values are obtained in scaling according to the TDY 2020. On the other hand, most critical values are computed from scaling according to the EN-8.

Percentage difference given in the Tables 4.10-4.11, 4.7-4.14, 4.16-4.17 and 4.19-4.24 below are calculated based on the following equation;

$$\% = \frac{B-A}{A} \quad (1)$$

A: The result parameter taken as base

B: Compared result parameter

Table 4.9 The maximum M_y values of pier P7 for M1 (kN.m)

	P7-M_y		
	SET-1	SET-2	SET-3
AASHTO LRFD	75157.7	69881.2	88810.8
EN-8	92641.16	76565.94	91175.93
TDY 2020	63133.23	59632.31	62134.71

Table 4.10 Specification-wise percentage differences of M_y values of pier P7 for M1

	Compared with AASHTO LRFD			Compared with EN-8			Compared with TDY 2020		
	SET-1	SET-2	SET-3	SET-1	SET-2	SET-3	SET-1	SET-2	SET-3
AASHTO LRFD	-	-	-	-19%	-9%	-3%	19%	17%	43%
EN-8	23%	10%	3%	-	-	-	47%	28%	47%
TDY 2020	-16%	-15%	-30%	-32%	-22%	-32%	-	-	-

EN-8 gives the largest moment values compared to other codes. TDY2020, on the other hand results in lowest M_y values.

Table 4.11 Ground motion set-wise percentage differences of M_y values of pier P7 for M1

	Compared with SET-1			Compared with SET-2			Compared with SET-3		
	SET-1	SET-2	SET-3	SET-1	SET-2	SET-3	SET-1	SET-2	SET-3
AASHTO LRFD	-	-7%	18%	8%	-	27%	-15%	-21%	-
EN-8	-	-17%	-2%	21%	-	19%	2%	-16%	-
TDY 2020	-	-6%	-2%	6%	-	4%	2%	-4%	-

Table 4.12 The maximum M_x values of pier P7 for M1 (kN.m)

	P7-M_x		
	SET-1	SET-2	SET-3
AASHTO LRFD	81595.47	99057.88	98761.96
EN-8	108533.6	108533.6	101392.1
TDY 2020	68541.03	84529.89	69096.84

Table 4.13 Specification-wise percentage differences of M_x values of pier P7 for M1

	Compared with AASHTO LRFD			Compared with EN-8			Compared with TDY 2020		
	SET-1	SET-2	SET-3	SET-1	SET-2	SET-3	SET-1	SET-2	SET-3
AASHTO LRFD	-	-	-	-25%	-9%	-3%	19%	17%	43%
EN-8	33%	10%	3%	-	-	-	58%	28%	47%
TDY 2020	-16%	-15%	-30%	-37%	-22%	-32%	-	-	-

EN-8 gives the largest moment values compared to other codes. TDY2020, on the other hand results in lowest M_x values.

Table 4.14 Ground motion set-wise percentage differences of M_x values of pier P7 for M1

	Compared with SET-1			Compared with SET-2			Compared with SET-3		
	SET-1	SET-2	SET-3	SET-1	SET-2	SET-3	SET-1	SET-2	SET-3
AASHTO LRFD	-	21%	21%	-18%	-	0%	-17%	0%	-
EN-8	-	0%	-7%	0%	-	-6%	7%	7%	-
TDY 2020	-	23%	1%	-19%	-	-18%	-1%	22%	-

Table 4.15 The maximum u_y values of pier P7 for M1 (m)

	P7- u_y		
	SET-1	SET-2	SET-3
AASHTO	0.0087	0.0082	0.0103
EN	0.0089	0.0089	0.0106
TDY	0.0073	0.0070	0.0072

Table 4.16 Specification-wise percentage differences of u_y values of pier P7 for M1

	Compared with AASHTO LRFD			Compared with EN-8			Compared with TDY 2020		
	SET-1	SET-2	SET-3	SET-1	SET-2	SET-3	SET-1	SET-2	SET-3
AASHTO	-	-	-	-2%	-9%	-3%	19%	17%	43%
EN	2%	10%	3%	-	-	-	22%	28%	47%
TDY	-16%	-15%	-30%	-18%	-22%	-32%	-	-	-

EN-8 gives the largest moment values compared to other codes. TDY2020, on the other hand results in lowest u_y values.

Table 4.17 Ground motion set-wise percentage differences of u_y values of pier P7 for M1

	Compared with SET-1			Compared with SET-2			Compared with SET-3		
	SET-1	SET-2	SET-3	SET-1	SET-2	SET-3	SET-1	SET-2	SET-3
AASHTO	-	-7%	18%	7%	-	27%	-15%	-21%	-
EN	-	0%	19%	0%	-	18.54%	-16%	-16%	-
TDY	-	-5%	-2%	5%	-	4%	2%	-4%	-

Table 4.18 The maximum u_x values of pier P7 for M1 (m)

	P7-u_x		
	SET-1	SET-2	SET-3
AASHTO	0.030	0.036	0.036
EN	0.037	0.040	0.037
TDY	0.025	0.031	0.025

Table 4.19 Specification-wise percentage differences of u_x values of pier P7 for M1

	Compared with AASHTO LRFD			Compared with EN-8			Compared with TDY 2020		
	SET-1	SET-2	SET-3	SET-1	SET-2	SET-3	SET-1	SET-2	SET-3
AASHTO	-	-	-	-19%	-9%	-3%	19%	17%	43%
EN	23%	10%	3%	-	-	-	47%	28%	47%
TDY	-16%	-15%	-30%	-32%	-22%	-32%	-	-	-

EN-8 gives the largest moment values compared to other codes. TDY2020, on the other hand results in lowest u_x values.

Table 4.20 Ground motion set-wise percentage differences of u_x values of pier P7 for M1

	Compared with SET-1			Compared with SET-2			Compared with SET-3		
	SET-1	SET-2	SET-3	SET-1	SET-2	SET-3	SET-1	SET-2	SET-3
AASHTO	-	21%	21%	-18%	-	0%	-17%	0%	-
EN	-	8%	1%	-7%	-	-7%	-1%	7%	-
TDY	-	23%	1%	-19%	-	-18%	-1%	22%	-

Table 4.21 Ground motion set-wise percentage differences of M_y values of all pier columns for M1

		Compared with SET-1			Compared with SET-2			Compared with SET-3		
		SET-1	SET-2	SET-3	SET-1	SET-2	SET-3	SET-1	SET-2	SET-3
P1- M_y	AASHTO	-	31%	38%	-24%	-	6%	-28%	-5%	-
	EN	-	16%	15%	-14%	-	-1%	-13%	1%	-
	TDY	-	33%	15%	-25%	-	-13%	-13%	15%	-
P2- M_y	AASHTO	-	88%	90%	-47%	-	1%	-47%	-1%	-
	EN	-	67%	58%	-40%	-	-5%	-37%	6%	-
	TDY	-	91%	58%	-48%	-	-17%	-37%	21%	-
P3- M_y	AASHTO	-	9%	33%	-8%	-	21%	-25%	-18%	-
	EN	-	-3%	10%	3%	-	14%	-9%	-12%	-
	TDY	-	11%	10%	-10%	-	-1%	-9%	1%	-
P4- M_y	AASHTO	-	8%	32%	-8%	-	22%	-24%	-18%	-
	EN	-	-4%	10%	4%	-	14%	-9%	-12%	-
	TDY	-	10%	10%	-9%	-	0%	-9%	0%	-
P5- M_y	AASHTO	-	14%	25%	-13%	-	9%	-20%	-8%	-
	EN	-	2%	4%	-2%	-	2%	-4%	-2%	-
	TDY	-	16%	4%	-14%	-	-11%	-4%	12%	-
P6- M_y	AASHTO	-	10%	23%	-9%	-	12%	-19%	-11%	-
	EN	-	-2%	3%	2%	-	5%	-3%	-5%	-
	TDY	-	12%	3%	-11%	-	-8%	-3%	9%	-
P7- M_y	AASHTO	-	-7%	18%	8%	-	27%	-15%	-21%	-
	EN	-	-17%	-2%	21%	-	19%	2%	-16%	-
	TDY	-	-6%	-2%	6%	-	4%	2%	-4%	-
P8- M_y	AASHTO	-	14%	24%	-12%	-	9%	-19%	-8%	-
	EN	-	1%	3%	-1%	-	2%	-3%	-2%	-
	TDY	-	15%	3%	-13%	-	-11%	-3%	12%	-
P9- M_y	AASHTO	-	55%	55%	-35%	-	0%	-35%	0%	-
	EN	-	38%	29%	-27%	-	-7%	-22%	7%	-
	TDY	-	57%	29%	-36%	-	-18%	-22%	22%	-

For most cases, SET-3 gives largest results for M_y whereas SET-1 results are generally smallest.

Table 4.22 Ground motion set-wise percentage differences of M_x values of all pier columns for M1

		Compared with SET-1			Compared with SET-2			Compared with SET-3		
		SET-1	SET-2	SET-3	SET-1	SET-2	SET-3	SET-1	SET-2	SET-3
P1- M_x	AASHTO	-	-7%	16%	8%	-	25%	-14%	-20%	-
	EN	-	-18%	-3%	21%	-	18%	3%	-15%	-
	TDY	-	-6%	-3%	6%	-	3%	3%	-3%	-
P2- M_x	AASHTO	-	-16%	16%	20%	-	38%	-14%	-28%	-
	EN	-	-26%	-4%	35%	-	30%	4%	-23%	-
	TDY	-	-15%	-4%	18%	-	13%	4%	-12%	-
P3- M_x	AASHTO	-	0%	14%	0%	-	14%	-12%	-13%	-
	EN	-	-11%	-5%	13%	-	7%	5%	-7%	-
	TDY	-	1%	-5%	-1%	-	-6%	5%	7%	-
P4- M_x	AASHTO	-	0%	14%	0%	-	14%	-12%	-12%	-
	EN	-	-11%	-5%	13%	-	7%	5%	-7%	-
	TDY	-	1%	-5%	-1%	-	-6%	5%	7%	-
P5- M_x	AASHTO	-	-9%	6%	10%	-	16%	-5%	-14%	-
	EN	-	-19%	-12%	24%	-	9%	14%	-8%	-
	TDY	-	-8%	-12%	8%	-	-5%	14%	5%	-
P6- M_x	AASHTO	-	-1%	8%	1%	-	8%	-7%	-8%	-
	EN	-	-12%	-10%	13%	-	2%	11%	-2%	-
	TDY	-	1%	-10%	-1%	-	-11%	11%	12%	-
P7- M_x	AASHTO	-	21%	21%	-18%	-	0%	-17%	0%	-
	EN	-	0%	-7%	0%	-	-7%	7%	7%	-
	TDY	-	23%	1%	-19%	-	-18%	-1%	22%	-
P8- M_x	AASHTO	-	-10%	5%	11%	-	17%	-5%	-14%	-
	EN	-	-12%	-12%	14%	-	0%	14%	0%	-
	TDY	-	-9%	-12%	9%	-	-4%	14%	4%	-
P9- M_x	AASHTO	-	4%	27%	-4%	-	21%	-21%	-18%	-
	EN	-	-7%	6%	8%	-	14%	-5%	-12%	-
	TDY	-	6%	6%	-6%	-	0%	-5%	0%	-

For most cases, SET-3 gives largest results for M_x whereas SET-2 results are generally smallest.

Table 4.23 Ground motion set-wise percentage differences of u_y values of all pier columns for M1

		Compared with SET-1			Compared with SET-2			Compared with SET-3		
		SET-1	SET-2	SET-3	SET-1	SET-2	SET-3	SET-1	SET-2	SET-3
P1- u_y	AASHTO	-	31%	38%	-24%	-	6%	-28%	-5%	-
	EN	-	16%	15%	-14%	-	-1%	-13%	1%	-
	TDY	-	33%	15%	-25%	-	-13%	-13%	16%	-
P2- u_y	AASHTO	-	88%	89%	-47%	-	1%	-47%	-1%	-
	EN	-	67%	58%	-40%	-	-6%	-37%	6%	-
	TDY	-	91%	58%	-48%	-	-17%	-37%	21%	-
P3- u_y	AASHTO	-	9%	32%	-9%	-	21%	-24%	-17%	-
	EN	-	-3%	10%	3%	-	13%	-9%	-12%	-
	TDY	-	11%	10%	-10%	-	-1%	-9%	1%	-
P4- u_y	AASHTO	-	9%	32%	-8%	-	21%	-24%	-18%	-
	EN	-	-3%	10%	3%	-	14%	-9%	-12%	-
	TDY	-	10%	10%	-9%	-	-1%	-9%	1%	-
P5- u_y	AASHTO	-	15%	25%	-13%	-	9%	-20%	-8%	-
	EN	-	2%	4%	-2%	-	2%	-4%	-2%	-
	TDY	-	17%	4%	-14%	-	-11%	-4%	12%	-
P6- u_y	AASHTO	-	11%	23%	-10%	-	11%	-19%	-10%	-
	EN	-	-2%	3%	2%	-	4%	-3%	-4%	-
	TDY	-	12%	3%	-11%	-	-9%	-3%	10%	-
P7- u_y	AASHTO	-	-7%	18%	7%	-	27%	-15%	-21%	-
	EN	-	0%	19%	0%	-	19%	-16%	-16%	-
	TDY	-	-5%	-2%	5%	-	4%	2%	-4%	-
P8- u_y	AASHTO	-	14%	24%	-12%	-	9%	-19%	-8%	-
	EN	-	3%	3%	-3%	-	0%	-3%	0%	-
	TDY	-	16%	3%	-14%	-	-11%	-3%	12%	-
P9- u_y	AASHTO	-	56%	55%	-36%	-	0%	-35%	0%	-
	EN	-	38%	29%	-28%	-	-7%	-22%	7%	-
	TDY	-	58%	29%	-37%	-	-18%	-22%	23%	-

For most cases, SET-3 gives largest results for u_y whereas SET-1 results are generally smallest.

Table 4.24 Ground motion set-wise percentage differences of u_x values of all pier columns for M1

		Compared with SET-1			Compared with SET-2			Compared with SET-3		
		SET-1	SET-2	SET-3	SET-1	SET-2	SET-3	SET-1	SET-2	SET-3
P1- u_x	AASHTO	-	-7%	16%	8%	-	25%	-14%	-20%	-
	EN	-	-17%	-3%	21%	-	18%	3%	-15%	-
	TDY	-	-6%	-3%	6%	-	3%	3%	-3%	-
P2- u_x	AASHTO	-	-16%	16%	20%	-	38%	-14%	-28%	-
	EN	-	-26%	-4%	34%	-	29%	4%	-23%	-
	TDY	-	-15%	-4%	18%	-	13%	4%	-12%	-
P3- u_x	AASHTO	-	0%	14%	0%	-	14%	-12%	-13%	-
	EN	-	-11%	-5%	13%	-	7%	5%	-7%	-
	TDY	-	1%	-5%	-1%	-	-6%	5%	7%	-
P4- u_x	AASHTO	-	0%	14%	0%	-	14%	-12%	-12%	-
	EN	-	-11%	-5%	13%	-	7%	5%	-7%	-
	TDY	-	1%	-5%	-1%	-	-6%	5%	7%	-
P5- u_x	AASHTO	-	-9%	6%	10%	-	16%	-5%	-14%	-
	EN	-	-19%	-12%	24%	-	9%	14%	-8%	-
	TDY	-	-8%	-12%	8%	-	-5%	14%	5%	-
P6- u_x	AASHTO	-	-1%	8%	1%	-	8%	-7%	-8%	-
	EN	-	-12%	-10%	13%	-	2%	11%	-2%	-
	TDY	-	1%	-10%	-1%	-	-11%	11%	12%	-
P7- u_x	AASHTO	-	21%	21%	-18%	-	0%	-17%	0%	-
	EN	-	8%	1%	-7%	-	-7%	-1%	7%	-
	TDY	-	23%	1%	-19%	-	-18%	-1%	22%	-
P8- u_x	AASHTO	-	-10%	5%	11%	-	17%	-5%	-14%	-
	EN	-	-20%	-13%	25%	-	9%	14%	-8%	-
	TDY	-	-8%	-13%	9%	-	-4%	14%	5%	-
P9- u_x	AASHTO	-	4%	27%	-4%	-	22%	-21%	-18%	-
	EN	-	-7%	6%	8%	-	14%	-5%	-12%	-
	TDY	-	6%	6%	-6%	-	0%	-5%	0%	-

For most cases, SET-3 gives largest results for u_x whereas SET-2 results are generally smallest.

4.1.2 Comparison of Results for Scaling Method-2

In Method-2, the maximum M_y values of SET-1 occur in pier P7 and the maximum M_x values of SET-1 occur in pier P2. In contrast, the maximum M_y values of SET-2 occur in pier P2 and the maximum M_x values of SET-2 occur in pier P7. The maximum values of M_x and M_y of SET-3 occur in pier P2.

Sorting of maximum M_y values:

For AASHTO LRFD: SET-3 > SET-2 > SET-1 (147076 > 122326 > 86906) (kN.m)

For EN-8: SET-2 > SET-3 > SET-1 (128898 > 128353 > 103340) (kN.m)

For TDY 2020: SET-2 > SET-3 > SET-1 (99208 > 87893 > 70556) (kN.m)

Sorting of maximum M_x values:

For AASHTO LRFD: SET-3 > SET-2 > SET-1 (105152 > 84493 > 81703) (kN.m)

For EN-8: SET-1 > SET-3 > SET-2 (97002 > 93527 > 91302) (kN.m)

For TDY 2020: SET-2 > SET-1 > SET-3 (70151 > 66237 > 64492) (kN.m)

In Method-2, the maximum u_x and u_y values of SET-1 and SET-3 occur in pier P7. The maximum u_x values of SET-2 occur in pier P7 while the maximum u_y values occur in pier P2.

Sorting of maximum u_y values:

For AASHTO LRFD: SET-3 > SET-1 > SET-2 (1.23 > 1.01 > 0.89) (cm)

For EN-8: SET-1 > SET-3 > SET-2 (1.20 > 1.11 > 0.94) (cm)

For TDY 2020: SET-1 > SET-3 > SET-2 (0.82 > 0.76 > 0.72) (cm)

Sorting of maximum u_x values:

For AASHTO LRFD: SET-3 > SET-2>SET-1 (3.71> 3.11> 2.95) (cm)

For EN-8: SET-1>SET-2> SET-1 (3.53> 3.36> 3.31) (cm)

For TDY 2020: SET-2> SET-1>SET-3 (2.58> 2.41> 2.28) (cm)

Moment and displacement values are not close to each other. The different sets for specific specification show different results to each other. The most critical moment and displacement value comes from AASHTO LRFD, however in average between sets, Eurocode-8 is more critical than the other specifications. TDY 2020 is least critical in terms of results as in the Method-1.

Percentage difference given in the Tables 4.26-4.27, 4.29-4.30, 4.32-4.33 and 4.35-4.40 below are calculated based on the Equation 1.

Table 4.25 The maximum M_y values of pier P7 for M2 (kN.m)

	P7-M_y		
	SET-1	SET-2	SET-3
AASHTO LRFD	86906.83	69090.53	105914.2
EN-8	103340.3	74320.56	95480.86
TDY 2020	70556.23	57202.01	65679.34

Table 4.26 Specification-wise percentage differences of M_y values of pier P7 for M2

	Compared with AASHTO LRFD			Compared with EN-8			Compared with TDY 2020		
	SET-1	SET-2	SET-3	SET-1	SET-2	SET-3	SET-1	SET-2	SET-3
AASHTO LRFD	-	-	-	-16%	-7%	11%	23%	21%	61%
EN-8	19%	8%	-9 %	-	-	-	46%	30%	45%
TDY 2020	-19%	-17%	-38%	-32%	-23%	-31%	-	-	-

EN-8 gives the largest moment values compared to other codes. TDY2020, on the other hand results in lowest M_y values like in Method-1.

Table 4.27 Ground motion set-wise percentage differences of M_y values of pier P7 for M2

	Compared with SET-1			Compared with SET-2			Compared with SET-3		
	SET-1	SET-2	SET-3	SET-1	SET-2	SET-3	SET-1	SET-2	SET-3
AASHTO LRFD	-	-21%	22%	26%	-	53%	-18%	-35%	-
EN-8	-	-28%	-8%	39%	-	28%	8%	-22%	-
TDY 2020	-	-19%	-7%	23%	-	15%	7%	-13%	-

Table 4.28 The maximum M_x values of pier P7 for M2 (kN.m)

	P7-M_x		
	SET-1	SET-2	SET-3
AASHTO LRFD	80081.45	84493.08	100730.9
EN-8	91302.34	91302.34	89910.34
TDY 2020	65511.68	70151.21	61838.24

Table 4.29 Specification-wise percentage differences of M_x values of pier P7 for M2

	Compared with AASHTO LRFD			Compared with EN-8			Compared with TDY 2020		
	SET-1	SET-2	SET-3	SET-1	SET-2	SET-3	SET-1	SET-2	SET-3
AASHTO LRFD	-	-	-	-12%	-7%	12%	22%	20%	63%
EN-8	14%	8%	-11%	-	-	-	39%	30%	45%
TDY 2020	-18%	-17%	-39%	-28%	-23%	-31%	-	-	-

EN-8 gives the largest moment values compared to other codes. TDY2020, on the other hand results in lowest M_x values like Method-1.

Table 4.30 Ground motion set-wise percentage differences of M_x values of pier P7 for M2

	Compared with SET-1			Compared with SET-2			Compared with SET-3		
	SET-1	SET-2	SET-3	SET-1	SET-2	SET-3	SET-1	SET-2	SET-3
AASHTO LRFD	-	6%	26%	-5%	-	19%	-20%	-16%	-
EN-8	-	0%	-2%	0%	-	-2%	2%	2%	-
TDY	-	7%	-6%	-7%	-	-12%	6%	13%	-

Table 4.31 The maximum u_y values of pier P7 for M2 (m)

	P7- u_y		
	SET-1	SET-2	SET-3
AASHTO	0.0101	0.0081	0.0123
EN	0.0087	0.0087	0.0111
TDY	0.0082	0.0067	0.0076

Table 4.32 Specification-wise percentage differences of u_y values of pier P7 for M2

	Compared with AASHTO LRFD			Compared with EN-8			Compared with TDY 2020		
	SET-1	SET-2	SET-3	SET-1	SET-2	SET-3	SET-1	SET-2	SET-3
AASHTO	-	-	-	17%	-7%	11%	23%	21%	61%
EN	-14%	8%	-10%	-	-	-	6%	30%	45%
TDY	-19%	-17%	-38%	-5%	-23%	-31%	-	-	-

EN-8 gives the largest displacement values compared to other codes by employing the SET-1 and SET-3 while AASHTO LRFD gives the largest values by employing the SET-2. TDY2020, on the other hand results in lowest u_y values like in Method-1.

Table 4.33 Ground motion set-wise percentage differences of u_y values of pier P7 for M2

	Compared with SET-1			Compared with SET-2			Compared with SET-3		
	SET-1	SET-2	SET-3	SET-1	SET-2	SET-3	SET-1	SET-2	SET-3
AASHTO	-	6%	26%	-5%	-	19%	-21%	-16%	-
EN	-	-5%	-6%	5%	-	-2%	7%	2%	-
TDY	-	7%	-6%	-7%	-	-12%	6%	13%	-

Table 4.34 The maximum u_x values of pier P7 for M2 (m)

	P7-u_x		
	SET-1	SET-2	SET-3
AASHTO	0.0295	0.0311	0.0371
EN	0.0354	0.0336	0.0331
TDY	0.0241	0.0258	0.0228

Table 4.35 Specification-wise percentage differences of u_x values of pier P7 for M2

	Compared with AASHTO LRFD			Compared with EN-8			Compared with TDY 2020		
	SET-1	SET-2	SET-3	SET-1	SET-2	SET-3	SET-1	SET-2	SET-3
AASHTO	-	-	-	-17%	-7%	12%	22%	20%	63%
EN	20%	8%	-11%	-	-	-	47%	30%	45%
TDY	-18%	-17%	-39%	-32%	-23%	-31%	-	-	-

EN-8 gives the largest displacement values compared to other codes. TDY2020, on the other hand results in lowest u_x values like Method-1.

Table 4.36 Ground motion set-wise percentage differences of u_x values of pier P7 for M2

	Compared with SET-1			Compared with SET-2			Compared with SET-3		
	SET-1	SET-2	SET-3	SET-1	SET-2	SET-3	SET-1	SET-2	SET-3
AASHTO	-	6%	26%	-5%	-	19%	-21%	-16%	-
EN	-	-5%	-6%	5%	-	-2%	7%	2%	-
TDY	-	7%	-6%	-7%	-	-12%	6%	13%	-

Table 4.37 Ground motion set-wise percentage differences of M_y values of all pier columns for M2

		Compared with SET-1			Compared with SET-2			Compared with SET-3		
		SET-1	SET-2	SET-3	SET-1	SET-2	SET-3	SET-1	SET-2	SET-3
P1- M_y	AASHTO	-	37%	63%	-27%	-	19%	-38%	-16%	-
	EN	-	21%	21%	-17%	-	0%	-18%	0%	-
	TDY	-	37%	22%	-27%	-	-11%	-18%	12%	-
P2- M_y	AASHTO	-	137%	185%	-58%	-	20%	-65%	-17%	-
	EN	-	108%	107%	-52%	-	0%	-52%	0%	-
	TDY	-	134%	108%	-57%	-	-11%	-52%	13%	-
P3- M_y	AASHTO	-	24%	67%	-19%	-	35%	-40%	-26%	-
	EN	-	10%	24%	-9%	-	13%	-20%	-12%	-
	TDY	-	24%	25%	-20%	-	1%	-20%	-1%	-
P4- M_y	AASHTO	-	24%	67%	-19%	-	35%	-40%	-26%	-
	EN	-	10%	24%	-9%	-	13%	-19%	-11%	-
	TDY	-	24%	25%	-19%	-	1%	-20%	-1%	-
P5- M_y	AASHTO	-	4%	39%	-4%	-	33%	-28%	-25%	-
	EN	-	-7%	3%	7%	-	10%	-3%	-9%	-
	TDY	-	5%	4%	-5%	-	-1%	-4%	1%	-
P6- M_y	AASHTO	-	-2%	33%	2%	-	36%	-25%	-27%	-
	EN	-	-12%	0%	14%	-	13%	0%	-12%	-
	TDY	-	-1%	1%	1%	-	2%	-1%	-2%	-
P7- M_y	AASHTO	-	-21%	22%	26%	-	53%	-18%	-35%	-
	EN	-	-28%	-8%	39%	-	28%	8%	-22%	-
	TDY	-	-19%	-7%	23%	-	15%	7%	-13%	-
P8- M_y	AASHTO	-	1%	34%	-1%	-	33%	-25%	-25%	-
	EN	-	-11%	0%	12%	-	12%	0%	-11%	-
	TDY	-	0%	1%	0%	-	1%	-1%	-1%	-
P9- M_y	AASHTO	-	73%	100%	-42%	-	16%	-50%	-13%	-
	EN	-	52%	47%	-34%	-	-4%	-32%	4%	-
	TDY	-	72%	48%	-42%	-	-14%	-32%	17%	-

For most cases, SET-3 gives largest results for M_y whereas SET-1 results are generally values like in Method-1.

Table 4.38 Ground motion set-wise percentage differences of M_x values of all pier columns for M2

		Compared with SET-1			Compared with SET-2			Compared with SET-3		
		SET-1	SET-2	SET-3	SET-1	SET-2	SET-3	SET-1	SET-2	SET-3
P1- M_x	AASHTO	-	-20%	23%	25%	-	53%	-18%	-35%	-
	EN	-	-27%	-8%	38%	-	27%	8%	-21%	-
	TDY	-	-18%	-7%	22%	-	14%	7%	-12%	-
P2- M_x	AASHTO	-	-25%	29%	34%	-	73%	-22%	-42%	-
	EN	-	-33%	-4%	49%	-	44%	4%	-30%	-
	TDY	-	-25%	-3%	33%	-	29%	3%	-23%	-
P3- M_x	AASHTO	-	-10%	27%	11%	-	40%	-21%	-29%	-
	EN	-	-19%	-5%	23%	-	17%	5%	-14%	-
	TDY	-	-8%	-4%	9%	-	5%	4%	-5%	-
P4- M_x	AASHTO	-	-10%	27%	11%	-	40%	-21%	-29%	-
	EN	-	-19%	-5%	23%	-	17%	5%	-14%	-
	TDY	-	-8%	-4%	9%	-	5%	4%	-4%	-
P5- M_x	AASHTO	-	-11%	21%	12%	-	35%	-17%	-26%	-
	EN	-	-21%	-9%	27%	-	15%	10%	-13%	-
	TDY	-	-11%	-8%	12%	-	3%	9%	-3%	-
P6- M_x	AASHTO	-	-9%	21%	10%	-	34%	-17%	-25%	-
	EN	-	-20%	-10%	24%	-	11%	12%	-10%	-
	TDY	-	-9%	-9%	10%	-	0%	10%	0%	-
P7- M_x	AASHTO	-	6%	26%	-5%	-	19%	-20%	-16%	-
	EN	-	0%	-2%	0%	-	-2%	2%	2%	-
	TDY	-	7%	-6%	-7%	-	-12%	6%	13%	-
P8- M_x	AASHTO	-	-13%	17%	15%	-	35%	-14%	-26%	-
	EN	-	-12%	-12%	14%	-	0%	14%	0%	-
	TDY	-	-14%	-11%	16%	-	3%	13%	-3%	-
P9- M_x	AASHTO	-	-19%	23%	23%	-	52%	-19%	-34%	-
	EN	-	-25%	-8%	34%	-	23%	9%	-19%	-
	TDY	-	-16%	-7%	19%	-	10%	8%	-9%	-

For most cases, SET-3 gives largest results for M_x whereas SET-2 results are generally smallest like in Method-1.

Table 4.39 Ground motion set-wise percentage differences of u_y values of all pier columns for M2

		Compared with SET-1			Compared with SET-2			Compared with SET-3		
		SET-1	SET-2	SET-3	SET-1	SET-2	SET-3	SET-1	SET-2	SET-3
P1- u_y	AASHTO	-	37%	62%	-27%	-	19%	-38%	-16%	-
	EN	-	21%	21%	-17%	-	0%	-18%	0%	-
	TDY	-	37%	22%	-27%	-	-11%	-18%	12%	-
P2- u_y	AASHTO	-	137%	185%	-58%	-	20%	-65%	-17%	-
	EN	-	107%	106%	-52%	-	-1%	-51%	1%	-
	TDY	-	134%	107%	-57%	-	-12%	-52%	13%	-
P3- u_y	AASHTO	-	24%	66%	-19%	-	35%	-40%	-26%	-
	EN	-	10%	24%	-9%	-	13%	-19%	-11%	-
	TDY	-	24%	25%	-19%	-	1%	-20%	-1%	-
P4- u_y	AASHTO	-	23%	66%	-19%	-	35%	-40%	-26%	-
	EN	-	10%	24%	-9%	-	13%	-19%	-11%	-
	TDY	-	24%	25%	-19%	-	1%	-20%	-1%	-
P5- u_y	AASHTO	-	4%	38%	-4%	-	33%	-28%	-25%	-
	EN	-	-7%	3%	8%	-	10%	-2%	-9%	-
	TDY	-	5%	3%	-5%	-	-1%	-3%	1%	-
P6- u_y	AASHTO	-	-2%	33%	2%	-	36%	-25%	-26%	-
	EN	-	-12%	0%	14%	-	13%	0%	-12%	-
	TDY	-	-1%	0%	1%	-	1%	0%	-1%	-
P7- u_y	AASHTO	-	-20%	22%	25%	-	53%	-18%	-35%	-
	EN	-	0%	28%	0%	-	28%	-22%	-22%	-
	TDY	-	-19%	-7%	23%	-	14%	7%	-13%	-
P8- u_y	AASHTO	-	1%	34%	-1%	-	32%	-25%	-24%	-
	EN	-	0%	0%	0%	-	0%	0%	0%	-
	TDY	-	1%	1%	-1%	-	1%	-1%	-1%	-
P9- u_y	AASHTO	-	73%	100%	-42%	-	15%	-50%	-13%	-
	EN	-	53%	47%	-34%	-	-4%	-32%	4%	-
	TDY	-	72%	48%	-42%	-	-14%	-32%	17%	-

For most cases, SET-3 gives largest results for u_y whereas SET-1 results are generally smallest like in Method-1.

Table 4.40 Ground motion set-wise percentage differences of u_x values of all pier columns for M2

		Compared with SET-1			Compared with SET-2			Compared with SET-3		
		SET-1	SET-2	SET-3	SET-1	SET-2	SET-3	SET-1	SET-2	SET-3
P1- u_x	AASHTO	-	-20%	23%	25%	-	53%	-18%	-35%	-
	EN	-	-27%	-8%	38%	-	27%	8%	-21%	-
	TDY	-	-18%	-7%	22%	-	14%	7%	-12%	-
P2- u_x	AASHTO	-	-25%	29%	34%	-	72%	-22%	-42%	-
	EN	-	-33%	-4%	49%	-	44%	4%	-30%	-
	TDY	-	-25%	-3%	33%	-	29%	3%	-23%	-
P3- u_x	AASHTO	-	-10%	27%	11%	-	40%	-21%	-29%	-
	EN	-	-19%	-5%	23%	-	17%	5%	-14%	-
	TDY	-	-8%	-4%	9%	-	5%	4%	-5%	-
P4- u_x	AASHTO	-	-10%	27%	11%	-	40%	-21%	-29%	-
	EN	-	-19%	-5%	23%	-	17%	5%	-14%	-
	TDY	-	-8%	-4%	9%	-	5%	4%	-4%	-
P5- u_x	AASHTO	-	-11%	21%	12%	-	35%	-17%	-26%	-
	EN	-	-21%	-9%	27%	-	15%	10%	-13%	-
	TDY	-	-11%	-9%	12%	-	3%	9%	-3%	-
P6- u_x	AASHTO	-	-9%	21%	10%	-	34%	-17%	-25%	-
	EN	-	-20%	-10%	24%	-	11%	12%	-10%	-
	TDY	-	-9%	-9%	10%	-	0%	10%	0%	-
P7- u_x	AASHTO	-	6%	26%	-5%	-	19%	-21%	-16%	-
	EN	-	-5%	-6%	5%	-	-2%	7%	2%	-
	TDY	-	7%	-6%	-7%	-	-12%	6%	13%	-
P8- u_x	AASHTO	-	-13%	17%	15%	-	35%	-14%	-26%	-
	EN	-	-23%	-12%	30%	-	14%	14%	-13%	-
	TDY	-	-14%	-11%	16%	-	3%	13%	-3%	-
P9- u_x	AASHTO	-	-19%	23%	23%	-	52%	-19%	-34%	-
	EN	-	-25%	-8%	34%	-	23%	9%	-19%	-
	TDY	-	-16%	-7%	19%	-	10%	8%	-9%	-

For most cases, SET-3 gives largest results for u_x whereas SET-2 results are generally smallest like in Method-1.

4.1.3 Comparison of Results for Scaling Method-3

In Method-3, the maximum M_x and M_y values of SET-1 occur in pier P7. The maximum M_y values of SET-2 occur in pier P2 and the maximum M_x values of SET-2 occur in pier P7. Differently, while the maximum values of M_x and M_y of SET-3 occur in pier P2 according to TDY 2020, the maximum values of M_y of SET-2 occur in P2 and the maximum values of M_x occur in P7 according to AASHTO LRFD and EN-8.

Sorting of maximum M_y values:

For AASHTO LRFD: SET-3 > SET-2 > SET-1 (94655 > 91628 > 81383) (kN.m)

For EN-8: SET-1 > SET-2 > SET-3 (98660 > 97311 > 95405) (kN.m)

For TDY 2020: SET-2 > SET-3 > SET-1 (81599 > 77151 > 70249) (kN.m)

Sorting of maximum M_x values :

For AASHTO LRFD: SET-3 > SET-2 > SET-1 (94497 > 84965 > 80015) (kN.m)

For EN-8: SET-2 > SET-3 > SET-1 (108533 > 101392 > 100576) (kN.m)

For TDY 2020: SET-1 > SET-2 > SET-3 (102376 > 97840 > 94156) (kN.m)

In Method-3, while the maximum u_x and u_y values of SET-1, SET-2 and SET-3 occurs in pier P7 unlike the moment values.

Sorting of maximum u_y values:

For AASHTO LRFD: SET-3 > SET-1 > SET-2 (1.06 > 0.95 > 0.76) cm

For EN-8: SET-1 > SET-3 > SET-2 (1.15 > 1.08 > 0.85) cm

For TDY 2020: SET-1 > SET-3 > SET-2 (0.82 > 0.76 > 0.63) cm

Sorting of maximum u_x values:

For AASHTO LRFD: SET-3 > SET-2>SET-1 (3.48>3.13>2.95) cm

For EN-8: SET-1>SET-2> SET-3 (3.77>3.60>3.47) cm

For TDY 2020: SET-2 > SET-1>SET-3 (2.54>2.52>2.28) cm

In this method, it can be seen that the moment values per different specifications are close to each other when comparing the other methods while the displacement values are not close to each other. And also, sets are not producing different moment and displacement values than each other when comparing the other methods. Most critical results comes from Eurocode-8 and less critical results come from AASHTO LRFD scaling methods.

Percentage difference given in the Tables 4.42-4.43, 4.45-4.46, 4.48-4.49 and 4.51-4.56 below are calculated based on the Equation 1.

Table 4.41 The maximum M_y values of pier P7 for M3 (kN.m)

	P7-M_y		
	SET-1	SET-2	SET-3
AASHTO LRFD	81383.71	65109.22	91377.92
EN-8	98660.82	72620.27	92801.71
TDY 2020	70249.96	53904.85	65023.12

Table 4.42 Specification-wise percentage differences of M_y values of pier P7 for M3

	Compared with AASHTO LRFD			Compared with EN-8			Compared with TDY 2020		
	SET-1	SET-2	SET-3	SET-1	SET-2	SET-3	SET-1	SET-2	SET-3
AASHTO LRFD	-	-	-	-18%	-10%	-2%	16%	21%	41%
EN-8	21%	12%	2%	-	-	-	40%	35%	43%
TDY 2020	-14%	-17%	-29%	-29%	-26%	-30%	-	-	-

EN-8 gives the largest moment values compared to other codes. TDY2020, on the other hand results in lowest M_y values like in Method-1 and Method-2.

Table 4.43 Ground motion set-wise percentage differences of M_y values of pier P7 for M3

	Compared with SET-1			Compared with SET-2			Compared with SET-3		
	SET-1	SET-2	SET-3	SET-1	SET-2	SET-3	SET-1	SET-2	SET-3
AASHTO LRFD	-	-20%	12%	25%	-	40%	-11%	-29%	-
EN-8	-	-26%	-6%	36%	-	28%	6%	-2%	-
TDY 2020	-	-23%	-7%	30%	-	21%	8%	-17%	-

Table 4.44 The maximum M_x values of pier P7 for M3 (kN.m)

	P7-M_x		
	SET-1	SET-2	SET-3
AASHTO LRFD	80015.1	84965.73	94497.79
EN-8	97840.14	97840.14	94156.15
TDY 2020	68506.79	68902.52	61987.29

Table 4.45 Specification-wise percentage differences of M_x values of pier P7 for M3

	Compared with AASHTO LRFD			Compared with EN-8			Compared with TDY 2020		
	SET-1	SET-2	SET-3	SET-1	SET-2	SET-3	SET-1	SET-2	SET-3
AASHTO LRFD	-	-	-	-18%	-13%	0%	17%	23%	52%
EN-8	22%	15%	-0.36%	-	-	-	43%	42%	52%
TDY 2020	-14%	-19%	-34%	-30%	-30%	-34%	-	-	-

EN-8 gives the largest moment values compared to other codes. TDY2020, on the other hand results in lowest M_x values like Method-1 and Method-2.

Table 4.46 Ground motion set-wise percentage differences of M_x values of pier P7 for M3

	Compared with SET-1			Compared with SET-2			Compared with SET-3		
	SET-1	SET-2	SET-3	SET-1	SET-2	SET-3	SET-1	SET-2	SET-3
AASHTO LRFD	-	6%	18%	-6%	-	11%	-15%	-10%	-
EN-8	-	0%	-4%	0%	-	-3.77%	4%	3.91%	-
TDY 2020	-	1%	-10%	-1%	-	-10%	11%	11%	-

Table 4.47 The maximum u_y values of pier P7 for M3 (m)

	P7-u_y		
	SET-1	SET-2	SET-3
AASHTO	0.0095	0.0076	0.0106
EN	0.0085	0.0085	0.0108
TDY	0.0082	0.0063	0.0076

Table 4.48 Specification-wise percentage differences of u_y values of pier P7 for M3

	Compared with AASHTO LRFD			Compared with EN-8			Compared with TDY 2020		
	SET-1	SET-2	SET-3	SET-1	SET-2	SET-3	SET-1	SET-2	SET-3
AASHTO	-	-	-	12%	-10%	-2%	16%	21%	41%
EN	-10%	12%	2%	-	-	-	4%	35%	43%
TDY	-14%	-17%	-29%	-4%	-26%	-30%	-	-	-

EN-8 gives the largest displacement values compared to other codes. TDY2020, on the other hand results in lowest u_y values like in Method-1 and Method-2.

Table 4.49 Ground motion set-wise percentage differences of u_y values of pier P7 for M3

	Compared with SET-1			Compared with SET-2			Compared with SET-3		
	SET-1	SET-2	SET-3	SET-1	SET-2	SET-3	SET-1	SET-2	SET-3
AASHTO	-	-20%	12%	25%	-	40%	-11%	-28%	-
EN	-	0%	27%	0%	-	27%	-21%	-21%	-
TDY	-	-23%	-7%	30%	-	20%	8%	-17%	-

Table 4.50 The maximum u_x values of pier P7 for M3 (m)

	P7-u_x		
	SET-1	SET-2	SET-3
AASHTO	0.0295	0.0313	0.0348
EN	0.0377	0.0360	0.0347
TDY	0.0252	0.0254	0.0228

Table 4.51 Specification-wise percentage differences of u_x values of pier P7 for M3

	Compared with AASHTO LRFD			Compared with EN-8			Compared with TDY 2020		
	SET-1	SET-2	SET-3	SET-1	SET-2	SET-3	SET-1	SET-2	SET-3
AASHTO	-	-	-	-22%	-13%	0%	17%	23%	52%
EN	28%	15%	-0.4%	-	-	-	49%	42%	52%
TDY	-14%	-19%	-34%	-33%	-30%	-34%	-	-	-

EN-8 gives the largest displacement values compared to other codes. TDY2020, on the other hand results in lowest u_x values like Method-1 and Method-2.

Table 4.52 Ground motion set-wise percentage differences of u_x values of pier P7 for M3

	Compared with SET-1			Compared with SET-2			Compared with SET-3		
	SET-1	SET-2	SET-3	SET-1	SET-2	SET-3	SET-1	SET-2	SET-3
AASHTO	-	6%	18%	-6%	-	11%	-15%	-10%	-
EN	-	-4%	-8%	5%	-	-4%	9%	4%	-
TDY	-	1%	-10%	-1%	-	-10%	11%	11%	-

Table 4.53 Ground motion set-wise percentage differences of M_y values of all pier columns for M3

		Compared with SET-1			Compared with SET-2			Compared with SET-3		
		SET-1	SET-2	SET-3	SET-1	SET-2	SET-3	SET-1	SET-2	SET-3
P1- M_y	AASHTO	-	29%	37%	-22%	-	6%	-27%	-6%	-
	EN	-	13%	14%	-12%	-	1%	-12%	-1%	-
	TDY	-	27%	19%	-21%	-	-6%	-16%	7%	-
P2- M_y	AASHTO	-	93%	99%	-48%	-	3%	-50%	-3%	-
	EN	-	68%	65%	-40%	-	-2%	-39%	2%	-
	TDY	-	97%	86%	-49%	-	-5%	-46%	6%	-
P3- M_y	AASHTO	-	8%	33%	-8%	-	23%	-25%	-19%	-
	EN	-	-5%	11%	5%	-	17%	-10%	-14%	-
	TDY	-	9%	17%	-8%	-	8%	-15%	-7%	-
P4- M_y	AASHTO	-	8%	33%	-8%	-	23%	-25%	-19%	-
	EN	-	-5%	11%	6%	-	17%	-10%	-15%	-
	TDY	-	9%	17%	-8%	-	8%	-15%	-7%	-
P5- M_y	AASHTO	-	2%	21%	-2%	-	19%	-17%	-16%	-
	EN	-	-8%	0%	9%	-	9%	0%	-8%	-
	TDY	-	-2%	2%	2%	-	4%	-2%	-4%	-
P6- M_y	AASHTO	-	-3%	18%	3%	-	21%	-15%	-17%	-
	EN	-	-12%	-2%	13%	-	11%	2%	-10%	-
	TDY	-	-7%	-1%	8%	-	7%	1%	-6%	-
P7- M_y	AASHTO	-	-20%	12%	25%	-	40%	-11%	-29%	-
	EN	-	-26%	-6%	36%	-	28%	6%	-22%	-
	TDY	-	-23%	-7%	30%	-	21%	8%	-17%	-
P8- M_y	AASHTO	-	0%	20%	0%	-	21%	-17%	-17%	-
	EN	-	-10%	0%	11%	-	11%	0%	-10%	-
	TDY	-	-6%	-1%	6%	-	5%	1%	-5%	-
P9- M_y	AASHTO	-	57%	57%	-36%	-	0%	-36%	0%	-
	EN	-	37%	30%	-27%	-	-5%	-23%	5%	-
	TDY	-	56%	41%	-36%	-	-10%	-29%	11%	-

For most cases, SET-3 gives largest results for M_y whereas SET-1 results are generally smallest unlikely in Method-1 and Method-2.

Table 4.54 Ground motion set-wise percentage differences of M_x values of all pier columns for M3

		Compared with SET-1			Compared with SET-2			Compared with SET-3		
		SET-1	SET-2	SET-3	SET-1	SET-2	SET-3	SET-1	SET-2	SET-3
P1- M_x	AASHTO	-	-21%	12%	26%	-	42%	-11%	-30%	-
	EN	-	-27%	-8%	38%	-	26%	9%	-21%	-
	TDY	-	-24%	-8%	31%	-	20%	9%	-17%	-
P2- M_x	AASHTO	-	-29%	14%	40%	-	60%	-12%	-37%	-
	EN	-	-35%	-7%	54%	-	43%	7%	-30%	-
	TDY	-	-32%	-6%	46%	-	37%	6%	-27%	-
P3- M_x	AASHTO	-	-12%	12%	14%	-	28%	-11%	-22%	-
	EN	-	-21%	-10%	27%	-	14%	11%	-12%	-
	TDY	-	-16%	-9%	20%	-	9%	10%	-8%	-
P4- M_x	AASHTO	-	-12%	12%	14%	-	28%	-11%	-22%	-
	EN	-	-21%	-10%	26%	-	14%	11%	-12%	-
	TDY	-	-16%	-9%	20%	-	9%	10%	-8%	-
P5- M_x	AASHTO	-	-12%	8%	14%	-	23%	-7%	-19%	-
	EN	-	-25%	-12%	33%	-	16%	14%	-14%	-
	TDY	-	-18%	-12%	21%	-	7%	14%	-6%	-
P6- M_x	AASHTO	-	-9%	10%	10%	-	20%	-9%	-17%	-
	EN	-	-20%	-12%	25%	-	10%	14%	-9%	-
	TDY	-	-15%	-12%	17%	-	3%	14%	-3%	-
P7- M_x	AASHTO	-	6%	18%	-6%	-	11%	-15%	-10%	-
	EN	-	0%	-4%	0%	-	-4%	4%	4%	-
	TDY	-	1%	-10%	-1%	-	-10%	11%	11%	-
P8- M_x	AASHTO	-	-14%	6%	17%	-	24%	-6%	-19%	-
	EN	-	-14%	-14%	16%	-	0%	16%	0%	-
	TDY	-	-19%	-14%	24%	-	7%	16%	-6%	-
P9- M_x	AASHTO	-	-15%	19%	18%	-	40%	-16%	-29%	-
	EN	-	-20%	-4%	25%	-	19%	4%	-16%	-
	TDY	-	-19%	-7%	23%	-	14%	8%	-12%	-

For most cases, SET-3 gives largest results for M_x whereas SET-2 results are generally smallest like in Method-1 and Method-2.

Table 4.55 Ground motion set-wise percentage differences of u_y values of all pier columns for M3

		Compared with SET-1			Compared with SET-2			Compared with SET-3		
		SET-1	SET-2	SET-3	SET-1	SET-2	SET-3	SET-1	SET-2	SET-3
P1- u_y	AASHTO	-	29%	37%	-22%	-	6%	-27%	-6%	-
	EN	-	13%	14%	-12%	-	1%	-12%	-1%	-
	TDY	-	27%	19%	-21%	-	-6%	-16%	7%	-
P2- u_y	AASHTO	-	93%	99%	-48%	-	3%	-50%	-3%	-
	EN	-	68%	64%	-40%	-	-2%	-39%	2%	-
	TDY	-	97%	86%	-49%	-	-6%	-46%	6%	-
P3- u_y	AASHTO	-	8%	33%	-8%	-	23%	-25%	-19%	-
	EN	-	-5%	11%	5%	-	17%	-10%	-14%	-
	TDY	-	8%	17%	-8%	-	8%	-15%	-7%	-
P4- u_y	AASHTO	-	8%	33%	-7%	-	23%	-25%	-19%	-
	EN	-	-5%	11%	6%	-	17%	-10%	-14%	-
	TDY	-	8%	17%	-8%	-	8%	-15%	-7%	-
P5- u_y	AASHTO	-	2%	21%	-2%	-	18%	-17%	-16%	-
	EN	-	-8%	0%	9%	-	8%	0%	-8%	-
	TDY	-	-2%	1%	2%	-	4%	-1%	-4%	-
P6- u_y	AASHTO	-	-3%	17%	3%	-	21%	-15%	-17%	-
	EN	-	-11%	-2%	13%	-	10%	2%	-9%	-
	TDY	-	-7%	-1%	8%	-	6%	1%	-6%	-
P7- u_y	AASHTO	-	-20%	12%	25%	-	40%	-11%	-28%	-
	EN	-	0%	27%	0%	-	27%	-21%	-21%	-
	TDY	-	-23%	-7%	30%	-	20%	8%	-17%	-
P8- u_y	AASHTO	-	0%	20%	0%	-	21%	-17%	-17%	-
	EN	-	0%	0%	0%	-	0%	0%	0%	-
	TDY	-	-6%	-1%	6%	-	5%	1%	-5%	-
P9- u_y	AASHTO	-	57%	57%	-36%	-	0%	-36%	0%	-
	EN	-	37%	30%	-27%	-	-5%	-23%	5%	-
	TDY	-	57%	41%	-36%	-	-10%	-29%	11%	-

For most cases, SET-3 gives largest results for u_y whereas SET-1 results are generally smallest unlikely in Method-1 and Method-2.

Table 4.56 Ground motion set-wise percentage differences of u_x values of all pier columns for M3

		Compared with SET-1			Compared with SET-2			Compared with SET-3		
		SET-1	SET-2	SET-3	SET-1	SET-2	SET-3	SET-1	SET-2	SET-3
P1- u_x	AASHTO	-	-21%	12%	26%	-	42%	-11%	-30%	-
	EN	-	-27%	-8%	38%	-	26%	9%	-21%	-
	TDY	-	-24%	-8%	31%	-	20%	9%	-17%	-
P2- u_x	AASHTO	-	-28%	14%	40%	-	59%	-12%	-37%	-
	EN	-	-35%	-7%	53%	-	43%	7%	-30%	-
	TDY	-	-32%	-6%	46%	-	37%	6%	-27%	-
P3- u_x	AASHTO	-	-12%	12%	14%	-	28%	-11%	-22%	-
	EN	-	-21%	-10%	27%	-	14%	11%	-12%	-
	TDY	-	-16%	-9%	20%	-	9%	10%	-8%	-
P4- u_x	AASHTO	-	-12%	12%	14%	-	28%	-11%	-22%	-
	EN	-	-21%	-10%	26%	-	14%	11%	-12%	-
	TDY	-	-16%	-9%	20%	-	9%	10%	-8%	-
P5- u_x	AASHTO	-	-12%	8%	14%	-	23%	-7%	-19%	-
	EN	-	-25%	-13%	33%	-	16%	14%	-14%	-
	TDY	-	-18%	-12%	21%	-	7%	14%	-6%	-
P6- u_x	AASHTO	-	-9%	10%	10%	-	20%	-9%	-17%	-
	EN	-	-20%	-12%	25%	-	10%	14%	-9%	-
	TDY	-	-15%	-12%	17%	-	3%	14%	-3%	-
P7- u_x	AASHTO	-	6%	18%	-6%	-	11%	-15%	-10%	-
	EN	-	-4%	-8%	5%	-	-4%	9%	4%	-
	TDY	-	1%	-10%	-1%	-	-10%	11%	11%	-
P8- u_x	AASHTO	-	-14%	6%	16%	-	24%	-6%	-19%	-
	EN	-	-26%	-14%	35%	-	16%	16%	-14%	-
	TDY	-	-19%	-14%	24%	-	6%	16%	-6%	-
P9- u_x	AASHTO	-	-15%	19%	18%	-	40%	-16%	-29%	-
	EN	-	-20%	-4%	25%	-	19%	4%	-16%	-
	TDY	-	-19%	-7%	23%	-	14%	8%	-12%	-

For most cases, SET-3 gives largest results for u_x whereas SET-2 results are generally smallest like in Method-1 and Method-2.

4.1.4 Summary of the Comparison Results

It can be seen that the most critical values of moments and displacements do not always occur in the same column and in the same ground motion set. While for a method SET-3 gives the critical moment values, SET-1 gives the critical displacement values. Sorting of the ground motion sets for displacement values is different than the sorting of the sets for moments for all of the specifications. Critical displacement values are observed in the highest column as expected. The percentage differences of both ground motion set-wise and specification-wise are the same in moment and displacement values. Thus, the summary of the comparison results are mostly focused on the moment values.

It can be concluded that when the specification-based comparison is considered, scaling according to the Eurocode-8 design spectrum resulted in the greater moment values than AASHTO LRFD and TDY 2020 for ground motion sets SET-1 and SET-2. However for the ground motion set SET-3, while the moment values for AASHTO LRFD become closer to Eurocode-8 by applying the Method-1 and Method-2, values for AASHTO LRFD are greater than the Eurocode-8 for Method-3. For all of these cases, scaling according to the TDY 2020 design spectrum gives the minimum moment values.

The moments in the pier column are given in the previous sections. When the results of 3 different sets are compared, the most consistent scaling method appears to be Eurocode-8. The moment values are not changing significantly in Eurocode-8 unlike in other specifications. Additionally, the most critical moment values are obtained when Eurocode-8 specification is employed. Besides comparing specifications, it can be seen that limiting the scaling factor (as in Method-3) provides closer results for different specifications with different sets. It increases the consistency.

When the ground motion-based comparison is considered, the results are observed to be variable between the nine pier columns for each specification as well.

As can be seen from Figure 4.13 and 4.14, for *AASHTO LRFD* design spectrum scaling, the maximum M_y moments occur in Method-2 for all of the columns. After Method-2, maximum values occur in Method-3 and Method-1 respectively.

The maximum M_x moments cannot be correlated between the methods because in each set for each pier different methods govern the design.

For the bridge transverse direction (M_y), when the three ground motion sets applied for each method are compared, SET-3 gives the maximum moment values for all of the columns. And for P1 to P5 SET-2 results are greater than SET-1, while for P5 to P9 SET-1 results are greater than SET-2.

For the bridge longitudinal direction (M_x), when the three ground motion sets applied for each method are compared, SET-3 gives the maximum moment values for all of the columns. And for P1 to P9, except P7, SET-1 results are greater than SET-2 that is greater than SET-1 for P7.

These observations show that the moment values show variation according to the ground motion set and the scaling method.

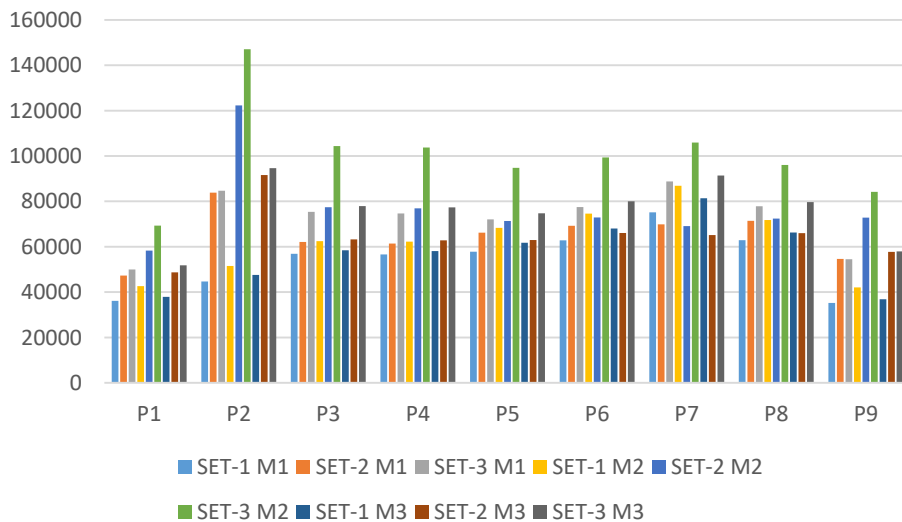


Figure 4.13. M_y values of all of the pier columns for three scaling methods applied according to AASHTO LRFD (kN.m)

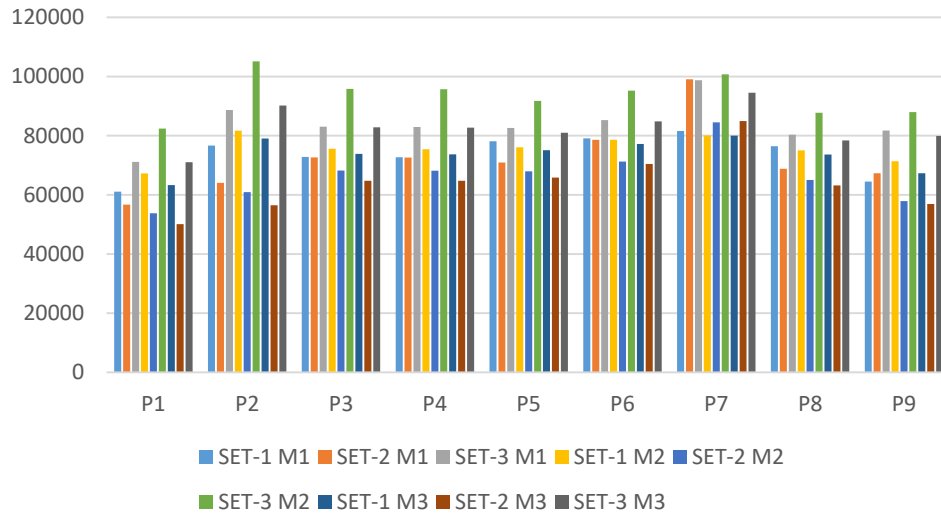


Figure 4.14. M_x values of all of the pier columns for three scaling methods applied according to AASHTO LRFD (kN.m)

It can be said that by following the AASHTO LRFD specification for the design, although for the transverse direction Method-2 gives the maximum moment values, there is an uncertainty for the longitudinal direction about which method to be used. Method-wise percentage differences can be seen from Tables 57-59. In the case of the selection of ground motion sets, similar uncertainty exists about which one to choose. Thus, different ground motion sets and methods should be employed in the design to obtain reliable results.

Table 4.57 AASHTO LRFD method-wise differences for SET-1

	AASHTO LRFD M2-M _y			AASHTO LRFD M3-M _x		
	Compared with M1			Compared with M1		
	SET-1 M1	SET-1 M2	SET-1 M3	SET-1 M1	SET-1 M2	SET-1 M3
P1	-	0.178	0.047	-	0.101	0.037
P2	-	0.154	0.065	-	0.066	0.031
P3	-	0.099	0.027	-	0.038	0.014
P4	-	0.100	0.026	-	0.038	0.014
P5	-	0.181	0.068	-	-0.027	-0.039
P6	-	0.188	0.084	-	-0.006	-0.024
P7	-	0.156	0.083	-	-0.019	-0.019
P8	-	0.141	0.054	-	-0.018	-0.037
P9	-	0.194	0.047	-	0.106	0.043

	Compared with M2			Compared with M2		
	SET-1 M1	SET-1 M2	SET-1 M3	SET-1 M1	SET-1 M2	SET-1 M3
P1	-0.151	-	-0.111	-0.092	-	-0.058
P2	-0.133	-	-0.076	-0.062	-	-0.032
P3	-0.090	-	-0.065	-0.036	-	-0.023
P4	-0.091	-	-0.067	-0.036	-	-0.023
P5	-0.154	-	-0.096	0.027	-	-0.013
P6	-0.159	-	-0.088	0.006	-	-0.018
P7	-0.135	-	-0.064	0.019	-	-0.001
P8	-0.124	-	-0.076	0.019	-	-0.019
P9	-0.162	-	-0.123	-0.096	-	-0.057

	Compared with M3			Compared with M3		
	SET-1 M1	SET-1 M2	SET-1 M3	SET-1 M1	SET-1 M2	SET-1 M3
P1	-0.045	0.125	-	-0.035	0.062	-
P2	-0.061	0.083	-	-0.030	0.034	-
P3	-0.027	0.070	-	-0.014	0.024	-
P4	-0.026	0.072	-	-0.014	0.024	-
P5	-0.064	0.106	-	0.041	0.013	-
P6	-0.077	0.097	-	0.024	0.018	-
P7	-0.077	0.068	-	0.020	0.001	-
P8	-0.051	0.083	-	0.038	0.019	-
P9	-0.045	0.140	-	-0.041	0.060	-

Table 4.58 AASHTO LRFD method-wise differences for SET-2

	AASHTO LRFD M2-M _y			AASHTO LRFD M3-M _x		
	Compared with M1			Compared with M1		
	SET-2 M1	SET-2 M2	SET-2 M3	SET-2 M1	SET-2 M2	SET-2 M3
P1	-	0.233	0.030	-	-0.051	-0.117
P2	-	0.459	0.093	-	-0.049	-0.118
P3	-	0.246	0.018	-	-0.061	-0.108
P4	-	0.253	0.023	-	-0.061	-0.108
P5	-	0.078	-0.049	-	-0.042	-0.072
P6	-	0.052	-0.047	-	-0.094	-0.104
P7	-	-0.011	-0.068	-	-0.147	-0.142
P8	-	0.014	-0.076	-	-0.056	-0.082
P9	-	0.334	0.058	-	-0.140	-0.154

	Compared with M2			Compared with M2		
	SET-2 M1	SET-2 M2	SET-2 M3	SET-2 M1	SET-2 M2	SET-2 M3
P1	-0.189	-	-0.164	0.054	-	-0.069
P2	-0.315	-	-0.251	0.052	-	-0.072
P3	-0.197	-	-0.183	0.065	-	-0.050
P4	-0.202	-	-0.183	0.065	-	-0.050
P5	-0.072	-	-0.117	0.044	-	-0.031
P6	-0.050	-	-0.094	0.104	-	-0.012
P7	0.011	-	-0.058	0.172	-	0.006
P8	-0.014	-	-0.089	0.059	-	-0.028
P9	-0.250	-	-0.207	0.162	-	-0.017

	Compared with M3			Compared with M3		
	SET-2 M1	SET-2 M2	SET-2 M3	SET-2 M1	SET-2 M2	SET-2 M3
P1	-0.030	0.196	-	0.132	0.074	-
P2	-0.085	0.335	-	0.134	0.078	-
P3	-0.018	0.224	-	0.121	0.053	-
P4	-0.023	0.225	-	0.121	0.053	-
P5	0.051	0.133	-	0.078	0.032	-
P6	0.049	0.104	-	0.117	0.012	-
P7	0.073	0.061	-	0.166	-0.006	-
P8	0.082	0.098	-	0.089	0.029	-
P9	-0.055	0.261	-	0.183	0.017	-

Table 4.59 AASHTO LRFD method-wise differences for SET-3

	AASHTO LRFD M2-M _y			AASHTO LRFD M3-M _x		
	Compared with M1			Compared with M1		
	SET-3 M1	SET-3 M2	SET-3 M3	SET-3 M1	SET-3 M2	SET-3 M3
P1	-	0.386	0.036	-	0.158	-0.001
P2	-	0.737	0.118	-	0.186	0.017
P3	-	0.384	0.034	-	0.153	-0.003
P4	-	0.388	0.035	-	0.154	-0.003
P5	-	0.315	0.036	-	0.111	-0.019
P6	-	0.283	0.033	-	0.117	-0.005
P7	-	0.193	0.029	-	0.020	-0.043
P8	-	0.233	0.023	-	0.092	-0.025
P9	-	0.545	0.064	-	0.076	-0.023

	Compared with M2			Compared with M2		
	SET-3 M1	SET-3 M2	SET-3 M3	SET-3 M1	SET-3 M2	SET-3 M3
P1	-0.279	-	-0.252	-0.137	-	-0.137
P2	-0.424	-	-0.356	-0.157	-	-0.143
P3	-0.278	-	-0.253	-0.133	-	-0.135
P4	-0.280	-	-0.254	-0.133	-	-0.136
P5	-0.239	-	-0.212	-0.100	-	-0.117
P6	-0.221	-	-0.195	-0.104	-	-0.109
P7	-0.161	-	-0.137	-0.020	-	-0.062
P8	-0.189	-	-0.171	-0.084	-	-0.107
P9	-0.353	-	-0.312	-0.070	-	-0.091

	Compared with M3			Compared with M3		
	SET-3 M1	SET-3 M2	SET-3 M3	SET-3 M1	SET-3 M2	SET-3 M3
P1	-0.035	0.337	-	0.001	0.159	-
P2	-0.105	0.554	-	-0.017	0.166	-
P3	-0.033	0.339	-	0.003	0.157	-
P4	-0.034	0.341	-	0.003	0.157	-
P5	-0.035	0.268	-	0.020	0.133	-
P6	-0.032	0.242	-	0.005	0.122	-
P7	-0.028	0.159	-	0.045	0.066	-
P8	-0.023	0.206	-	0.025	0.120	-
P9	-0.060	0.453	-	0.023	0.100	-

As can be seen from Figure 4.15 and 4.16, for **Eurocode-8** design spectrum based scaling, the maximum M_y moments generally occur in Method-2 for all of the columns in the cases of different ground motion sets. After Method-2, maximum values occur in Method-3 and Method-1 respectively.

The maximum M_x moments cannot be correlated between the methods because in each set for each pier different methods govern the design. It can be said that for SET-1 and SET-2, three methods give approximately the same results. However, for SET-2, Method-1 gives the maximum M_x moment for all of the pier columns.

For the bridge transverse direction (M_y), when the three ground motion sets applied for each method are compared, maximum M_y moments cannot be correlated between the ground motion sets because in each method for each pier a different set govern the design.

For the bridge longitudinal direction (M_x), when the three ground motion sets applied for each method are compared, SET-1 gives the maximum moment values for all of the columns except P7 where maximum M_x moment occurs with SET-2 of Method-1. After SET-1, sorting of the maximum values are variable among the SET-2 and SET-3 for different columns.

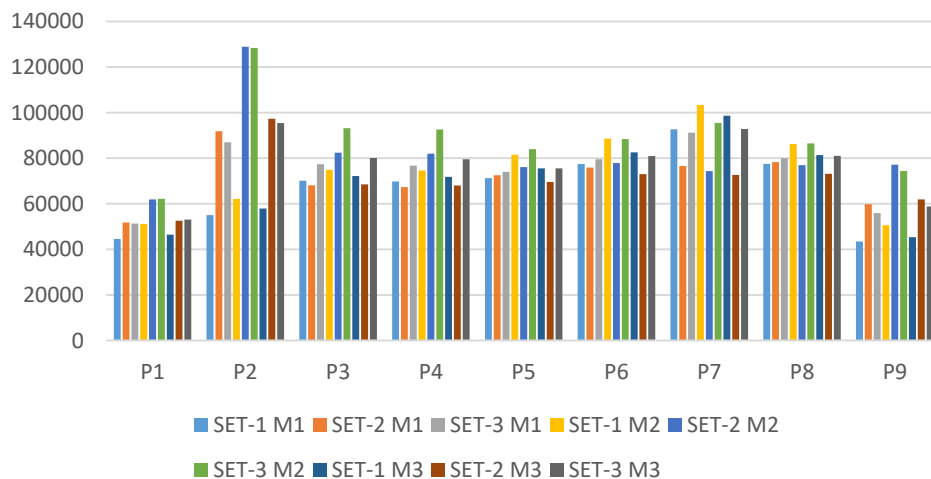


Figure 4.15. M_y values of all of the pier columns for three scaling methods applied according to EN-8 (kN.m)

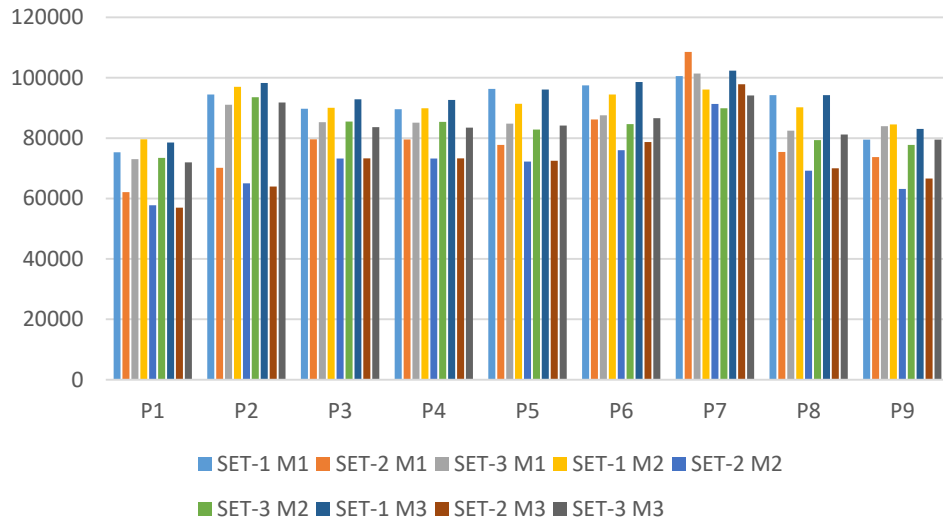


Figure 4.16. M_x values of all of the pier columns for three scaling methods applied according to EN-8 (kN.m)

It can be said that by following the Eurocode-8 specification for the design, although for the transverse direction Method-2 gives the maximum moment values, there is an uncertainty for the longitudinal direction about which method to be used. Method-wise percentage differences can be seen from Tables 60-62. In the case of the selection of ground motion sets, similar uncertainty exists about which one to choose. Thus, different ground motion sets and methods should be employed in the design to obtain reliable results.

Table 4.60 EN-8 method-wise differences for SET-1

	EN M2-M _y			EN M3-M _x		
	Compared with M1			Compared with M1		
	SET-1 M1	SET-1 M2	SET-1 M3	SET-1 M1	SET-1 M2	SET-1 M3
P1	-	0.148	0.042	-	0.057	0.043
P2	-	0.128	0.052	-	0.027	0.040
P3	-	0.069	0.029	-	0.003	0.034
P4	-	0.069	0.029	-	0.003	0.034
P5	-	0.144	0.060	-	-0.051	-0.002
P6	-	0.145	0.066	-	-0.031	0.011
P7	-	0.115	0.065	-	-0.045	0.018
P8	-	0.112	0.050	-	-0.043	0.000
P9	-	0.166	0.044	-	0.063	0.045

	Compared with M2			Compared with M2		
	SET-1 M1	SET-1 M2	SET-1 M3	SET-1 M1	SET-1 M2	SET-1 M3
P1	-0.129	-	-0.092	-0.054	-	-0.013
P2	-0.114	-	-0.067	-0.026	-	0.013
P3	-0.064	-	-0.037	-0.003	-	0.031
P4	-0.065	-	-0.038	-0.003	-	0.031
P5	-0.126	-	-0.073	0.054	-	0.052
P6	-0.126	-	-0.068	0.032	-	0.044
P7	-0.104	-	-0.045	0.047	-	0.065
P8	-0.100	-	-0.056	0.044	-	0.045
P9	-0.142	-	-0.105	-0.059	-	-0.017

	Compared with M3			Compared with M3		
	SET-1 M1	SET-1 M2	SET-1 M3	SET-1 M1	SET-1 M2	SET-1 M3
P1	-0.041	0.101	-	-0.042	0.014	-
P2	-0.050	0.072	-	-0.039	-0.013	-
P3	-0.028	0.038	-	-0.033	-0.030	-
P4	-0.028	0.040	-	-0.033	-0.030	-
P5	-0.057	0.079	-	0.002	-0.049	-
P6	-0.062	0.073	-	-0.011	-0.042	-
P7	-0.061	0.047	-	-0.018	-0.061	-
P8	-0.047	0.059	-	0.000	-0.043	-
P9	-0.042	0.117	-	-0.043	0.018	-

Table 4.61 EN-8 method-wise differences for SET-2

	EN M2-M _y			EN M3-M _x		
	Compared with M1			Compared with M1		
	SET-2 M1	SET-2 M2	SET-2 M3	SET-2 M1	SET-2 M2	SET-2 M3
P1	-	0.195	0.014	-	-0.070	-0.082
P2	-	0.404	0.060	-	-0.073	-0.088
P3	-	0.211	0.007	-	-0.080	-0.079
P4	-	0.218	0.010	-	-0.079	-0.079
P5	-	0.049	-0.041	-	-0.071	-0.067
P6	-	0.026	-0.038	-	-0.118	-0.087
P7	-	-0.029	-0.052	-	-0.159	-0.099
P8	-	-0.016	-0.065	-	-0.082	-0.072
P9	-	0.290	0.035	-	-0.143	-0.097

	Compared with M2			Compared with M2		
	SET-2 M1	SET-2 M2	SET-2 M3	SET-2 M1	SET-2 M2	SET-2 M3
P1	-0.163	-	-0.152	0.075	-	-0.014
P2	-0.288	-	-0.245	0.079	-	-0.016
P3	-0.174	-	-0.169	0.087	-	0.001
P4	-0.179	-	-0.171	0.086	-	0.001
P5	-0.047	-	-0.086	0.076	-	0.004
P6	-0.026	-	-0.062	0.133	-	0.035
P7	0.030	-	-0.023	0.189	-	0.072
P8	0.017	-	-0.049	0.089	-	0.011
P9	-0.225	-	-0.197	0.167	-	0.055

	Compared with M3			Compared with M3		
	SET-2 M1	SET-2 M2	SET-2 M3	SET-2 M1	SET-2 M2	SET-2 M3
P1	-0.014	0.179	-	0.090	0.014	-
P2	-0.056	0.325	-	0.097	0.017	-
P3	-0.007	0.203	-	0.086	-0.001	-
P4	-0.010	0.206	-	0.086	-0.001	-
P5	0.043	0.094	-	0.072	-0.004	-
P6	0.039	0.067	-	0.095	-0.034	-
P7	0.054	0.023	-	0.109	-0.067	-
P8	0.069	0.052	-	0.077	-0.011	-
P9	-0.034	0.246	-	0.107	-0.052	-

Table 4.62 EN-8 method-wise differences for SET-3

	EN M2-M _y			EN M3-M _x		
	Compared with M1			Compared with M1		
	SET-3 M1	SET-3 M2	SET-3 M3	SET-3 M1	SET-3 M2	SET-3 M3
P1	-	0.211	0.034	-	0.006	-0.015
P2	-	0.476	0.097	-	0.027	0.009
P3	-	0.204	0.035	-	0.002	-0.020
P4	-	0.208	0.037	-	0.003	-0.019
P5	-	0.135	0.021	-	-0.023	-0.007
P6	-	0.111	0.018	-	-0.033	-0.011
P7	-	0.047	0.018	-	-0.113	-0.071
P8	-	0.082	0.013	-	-0.038	-0.016
P9	-	0.331	0.052	-	-0.074	-0.053

	Compared with M2			Compared with M2		
	SET-3 M1	SET-3 M2	SET-3 M3	SET-3 M1	SET-3 M2	SET-3 M3
P1	-0.174	-	-0.147	-0.006	-	-0.020
P2	-0.323	-	-0.257	-0.027	-	-0.018
P3	-0.169	-	-0.141	-0.002	-	-0.022
P4	-0.172	-	-0.141	-0.003	-	-0.022
P5	-0.119	-	-0.100	0.023	-	0.016
P6	-0.100	-	-0.084	0.034	-	0.023
P7	-0.045	-	-0.028	0.128	-	0.047
P8	-0.075	-	-0.063	0.040	-	0.024
P9	-0.249	-	-0.210	0.080	-	0.022

	Compared with M3			Compared with M3		
	SET-3 M1	SET-3 M2	SET-3 M3	SET-3 M1	SET-3 M2	SET-3 M3
P1	-0.032	0.172	-	0.015	0.021	-
P2	-0.089	0.345	-	-0.009	0.019	-
P3	-0.034	0.163	-	0.020	0.022	-
P4	-0.036	0.164	-	0.020	0.022	-
P5	-0.020	0.112	-	0.007	-0.016	-
P6	-0.018	0.092	-	0.011	-0.023	-
P7	-0.018	0.029	-	0.077	-0.045	-
P8	-0.013	0.067	-	0.016	-0.023	-
P9	-0.049	0.265	-	0.056	-0.022	-

As can be seen from Figure 4.17 and 4.18, for **TDY-2020** design spectrum scaling, the maximum M_y moments generally occur in Method-2 for all of the columns. After Method-2, maximum values occur in Method-3 and Method-1 respectively.

The maximum M_x moments cannot be correlated between the methods because in each set for each pier different methods govern the design. It can be said that for SET-1 and SET-2, three methods give approximately the same results. However, for the SET-2, Method-1 gives the maximum M_x moment for all of the pier columns.

For the bridge transverse direction (M_y), when the three ground motion sets applied for each method are compared, maximum M_y moments cannot be correlated between the ground motion sets because in each method for each pier a different set governs the design.

For the bridge longitudinal direction (M_x), when the three ground motion sets applied for each method are compared, SET-1 gives the maximum moment values for all of the columns except P7 where maximum M_x moment occurs with SET-2 of Method-1 and Method-2. After SET-1, sorting of the maximum values are variable among the SET-2 and SET-3 for different columns.

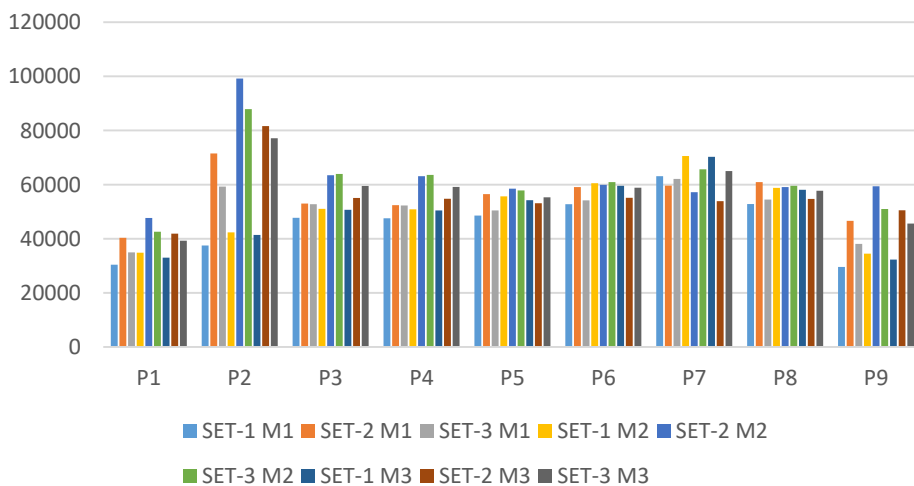


Figure 4.17. M_y values of all of the pier columns for three scaling methods applied according to TDY 2020 (kN.m)

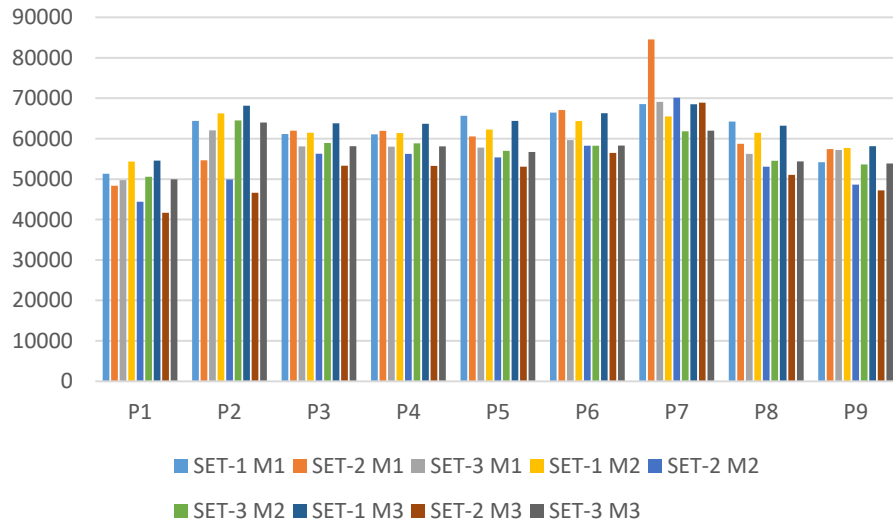


Figure 4.18. M_x values of all of the pier columns for three scaling methods applied according to TDY 2020 (kN.m)

It can be said that by following the TDY 2020 specification for the design, although for the transverse direction Method-2 gives the maximum moment values, there is an uncertainty for the longitudinal direction about which method to be used. Method-wise percentage differences can be seen from Tables 63-65. In the case of the selection of ground motion sets, similar uncertainty exists about which one to choose. Thus, different ground motion sets and methods should be employed in the design to obtain reliable results.

Table 4.63 TDY 2020 method-wise differences for SET-1

	TDY M2-M _y			TDY M3-M _x		
	Compared with M1			Compared with M1		
	SET-1 M1	SET-1 M2	SET-1 M3	SET-1 M1	SET-1 M2	SET-1 M3
P1	-	0.148	0.086	-	0.059	0.063
P2	-	0.129	0.103	-	0.029	0.059
P3	-	0.069	0.061	-	0.005	0.043
P4	-	0.070	0.060	-	0.005	0.043
P5	-	0.146	0.117	-	-0.051	-0.019
P6	-	0.147	0.129	-	-0.031	-0.002
P7	-	0.118	0.113	-	-0.044	0.000
P8	-	0.113	0.100	-	-0.043	-0.016
P9	-	0.165	0.091	-	0.065	0.073

	Compared with M2			Compared with M2		
	SET-1 M1	SET-1 M2	SET-1 M3	SET-1 M1	SET-1 M2	SET-1 M3
P1	-0.129	-	-0.054	-0.056	-	0.004
P2	-0.114	-	-0.023	-0.028	-	0.029
P3	-0.065	-	-0.007	-0.005	-	0.038
P4	-0.065	-	-0.009	-0.005	-	0.038
P5	-0.127	-	-0.025	0.054	-	0.034
P6	-0.128	-	-0.016	0.032	-	0.030
P7	-0.105	-	-0.004	0.046	-	0.046
P8	-0.102	-	-0.012	0.045	-	0.028
P9	-0.142	-	-0.064	-0.061	-	0.007

	Compared with M3			Compared with M3		
	SET-1 M1	SET-1 M2	SET-1 M3	SET-1 M1	SET-1 M2	SET-1 M3
P1	-0.079	0.057	-	-0.060	-0.004	-
P2	-0.094	0.023	-	-0.055	-0.028	-
P3	-0.058	0.008	-	-0.042	-0.037	-
P4	-0.057	0.009	-	-0.041	-0.036	-
P5	-0.105	0.026	-	0.019	-0.033	-
P6	-0.114	0.016	-	0.002	-0.029	-
P7	-0.101	0.004	-	0.000	-0.044	-
P8	-0.091	0.012	-	0.016	-0.027	-
P9	-0.084	0.068	-	-0.068	-0.007	-

Table 4.64 TDY 2020 method-wise differences for SET-2

	TDY M2-My			TDY M3-Mx		
	Compared with M1			Compared with M1		
	SET-2 M1	SET-2 M2	SET-2 M3	SET-2 M1	SET-2 M2	SET-2 M3
P1	-	0.182	0.038	-	-0.082	-0.138
P2	-	0.387	0.141	-	-0.087	-0.147
P3	-	0.197	0.039	-	-0.093	-0.140
P4	-	0.204	0.045	-	-0.092	-0.140
P5	-	0.035	-0.060	-	-0.085	-0.123
P6	-	0.014	-0.067	-	-0.132	-0.158
P7	-	-0.041	-0.096	-	-0.170	-0.185
P8	-	-0.030	-0.102	-	-0.096	-0.131
P9	-	0.275	0.084	-	-0.153	-0.178

	Compared with M2			Compared with M2		
	SET-2 M1	SET-2 M2	SET-2 M3	SET-2 M1	SET-2 M2	SET-2 M3
P1	-0.154	-	-0.121	0.089	-	-0.061
P2	-0.279	-	-0.177	0.095	-	-0.066
P3	-0.165	-	-0.132	0.102	-	-0.053
P4	-0.170	-	-0.132	0.102	-	-0.053
P5	-0.034	-	-0.092	0.093	-	-0.041
P6	-0.013	-	-0.079	0.152	-	-0.031
P7	0.042	-	-0.058	0.205	-	-0.018
P8	0.031	-	-0.074	0.107	-	-0.038
P9	-0.215	-	-0.149	0.180	-	-0.029

	Compared with M3			Compared with M3		
	SET-2 M1	SET-2 M2	SET-2 M3	SET-2 M1	SET-2 M2	SET-2 M3
P1	-0.037	0.138	-	0.161	0.065	-
P2	-0.123	0.216	-	0.173	0.070	-
P3	-0.038	0.152	-	0.163	0.055	-
P4	-0.043	0.152	-	0.163	0.056	-
P5	0.064	0.101	-	0.141	0.043	-
P6	0.072	0.086	-	0.188	0.031	-
P7	0.106	0.061	-	0.227	0.018	-
P8	0.113	0.080	-	0.151	0.040	-
P9	-0.078	0.176	-	0.216	0.030	-

Table 4.65 TDY 2020 method-wise differences for SET-3

	TDY M2-My			TDY M3-Mx		
	Compared with M1			Compared with M1		
	SET-3 M1	SET-3 M2	SET-3 M3	SET-3 M1	SET-3 M2	SET-3 M3
P1	-	0.218	0.124	-	0.016	0.003
P2	-	0.483	0.302	-	0.040	0.032
P3	-	0.213	0.128	-	0.014	0.001
P4	-	0.216	0.131	-	0.014	0.001
P5	-	0.147	0.096	-	-0.014	-0.018
P6	-	0.124	0.086	-	-0.023	-0.023
P7	-	0.057	0.046	-	-0.105	-0.103
P8	-	0.093	0.060	-	-0.030	-0.033
P9	-	0.337	0.197	-	-0.062	-0.059

	Compared with M2			Compared with M2		
	SET-3 M1	SET-3 M2	SET-3 M3	SET-3 M1	SET-3 M2	SET-3 M3
P1	-0.179	-	-0.077	-0.016	-	-0.012
P2	-0.326	-	-0.122	-0.038	-	-0.007
P3	-0.175	-	-0.070	-0.014	-	-0.013
P4	-0.178	-	-0.070	-0.014	-	-0.013
P5	-0.128	-	-0.045	0.014	-	-0.005
P6	-0.110	-	-0.034	0.024	-	0.000
P7	-0.054	-	-0.010	0.117	-	0.002
P8	-0.085	-	-0.031	0.031	-	-0.003
P9	-0.252	-	-0.105	0.067	-	0.004

	Compared with M3			Compared with M3		
	SET-3 M1	SET-3 M2	SET-3 M3	SET-3 M1	SET-3 M2	SET-3 M3
P1	-0.110	0.083	-	-0.003	0.013	-
P2	-0.232	0.139	-	-0.031	0.007	-
P3	-0.113	0.075	-	-0.001	0.013	-
P4	-0.116	0.075	-	-0.001	0.013	-
P5	-0.088	0.047	-	0.019	0.005	-
P6	-0.079	0.035	-	0.024	0.000	-
P7	-0.044	0.010	-	0.115	-0.002	-
P8	-0.056	0.032	-	0.034	0.003	-
P9	-0.164	0.118	-	0.062	-0.004	-

It appears that in all cases Method 2 gives the largest values for M_y in transverse direction. This is can be explained by having no upper limit for scaling. However, for M_x in longitudinal direction it cannot be decided that which method give the maximum values. Also, in both directions, it seems to be not clear that which ground motion set should be used. Thus, different ground motion sets and methods should be employed in the seismic design of bridges having fundamental periods greater than 1 ($T_n > 1$) to obtain reliable and accurate results for each bridge design specification.

4.2 Comparison of Results for V08 Bridge

Before the comparison of the analysis results, first the spectral acceleration values of the mean spectra of the selected set of earthquakes are compared. Maximum spectral acceleration values of mean response spectrum of the scaled time histories change both according to specifications and methods. Mean spectra of the ground motion sets scaled according to three scaling methods (M1, M2 and M3) are shown in Figures 4.19-4.27 per specification. For TDY 2020 design spectrum, maximum S_a resulted in Method-2 conducted on ground motion set SET-2 as 1.62g, while for AASHTO LRFD and EN-8 design spectra, maximum S_a resulted in Method-2 conducted on ground motion set SET-3 as 1.61g and 2.31 respectively (Table 4.66).

Table 4.66 Maximum spectral acceleration (S_a) values (g)

	AASHTO LRFD			EN-8			TDY		
	M1	M2	M3	M1	M2	M3	M1	M2	M3
SET-1	0.933	1.043	0.950	1.730	1.838	1.732	1.138	1.212	1.196
SET-2	1.016	1.248	0.955	1.712	2.060	1.728	1.286	1.622	1.425
SET-3	1.287	1.613	1.282	2.013	2.305	2.025	1.324	1.521	1.339

Spectral acceleration values at $T=1.00$ sec. (fundamental period of V08) of mean response spectrum of the scaled time histories have different pattern than the maximum values (Table 4.67). For both AASHTO LRFD and TDY design spectrum, the maximum value occurs for Method-3. However, while for AASHTO LRFD Method-3 of SET-3 governs, for TDY Method-3 of SET-2 governs. For EN-8 maximum value occurs for Method-2 on SET-2.

Table 4.67 Spectral acceleration (S_a) values at $T=1.00$ sec. (g)

	AASHTO LRFD			EN-8			TDY		
	M1	M2	M3	M1	M2	M3	M1	M2	M3
SET-1	0.324	0.319	0.323	0.605	0.610	0.607	0.398	0.401	0.411
SET-2	0.320	0.318	0.317	0.592	0.616	0.607	0.445	0.464	0.470
SET-3	0.341	0.339	0.343	0.542	0.511	0.543	0.357	0.336	0.341

The maximum acceleration values (Table 4.66) regardless of the scaling methods in time interval 0-4 seconds based on the selected ground motion sets are sorted as follows per specification:

For AASHTO LRFD: SET-3 > SET-2 > SET-1

For EN-8: SET-3 > SET-2 > SET-1

For TDY 2020: SET-2 > SET-3 > SET-1

To sum up, in time interval 0-4 seconds, Method-2 resulted in the maximum spectral acceleration values for all the three sets and the specifications. However, at the fundamental period of the bridge, Method-2 and Method-3 give the maximum S_a values.

In overall, EN-8 response spectrum scaling and Method-2 give the maximum acceleration values.

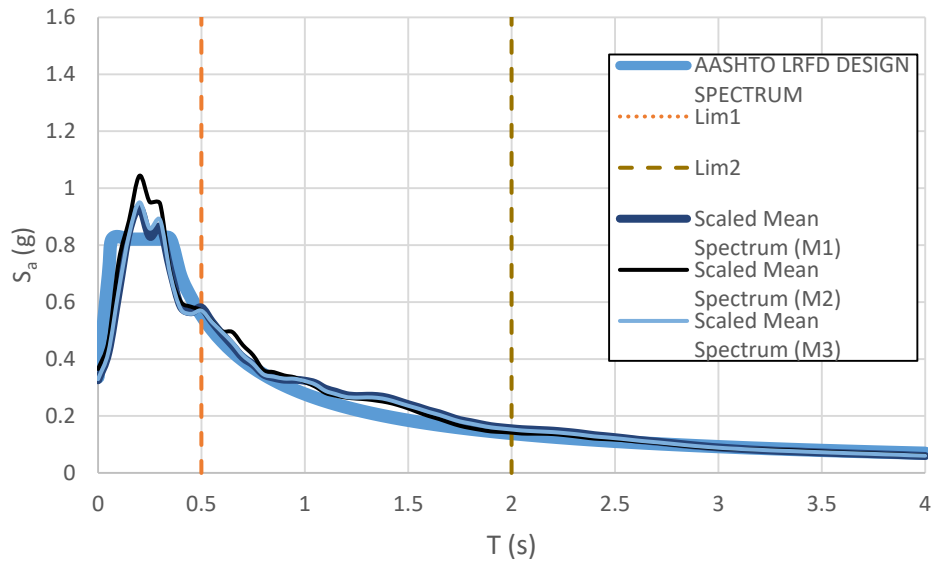


Figure 4.19. Scaled mean spectra for M1,M2 and M3 and AASHTO LRFD design response spectrum for SET-1

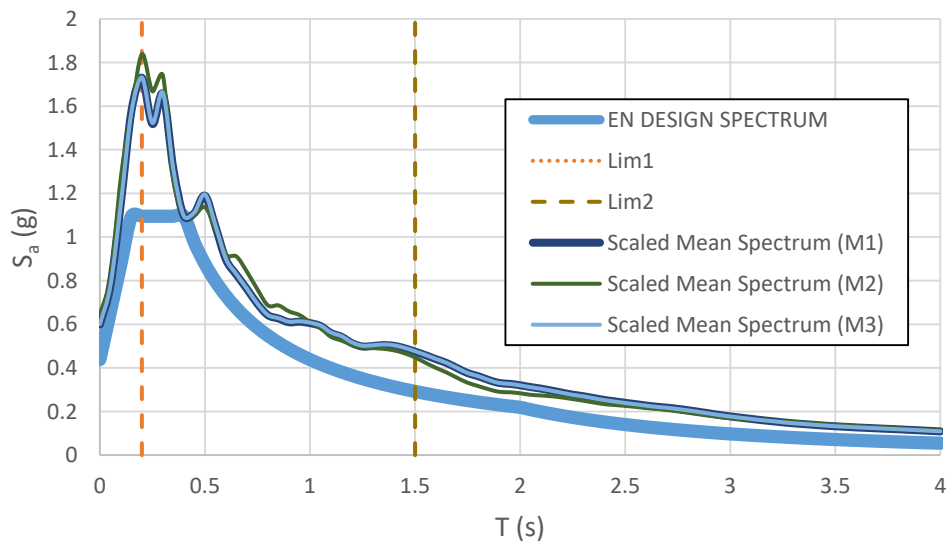


Figure 4.20. Scaled mean spectra for M1,M2 and M3 and EN 8 design response spectrum for SET-1

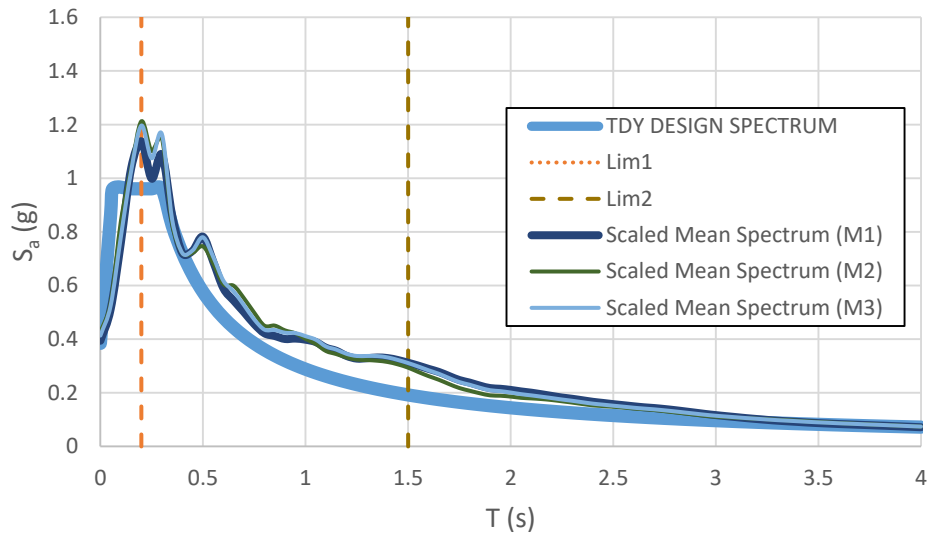


Figure 4.21. Scaled mean spectra for M1,M2 and M3 and TDY design response spectrum for SET-1

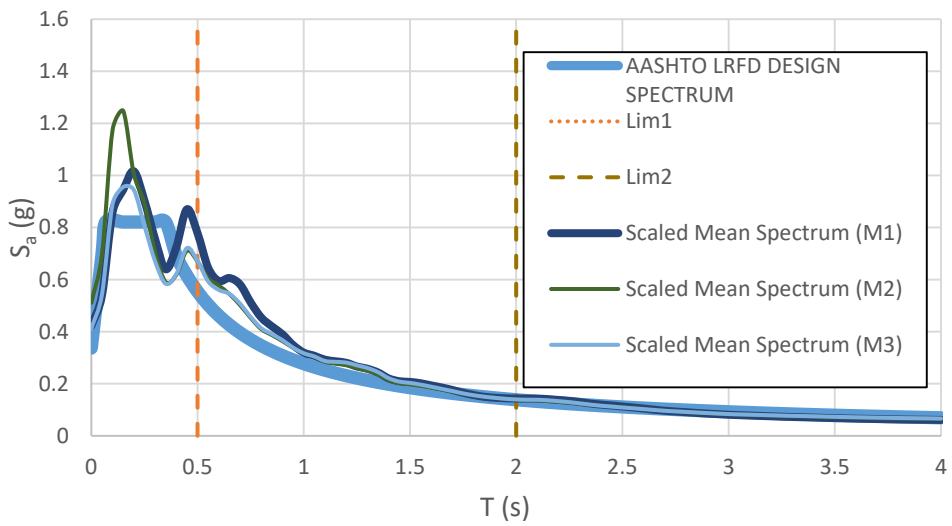


Figure 4.22. Scaled mean spectra for M1,M2 and M3 and AASHTO LRFD design response spectrum for SET-2

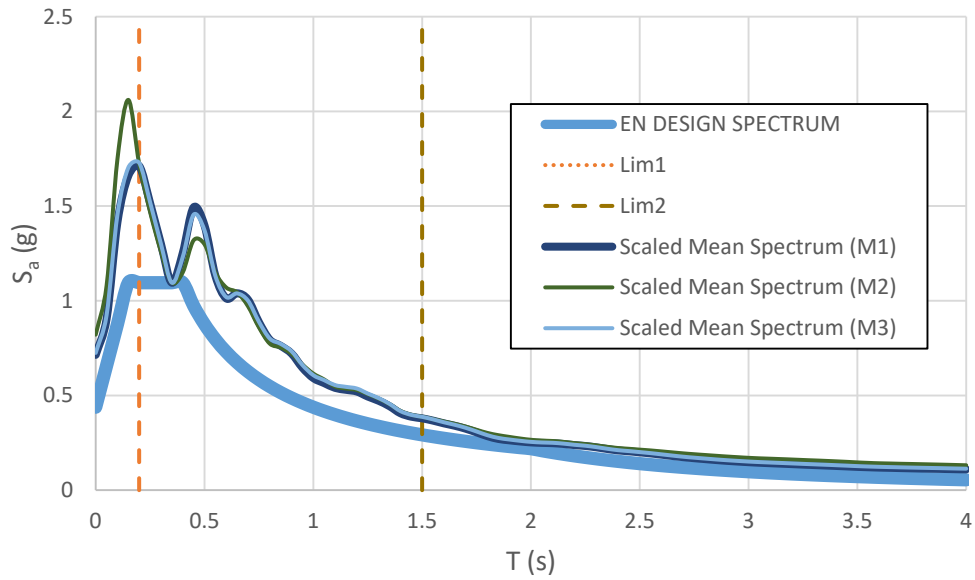


Figure 4.23. Scaled mean spectra for M1,M2 and M3 and EN 8 design response spectrum for SET-2

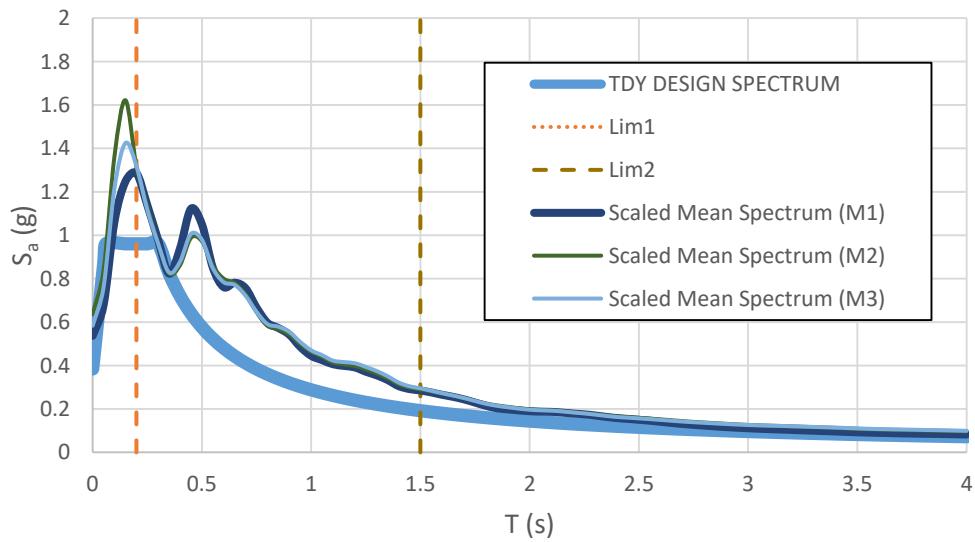


Figure 4.24. Scaled mean spectra for M1,M2 and M3 and TDY design response spectrum for SET-2

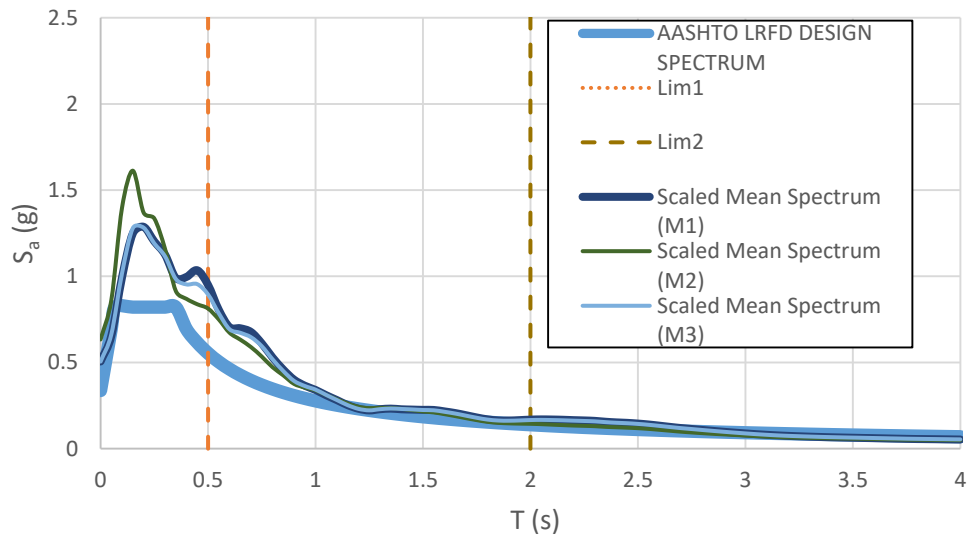


Figure 4.25. Scaled mean spectra for M1,M2 and M3 and AASHTO LRFD design response spectrum for SET-3

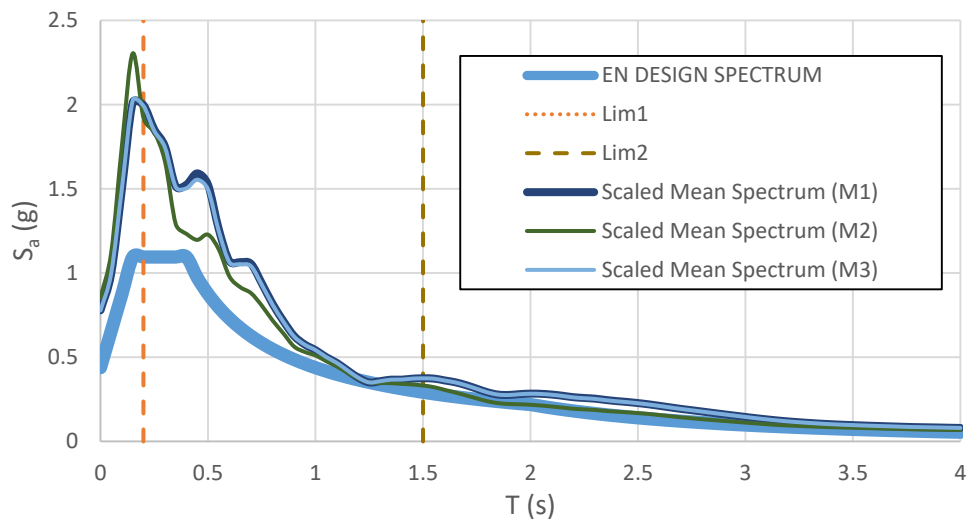


Figure 4.26. Scaled mean spectra for M1,M2 and M3 and EN 8 design response spectrum for SET-3

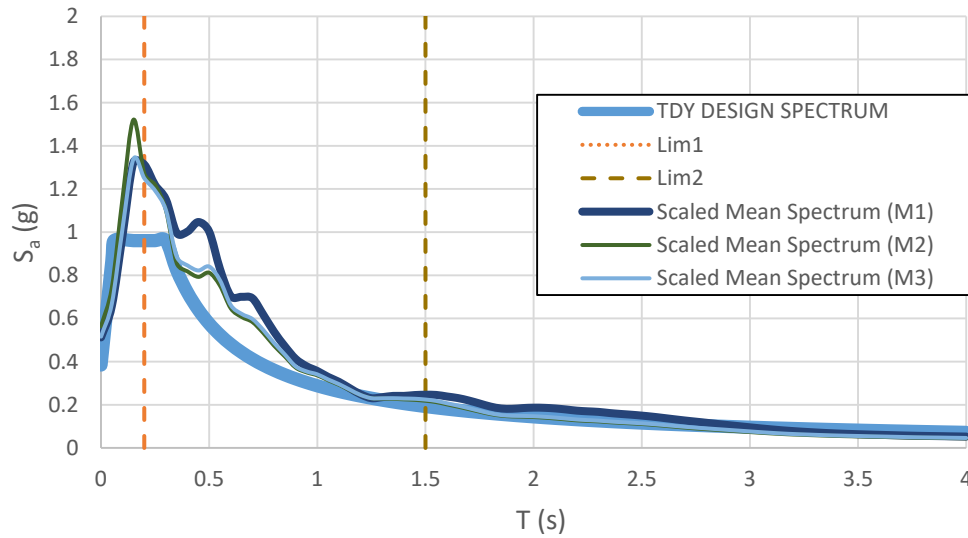


Figure 4.27. Scaled mean spectra for M1,M2 and M3 and TDY design response spectrum for SET-3

Comparison of the analysis results is made both for ground motion set-wise and bridge specification-wise and given in detail in the subsections 4.2.1 to 4.2.4 per scaling method. Although the seismic demand parameters M_x - M_y and u_x - u_y are taken as mean values of seven scaled earthquake ground motions, the results seem to be not strictly dependent on the ratio of the mean spectrum S_a values. For example, as shown in Table 4.67, for AASHTO LRFD spectral acceleration values are sorted larger to smaller as SET-3 > SET-1 > SET-2 at $t=1.00$ sec for all of the three scaling methods. On the contrary, moment and displacement values are sorted as SET-3 > SET-2 > SET-1 in both transverse direction (M_y) and longitudinal direction (M_x) for Method-1. For other methods and for EN-8 and TDY 2020 this comparison is likewise but sorting of sets differs.

This result can be explained with the diversity of the predominant periods of the earthquakes like V03 Bridge. V08 Bridge has 5 piers and when the seismic demand parameters are compared, it can be seen that dominant earthquakes are different for each pier column. To illustrate, while Sitka earthquake gives the maximum moment and displacement values for pier P2, Tottori earthquake governs for pier P3 in the same analysis with the same set of ground motions.

The change in the mean maximum moment values of the columns for the three bridge specifications is summarized for each scaling methods. Because the specification-wise percentage differences between the three ground motion sets are approximately the same for each pier column, results are tabulated according to P3 for demonstration in the next subsections 4.2.1, 4.2.2 and 4.2.3. However, ground motion set-wise percentage differences considerably vary for each pier column.

4.2.1 Comparison of Results for Scaling Method-1

In Method-1, while the maximum M_x and M_y values of SET-1 and SET-3 occur in pier P3, maximum M_y of SET-2 occurs in P2 and maximum M_x of SET-3 occurs in P3.

Sorting of maximum M_y values:

For AASHTO LRFD: SET-2 > SET-3 > SET-1 (163255 > 165978 > 139252) (kN.m)

For EN-8: SET-2 > SET-1 > SET-3 (198172 > 177888 > 173698) (kN.m)

For TDY 2020: SET2 > SET-1 > SET-3 (199151 > 116973 > 114218) (kN.m)

Sorting of maximum M_x values:

For AASHTO LRFD: SET-2 > SET-3 > SET-1 (131161 > 130152 > 117377) (kN.m)

For EN-8: SET-2 > SET-1 > SET-3 (156919 > 149944 > 138478) (kN.m)

For TDY 2020: SET-2 > SET-1 > SET-3 (162647 > 98598 > 91058) (kN.m)

In Method-1, the maximum u_x and u_y values of SET-1 and SET-3 occur in pier P3 unlike the moment values.

Sorting of maximum u_y values:

For AASHTO LRFD: SET-3 > SET-2 > SET-1 (1.95 > 1.93 > 1.66) (cm)

For EN-8: SET-2 > SET-1 > SET-3 (2.31 > 2.12 > 2.07) (cm)

For TDY 2020: SET2 > SET-1 > SET-3 (2.35 > 1.40 > 1.36) (cm)

Sorting of maximum u_x values:

For AASHTO LRFD: SET-2 > SET-3 > SET-1 (4.30 > 4.27 > 3.85) (cm)

For EN-8: SET-2 > SET-1 > SET-3 (5.14 > 4.92 > 4.54) (cm)

For TDY 2020: SET-2 > SET-1 > SET-3 (5.33 > 3.23 > 2.99) (cm)

Moment and displacement values are not very close to each other as it can be seen from the given results. When the results are sorted, it can be seen that specifications point to different sets as critical and there is a considerable amount of difference between both M_x, M_y and u_x, u_y values. Besides, the lowest moment values are obtained in scaling according to the TDY 2020. On the other hand, most critical values are computed from scaling according to the EN-8. On the other hand, the lowest displacement values are obtained in scaling according to the TDY 2020 except the SET-2 both in transverse and longitudinal directions. The most critical values are computed from scaling according to the EN-8 in SET-1 and SET-3.

Percentage difference given in the Tables 4.69-4.70, 4.72-4.73, 4.75-4.76 and 4.78-4.83 below are calculated based on the following equation;

$$\% = \frac{B-A}{A} \quad \text{Eq. (1)}$$

A: The result parameter taken as base

B: Compared result parameter

Table 4.68 The maximum M_y values of pier P3 for M1 (kN.m)

	P3-M_y		
	SET-1	SET-2	SET-3
AASHTO	139252.7	160288.8	163255.2
EN	177888.7	192295.5	173698.3
TDY	116973.7	195728.3	114218.2

Table 4.69 Specification-wise percentage differences of M_y values of pier P3 for M1

	Compared with AASHTO LRFD			Compared with EN-8			Compared with TDY 2020		
	SET-1	SET-2	SET-3	SET-1	SET-2	SET-3	SET-1	SET-2	SET-3
AASHTO	-	-	-	-22%	-17%	-6%	19%	-18%	43%
EN	28%	20%	6%	-	-	-	52%	-2%	52%
TDY	-16%	22%	-30%	-34%	2%	-34%	-	-	-

EN-8 gives the largest moment values compared to other codes. TDY2020, on the other hand results in lowest M_y values like the results of V03 Bridge.

Table 4.70 Ground motion set-wise percentage differences of M_y values of pier P3 for M1

	Compared with SET-1			Compared with SET-2			Compared with SET-3		
	SET-1	SET-2	SET-3	SET-1	SET-2	SET-3	SET-1	SET-2	SET-3
AASHTO	-	15%	17%	-13%	-	2%	-15%	-2%	-
EN	-	8%	-2%	-7%	-	-9.67%	2%	10.71%	-
TDY	-	67%	-2%	-40%	-	-42%	2%	71%	-

Table 4.71 The maximum M_x values of pier P3 for M1 (kN.m)

	P3-M_x		
	SET-1	SET-2	SET-3
AASHTO	117377.5	131161.4	130152.5
EN	149944.1	156919.2	138478.1
TDY	98598.28	162647.8	91058.59

Table 4.72 Specification-wise percentage differences of M_x values of pier P3 for M1

	Compared with AASHTO LRFD			Compared with EN-8			Compared with TDY 2020		
	SET-1	SET-2	SET-3	SET-1	SET-2	SET-3	SET-1	SET-2	SET-3
AASHTO	-	-	-	-22%	-16%	-6%	19%	-19%	43%
EN	28%	20%	6%	-	-	-	52%	-4%	52%
TDY	-16%	24%	-30%	-34%	4%	-34%	-	-	-

EN-8 gives the largest moment values compared to other codes. TDY2020, on the other hand results in lowest M_x values like the results of V03 Bridge.

Table 4.73 Ground motion set-wise percentage differences of M_x values of pier P3 for M1

	Compared with SET-1			Compared with SET-2			Compared with SET-3		
	SET-1	SET-2	SET-3	SET-1	SET-2	SET-3	SET-1	SET-2	SET-3
AASHTO	-	12%	11%	-11%	-	-1%	-10%	1%	-
EN	-	5%	-8%	-4%	-	-11.75%	8%	13.32%	-
TDY	-	65%	-8%	-39%	-	-44%	8%	79%	-

Table 4.74 The maximum u_y values of pier P3 for M1 (m)

	P3- u_y		
	SET-1	SET-2	SET-3
AASHTO	0.0166	0.0193	0.0195
EN	0.0212	0.0231	0.0207
TDY	0.0140	0.0235	0.0136

Table 4.75 Specification-wise percentage differences of u_y values of pier P3 for M1

	Compared with AASHTO LRFD			Compared with EN-8			Compared with TDY 2020		
	SET-1	SET-2	SET-3	SET-1	SET-2	SET-3	SET-1	SET-2	SET-3
AASHTO	-	-	-	-22%	-17%	-6%	19%	-18%	43%
EN	28%	20%	6%	-	-	-	52%	-2%	52%
TDY	-16%	22%	-30%	-34%	2%	-34%	-	-	-

EN-8 gives the largest moment values compared to other codes. TDY2020, on the other hand results in lowest u_y values except SET-2.

Table 4.76 Ground motion set-wise percentage differences of u_y values of pier P3 for M1

	Compared with SET-1			Compared with SET-2			Compared with SET-3		
	SET-1	SET-2	SET-3	SET-1	SET-2	SET-3	SET-1	SET-2	SET-3
AASHTO	-	16%	17%	-14%	-	1%	-15%	-1%	-
EN	-	9%	-2%	-8%	-	-10%	2%	12%	-
TDY	-	69%	-2%	-41%	-	-42%	2%	73%	-

Table 4.77 The maximum u_x values of pier P3 for M1 (m)

	P3-u_x		
	SET-1	SET-2	SET-3
AASHTO	0.0385	0.0430	0.0427
EN	0.0492	0.0514	0.0454
TDY	0.0323	0.0533	0.0299

Table 4.78 Specification-wise percentage differences of u_x values of pier P3 for M1

	Compared with AASHTO LRFD			Compared with EN-8			Compared with TDY 2020		
	SET-1	SET-2	SET-3	SET-1	SET-2	SET-3	SET-1	SET-2	SET-3
AASHTO	-	-	-	-22%	-16%	-6%	19%	-19%	43%
EN	28%	20%	6%	-	-	-	52%	-4%	52%
TDY	-16%	24%	-30%	-34%	4%	-34%	-	-	-

EN-8 gives the largest moment values compared to other codes. TDY2020, on the other hand results in lowest u_x values except SET-2.

Table 4.79 Ground motion set-wise percentage differences of u_x values of pier P3 for M1

	Compared with SET-1			Compared with SET-2			Compared with SET-3		
	SET-1	SET-2	SET-3	SET-1	SET-2	SET-3	SET-1	SET-2	SET-3
AASHTO	-	12%	11%	-10%	-	-1%	-10%	1%	-
EN	-	5%	-8%	-4%	-	-12%	8%	13%	-
TDY	-	65%	-8%	-39%	-	-44%	8%	79%	-

Table 4.80 Ground motion set-wise percentage differences of M_y values of all pier columns for M1

		Compared with SET-1			Compared with SET-2			Compared with SET-3		
		SET-1	SET-2	SET-3	SET-1	SET-2	SET-3	SET-1	SET-2	SET-3
P1-M_y	AASHTO	-	22%	20%	-18%	-	-2%	-17%	2%	-
	EN	-	10%	0%	-9%	-	-9%	0%	10%	-
	TDY	-	64%	0%	-39%	-	-39%	0%	63%	-
P2-M_y	AASHTO	-	22%	20%	-18%	-	-2%	-16%	2%	-
	EN	-	14%	0%	-13%	-	-13%	0%	15%	-
	TDY	-	75%	0%	-43%	-	-43%	0%	75%	-
P3-M_y	AASHTO	-	15%	17%	-13%	-	2%	-15%	-2%	-
	EN	-	8%	-2%	-7%	-	-10%	2%	11%	-
	TDY	-	67%	-2%	-40%	-	-42%	2%	71%	-
P4-M_y	AASHTO	-	54%	35%	-35%	-	-12%	-26%	14%	-
	EN	-	35%	12%	-26%	-	-17%	-11%	21%	-
	TDY	-	92%	12%	-48%	-	-42%	-11%	71%	-
P5-M_y	AASHTO	-	76%	38%	-43%	-	-22%	-28%	28%	-
	EN	-	52%	15%	-34%	-	-24%	-13%	32%	-
	TDY	-	107%	15%	-52%	-	-45%	-13%	80%	-

For most cases, SET-2 gives largest results for M_y whereas SET-1 results are generally smallest.

Table 4.81 Ground motion set-wise percentage differences of M_x values of all pier columns for M1

		Compared with SET-1			Compared with SET-2			Compared with SET-3		
		SET-1	SET-2	SET-3	SET-1	SET-2	SET-3	SET-1	SET-2	SET-3
P1-M_x	AASHTO	-	23%	26%	-18%	-	3%	-21%	-3%	-
	EN	-	14%	5%	-12%	-	-7%	-5%	8%	-
	TDY	-	74%	5%	-43%	-	-40%	-5%	65%	-
P2-M_x	AASHTO	-	16%	13%	-13%	-	-2%	-12%	2%	-
	EN	-	8%	-6%	-7%	-	-13%	6%	14%	-
	TDY	-	68%	-6%	-40%	-	-44%	6%	78%	-
P3-M_x	AASHTO	-	12%	11%	-11%	-	-1%	-10%	1%	-
	EN	-	5%	-8%	-4%	-	-12%	8%	13%	-
	TDY	-	65%	-8%	-39%	-	-44%	8%	79%	-
P4-M_x	AASHTO	-	27%	18%	-21%	-	-7%	-16%	7%	-
	EN	-	20%	-1%	-17%	-	-18%	1%	21%	-
	TDY	-	80%	-1%	-44%	-	-45%	1%	83%	-
P5-M_x	AASHTO	-	41%	30%	-29%	-	-8%	-23%	9%	-
	EN	-	28%	8%	-22%	-	-15%	-8%	18%	-
	TDY	-	89%	8%	-47%	-	-43%	-8%	74%	-

For most cases, SET-2 gives largest results for M_x whereas SET-1 results are generally smallest.

Table 4.82 Ground motion set-wise percentage differences of u_y values of all pier columns for M1

		Compared with SET-1			Compared with SET-2			Compared with SET-3		
		SET-1	SET-2	SET-3	SET-1	SET-2	SET-3	SET-1	SET-2	SET-3
P1- u_y	AASHTO	-	22%	20%	-18%	-	-2%	-16%	2%	-
	EN	-	10%	0%	-9%	-	-10%	0%	11%	-
	TDY	-	64%	0%	-39%	-	-39%	0%	65%	-
P2- u_y	AASHTO	-	23%	20%	-19%	-	-2%	-17%	2%	-
	EN	-	15%	0%	-13%	-	-13%	0%	15%	-
	TDY	-	76%	0%	-43%	-	-43%	0%	76%	-
P3- u_y	AASHTO	-	16%	17%	-14%	-	1%	-15%	-1%	-
	EN	-	9%	-2%	-8%	-	-10%	2%	11%	-
	TDY	-	69%	-2%	-41%	-	-42%	2%	73%	-
P4- u_y	AASHTO	-	46%	35%	-31%	-	-7%	-26%	8%	-
	EN	-	55%	12%	-35%	-	-27%	-11%	38%	-
	TDY	-	90%	12%	-47%	-	-41%	-11%	69%	-
P5- u_y	AASHTO	-	76%	38%	-43%	-	-22%	-27%	28%	-
	EN	-	52%	15%	-34%	-	-24%	-13%	32%	-
	TDY	-	107%	15%	-52%	-	-45%	-13%	81%	-

For most cases, SET-2 gives largest results for u_y whereas SET-1 results are generally smallest.

Table 4.83 Ground motion set-wise percentage differences of u_x values of all pier columns for M1

		Compared with SET-1			Compared with SET-2			Compared with SET-3		
		SET-1	SET-2	SET-3	SET-1	SET-2	SET-3	SET-1	SET-2	SET-3
P1-u_x	AASHTO	-	23%	26%	-18%	-	3%	-21%	-3%	-
	EN	-	14%	5%	-12%	-	-7%	-5%	8%	-
	TDY	-	74%	5%	-43%	-	-40%	-5%	65%	-
P2-u_x	AASHTO	-	16%	13%	-14%	-	-2%	-12%	2%	-
	EN	-	8%	-6%	-7%	-	-13%	6%	15%	-
	TDY	-	68%	-6%	-40%	-	-44%	6%	78%	-
P3-u_x	AASHTO	-	12%	11%	-10%	-	-1%	-10%	1%	-
	EN	-	5%	-8%	-4%	-	-12%	8%	13%	-
	TDY	-	65%	-8%	-39%	-	-44%	8%	79%	-
P4-u_x	AASHTO	-	27%	18%	-21%	-	-7%	-15%	7%	-
	EN	-	34%	-1%	-25%	-	-27%	1%	36%	-
	TDY	-	80%	-1%	-45%	-	-45%	1%	83%	-
P5-u_x	AASHTO	-	41%	30%	-29%	-	-8%	-23%	9%	-
	EN	-	28%	8%	-22%	-	-15%	-8%	18%	-
	TDY	-	89%	8%	-47%	-	-43%	-8%	74%	-

For most cases, SET-2 gives largest results for u_x whereas SET-1 results are generally smallest.

4.2.2 Comparison of Results for Scaling Method-2

In Method-2, the maximum M_x and M_y values of SET-1 occur in pier P3. In contrast, the maximum M_y values of SET-2 occur in pier P2 and the maximum M_x values of SET-2 occur in pier P3. And the maximum values of M_x values of SET-3 occur in pier P3. However, the maximum values of M_y occur in P3 for AASHTO LRFD scaling while the maximum M_y values occur in P2 for EN-8 and TDY scaling.

Sorting of maximum M_y values:

For AASHTO LRFD: SET-3 > SET-2 > SET-1 (176488 > 165978 > 155531) (kN.m)

For EN-8: SET-1 > SET-2 > SET-3 (198237 > 198172 > 178568) (kN.m)

For TDY 2020: SET-2 > SET-1 > SET-3 (150310 > 130584 > 117821) (kN.m)

Sorting of maximum M_x values:

For AASHTO LRFD: SET-3 > SET-2 > SET-1 (145369 > 131161 > 126285) (kN.m)

For EN-8: SET-1 > SET-2 > SET-3 (162565 > 156919 > 141980) (kN.m)

For TDY 2020: SET-2 > SET-1 > SET-3 (119023 > 106983 > 93620) (kN.m)

In Method-2, the maximum u_x and u_y values occur in pier P3 unlike the moment values.

Sorting of maximum u_y values:

For AASHTO LRFD: SET-3 > SET-2 > SET-1 (2.10 > 1.93 > 1.85) (cm)

For EN-8: SET-1 > SET-2 > SET-3 (2.37 > 2.31 > 2.10) (cm)

For TDY 2020: SET-2 > SET-1 > SET-3 (1.75 > 1.56 > 1.39) (cm)

Sorting of maximum u_x values:

For AASHTO LRFD: SET-3 > SET-2 > SET-1 (4.77 > 4.30 > 4.14) (cm)

For EN-8: SET-1 > SET-2 > SET-3 (5.33 > 5.14 > 4.65) (cm)

For TDY 2020: SET-2 > SET-1 > SET-3 (3.90 > 3.51 > 3.07) (cm)

The difference in the moment values are greater than the ones in Method-1 as it can be seen from the given results. When the results are sorted, it can be seen that specifications point to different sets as critical and there is a considerable amount of difference between both M_x , M_y and u_x , u_y values. Besides, the lowest moment and displacement values are obtained in scaling according to the TDY 2020. On the other hand, most critical values are computed from scaling according to the EN-8.

Percentage difference given in the Tables 4.85-4.86, 4.88-4.89, 4.91-4.92 and 4.92-4.99 below are calculated based on the Equation 1.

Table 4.84 The maximum M_y values of pier P3 for M2 (kN.m)

	P3-M_y		
	SET-1	SET-2	SET-3
AASHTO	155531.7	160288.8	176488.7
EN	198237.1	192295.5	176004.7
TDY	130584	145678.5	116227.9

Table 4.85 Specification-wise percentage differences of M_y values of pier P3 for M2

	Compared with AASHTO LRFD			Compared with EN-8			Compared with TDY 2020		
	SET-1	SET-2	SET-3	SET-1	SET-2	SET-3	SET-1	SET-2	SET-3
AASHTO	-	-	-	-22%	-17%	0%	19%	10%	52%
EN	27%	20%	-0.27%	-	-	-	52%	32%	51%
TDY	-16%	-9%	-34%	-34%	-24%	-34%	-	-	-

EN-8 gives the largest moment values compared to other codes. TDY2020, on the other hand results in lowest M_y values like the results of Method-1..

Table 4.86 Ground motion set-wise percentage differences of M_y values of pier P3 for M2

	Compared with SET-1			Compared with SET-2			Compared with SET-3		
	SET-1	SET-2	SET-3	SET-1	SET-2	SET-3	SET-1	SET-2	SET-3
AASHTO	-	3%	13%	-3%	-	10%	-12%	-9%	-
EN	-	-3%	-11%	3%	-	-9%	13%	9%	-
TDY	-	12%	-11%	-10%	-	-20%	12%	25%	-

Table 4.87 The maximum M_x values of pier P3 for M2 (kN.m)

	P3- M_x		
	SET-1	SET-2	SET-3
AASHTO	126285	131161.4	145369.2
EN	162565.2	156919.2	141980
TDY	106983.8	119023.9	93620.89

Table 4.88 Specification-wise percentage differences of M_x values of pier P3 for M2

	Compared with AASHTO LRFD			Compared with EN-8			Compared with TDY 2020		
	SET-1	SET-2	SET-3	SET-1	SET-2	SET-3	SET-1	SET-2	SET-3
AASHTO	-	-	-	-22%	-16%	2%	18%	10%	55%
EN	29%	20%	-2 %	-	-	-	52%	32%	52%
TDY	-15%	-9%	-36%	-34%	-24%	-34%	-	-	-

EN-8 gives the largest moment values compared to other codes. TDY2020, on the other hand results in lowest M_x values like the results of Method-1.

Table 4.89 Ground motion set-wise percentage differences of M_x values of pier P3 for M2

	Compared with SET-1			Compared with SET-2			Compared with SET-3		
	SET-1	SET-2	SET-3	SET-1	SET-2	SET-3	SET-1	SET-2	SET-3
AASHTO	-	4%	15%	-4%	-	11%	-13%	-10%	-
EN	-	-3%	-13%	4%	-	-9.52%	14%	10.52%	-
TDY	-	11%	-12%	-10%	-	-21%	14%	27%	-

Table 4.90 The maximum u_y values of pier P3 for M2 (m)

	P3- u_y		
	SET-1	SET-2	SET-3
AASHTO	0.0185	0.0193	0.0210
EN	0.0237	0.0231	0.0210
TDY	0.0156	0.0175	0.0139

Table 4.91 Specification-wise percentage differences of u_y values of pier P3 for M2

	Compared with AASHTO LRFD			Compared with EN-8			Compared with TDY 2020		
	SET-1	SET-2	SET-3	SET-1	SET-2	SET-3	SET-1	SET-2	SET-3
AASHTO	-	-	-	-22%	-17%	0%	19%	10%	51%
EN	28%	20%	0%	-	-	-	52%	32%	51%
TDY	-16%	-9%	-34%	-34%	-24%	-34%	-	-	-

EN-8 gives the largest moment values compared to other codes. TDY2020, on the other hand results in lowest u_y values.

Table 4.92 Ground motion set-wise percentage differences of u_y values of pier P3 for M2

	Compared with SET-1			Compared with SET-2			Compared with SET-3		
	SET-1	SET-2	SET-3	SET-1	SET-2	SET-3	SET-1	SET-2	SET-3
AASHTO	-	4%	13%	-4%	-	9%	-12%	-8%	-
EN	-	-2%	-11%	2%	-	-9%	13%	10%	-
TDY	-	12%	-11%	-11%	-	-21%	12%	26%	-

Table 4.93 The maximum u_x values of pier P3 for M2 (m)

	P3-u_x		
	SET-1	SET-2	SET-3
AASHTO	0.0414	0.0430	0.0477
EN	0.0533	0.0514	0.0465
TDY	0.0351	0.0390	0.0307

Table 4.94 Specification-wise percentage differences of u_x values of pier P3 for M2

	Compared with AASHTO LRFD			Compared with EN-8			Compared with TDY 2020		
	SET-1	SET-2	SET-3	SET-1	SET-2	SET-3	SET-1	SET-2	SET-3
AASHTO	-	-	-	-22%	-16%	2%	18%	10%	55%
EN	29%	20%	-2.33%	-	-	-	52%	32%	52%
TDY	-15%	-9%	-36%	-34%	-24%	-34%	-	-	-

EN-8 gives the largest moment values compared to other codes. TDY2020, on the other hand results in lowest u_x values.

Table 4.95 Ground motion set-wise percentage differences of u_x values of pier P3 for M2

	Compared with SET-1			Compared with SET-2			Compared with SET-3		
	SET-1	SET-2	SET-3	SET-1	SET-2	SET-3	SET-1	SET-2	SET-3
AASHTO	-	4%	15%	-4%	-	11%	-13%	-10%	-
EN	-	-3%	-13%	4%	-	-10%	15%	11%	-
TDY	-	11%	-12%	-10%	-	-21%	14%	27%	-

Table 4.96 Ground motion set-wise percentage differences of M_y values of all pier columns for M2

		Compared with SET-1			Compared with SET-2			Compared with SET-3		
		SET-1	SET-2	SET-3	SET-1	SET-2	SET-3	SET-1	SET-2	SET-3
P1- M_y	AASHTO	-	10%	28%	-9%	-	16%	-22%	-14%	-
	EN	-	0%	-5%	0%	-	-5%	5%	5%	-
	TDY	-	16%	-5%	-14%	-	-18%	5%	21%	-
P2- M_y	AASHTO	-	7%	12%	-7%	-	5%	-11%	-5%	-
	EN	-	0%	-10%	0%	-	-10%	11%	11%	-
	TDY	-	15%	-10%	-13%	-	-22%	11%	28%	-
P3- M_y	AASHTO	-	3%	13%	-3%	-	10%	-12%	-9%	-
	EN	-	-3%	-11%	3%	-	-8%	13%	9%	-
	TDY	-	12%	-11%	-10%	-	-20%	12%	25%	-
P4- M_y	AASHTO	-	30%	45%	-23%	-	11%	-31%	-10%	-
	EN	-	15%	9%	-13%	-	-5%	-8%	5%	-
	TDY	-	34%	9%	-25%	-	-19%	-9%	23%	-
P5- M_y	AASHTO	-	51%	56%	-34%	-	3%	-36%	-3%	-
	EN	-	31%	15%	-23%	-	-12%	-13%	14%	-
	TDY	-	54%	15%	-35%	-	-25%	-13%	34%	-

For most cases, SET-2 gives largest results for M_y whereas SET-1 results are generally smallest like the results of Method-1.

Table 4.97 Ground motion set-wise percentage differences of M_x values of all pier columns for M2

		Compared with SET-1			Compared with SET-2			Compared with SET-3		
		SET-1	SET-2	SET-3	SET-1	SET-2	SET-3	SET-1	SET-2	SET-3
P1-M_x	AASHTO	-	5%	27%	-4%	-	21%	-21%	-18%	-
	EN	-	-2%	-2%	3%	-	0%	2%	0%	-
	TDY	-	12%	-2%	-11%	-	-13%	2%	15%	-
P2-M_x	AASHTO	-	9%	21%	-8%	-	11%	-17%	-10%	-
	EN	-	1%	-9%	-1%	-	-9%	10%	10%	-
	TDY	-	16%	-9%	-14%	-	-21%	9%	27%	-
P3-M_x	AASHTO	-	4%	15%	-4%	-	11%	-13%	-10%	-
	EN	-	-3%	-13%	4%	-	-10%	14%	11%	-
	TDY	-	11%	-12%	-10%	-	-21%	14%	27%	-
P4-M_x	AASHTO	-	8%	17%	-8%	-	8%	-14%	-7%	-
	EN	-	3%	-11%	-3%	-	-13%	12%	15%	-
	TDY	-	18%	-10%	-15%	-	-24%	12%	32%	-
P5-M_x	AASHTO	-	23%	34%	-19%	-	9%	-26%	-9%	-
	EN	-	12%	1%	-10%	-	-10%	-1%	11%	-
	TDY	-	29%	1%	-23%	-	-22%	-1%	28%	-

For most cases, SET-2 gives largest results for M_x whereas SET-1 results are generally smallest like the results of Method-1.

Table 4.98 Ground motion set-wise percentage differences of u_y values of all pier columns for M2

		Compared with SET-1			Compared with SET-2			Compared with SET-3		
		SET-1	SET-2	SET-3	SET-1	SET-2	SET-3	SET-1	SET-2	SET-3
P1- u_y	AASHTO	-	10%	27%	-9%	-	16%	- 21%	- 14%	-
	EN	-	0%	-6%	0%	-	-5%	6%	6%	-
	TDY	-	16%	-5%	- 14%	-	- 18%	6%	22%	-
P2- u_y	AASHTO	-	7%	12%	-7%	-	5%	- 11%	-4%	-
	EN	-	0%	- 10%	0%	-	- 10%	11%	11%	-
	TDY	-	15%	- 10%	- 13%	-	- 22%	11%	28%	-
P3- u_y	AASHTO	-	4%	13%	-4%	-	9%	- 12%	-8%	-
	EN	-	-2%	- 11%	2%	-	-9%	13%	10%	-
	TDY	-	12%	- 11%	- 11%	-	- 21%	12%	26%	-
P4- u_y	AASHTO	-	30%	44%	- 23%	-	11%	- 30%	- 10%	-
	EN	-	15%	9%	- 13%	-	-5%	-8%	6%	-
	TDY	-	34%	9%	- 26%	-	- 19%	-8%	23%	-
P5- u_y	AASHTO	-	51%	56%	- 34%	-	3%	- 36%	-3%	-
	EN	-	31%	15%	- 23%	-	- 12%	- 13%	14%	-
	TDY	-	54%	15%	- 35%	-	- 25%	- 13%	34%	-

For most cases, SET-2 gives largest results for u_y whereas SET-1 results are generally smallest like the results of Method-1.

Table 4.99 Ground motion set-wise percentage differences of u_x values of all pier columns for M2

		Compared with SET-1			Compared with SET-2			Compared with SET-3		
		SET-1	SET-2	SET-3	SET-1	SET-2	SET-3	SET-1	SET-2	SET-3
P1- u_x	AASHTO	-	5%	27%	-4%	-	21%	-	-	-
	EN	-	-2%	-2%	3%	-	0%	2%	0%	-
	TDY	-	12%	-2%	-	-	-	2%	15%	-
P2- u_x	AASHTO	-	9%	21%	-8%	-	11%	-	-	-
	EN	-	1%	-9%	-1%	-	-9%	10%	10%	-
	TDY	-	16%	-9%	-	-	-	9%	27%	-
P3- u_x	AASHTO	-	4%	15%	-4%	-	11%	-	-	-
	EN	-	-3%	-	4%	-	-	15%	11%	-
	TDY	-	11%	-	-	-	-	14%	27%	-
P4- u_x	AASHTO	-	9%	17%	-8%	-	8%	-	-	-
	EN	-	3%	-	-3%	-	-	12%	15%	-
	TDY	-	18%	-	-	-	-	12%	32%	-
P5- u_x	AASHTO	-	23%	34%	-	-	9%	-	-	-
	EN	-	12%	1%	-	-	-	-1%	11%	-
	TDY	-	29%	1%	-	-	-	-1%	28%	-

For most cases, SET-2 gives largest results for u_x whereas SET-1 results are generally smallest.

4.2.3 Comparison of Results for Scaling Method-3

In Method-3, the maximum M_x and M_y values of SET-1 occur in pier P3. The maximum M_y values of SET-2 occur in pier P2 and the maximum M_x values of SET-2 occur in pier P3. Differently, while the maximum values of M_x and M_y of SET-3 occur in pier P3 according to AASHTO LRFD and EN-8, the maximum values of M_y of SET-3 occur in P2 and the maximum values of M_x occur in P3 according to TDY 2020.

Sorting of maximum M_y values:

For AASHTO LRFD: SET-2 > SET-3>SET-1 (162301> 161692> 145423) (kN.m)

For EN-8: SET-2>SET-1> SET-3 (203082> 179202> 172912) (kN.m)

For TDY 2020:SET2 > SET-1> SET-3 (151965> 129233> 116759) (kN.m)

Sorting of maximum M_x values:

For AASHTO LRFD: SET-2 > SET-3>SET-1 (132017> 129583> 120995) (kN.m)

For EN-8: SET-2>SET-1> SET-3 (166267> 151150> 138045) (kN.m)

For TDY 2020: SET-2> SET-1 >SET-3 (122406> 107574> 93904) (kN.m)

In Method-3, the maximum u_x and u_y values occur in pier P3 unlike the moment values.

Sorting of maximum u_y values:

For AASHTO LRFD: SET-3 > SET-2>SET-1 (1.93> 1.92> 1.73) (cm)

For EN-8: SET-2>SET-1> SET-3 (2.40> 2.14> 2.06) (cm)

For TDY 2020:SET2 > SET-1> SET-3 (1.79> 1.54> 1.38) (cm)

Sorting of maximum u_x values:

For AASHTO LRFD: SET-2 > SET-3 > SET-1 (4.33 > 4.29 > 3.97) (cm)

For EN-8: SET-2 > SET-1 > SET-3 (5.45 > 4.96 > 4.53) (cm)

For TDY 2020: SET-2 > SET-1 > SET-3 (4.01 > 3.53 > 3.08) (cm)

The difference in the moment values are greater than the ones in Method-1 and Method-2 as it can be seen from the given results. When the results are sorted, it can be seen that specifications point to different sets as critical and there is a considerable amount of difference between both M_x , M_y and u_x , u_y values. Besides, the lowest moment values are obtained in scaling according to the TDY 2020. On the other hand, most critical values are computed from scaling according to the EN-8.

Percentage difference given in the Tables 4.101-4.102, 4.104-4.105, 4.107-4.108 and 4.110-4.115 below are calculated based on the Equation 1.

Table 4.100 The maximum M_y values of pier P3 for M3 (kN.m)

	P3-M_y		
	SET-1	SET-2	SET-3
AASHTO	145423.4	159171.5	161692.6
EN	179202	199351.8	172912.5
TDY	129233.8	148698.2	115591.6

Table 4.101 Specification-wise percentage differences of M_y values of pier P3 for M3

	Compared with AASHTO LRFD			Compared with EN-8			Compared with TDY 2020		
	SET-1	SET-2	SET-3	SET-1	SET-2	SET-3	SET-1	SET-2	SET-3
AASHTO	-	-	-	-19%	-20%	-6%	13%	7%	40%
EN	23%	25%	7%	-	-	-	39%	34%	50%
TDY	-11%	-7%	-29%	-28%	-25%	-33%	-	-	-

EN-8 gives the largest moment values compared to other codes. TDY2020, on the other hand results in lowest M_y values like the results of Method-1 and Method-2.

Table 4.102 Ground motion set-wise percentage differences of M_y values of pier P3 for M3

	Compared with SET-1			Compared with SET-2			Compared with SET-3		
	SET-1	SET-2	SET-3	SET-1	SET-2	SET-3	SET-1	SET-2	SET-3
AASHTO	-	9%	11%	-9%	-	2%	-10%	-2%	-
EN	-	11%	-4%	-10%	-	-13%	4%	15%	-
TDY	-	15%	-11%	-13%	-	-22%	12%	29%	-

Table 4.103 The maximum M_x values of pier P3 for M3 (kN.m)

	P3- M_x		
	SET-1	SET-2	SET-3
AASHTO	120995	132017.3	129583.2
EN	151150.8	166267.9	138045.9
TDY	107574.5	122406.7	93904.17

Table 4.104 Specification-wise percentage differences of M_x values of pier P3 for M3

	Compared with AASHTO LRFD			Compared with EN-8			Compared with TDY 2020		
	SET-1	SET-2	SET-3	SET-1	SET-2	SET-3	SET-1	SET-2	SET-3
AASHTO	-	-	-	-20%	-21%	-6%	12%	8%	38%
EN	25%	26%	7%	-	-	-	41%	36%	47%
TDY	-11%	-7%	-28%	-29%	-26%	-32%	-	-	-

EN-8 gives the largest moment values compared to other codes. TDY2020, on the other hand results in lowest M_x values like the results of Method-1.

Table 4.105 Ground motion set-wise percentage differences of M_x values of pier P3 for M3

	Compared with SET-1			Compared with SET-2			Compared with SET-3		
	SET-1	SET-2	SET-3	SET-1	SET-2	SET-3	SET-1	SET-2	SET-3
AASHTO	-	9%	7%	-8%	-	-2%	-7%	2%	-
EN	-	10%	-9%	-9%	-	-17%	9%	20%	-
TDY	-	14%	-13%	-12%	-	-23%	15%	30%	-

Table 4.106 The maximum u_y values of pier P3 for M3 (m)

	P3- u_y		
	SET-1	SET-2	SET-3
AASHTO	0.0174	0.0191	0.0193
EN	0.0214	0.0240	0.0206
TDY	0.0154	0.0179	0.0138

Table 4.107 Specification-wise percentage differences of u_y values of pier P3 for M3

	Compared with AASHTO LRFD			Compared with EN-8			Compared with TDY 2020		
	SET-1	SET-2	SET-3	SET-1	SET-2	SET-3	SET-1	SET-2	SET-3
AASHTO	-	-	-	-19%	-20%	-6%	13%	7%	40%
EN	23%	25%	7%	-	-	-	39%	34%	49%
TDY	-11%	-7%	-28%	-28%	-25%	-33%	-	-	-

EN-8 gives the largest displacement values compared to other codes. TDY2020, on the other hand results in lowest u_y values.

Table 4.108 Ground motion set-wise percentage differences of u_y values of pier P3 for M3

	Compared with SET-1			Compared with SET-2			Compared with SET-3		
	SET-1	SET-2	SET-3	SET-1	SET-2	SET-3	SET-1	SET-2	SET-3
AASHTO	-	10%	11%	-9%	-	1%	-10%	-1%	-
EN	-	12%	-3%	-11%	-	-14%	4%	16%	-
TDY	-	16%	-11%	-14%	-	-23%	12%	29%	-

Table 4.109 The maximum u_x values of pier P3 for M3 (m)

	P3-u_x		
	SET-1	SET-2	SET-3
AASHTO	0.0397	0.0433	0.0425
EN	0.0496	0.0545	0.0453
TDY	0.0353	0.0401	0.0308

Table 4.110 Specification-wise percentage differences of u_x values of pier P3 for M3

	Compared with AASHTO LRFD			Compared with EN-8			Compared with TDY 2020		
	SET-1	SET-2	SET-3	SET-1	SET-2	SET-3	SET-1	SET-2	SET-3
AASHTO	-	-	-	-20%	-21%	-6%	12%	8%	38%
EN	25%	26%	7%	-	-	-	41%	36%	47%
TDY	-11%	-7%	-28%	-29%	-26%	-32%	-	-	-

EN-8 gives the largest displacement values compared to other codes. TDY2020, on the other hand results in lowest u_x values.

Table 4.111 Ground motion set-wise percentage differences of u_x values of pier P3 for M3

	Compared with SET-1			Compared with SET-2			Compared with SET-3		
	SET-1	SET-2	SET-3	SET-1	SET-2	SET-3	SET-1	SET-2	SET-3
AASHTO	-	9%	7%	-8%	-	-2%	-7%	2%	-
EN	-	10%	-9%	-9%	-	-17%	10%	20%	-
TDY	-	14%	-13%	-12%	-	-23%	15%	30%	-

Table 4.112 Ground motion set-wise percentage differences of M_y values of all pier columns for M3

		Compared with SET-1			Compared with SET-2			Compared with SET-3		
		SET-1	SET-2	SET-3	SET-1	SET-2	SET-3	SET-1	SET-2	SET-3
P1- M_y	AASHTO	-	10%	17%	-9%	-	7%	-15%	-6%	-
	EN	-	10%	0%	-9%	-	-9%	0%	10%	-
	TDY	-	17%	-7%	-14%	-	-20%	7%	25%	-
P2- M_y	AASHTO	-	15%	14%	-13%	-	-1%	-12%	1%	-
	EN	-	16%	-2%	-14%	-	-15%	2%	18%	-
	TDY	-	20%	-8%	-17%	-	-23%	8%	30%	-
P3- M_y	AASHTO	-	9%	11%	-9%	-	2%	-10%	-2%	-
	EN	-	11%	-4%	-10%	-	-13%	4%	15%	-
	TDY	-	15%	-11%	-13%	-	-22%	12%	29%	-
P4- M_y	AASHTO	-	28%	28%	-22%	-	1%	-22%	-1%	-
	EN	-	29%	11%	-22%	-	-14%	-10%	16%	-
	TDY	-	34%	7%	-26%	-	-20%	-7%	25%	-
P5- M_y	AASHTO	-	42%	34%	-30%	-	-6%	-25%	6%	-
	EN	-	39%	14%	-28%	-	-18%	-13%	22%	-
	TDY	-	53%	11%	-35%	-	-27%	-10%	38%	-

For most cases, SET-2 gives largest results for M_y whereas SET-1 results are generally smallest like the results of Method-1 and Method-2.

Table 4.113 Ground motion set-wise percentage differences of M_x values of all pier columns for M3

		Compared with SET-1			Compared with SET-2			Compared with SET-3		
		SET-1	SET-2	SET-3	SET-1	SET-2	SET-3	SET-1	SET-2	SET-3
P1- M_x	AASHTO	-	11%	18%	-10%	-	6%	-15%	-6%	-
	EN	-	16%	4%	-13%	-	-10%	-4%	11%	-
	TDY	-	15%	-1%	-13%	-	-14%	1%	17%	-
P2- M_x	AASHTO	-	11%	10%	-10%	-	-1%	-9%	2%	-
	EN	-	12%	-7%	-11%	-	-17%	7%	20%	-
	TDY	-	17%	-10%	-14%	-	-23%	12%	30%	-
P3- M_x	AASHTO	-	9%	7%	-8%	-	-2%	-7%	2%	-
	EN	-	10%	-9%	-9%	-	-17%	9%	20%	-
	TDY	-	14%	-13%	-12%	-	-23%	15%	30%	-
P4- M_x	AASHTO	-	20%	13%	-17%	-	-6%	-12%	6%	-
	EN	-	20%	-3%	-17%	-	-19%	3%	23%	-
	TDY	-	24%	-8%	-20%	-	-26%	8%	35%	-
P5- M_x	AASHTO	-	26%	25%	-20%	-	0%	-20%	0%	-
	EN	-	26%	7%	-21%	-	-15%	-7%	17%	-
	TDY	-	33%	1%	-25%	-	-24%	-1%	31%	-

For most cases, SET-2 gives largest results for M_x whereas SET-1 results are generally smallest like the results of Method-1 and Method-2.

Table 4.114 Ground motion set-wise percentage differences of u_y values of all pier columns for M3

		Compared with SET-1			Compared with SET-2			Compared with SET-3		
		SET-1	SET-2	SET-3	SET-1	SET-2	SET-3	SET-1	SET-2	SET-3
P1- u_y	AASHTO	-	10%	17%	-9%	-	6%	-14%	-6%	-
	EN	-	10%	-1%	-9%	-	-10%	1%	11%	-
	TDY	-	17%	-7%	-15%	-	-21%	8%	26%	-
P2- u_y	AASHTO	-	15%	13%	-13%	-	-1%	-12%	1%	-
	EN	-	17%	-1%	-15%	-	-16%	1%	19%	-
	TDY	-	21%	-8%	-17%	-	-23%	8%	31%	-
P3- u_y	AASHTO	-	10%	11%	-9%	-	1%	-10%	-1%	-
	EN	-	12%	-3%	-11%	-	-14%	4%	16%	-
	TDY	-	16%	-11%	-14%	-	-23%	12%	29%	-
P4- u_y	AASHTO	-	28%	28%	-22%	-	0%	-22%	0%	-
	EN	-	30%	11%	-23%	-	-14%	-10%	16%	-
	TDY	-	35%	7%	-26%	-	-21%	-7%	26%	-
P5- u_y	AASHTO	-	43%	34%	-30%	-	-6%	-25%	7%	-
	EN	-	40%	14%	-28%	-	-18%	-12%	22%	-
	TDY	-	53%	11%	-35%	-	-28%	-10%	38%	-

For most cases, SET-2 gives largest results for u_y whereas SET-1 results are generally smallest like the results of Method-1 and Method-2.

Table 4.115 Ground motion set-wise percentage differences of u_x values of all pier columns for M3

		Compared with SET-1			Compared with SET-2			Compared with SET-3		
		SET-1	SET-2	SET-3	SET-1	SET-2	SET-3	SET-1	SET-2	SET-3
P1-u_x	AASHTO	-	11%	18%	-10%	-	6%	-15%	-6%	-
	EN	-	16%	4%	-13%	-	-10%	-4%	11%	-
	TDY	-	15%	-1%	-13%	-	-14%	1%	17%	-
P2-u_x	AASHTO	-	12%	10%	-10%	-	-2%	-9%	2%	-
	EN	-	12%	-7%	-11%	-	-17%	7%	20%	-
	TDY	-	17%	-10%	-14%	-	-23%	12%	30%	-
P3-u_x	AASHTO	-	9%	7%	-8%	-	-2%	-7%	2%	-
	EN	-	10%	-9%	-9%	-	-17%	10%	20%	-
	TDY	-	14%	-13%	-12%	-	-23%	15%	30%	-
P4-u_x	AASHTO	-	20%	13%	-17%	-	-6%	-12%	6%	-
	EN	-	20%	-3%	-17%	-	-19%	3%	23%	-
	TDY	-	25%	-8%	-20%	-	-26%	8%	35%	-
P5-u_x	AASHTO	-	26%	25%	-20%	-	0%	-20%	0%	-
	EN	-	26%	7%	-21%	-	-15%	-7%	17%	-
	TDY	-	33%	1%	-25%	-	-24%	-1%	31%	-

For most cases, SET-2 gives largest results for u_x whereas SET-1 results are generally smallest like the results of Method-1 and Method-2.

4.2.4 Summary of the Comparison Results

It can be seen that the most critical values of moments and displacements do not always occur in the same column and in the same ground motion set. While for a method SET-3 gives the critical moment values, SET-1 gives the critical displacement values. Sorting of the ground motion sets for displacement values become less different than the sorting of the sets for moments unlike in V03 Bridge. Critical displacement values are observed in the highest column as expected. The percentage differences of both ground motion set-wise and specification-wise are the same in moment and displacement values. Thus, the summary of the comparison results are mostly focused on the moment values.

It can be concluded that when the specification-based comparison is considered, scaling according to the Eurocode-8 design spectrum resulted in the greater moment values than AASHTO LRFD and TDY 2020 for ground motion sets SET-1 and SET-2.

However only for the ground motion set SET-3, while the moment values for AASHTO LRFD are greater than Eurocode-8 by applying the Method-2, values for AASHTO LRFD become less than Eurocode-8 for Method-1 and Method-3.

Although scaling according to the TDY 2020 design spectrum gives the minimum moment values with significant differences for Method-2 and Method-3, the moment values become approximately the same with Eurocode-8 for ground motion set SET-2 of Method-1.

The moments in the pier column are given in the previous chapters. The moments show that the most consistent scaling method appears to be Eurocode-8. The moment values are not changing in Eurocode-8 unlike in other specifications in different sets. Also, most critical moment values comes from Eurocode-8 specification. Least critical method appears to be TDY as in V03 Bridge. There is lack of consistency between the codes.

When the scaling method-based comparison is considered, results are variable between the five pier columns for specification as well.

As can be seen from Figure 4.28 and 4.29, for *AASHTO LRFD* design spectrum scaling, maximum M_x and M_y moments occurs in Method-2 for all of the columns for the ground motion SET-1 and SET-3. By Method-1 and Method-3, moment values are close to each other. However for SET-2, moment values are close to each other among all of the methods.

For the bridge transverse (M_y) and longitudinal direction (M_x), when the three ground motion sets applied for each method are compared, SET-2 and SET-3 gives the maximum and more or less the same moment values for all of the columns, and those values are greater than the SET-1.

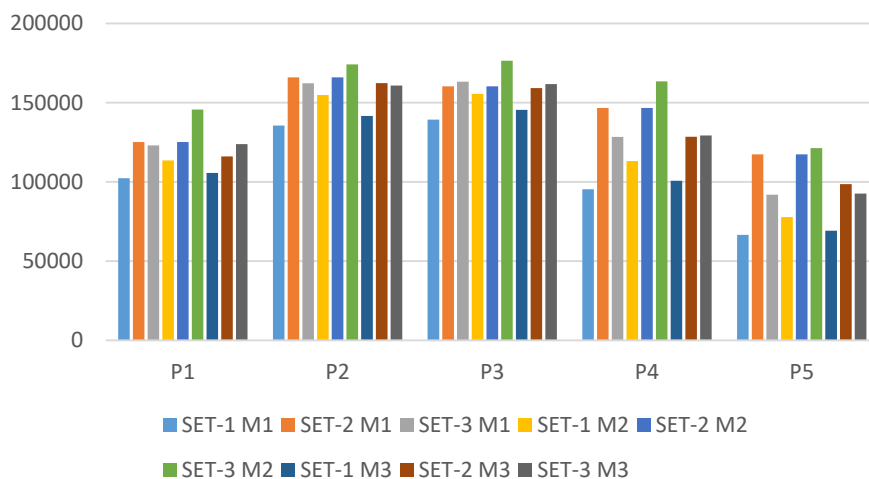


Figure 4.28. M_y values of all of the pier columns for three scaling methods applied according to AASHTO LRFD (kN.m)

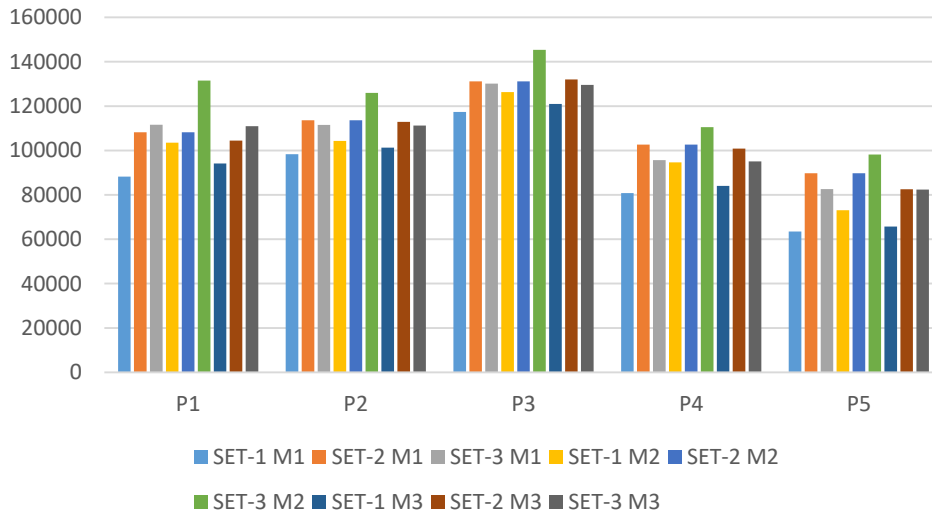


Figure 4.29. M_x values of all of the pier columns for three scaling methods applied according to AASHTO LRFD (kN.m)

It can be said that by following the AASHTO LRFD specification for the design, for the transverse and longitudinal directions Method-2 gives the maximum moment values. Method-wise percentage differences can be seen from Tables 116-118. In the case of the selection of ground motion sets, SET-2 and SET-3 gives the maximum moment values. It can be concluded that, time history analysis AASHTO LRFD design spectrum for a bridge having a fundamental period equals to 1 ($T_n=1$) can be done by using scaling method Method-2 and ground motion set SET-2 or SET-3.

Table 4.116 AASHTO LRFD method-wise differences for SET-1

	AASHTO LRFD M2-M _y			AASHTO LRFD M3-M _x		
	Compared with M1			Compared with M1		
	SET-1 M1	SET-1 M2	SET-1 M3	SET-1 M1	SET-1 M2	SET-1 M3
P1	-	0.110	0.032	-	0.173	0.066
P2	-	0.142	0.045	-	0.061	0.030
P3	-	0.117	0.044	-	0.076	0.031
P4	-	0.186	0.056	-	0.172	0.040
P5	-	0.168	0.039	-	0.151	0.035

	Compared with M2			Compared with M2		
	SET-1 M1	SET-1 M2	SET-1 M3	SET-1 M1	SET-1 M2	SET-1 M3
P1	-0.099	-	-0.070	-0.147	-	-0.091
P2	-0.125	-	-0.085	-0.057	-	-0.029
P3	-0.105	-	-0.065	-0.071	-	-0.042
P4	-0.157	-	-0.110	-0.147	-	-0.112
P5	-0.144	-	-0.110	-0.131	-	-0.101

	Compared with M3			Compared with M3		
	SET-1 M1	SET-1 M2	SET-1 M3	SET-1 M1	SET-1 M2	SET-1 M3
P1	-0.031	0.075	-	-0.062	0.100	-
P2	-0.043	0.093	-	-0.029	0.030	-
P3	-0.042	0.070	-	-0.030	0.044	-
P4	-0.053	0.123	-	-0.039	0.127	-
P5	-0.038	0.123	-	-0.034	0.112	-

Table 4.117 AASHTO LRFD method-wise differences for SET-2

	AASHTO LRFD M2-M _y			AASHTO LRFD M3-M _x		
	Compared with M1			Compared with M1		
	SET-2 M1	SET-2 M2	SET-2 M3	SET-2 M1	SET-2 M2	SET-2 M3
P1	-	0.000	-0.073	-	0.000	-0.035
P2	-	0.000	-0.022	-	0.000	-0.006
P3	-	0.000	-0.007	-	0.000	0.007
P4	-	0.000	-0.124	-	0.000	-0.017
P5	-	0.000	-0.160	-	0.000	-0.080

	Compared with M2			Compared with M2		
	SET-2 M1	SET-2 M2	SET-2 M3	SET-2 M1	SET-2 M2	SET-2 M3
P1	0.000	-	-0.073	0.000	-	-0.035
P2	0.000	-	-0.022	0.000	-	-0.006
P3	0.000	-	-0.007	0.000	-	0.007
P4	0.000	-	-0.124	0.000	-	-0.017
P5	0.000	-	-0.160	0.000	-	-0.080

	Compared with M3			Compared with M3		
	SET-2 M1	SET-2 M2	SET-2 M3	SET-2 M1	SET-2 M2	SET-2 M3
P1	0.078	0.078	-	0.036	0.036	-
P2	0.023	0.023	-	0.007	0.007	-
P3	0.007	0.007	-	-0.006	-0.006	-
P4	0.142	0.142	-	0.018	0.018	-
P5	0.191	0.191	-	0.087	0.087	-

Table 4.118 AASHTO LRFD method-wise differences for SET-3

	AASHTO LRFD M2-M _y			AASHTO LRFD M3-M _x		
	Compared with M1			Compared with M1		
	SET-3 M1	SET-3 M2	SET-3 M3	SET-3 M1	SET-3 M2	SET-3 M3
P1	-	0.184	0.006	-	0.178	-0.006
P2	-	0.074	-0.009	-	0.130	-0.003
P3	-	0.081	-0.010	-	0.117	-0.004
P4	-	0.273	0.006	-	0.155	-0.006
P5	-	0.320	0.008	-	0.188	-0.003

	Compared with M2			Compared with M2		
	SET-3 M1	SET-3 M2	SET-3 M3	SET-3 M1	SET-3 M2	SET-3 M3
P1	-0.155	-	-0.150	-0.151	-	-0.156
P2	-0.069	-	-0.077	-0.115	-	-0.117
P3	-0.075	-	-0.084	-0.105	-	-0.109
P4	-0.214	-	-0.209	-0.134	-	-0.140
P5	-0.243	-	-0.236	-0.158	-	-0.161

	Compared with M3			Compared with M3		
	SET-3 M1	SET-3 M2	SET-3 M3	SET-3 M1	SET-3 M2	SET-3 M3
P1	-0.006	0.176	-	0.006	0.185	-
P2	0.009	0.083	-	0.003	0.133	-
P3	0.010	0.092	-	0.004	0.122	-
P4	-0.006	0.265	-	0.006	0.162	-
P5	-0.008	0.309	-	0.003	0.192	-

As can be seen from Figure 4.30 and 4.31, for *Eurocode-8* design spectrum scaling, the maximum M_x and M_y moments occurs in Method-2 for all of the columns for the ground motion set SET-1. By Method-1 and Method-3, moment values are close to each other. However for SET-2 and SET-3, moment values are close to each other among all of the methods.

For the bridge transverse (M_y) and longitudinal direction (M_x), when the three ground motion sets applied for each method are compared, SET-2 gives the maximum values for Method-1 and Method-3, while for the Method-2 moment values are close to each other among all of the ground motion sets.

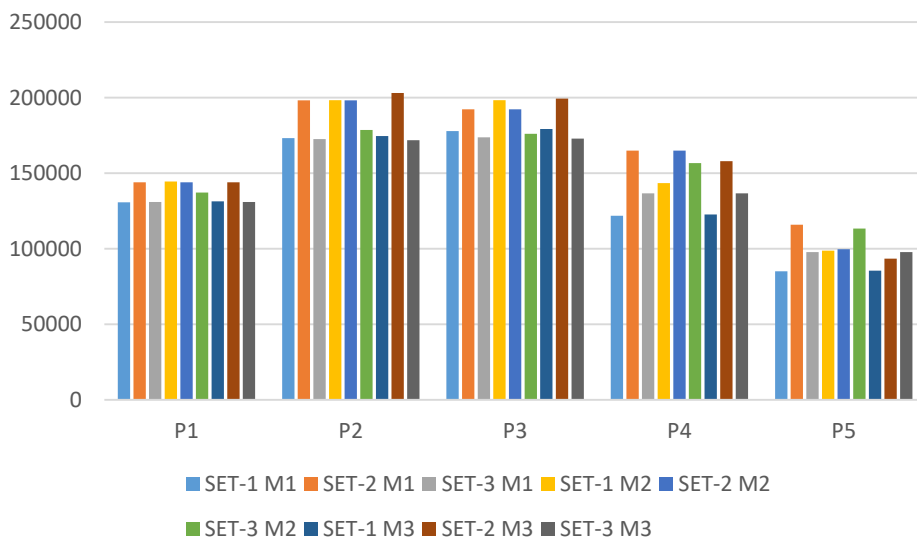


Figure 4.30. M_y values of all of the pier columns for three scaling methods applied according to EN-8 (kN.m)

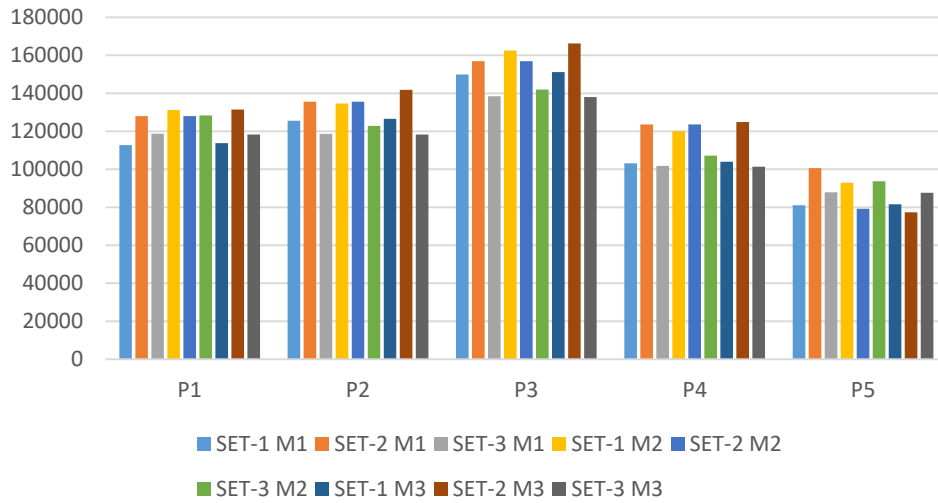


Figure 4.31. M_x values of all of the pier columns for three scaling methods applied according to EN-8 (kN.m)

It can be said that by following the Eurocode-8 specification for the design, for the transverse and longitudinal directions Method-2 gives the maximum moment values by employing the ground motion SET-1. However by employing the SET-2, Method-3 gives the maximum moment values. Method-wise percentage differences can be seen from Tables 119-124. Thus, different ground motion sets and methods should be employed in the design to obtain reliable results.

Table 4.119 EN-8 method-wise differences for SET-1

	EN M2-M _y			EN M3-M _x		
	Compared with M1			Compared with M1		
	SET-1 M1	SET-1 M2	SET-1 M3	SET-1 M1	SET-1 M2	SET-1 M3
P1	-	0.105	0.004	-	0.164	0.009
P2	-	0.145	0.008	-	0.072	0.008
P3	-	0.114	0.007	-	0.084	0.008
P4	-	0.178	0.007	-	0.164	0.008
P5	-	0.161	0.005	-	0.147	0.006

	Compared with M2			Compared with M2		
	SET-1 M1	SET-1 M2	SET-1 M3	SET-1 M1	SET-1 M2	SET-1 M3
P1	-0.095	-	-0.091	-0.141	-	-0.133
P2	-0.127	-	-0.120	-0.067	-	-0.060
P3	-0.103	-	-0.096	-0.078	-	-0.070
P4	-0.151	-	-0.145	-0.141	-	-0.134
P5	-0.139	-	-0.134	-0.128	-	-0.123

	Compared with M3			Compared with M3		
	SET-1 M1	SET-1 M2	SET-1 M3	SET-1 M1	SET-1 M2	SET-1 M3
P1	-0.004	0.100	-	-0.009	0.154	-
P2	-0.008	0.136	-	-0.008	0.064	-
P3	-0.007	0.106	-	-0.008	0.076	-
P4	-0.007	0.170	-	-0.008	0.155	-
P5	-0.005	0.155	-	-0.006	0.140	-

Table 4.120 EN-8 method-wise differences for SET-2

	EN M2-M _y			EN M3-M _x		
	Compared with M1			Compared with M1		
	SET-2 M1	SET-2 M2	SET-2 M3	SET-2 M1	SET-2 M2	SET-2 M3
P1	-	0.000	0.000	-	0.000	0.027
P2	-	0.000	0.025	-	0.000	0.046
P3	-	0.000	0.037	-	0.000	0.060
P4	-	0.000	-0.042	-	0.000	0.011
P5	-	-0.140	-0.194	-	-0.213	-0.231

	Compared with M2			Compared with M2		
	SET-2 M1	SET-2 M2	SET-2 M3	SET-2 M1	SET-2 M2	SET-2 M3
P1	0.000	-	0.000	0.000	-	0.027
P2	0.000	-	0.025	0.000	-	0.046
P3	0.000	-	0.037	0.000	-	0.060
P4	0.000	-	-0.042	0.000	-	0.011
P5	0.163	-	-0.062	0.270	-	-0.023

	Compared with M3			Compared with M3		
	SET-2 M1	SET-2 M2	SET-2 M3	SET-2 M1	SET-2 M2	SET-2 M3
P1	0.000	0.000	-	-0.026	-0.026	-
P2	-0.024	-0.024	-	-0.044	-0.044	-
P3	-0.035	-0.035	-	-0.056	-0.056	-
P4	0.044	0.044	-	-0.010	-0.010	-
P5	0.240	0.066	-	0.300	0.024	-

Table 4.121 EN-8 method-wise differences for SET-3

	EN M2-M _y			EN M3-M _x		
	Compared with M1			Compared with M1		
	SET-3 M1	SET-3 M2	SET-3 M3	SET-3 M1	SET-3 M2	SET-3 M3
P1	-	0.048	0.000	-	0.081	-0.004
P2	-	0.035	-0.004	-	0.036	-0.003
P3	-	0.013	-0.005	-	0.025	-0.003
P4	-	0.146	0.000	-	0.053	-0.004
P5	-	0.160	0.000	-	0.066	-0.003

	Compared with M2			Compared with M2		
	SET-3 M1	SET-3 M2	SET-3 M3	SET-3 M1	SET-3 M2	SET-3 M3
P1	-0.046	-	-0.046	-0.075	-	-0.078
P2	-0.033	-	-0.038	-0.034	-	-0.037
P3	-0.013	-	-0.018	-0.025	-	-0.028
P4	-0.128	-	-0.128	-0.050	-	-0.054
P5	-0.138	-	-0.138	-0.062	-	-0.065

	Compared with M3			Compared with M3		
	SET-3 M1	SET-3 M2	SET-3 M3	SET-3 M1	SET-3 M2	SET-3 M3
P1	0.000	0.048	-	0.004	0.085	-
P2	0.004	0.039	-	0.003	0.038	-
P3	0.005	0.018	-	0.003	0.028	-
P4	0.000	0.147	-	0.004	0.057	-
P5	0.000	0.160	-	0.003	0.069	-

As can be seen from Figure 4.32 and 4.33, for **TDY-2020** design spectrum scaling, maximum M_x and M_y moments occurs in Method-1 for all of the columns for the ground motion set SET-2. By Method-2 and Method-3, moment values are close to each other. However for SET-1 and SET-3, moment values are close to each other among all of the methods.

For the bridge transverse (M_y) and longitudinal direction (M_x), when the three ground motion sets applied for each method are compared, SET-2 gives the maximum values for all three methods. And by using the ground motion set SET-1 is greater than SET-3 for Method-2 and Method-3, while they are close to each other for Method-1.

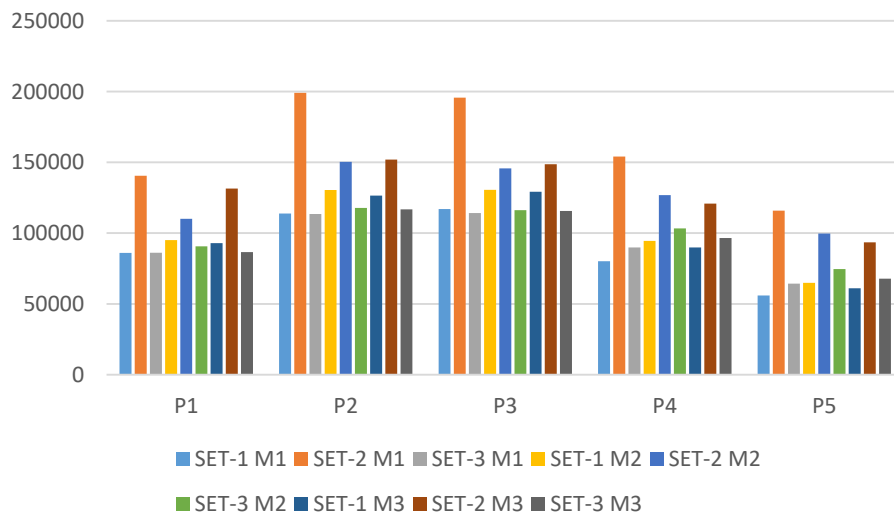


Figure 4.32. M_y values of all of the pier columns for three scaling methods applied according to TDY 2020 (kN.m)

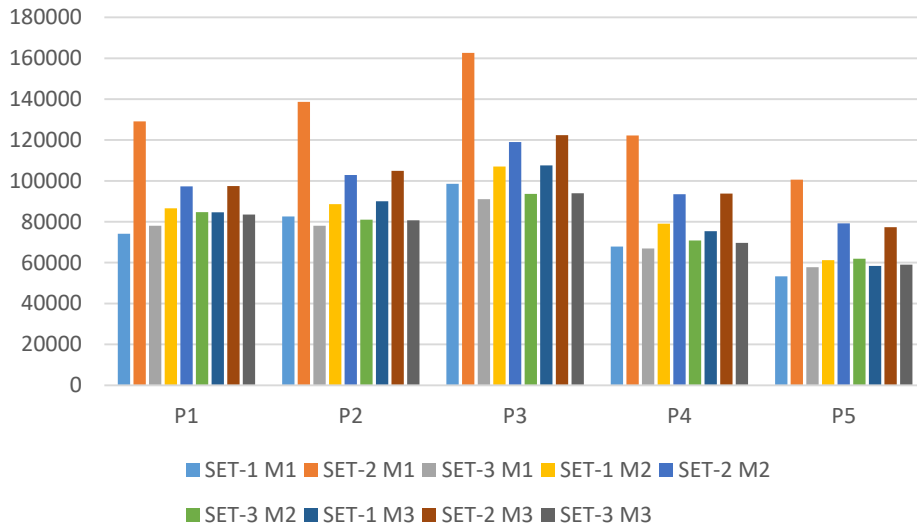


Figure 4.33. M_x values of all of the pier columns for three scaling methods applied according to TDY 2020 (kN.m)

It can be said that by following the TDY 2020 specification for the design, for the transverse and longitudinal directions Method-1 gives the maximum moment values by employing the ground motion SET-2. Method-wise percentage differences can be seen from Tables 122-124. It can be concluded that, time history analysis TDY 2020 design spectrum for a bridge having a fundamental period equals to 1 ($T_n=1$) can be done by using scaling method Method-1 and ground motion set SET-2.

Table 4.122 TDY 2020 method-wise differences for SET-1

	TDY M2-M _y			TDY M3-M _x		
	Compared with M1			Compared with M1		
	SET-1 M1	SET-1 M2	SET-1 M3	SET-1 M1	SET-1 M2	SET-1 M3
P1	-	0.106	0.080	-	0.168	0.142
P2	-	0.146	0.111	-	0.073	0.090
P3	-	0.116	0.105	-	0.085	0.091
P4	-	0.180	0.122	-	0.166	0.111
P5	-	0.161	0.092	-	0.148	0.095

	Compared with M2			Compared with M2		
	SET-1 M1	SET-1 M2	SET-1 M3	SET-1 M1	SET-1 M2	SET-1 M3
P1	-0.096	-	-0.023	-0.144	-	-0.022
P2	-0.127	-	-0.030	-0.068	-	0.016
P3	-0.104	-	-0.010	-0.078	-	0.006
P4	-0.152	-	-0.049	-0.142	-	-0.047
P5	-0.138	-	-0.059	-0.129	-	-0.046

	Compared with M3			Compared with M3		
	SET-1 M1	SET-1 M2	SET-1 M3	SET-1 M1	SET-1 M2	SET-1 M3
P1	-0.074	0.024	-	-0.124	0.022	-
P2	-0.100	0.031	-	-0.082	-0.015	-
P3	-0.095	0.010	-	-0.083	-0.005	-
P4	-0.109	0.051	-	-0.100	0.049	-
P5	-0.084	0.063	-	-0.087	0.048	-

Table 4.123 TDY 2020 method-wise differences for SET-2

	TDY M2-M _y			TDY M3-M _x		
	Compared with M1			Compared with M1		
	SET-2 M1	SET-2 M2	SET-2 M3	SET-2 M1	SET-2 M2	SET-2 M3
P1	-	-0.217	-0.065	-	-0.246	-0.245
P2	-	-0.245	-0.237	-	-0.258	-0.243
P3	-	-0.256	-0.240	-	-0.268	-0.247
P4	-	-0.177	-0.216	-	-0.235	-0.233
P5	-	-0.140	-0.194	-	-0.213	-0.231

	Compared with M2			Compared with M2		
	SET-2 M1	SET-2 M2	SET-2 M3	SET-2 M1	SET-2 M2	SET-2 M3
P1	0.277	-	0.194	0.327	-	0.002
P2	0.325	-	0.011	0.347	-	0.019
P3	0.344	-	0.021	0.367	-	0.028
P4	0.215	-	-0.047	0.308	-	0.004
P5	0.163	-	-0.062	0.270	-	-0.023

	Compared with M3			Compared with M3		
	SET-2 M1	SET-2 M2	SET-2 M3	SET-2 M1	SET-2 M2	SET-2 M3
P1	0.069	-0.163	-	0.325	-0.002	-
P2	0.311	-0.011	-	0.322	-0.019	-
P3	0.316	-0.020	-	0.329	-0.028	-
P4	0.275	0.049	-	0.303	-0.004	-
P5	0.240	0.066	-	0.300	0.024	-

Table 4.124 TDY 2020 method-wise differences for SET-3

	TDY M2-M _y			TDY M3-M _x		
	Compared with M1			Compared with M1		
	SET-3 M1	SET-3 M2	SET-3 M3	SET-3 M1	SET-3 M2	SET-3 M3
P1	-	0.053	0.006	-	0.085	0.070
P2	-	0.038	0.029	-	0.039	0.034
P3	-	0.018	0.012	-	0.028	0.031
P4	-	0.149	0.074	-	0.059	0.041
P5	-	0.160	0.055	-	0.071	0.021

	Compared with M2			Compared with M2		
	SET-3 M1	SET-3 M2	SET-3 M3	SET-3 M1	SET-3 M2	SET-3 M3
P1	-0.050	-	-0.044	-0.078	-	-0.013
P2	-0.037	-	-0.009	-0.038	-	-0.005
P3	-0.017	-	-0.005	-0.027	-	0.003
P4	-0.130	-	-0.065	-0.056	-	-0.017
P5	-0.138	-	-0.090	-0.066	-	-0.047

	Compared with M3			Compared with M3		
	SET-3 M1	SET-3 M2	SET-3 M3	SET-3 M1	SET-3 M2	SET-3 M3
P1	-0.006	0.046	-	-0.066	0.014	-
P2	-0.028	0.009	-	-0.033	0.005	-
P3	-0.012	0.006	-	-0.030	-0.003	-
P4	-0.069	0.070	-	-0.040	0.017	-
P5	-0.052	0.099	-	-0.020	0.049	-

It appears that in all cases Method 2 gives the largest moment values of M_x and M_y for AASHTO LRFD and TDY 2020. This can be explained by having no upper limit for scaling. Besides, in both directions, SET-2 gives the maximum values with Method-2. Unlikely, for Eurocode-8, there is an uncertainty about which method and set to be used. Thus, different ground motion sets and methods should be employed in the seismic design of bridges having fundamental periods equal to 1 (T_n=1) to obtain reliable and accurate results for Eurocode-8 bridge design specification, while for AASHTO LRFD and TDY Method-2 and SET-2 can be accepted.

4.3 Comparison of Results for V14 Bridge

Before the comparison of the analysis results, first the spectral acceleration values of the mean spectra of the selected set of earthquakes are compared. Maximum spectral acceleration values of mean response spectrum of the scaled time histories change both according to specifications and methods. Mean spectra of the ground motion sets scaled according to three scaling methods (M1, M2 and M3) are shown in Figures 4.34-4.42 per specification. For TDY 2020 design spectrum, maximum S_a resulted in Method-3 conducted on ground motion set SET-2 as 1.28g, while for AASHTO LRFD and EN-8 design spectra, maximum S_a resulted in Method-3 conducted on ground motion set SET-3 as 1.45g and 1.67g respectively (Table 4.125).

Table 4.125 Maximum spectral acceleration (S_a) values (g)

	AASHTO LRFD			EN-8			TDY		
	M1	M2	M3	M1	M2	M3	M1	M2	M3
SET-1	1.054	1.153	1.071	1.638	1.728	1.645	1.084	1.148	1.139
SET-2	0.926	1.343	1.010	1.620	1.535	1.653	1.226	1.262	1.280
SET-3	1.227	1.449	1.235	1.630	1.591	1.667	1.079	1.068	1.068

Spectral acceleration values at $T=0.73$ sec. (fundamental period of V14) of mean response spectrum of the scaled time histories have different pattern than the maximum values (Table 4.126). For both AASHTO LRFD design spectrum, the maximum value occurs for Method-1 conducted on ground motion set SET-3, while for EN-8 and TDY 2020 spectrum maximum S_a occurs Method-3 of SET-2 and Method-2 of SET-3 respectively.

Table 4.126 Spectral acceleration (S_a) values at $T=0.73$ sec. (g)

	AASHTO LRFD			EN-8			TDY		
	M1	M2	M3	M1	M2	M3	M1	M2	M3
SET-1	0.430	0.452	0.435	0.656	0.727	0.659	0.435	0.480	0.453
SET-2	0.467	0.486	0.490	0.840	0.833	0.844	0.636	0.648	0.632
SET-3	0.582	0.476	0.559	0.761	0.722	0.728	0.504	0.485	0.485

The maximum acceleration values (Table 4.125) regardless of the scaling methods in time interval 0-4 seconds based on the selected ground motion sets are sorted as follows per specification:

For AASHTO LRFD: SET-3 > SET-2 > SET-1

For EN-8: SET-3 > SET-1 > SET-2

For TDY 2020: SET-2 > SET-1 > SET-3

To sum up, in time interval 0-4 seconds, Method-2 and Method-3 resulted in the maximum spectral acceleration values for all the three sets and the specifications. However, at the fundamental period of the bridge, one of the three methods give the maximum S_a values for each specification.

In overall, EN-8 response spectrum scaling and Method-2 give the maximum acceleration values.

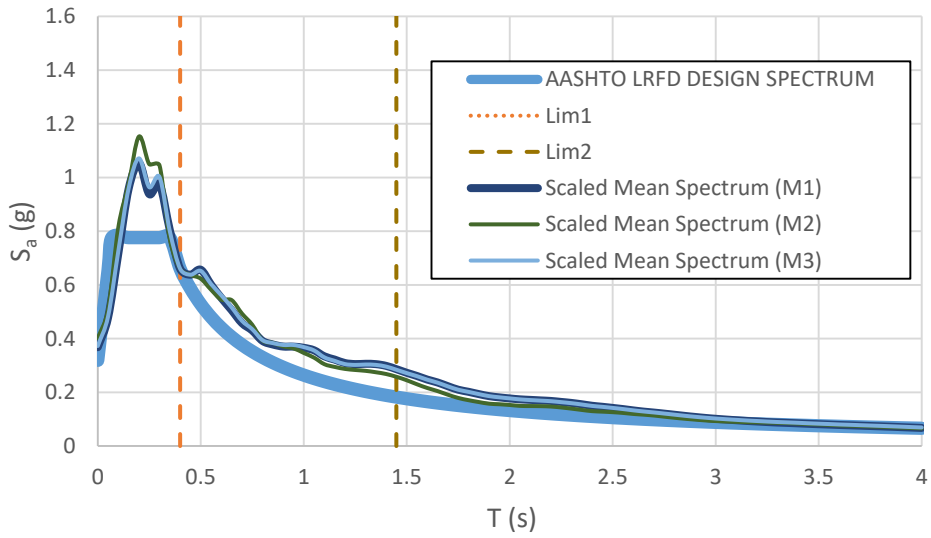


Figure 4.34. Scaled mean spectra for M1,M2 and M3 and AASHTO LRFD design response spectrum for SET-1

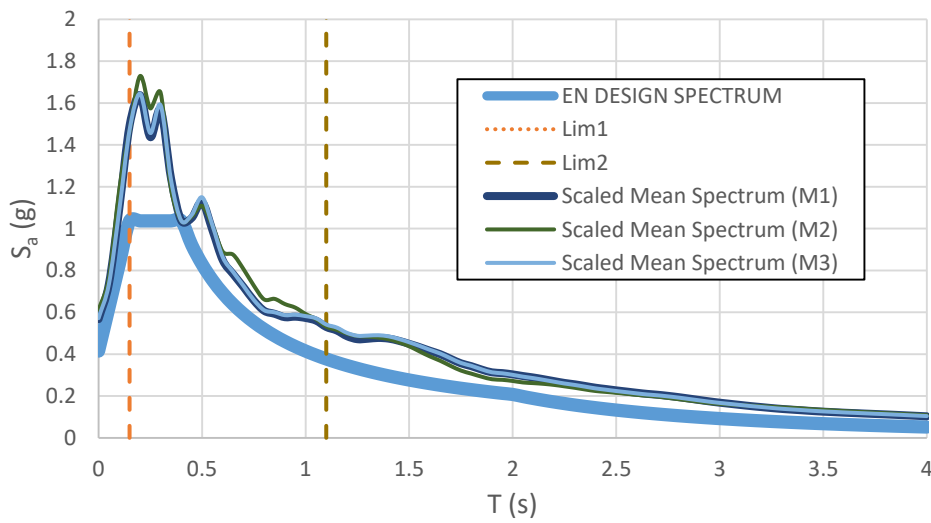


Figure 4.35. Scaled mean spectra for M1,M2 and M3 and EN 8 design response spectrum for SET-1

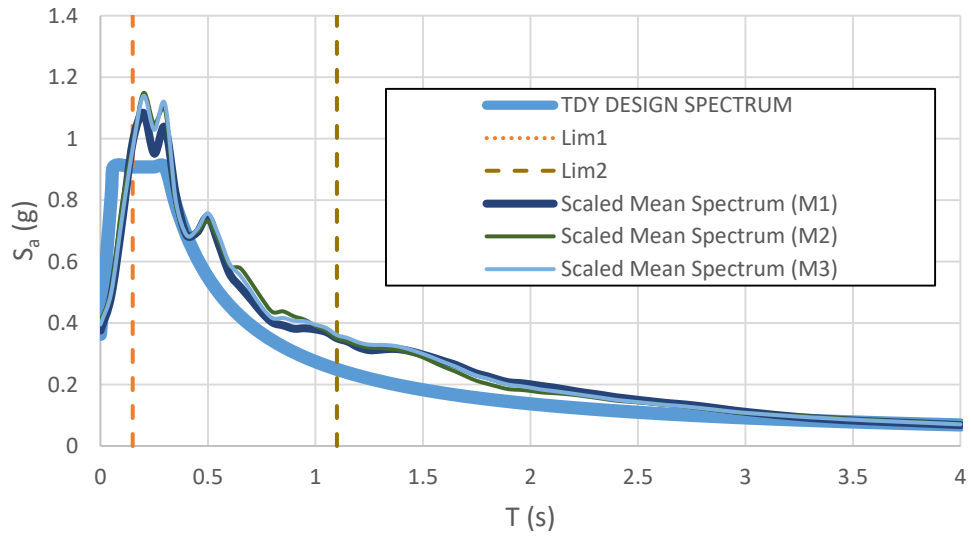


Figure 4.36. Scaled mean spectra for M1,M2 and M3 and TDY design response spectrum for SET-1

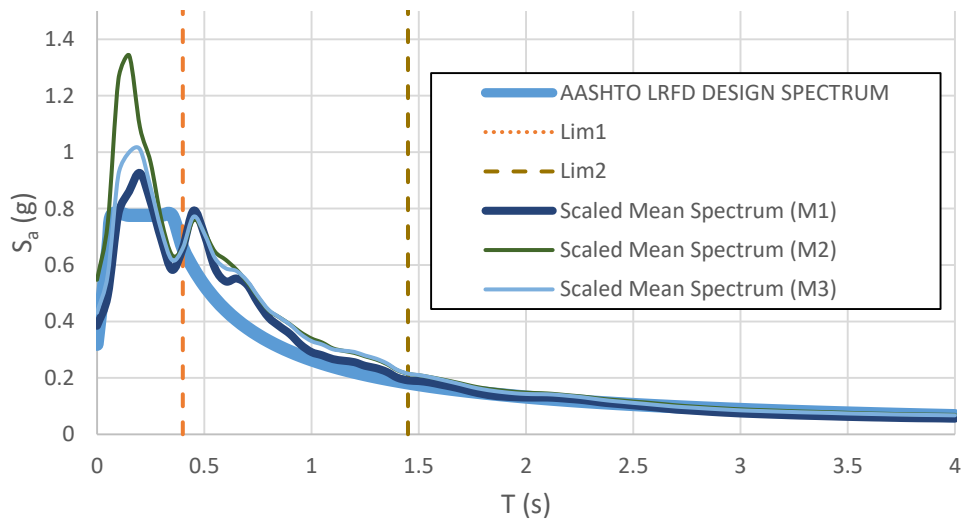


Figure 4.37. Scaled mean spectra for M1,M2 and M3 and AASHTO LRFD design response spectrum for SET-2

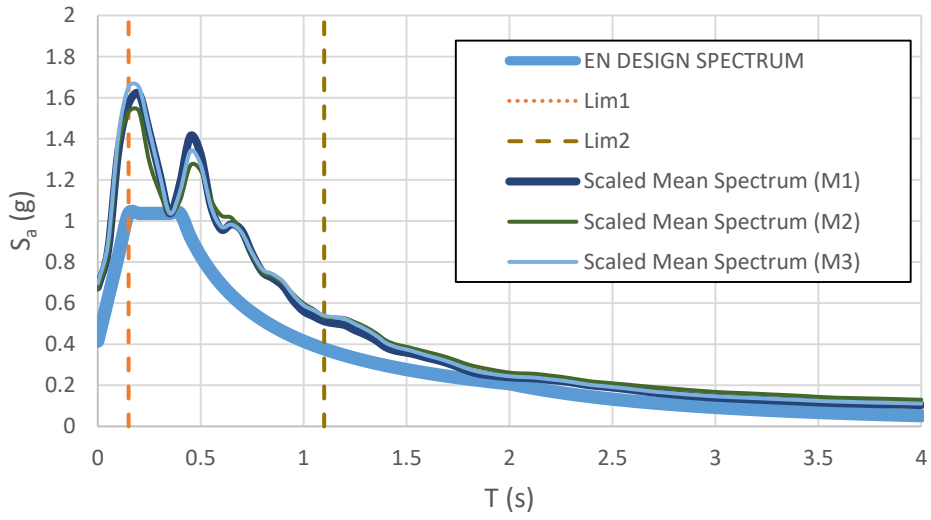


Figure 4.38. Scaled mean spectra for M1,M2 and M3 and EN 8 design response spectrum for SET-2

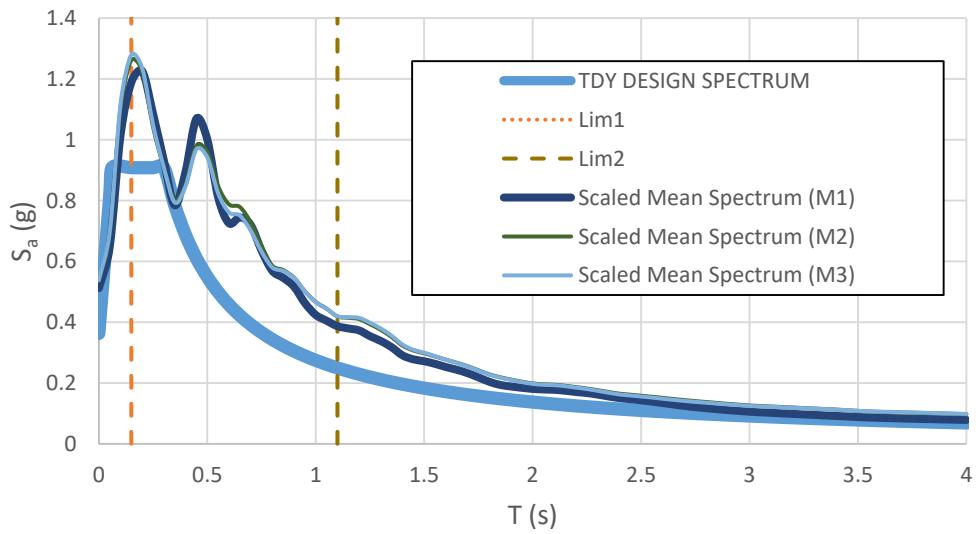


Figure 4.39. Scaled mean spectra for M1,M2 and M3 and TDY design response spectrum for SET-2

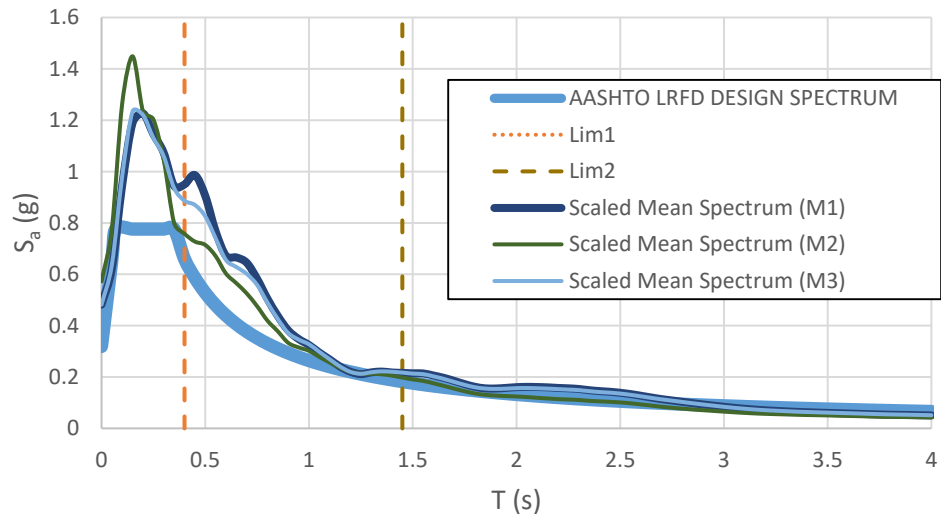


Figure 4.40. Scaled mean spectra for M1,M2 and M3 and AASHTO LRFD design response spectrum for SET-3

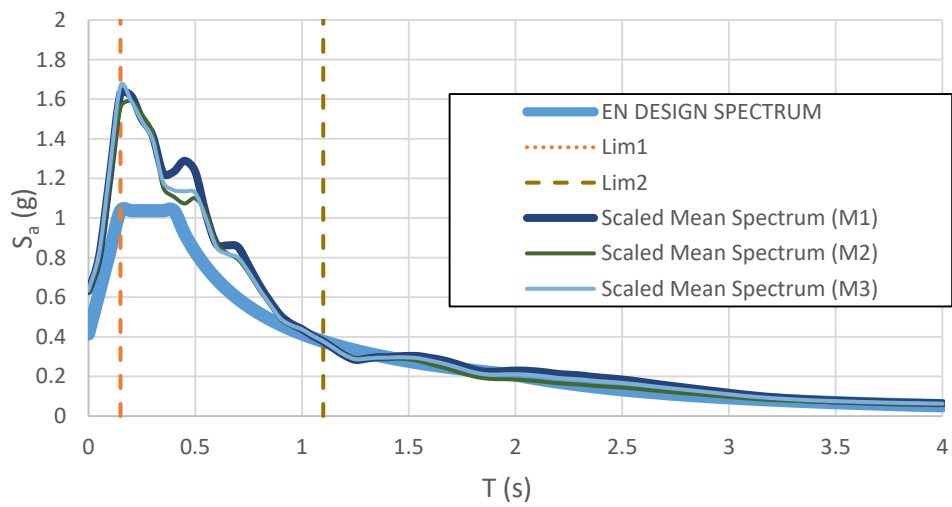


Figure 4.41. Scaled mean spectra for M1,M2 and M3 and EN 8 design response spectrum for SET-3

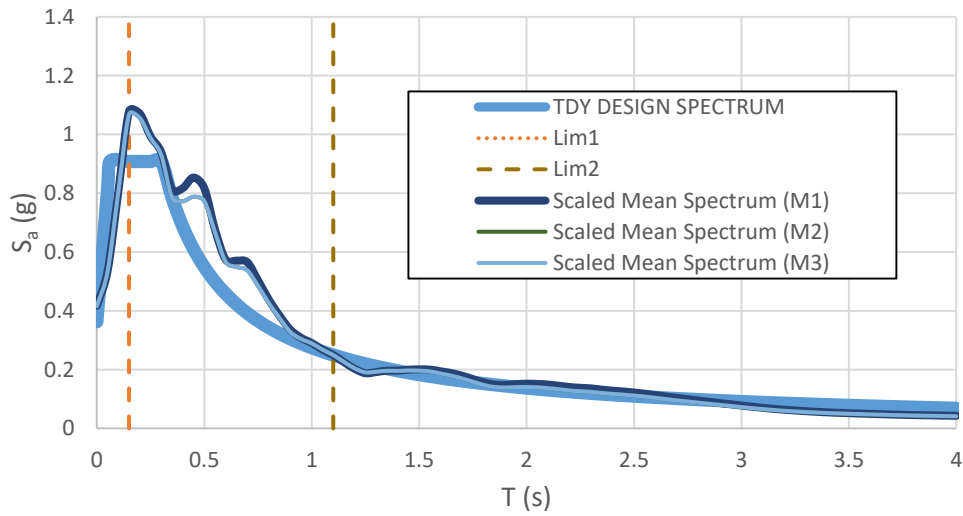


Figure 4.42. Scaled mean spectra for M1,M2 and M3 and TDY design response spectrum for SET-3

Comparison of the analysis results is made both for ground motion set-wise and bridge specification-wise and given in detail in the subsections 4.3.1 to 4.3.4 per scaling method. Although the seismic demand parameters M_x - M_y and u_x - u_y are taken as mean values of seven scaled earthquake ground motions, results seem to be not strictly dependent on the ratio of the mean spectrum S_a values. For example, as shown in Table 4.126, EN-8 spectral acceleration values are sorted larger to smaller as SET-2 > SET-3 > SET-1 at $t=0.73$ sec for all of the three scaling methods. On the contrary, moment and displacement values are sorted as SET-2 > SET-1 > SET-3 in both transverse direction (M_y) and longitudinal direction (M_x) for Method-1. For other methods and for AASHTO LRFD and TDY 2020 this comparison is likewise but sorting of sets differs.

This result can be explained with the diversity of the predominant periods of the earthquakes and the selected ground motion parameters. V14 Bridge has 2 piers and when the seismic demand parameters are compared, it can be seen that dominant earthquakes are different for each pier column and for each set. To illustrate, while Hector earthquake gives the maximum moment and displacement values for pier P1, Manjil earthquake governs for pier P2 in the same analysis with the same set of ground motions.

The change in the mean maximum moment values of the columns for the three bridge specifications is summarized for each scaling methods. Because the specification-wise percentage differences between the three ground motion sets are approximately the same for each pier column, results are tabulated according to P2 for demonstration in the next subsections 4.3.1, 4.3.2 and 4.3.3. However, ground motion set-wise percentage differences considerably vary for each pier column.

4.3.1 Comparison of Results for Scaling Method-1

In Method-1, the maximum M_x and M_y values occur in pier P2 for all of the ground motion sets.

Sorting of maximum M_y values:

For AASHTO LRFD: SET-3 > SET-2 > SET-1 (52326 > 45189 > 43029) (kN.m)

For EN-8: SET-2 > SET-3 > SET-1 (54297 > 47288 > 46031) (kN.m)

For TDY 2020: SET2 > SET-3 > SET-1 (41083 > 31307 > 30475) (kN.m)

Sorting of maximum M_x values:

For AASHTO LRFD: SET-3 > SET-2 > SET-1 (46058 > 45060 > 31226) (kN.m)

For EN-8: SET-2 > SET-3 > SET-1 (54142 > 41623 > 33404) (kN.m)

For TDY 2020: SET-2 > SET-3 > SET-1 (40967 > 27557 > 22116) (kN.m)

In Method-1, the maximum u_x and u_y values occur in pier P2 for all of the ground motion sets.

Sorting of maximum u_y values:

For AASHTO LRFD: SET-3 > SET-2 > SET-1 (2.44 > 2.10 > 2.00) (cm)

For EN-8: SET-2 > SET-3 > SET-1 (2.53 > 2.14 > 2.20) (cm)

For TDY 2020: SET2 > SET-3 > SET-1 (1.92 > 1.46 > 1.42) (cm)

Sorting of maximum u_x values:

For AASHTO LRFD: SET-3 > SET-2 > SET-1 (6.02 > 5.89 > 4.08) (cm)

For EN-8: SET-2 > SET-3 > SET-1 (7.08 > 5.44 > 4.37) (cm)

For TDY 2020: SET-2 > SET-3 > SET-1 (5.33 > 3.60 > 2.89) (cm)

Percentage difference given in the Tables 4.128, 4.129, 4.135, 4.134-4.138 below are calculated based on Equation 1.

$$\% = \frac{B-A}{A} \quad \text{Eq. (1)}$$

A: The result parameter taken as base

B: Compared result parameter

Moment and displacement values are not very close to each other as it can be seen from the given results. When the results are sorted, it can be seen that specifications point to different sets as critical and there is a considerable amount of difference between both M_x , M_y and u_x , u_y values. Besides, the lowest moment and displacement values are obtained in scaling according to the TDY 2020. On the other hand, most critical values are computed from scaling according to the EN-8.

Table 4.127 The maximum M_y values of pier P2 for M1 (kN.m)

	P2-M_y		
	SET-1	SET-2	SET-3
AASHTO	43029.56	45189.21	52326.23
EN	46031.26	54297.05	47288.24
TDY	30475.87	41083.87	31307.92

Table 4.128 Specification-wise percentage differences of M_y values of pier P2 for M1

	Compared with AASHTO LRFD			Compared with EN-8			Compared with TDY 2020		
	SET-1	SET-2	SET-3	SET-1	SET-2	SET-3	SET-1	SET-2	SET-3
AASHTO	-	-	-	-7%	-17%	11%	41%	10%	67%
EN	7%	20%	-10%	-	-	-	51%	32%	51%
TDY	-29%	-9%	-40%	-34%	-24%	-34%	-	-	-

EN-8 gives the largest moment values compared to other codes. TDY2020, on the other hand results in lowest M_y values like the results of V03 and V08 Bridge.

Table 4.129 The maximum M_x values of pier P2 for M1 (kN.m)

	P2- M_x		
	SET-1	SET-2	SET-3
AASHTO	31226.52	52950.44	53456.93
EN	33404.86	63622.55	48310.08
TDY	22116.32	48140.02	31984.6

Table 4.130 Specification-wise percentage differences of M_x values of pier P2 for M1

	Compared with AASHTO LRFD			Compared with EN-8			Compared with TDY 2020		
	SET-1	SET-2	SET-3	SET-1	SET-2	SET-3	SET-1	SET-2	SET-3
AASHTO	-	-	-	-7%	-17%	11%	41%	10%	67%
EN	7%	20%	-10%	-	-	-	51%	32%	51%
TDY	-29%	-9%	-40%	-34%	-24%	-34%	-	-	-

EN-8 gives the largest moment values compared to other codes. TDY2020, on the other hand results in lowest M_x values like the results of V03 and V08 Bridge.

Table 4.131 The maximum u_y values of pier P2 for M1 (m)

	P2-u_y		
	SET-1	SET-2	SET-3
AASHTO	0.0200	0.0211	0.0244
EN	0.0214	0.0253	0.0220
TDY	0.0141	0.0192	0.0146

Table 4.132 Specification-wise percentage differences of u_y values of pier P2 for M1

	Compared with AASHTO LRFD			Compared with EN-8			Compared with TDY 2020		
	SET-1	SET-2	SET-3	SET-1	SET-2	SET-3	SET-1	SET-2	SET-3
AASHTO	-	-	-	-7%	-17%	11%	41%	10%	67%
EN	7%	20%	-10%	-	-	-	51%	32%	51%
TDY	-29%	-9%	-40%	-34%	-24%	-34%	-	-	-

EN-8 gives the largest displacement values compared to other codes. TDY2020, on the other hand results in lowest u_y values like the results of V03 and V08 Bridge.

Table 4.133 The maximum u_x values of pier P2 for M1 (m)

	P2-u_x		
	SET-1	SET-2	SET-3
AASHTO	0.0408	0.0589	0.0602
EN	0.0437	0.0708	0.0544
TDY	0.0289	0.0535	0.0360

Table 4.134 Specification-wise percentage differences of u_x values of pier P2 for M1

	Compared with AASHTO LRFD			Compared with EN-8			Compared with TDY 2020		
	SET-1	SET-2	SET-3	SET-1	SET-2	SET-3	SET-1	SET-2	SET-3
AASHTO	-	-	-	-7%	-17%	11%	41%	10%	67%
EN	7%	20%	-10%	-	-	-	51%	32%	51%
TDY	-29%	-9%	-40%	-34%	-24%	-34%	-	-	-

EN-8 gives the largest displacement values compared to other codes. TDY2020, on the other hand results in lowest u_x values like the results of V03 and V08 Bridge.

Table 4.135 Ground motion set-wise percentage differences of M_y values of all pier columns for M1

		Compared with SET-1			Compared with SET-2			Compared with SET-3		
		SET-1	SET-2	SET-3	SET-1	SET-2	SET-3	SET-1	SET-2	SET-3
P1-M_y	AASHTO	-	7%	21%	-7%	-	13%	-17%	-11%	-
	EN	-	21%	2%	-17%	-	-15%	-2%	18%	-
	TDY	-	38%	2%	-27%	-	-26%	-2%	35%	-
P2-M_y	AASHTO	-	5%	22%	-5%	-	16%	-18%	-14%	-
	EN	-	18%	3%	-15%	-	-13%	-3%	15%	-
	TDY	-	35%	3%	-26%	-	-24%	-3%	31%	-

For most cases, SET-2 gives largest results for M_y whereas SET-1 results are generally smallest.

Table 4.136 Ground motion set-wise percentage differences of M_x values of all pier columns for M1

		Compared with SET-1			Compared with SET-2			Compared with SET-3		
		SET-1	SET-2	SET-3	SET-1	SET-2	SET-3	SET-1	SET-2	SET-3
P1-M_x	AASHTO	-	50%	52%	-33%	-	1%	-34%	-1%	-
	EN	-	69%	28%	-41%	-	-24%	-22%	32%	-
	TDY	-	93%	28%	-48%	-	-34%	-22%	51%	-
P2-M_x	AASHTO	-	70%	71%	-41%	-	1%	-42%	-1%	-
	EN	-	90%	45%	-47%	-	-24%	-31%	32%	-
	TDY	-	118%	45%	-54%	-	-34%	-31%	51%	-

For most cases, SET-2 gives largest results for M_x whereas SET-1 results are generally smallest

Table 4.137 Ground motion set-wise percentage differences of u_y values of all pier columns for M1

		Compared with SET-1			Compared with SET-2			Compared with SET-3		
		SET-1	SET-2	SET-3	SET-1	SET-2	SET-3	SET-1	SET-2	SET-3
P1-u_y	AASHTO	-	7%	21%	-7%	-	13%	-17%	-11%	-
	EN	-	21%	2%	-17%	-	-15%	-2%	18%	-
	TDY	-	38%	2%	-27%	-	-26%	-2%	35%	-
P2-u_y	AASHTO	-	5%	22%	-5%	-	16%	-18%	-14%	-
	EN	-	18%	3%	-16%	-	-13%	-3%	15%	-
	TDY	-	35%	3%	-26%	-	-24%	-3%	31%	-

For most cases, SET-2 gives largest results for u_y whereas SET-1 results are generally smallest.

Table 4.138 Ground motion set-wise percentage differences of u_x values of all pier columns for M1

		Compared with SET-1			Compared with SET-2			Compared with SET-3		
		SET-1	SET-2	SET-3	SET-1	SET-2	SET-3	SET-1	SET-2	SET-3
P1-u_x	AASHTO	-	50%	51%	-33%	-	1%	-34%	-1%	-
	EN	-	68%	28%	-41%	-	-24%	-22%	32%	-
	TDY	-	93%	28%	-48%	-	-34%	-22%	50%	-
P2-u_x	AASHTO	-	44%	47%	-31%	-	2%	-32%	-2%	-
	EN	-	62%	25%	-38%	-	-23%	-20%	30%	-
	TDY	-	85%	25%	-46%	-	-33%	-20%	49%	-

For most cases, SET-2 gives largest results for u_x whereas SET-1 results are generally smallest.

4.3.2 Comparison of Results for Scaling Method-2

In Method-2, the maximum M_x and M_y values occur in pier P2 for all of the ground motion sets.

Sorting of maximum M_y values:

For AASHTO LRFD: SET-2 > SET-3 > SET-1 (50912 > 49579 > 40907) (kN.m)

For EN-8: SET-2 > SET-1 > SET-3 (54660 > 46587 > 45300) (kN.m)

For TDY 2020: SET2 > SET-1 > SET-3 (42430 > 30803 > 30498) (kN.m)

Sorting of maximum M_x values:

For AASHTO LRFD: SET-2 > SET-3 > SET-1 (46697 > 40647 > 37196) (kN.m)

For EN-8: SET-2 > SET-1 > SET-3 (52866 > 41095 > 40426) (kN.m)

For TDY 2020: SET-2 > SET-1 > SET-3 (41189 > 27199 > 26683) (kN.m)

In Method-2, the maximum u_x and u_y values occur in pier P2 for all of the ground motion sets.

Sorting of maximum u_y values:

For AASHTO LRFD: SET-2 > SET-3 > SET-1 (2.37 > 2.30 > 1.90) (cm)

For EN-8: SET-2 > SET-1 > SET-3 (2.54 > 2.16 > 2.10) (cm)

For TDY 2020: SET2 > SET-1 > SET-3 (1.98 > 1.43 > 1.42) (cm)

Sorting of maximum u_x values:

For AASHTO LRFD: SET-2 > SET-3 > SET-1 (6.10 > 5.31 > 4.86) (cm)

For EN-8: SET-2 > SET-1 > SET-3 (6.91 > 5.37 > 5.28) (cm)

For TDY 2020: SET-2 > SET-1 > SET-3 (5.38 > 3.55 > 3.49) (cm)

Moment and displacement values are not very close to each other as it can be seen from the given results. When the results are sorted, it can be seen that specifications point to different sets as critical and there is a considerable amount of difference between both M_x , M_y and u_x , u_y values. Besides, the lowest moment values are obtained in scaling according to the TDY 2020. On the other hand, most critical values are computed from scaling according to the EN-8.

Percentage difference given in the Tables 4.140, 4.142, 4.144, 4.146-4.150 below are calculated based on the Equation 1.

Table 4.139 The maximum M_y values of pier P2 for M2 (kN.m)

	P2- M_y		
	SET-1	SET-2	SET-3
AASHTO	40907.41	50912.37	49579.99
EN	46587	54660.47	45300.03
TDY	30803.43	42430.18	30498.2

Table 4.140 Specification-wise percentage differences of M_y values of pier P2 for M2

	Compared with AASHTO LRFD			Compared with EN-8			Compared with TDY 2020		
	SET-1	SET-2	SET-3	SET-1	SET-2	SET-3	SET-1	SET-2	SET-3
AASHTO	-	-	-	-12%	-7%	9%	33%	20%	63%
EN	14%	7%	-9%	-	-	-	51%	29%	49%
TDY	-25%	-17%	-38%	-34%	-22%	-33%	-	-	-

EN-8 gives the largest moment values compared to other codes. TDY2020, on the other hand results in lowest M_y values like the results of Method-1.

Table 4.141 The maximum M_x values of pier P2 for M2 (kN.m)

	P2-M_x		
	SET-1	SET-2	SET-3
AASHTO	37196.09	54999.01	48187.18
EN	41095.34	61548.99	46858.73
TDY	27199.98	48000.64	30902.27

Table 4.142 Specification-wise percentage differences of M_x values of pier P2 for M2

	Compared with AASHTO LRFD			Compared with EN-8			Compared with TDY 2020		
	SET-1	SET-2	SET-3	SET-1	SET-2	SET-3	SET-1	SET-2	SET-3
AASHTO	-	-	-	-9%	-11%	3%	37%	15%	56%
EN	10%	12%	-3%	-	-	-	51%	28%	52%
TDY	-27%	-13%	-36%	-34%	-22%	-34%	-	-	-

EN-8 gives the largest moment values compared to other codes. TDY2020, on the other hand results in lowest M_x values like the results of Method-1.

Table 4.143 The maximum u_y values of pier P2 for M2 (m)

	P2-u_y		
	SET-1	SET-2	SET-3
AASHTO	0.019	0.024	0.023
EN	0.022	0.025	0.021
TDY	0.014	0.020	0.014

Table 4.144 Specification-wise percentage differences of u_y values of pier P2 for M2

	Compared with AASHTO LRFD			Compared with EN-8			Compared with TDY 2020		
	SET-1	SET-2	SET-3	SET-1	SET-2	SET-3	SET-1	SET-2	SET-3
AASHTO	-	-	-	-12%	-7%	9%	33%	20%	62%
EN	14%	7%	-9%	-	-	-	51%	29%	48%
TDY	-25%	-17%	-38%	-34%	-22%	-33%	-	-	-

EN-8 gives the largest displacement values compared to other codes. TDY2020, on the other hand results in lowest u_y values like the results of Method-1.

Table 4.145 The maximum u_x values of pier P2 for M2 (m)

	P2- u_x		
	SET-1	SET-2	SET-3
AASHTO	0.049	0.061	0.053
EN	0.054	0.069	0.053
TDY	0.036	0.054	0.035

Table 4.146 Specification-wise percentage differences of u_x values of pier P2 for M2

	Compared with AASHTO LRFD			Compared with EN-8			Compared with TDY 2020		
	SET-1	SET-2	SET-3	SET-1	SET-2	SET-3	SET-1	SET-2	SET-3
AASHTO	-	-	-	-9%	-12%	0%	37%	13%	52%
EN	10%	13%	-0.45%	-	-	-	51%	28%	51%
TDY	-27%	-12%	-34%	-34%	-22%	-34%	-	-	-

EN-8 gives the largest displacement values compared to other codes. TDY2020, on the other hand results in lowest u_x values like the results of Method-1.

Table 4.147 Ground motion set-wise percentage differences of M_y values of all pier columns for M2

		Compared with SET-1			Compared with SET-2			Compared with SET-3		
		SET-1	SET-2	SET-3	SET-1	SET-2	SET-3	SET-1	SET-2	SET-3
P1-M_y	AASHTO	-	17%	15%	-14%	-	-2%	-13%	2%	-
	EN	-	12%	-7%	-11%	-	-17%	7%	20%	-
	TDY	-	32%	-7%	-24%	-	-30%	8%	42%	-
P2-M_y	AASHTO	-	24%	21%	-20%	-	-3%	-17%	3%	-
	EN	-	17%	-3%	-15%	-	-17%	3%	21%	-
	TDY	-	38%	-1%	-27%	-	-28%	1%	39%	-

For most cases, SET-2 gives largest results for M_y whereas SET-1 results are generally smallest like the results of Method-1.

Table 4.148 Ground motion set-wise percentage differences of M_x values of all pier columns for M2

		Compared with SET-1			Compared with SET-2			Compared with SET-3		
		SET-1	SET-2	SET-3	SET-1	SET-2	SET-3	SET-1	SET-2	SET-3
P1- M_x	AASHTO	-	30%	14%	-23%	-	-12%	-12%	14%	-
	EN	-	32%	1%	-24%	-	-24%	-1%	31%	-
	TDY	-	56%	0%	-36%	-	-36%	0%	55%	-
P2- M_x	AASHTO	-	48%	30%	-32%	-	-12%	-23%	14%	-
	EN	-	50%	14%	-33%	-	-24%	-12%	31%	-
	TDY	-	76%	14%	-43%	-	-36%	-12%	55%	-

For most cases, SET-2 gives largest results for M_x whereas SET-1 results are generally smallest like the results of Method-1.

Table 4.149 Ground motion set-wise percentage differences of u_y values of all pier columns for M2

		Compared with SET-1			Compared with SET-2			Compared with SET-3		
		SET-1	SET-2	SET-3	SET-1	SET-2	SET-3	SET-1	SET-2	SET-3
P1- u_y	AASHTO	-	16%	15%	-14%	-	-2%	-13%	2%	-
	EN	-	12%	-7%	-11%	-	-17%	7%	20%	-
	TDY	-	32%	-7%	-24%	-	-30%	7%	42%	-
P2- u_y	AASHTO	-	25%	21%	-20%	-	-3%	-18%	3%	-
	EN	-	18%	-3%	-15%	-	-17%	3%	21%	-
	TDY	-	38%	-1%	-28%	-	-28%	1%	39%	-

For most cases, SET-2 gives largest results for u_y whereas SET-1 results are generally smallest like the results of Method-1.

Table 4.150 Ground motion set-wise percentage differences of u_x values of all pier columns for M2

		Compared with SET-1			Compared with SET-2			Compared with SET-3		
		SET-1	SET-2	SET-3	SET-1	SET-2	SET-3	SET-1	SET-2	SET-3
P1-u_x	AASHTO	-	30%	14%	-23%	-	-12%	-12%	14%	-
	EN	-	32%	1%	-24%	-	-24%	-1%	31%	-
	TDY	-	56%	0%	-36%	-	-36%	0%	55%	-
P2-u_x	AASHTO	-	25%	9%	-20%	-	-13%	-8%	15%	-
	EN	-	29%	-2%	-22%	-	-24%	2%	31%	-
	TDY	-	51%	-2%	-34%	-	-35%	2%	54%	-

For most cases, SET-2 gives largest results for u_x whereas SET-1 results are generally smallest like the results of Method-1.

4.3.3 Comparison of Results for Scaling Method-3

In Method-3, the maximum M_x and M_y values occur in pier P2 for all of the ground motion sets.

Sorting of maximum M_y values:

For AASHTO LRFD: SET-3 > SET-2 > SET-1 (49461 > 47501 > 43129) (kN.m)

For EN-8: SET-2 > SET-1 > SET-3 (54206 > 47131 > 45340) (kN.m)

For TDY 2020: SET2 > SET-1 > SET-3 (41275 > 31985 > 30498) (kN.m)

Sorting of maximum M_x values:

For AASHTO LRFD: SET-2 > SET-3 > SET-1 (46266 > 41992 > 32211) (kN.m)

For EN-8: SET-2 > SET-3 > SET-1 (53734 > 39354 > 34536) (kN.m)

For TDY 2020: SET-2 > SET-3 > SET-1 (39444 > 26683 > 25299) (kN.m)

In Method-3, the maximum u_x and u_y values occur in pier P2 for all of the ground motion sets.

Sorting of maximum u_y values:

For AASHTO LRFD: SET-3 > SET-2 > SET-1 (2.30 > 2.21 > 2.00) (cm)

For EN-8: SET-2 > SET-1 > SET-3 (2.53 > 2.19 > 2.11) (cm)

For TDY 2020: SET2 > SET-1 > SET-3 (1.92 > 1.49 > 1.42) (cm)

Sorting of maximum u_x values:

For AASHTO LRFD: SET-2 > SET-3 > SET-1 (6.05 > 5.49 > 4.21) (cm)

For EN-8: SET-2 > SET-3 > SET-1 (7.02 > 5.14 > 4.52) (cm)

For TDY 2020: SET-2 > SET-3 > SET-1 (5.15 > 3.49 > 3.31) (cm)

Moment and displacement values are not very close to each other as it can be seen from the given results. When the results are sorted, it can be seen that specifications point to different sets as critical and there is a considerable amount of difference between both M_x , M_y and u_x , u_y values. Besides, the lowest moment values are obtained in scaling according to the TDY 2020. On the other hand, most critical values are computed from scaling according to the EN-8.

Percentage difference given in the Tables 4.152, 4.154, 4.156, 4.158-4.164 below are calculated based on Equation 1.

Table 4.151 The maximum M_y values of pier P2 for M3 (kN.m)

	P2-M_y		
	SET-1	SET-2	SET-3
AASHTO	43129.16	47501.88	49461.42
EN	47131.51	54206.27	45340.99
TDY	31985.87	41275.57	30498.2

Table 4.152 Specification-wise percentage differences of M_y values of pier P2 for M3

	Compared with AASHTO LRFD			Compared with EN-8			Compared with TDY 2020		
	SET-1	SET-2	SET-3	SET-1	SET-2	SET-3	SET-1	SET-2	SET-3
AASHTO	-	-	-	-8%	-12%	9%	35%	15%	62%
EN	9%	14%	-8%	-	-	-	47%	31%	49%
TDY	-26%	-13%	-38%	-32%	-24%	-33%	-	-	-

EN-8 gives the largest moment values compared to other codes. TDY2020, on the other hand results in lowest M_y values like the results of Method-1 and Method-2.

Table 4.153 The maximum M_x values of pier P2 for M3 (kN.m)

	P2-M_x		
	SET-1	SET-2	SET-3
AASHTO	32211.35	54137.74	48319.48
EN	34536.18	62949.39	45517.82
TDY	25299.17	46106	30902.27

Table 4.154 Specification-wise percentage differences of M_x values of pier P2 for M3

	Compared with AASHTO LRFD			Compared with EN-8			Compared with TDY 2020		
	SET-1	SET-2	SET-3	SET-1	SET-2	SET-3	SET-1	SET-2	SET-3
AASHTO	-	-	-	-7%	-14%	6%	27%	17%	56%
EN	7%	16%	-5.80%	-	-	-	37%	37%	47%
TDY	-21%	-15%	-36%	-27%	-27%	-32%	-	-	-

EN-8 gives the largest moment values compared to other codes. TDY2020, on the other hand results in lowest M_x values like the results of Method-1 and Method-2.

Table 4.155 The maximum u_y values of pier P2 for M3 (m)

	P2-u_y		
	SET-1	SET-2	SET-3
AASHTO	0.0200	0.0221	0.0230
EN	0.0219	0.0253	0.0211
TDY	0.0148	0.0192	0.0142

Table 4.156 Specification-wise percentage differences of u_y values of pier P2 for M3

	Compared with AASHTO LRFD			Compared with EN-8			Compared with TDY 2020		
	SET-1	SET-2	SET-3	SET-1	SET-2	SET-3	SET-1	SET-2	SET-3
AASHTO	-	-	-	-9%	-12%	9%	35%	15%	62%
EN	9%	14%	-8%	-	-	-	47%	31%	49%
TDY	-26%	-13%	-38%	-32%	-24%	-33%	-	-	-

EN-8 gives the largest displacement values compared to other codes. TDY2020, on the other hand results in lowest u_y values like the results of Method-1 and Method-2.

Table 4.157 The maximum u_x values of pier P2 for M3 (m)

	P2- u_x		
	SET-1	SET-2	SET-3
AASHTO	0.0421	0.0605	0.0549
EN	0.0452	0.0702	0.0514
TDY	0.0331	0.0515	0.0349

Table 4.158 Specification-wise percentage differences of u_x values of pier P2 for M3

	Compared with AASHTO LRFD			Compared with EN-8			Compared with TDY 2020		
	SET-1	SET-2	SET-3	SET-1	SET-2	SET-3	SET-1	SET-2	SET-3
AASHTO	-	-	-	-7%	-14%	7%	27%	17%	57%
EN	7%	16%	-6%	-	-	-	37%	36%	47%
TDY	-21%	-15%	-36%	-27%	-27%	-32%	-	-	-

EN-8 gives the largest displacement values compared to other codes. TDY2020, on the other hand results in lowest u_x values like the results of Method-1 and Method-2.

Table 4.159 Ground motion set-wise percentage differences of M_y values of all pier columns for M3

		Compared with SET-1			Compared with SET-2			Compared with SET-3		
		SET-1	SET-2	SET-3	SET-1	SET-2	SET-3	SET-1	SET-2	SET-3
P1-M_y	AASHTO	-	12%	13%	-11%	-	1%	-12%	-1%	-
	EN	-	17%	-4%	-15%	-	-18%	4%	22%	-
	TDY	-	28%	-7%	-22%	-	-28%	8%	39%	-
P2-M_y	AASHTO	-	10%	15%	-9%	-	4%	-13%	-4%	-
	EN	-	15%	-4%	-13%	-	-16%	4%	20%	-
	TDY	-	29%	-5%	-23%	-	-26%	5%	35%	-

For most cases, SET-2 gives largest results for M_y whereas SET-1 results are generally smallest like the results of Method-1 and Method-2.

Table 4.160 Ground motion set-wise percentage differences of M_x values of all pier columns for M3

		Compared with SET-1			Compared with SET-2			Compared with SET-3		
		SET-1	SET-2	SET-3	SET-1	SET-2	SET-3	SET-1	SET-2	SET-3
P1-M_x	AASHTO	-	49%	33%	-33%	-	-11%	-25%	12%	-
	EN	-	61%	16%	-38%	-	-28%	-14%	38%	-
	TDY	-	60%	7%	-37%	-	-33%	-7%	49%	-
P2-M_x	AASHTO	-	68%	50%	-41%	-	-11%	-33%	12%	-
	EN	-	82%	32%	-45%	-	-28%	-24%	38%	-
	TDY	-	82%	22%	-45%	-	-33%	-18%	49%	-

For most cases, SET-2 gives largest results for M_x whereas SET-1 results are generally smallest like the results of Method-1 and Method-2.

Table 4.161 Ground motion set-wise percentage differences of u_y values of all pier columns for M3

		Compared with SET-1			Compared with SET-2			Compared with SET-3		
		SET-1	SET-2	SET-3	SET-1	SET-2	SET-3	SET-1	SET-2	SET-3
P1-u_y	AASHTO	-	12%	13%	-11%	-	1%	-12%	-1%	-
	EN	-	17%	-4%	-15%	-	-18%	4%	22%	-
	TDY	-	28%	-7%	-22%	-	-28%	8%	38%	-
P2-u_y	AASHTO	-	10%	15%	-10%	-	4%	-13%	-4%	-
	EN	-	15%	-4%	-13%	-	-16%	4%	20%	-
	TDY	-	29%	-4%	-23%	-	-26%	5%	35%	-

For most cases, SET-2 gives largest results for u_y whereas SET-1 results are generally smallest like the results of Method-1 and Method-2.

Table 4.162 Ground motion set-wise percentage differences of u_x values of all pier columns for M3

		Compared with SET-1			Compared with SET-2			Compared with SET-3		
		SET-1	SET-2	SET-3	SET-1	SET-2	SET-3	SET-1	SET-2	SET-3
P1-u_x	AASHTO	-	49%	33%	-33%	-	-11%	-25%	12%	-
	EN	-	61%	16%	-38%	-	-28%	-14%	38%	-
	TDY	-	60%	7%	-37%	-	-33%	-7%	49%	-
P2-u_x	AASHTO	-	44%	30%	-30%	-	-9%	-23%	10%	-
	EN	-	56%	14%	-36%	-	-27%	-12%	37%	-
	TDY	-	56%	5%	-36%	-	-32%	-5%	48%	-

For most cases, SET-2 gives largest results for u_x whereas SET-1 results are generally smallest like the results of Method-1 and Method-2.

4.3.4 Summary of the Comparison Results

It can be seen that the most critical values of moments and displacements occur in the same column and in the same ground motion set for all of the methods. Sorting of the ground motion sets are the same in moments and displacements unlike the bridges V03 and V08. The percentage differences of both ground motion set-wise and specification-wise are the same in moment and displacement values. Thus, the summary of the comparison results are mostly focused on the moment values.

It can be concluded that when the specification-based comparison is considered, scaling according to the Eurocode-8 design spectrum resulted in the greater moment values than AASHTO LRFD and TDY 2020 for all of three ground motion sets. For all of these cases, scaling according to the TDY 2020 design spectrum gives the minimum moment values.

When the scaling method-based comparison is considered, results are variable between the two pier columns for per specification as well.

As can be seen from Figure 4.43 and 4.44, for *AASHTO LRFD* design spectrum scaling, there is a consistency between the methods. In other words the maximum M_x and M_y moment values that are not varying in a vast scale among the scaling methods.

For the bridge transverse (M_y) direction, when the three ground motion sets applied for each method are compared, maximum values are obtained by SET-3 of Method-1 and Method-3, and SET-2 of Method-2.

For the bridge longitudinal (M_x) direction, when the three ground motion sets applied for each method are compared, maximum values are obtained by SET-2 of Method-2 and Method-3. In the Method-1 SET-2 and SET-3 gives the approximately the same values. For both directions SET-1 gives the minimum moment values.

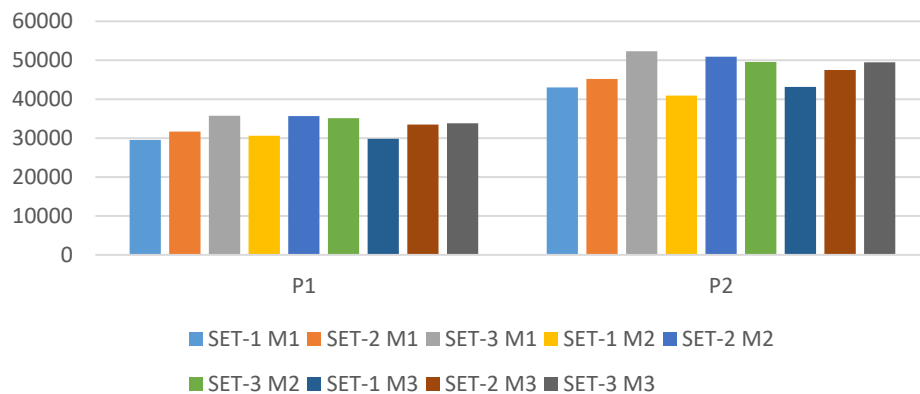


Figure 4.43. M_y values of all of the pier columns for three scaling methods applied according to AASHTO LRFD (kN.m)

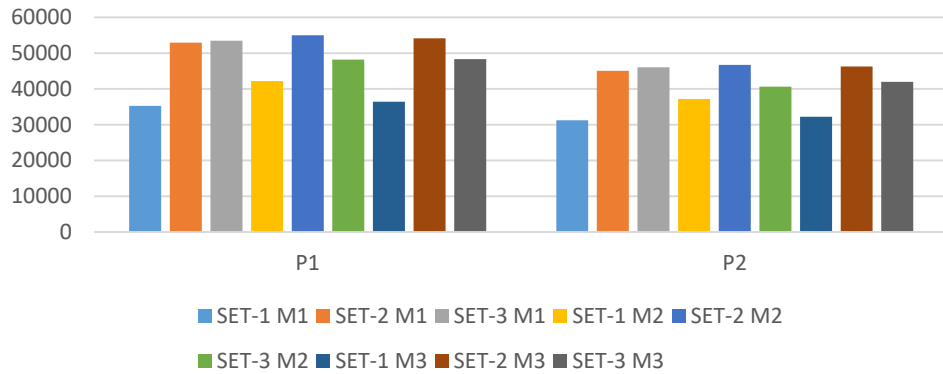


Figure 4.44. M_x values of all of the pier columns for three scaling methods applied according to AASHTO LRFD (kN.m)

It can be said that by following the AASHTO LRFD specification for the design, there is a consistency between the methods. Thus each method can be chosen for the time history analysis. In the case of the selection of ground motion sets, an uncertainty exists about which one to choose. Method-wise percentage differences can be seen in the Tables 163-165. Thus, different ground motion sets and one of the methods should be employed in the design to obtain reliable results.

Table 4.163 AASHTO LRFD method-wise differences for SET-1

	AASHTO LRFD M2-M _y			AASHTO LRFD M3-M _x		
	Compared with M1			Compared with M1		
	SET-1 M1	SET-1 M2	SET-1 M3	SET-1 M1	SET-1 M2	SET-1 M3
P1	-	0.036	0.010	-	0.196	0.032
P2	-	-0.049	0.002	-	0.191	0.032

	Compared with M2			Compared with M2		
	SET-1 M1	SET-1 M2	SET-1 M3	SET-1 M1	SET-1 M2	SET-1 M3
P1	-0.035	-	-0.025	-0.164	-	-0.138
P2	0.052	-	0.054	-0.160	-	-0.134

	Compared with M3			Compared with M3		
	SET-1 M1	SET-1 M2	SET-1 M3	SET-1 M1	SET-1 M2	SET-1 M3
P1	-0.010	0.026	-	-0.031	0.159	-
P2	-0.002	-0.052	-	-0.031	0.155	-

Table 4.164 AASHTO LRFD method-wise differences for SET-2

	AASHTO LRFD M2-M _y			AASHTO LRFD M3-M _x		
	Compared with M1			Compared with M1		
	SET-2 M1	SET-2 M2	SET-2 M3	SET-2 M1	SET-2 M2	SET-2 M3
P1	-	0.126	0.056	-	0.039	0.022
P2	-	0.127	0.051	-	0.036	0.027

	Compared with M2			Compared with M2		
	SET-2 M1	SET-2 M2	SET-2 M3	SET-2 M1	SET-2 M2	SET-2 M3
P1	-0.112	-	-0.062	-0.037	-	-0.016
P2	-0.112	-	-0.067	-0.035	-	-0.009

	Compared with M3			Compared with M3		
	SET-2 M1	SET-2 M2	SET-2 M3	SET-2 M1	SET-2 M2	SET-2 M3
P1	-0.053	0.066	-	-0.022	0.016	-
P2	-0.049	0.072	-	-0.026	0.009	-

Table 4.165 AASHTO LRFD method-wise differences for SET-3

	AASHTO LRFD M2-M _y			AASHTO LRFD M3-M _x		
	Compared with M1			Compared with M1		
	SET-3 M1	SET-3 M2	SET-3 M3	SET-3 M1	SET-3 M2	SET-3 M3
P1	-	-0.017	-0.053	-	-0.099	-0.096
P2	-	-0.052	-0.055	-	-0.117	-0.088

	Compared with M2			Compared with M2		
	SET-3 M1	SET-3 M2	SET-3 M3	SET-3 M1	SET-3 M2	SET-3 M3
	P1	0.018	-	-0.037	0.109	-
P2	0.055	-	-0.002	0.133	-	0.033

	Compared with M3			Compared with M3		
	SET-3 M1	SET-3 M2	SET-3 M3	SET-3 M1	SET-3 M2	SET-3 M3
	P1	0.056	0.038	-	0.106	-0.003
P2	0.058	0.002	-	0.097	-0.032	-

As can be seen from Figure 4.45 and 4.46, for *Eurocode-8* design spectrum scaling, there is a consistency between the methods. In other words the maximum M_x and M_y moment values that are not varying in a vast scale among the scaling methods like those in AASHTO LRFD.

For the bridge transverse (M_y) and longitudinal direction (M_x), when the three ground motion sets applied for each method are compared, SET-2 gives the maximum values for all of the three scaling methods. However, the sorting of the other sets are not certain because they change according to method and pier column.

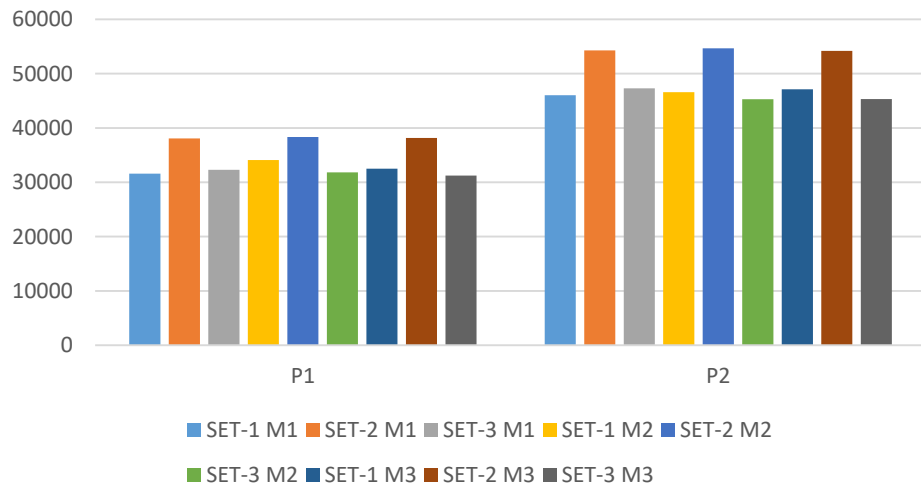


Figure 4.45. M_y values of all of the pier columns for three scaling methods applied according to EN-8 (kN.m)

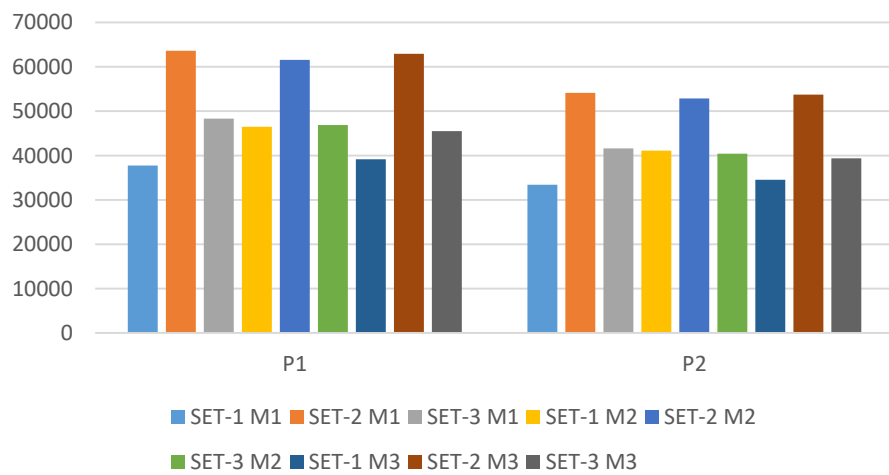


Figure 4.46. M_x values of all of the pier columns for three scaling methods applied according to EN-8 (kN.m)

It can be said that by following the Eurocode-8 specification for the design, there is a consistency between the methods. Thus each method can be chosen for the time history analysis. Method-wise percentage differences can be seen in the Tables 166-168. In the case of the selection of ground motion sets, SET-2 gives the maximum moments. Thus, SET-2 and any of the methods should be employed in the design to obtain reliable results.

Table 4.166 EN-8 method-wise differences for SET-1

	EN M2-M _y			EN M3-M _x		
	Compared with M1			Compared with M1		
	SET-1 M1	SET-1 M2	SET-1 M3	SET-1 M1	SET-1 M2	SET-1 M3
P1	-	0.079	0.029	-	0.232	0.038
P2	-	0.012	0.024	-	0.230	0.034

	Compared with M2			Compared with M2		
	SET-1 M1	SET-1 M2	SET-1 M3	SET-1 M1	SET-1 M2	SET-1 M3
P1	-0.073	-	-0.046	-0.188	-	-0.158
P2	-0.012	-	0.012	-0.187	-	-0.160

	Compared with M3			Compared with M3		
	SET-1 M1	SET-1 M2	SET-1 M3	SET-1 M1	SET-1 M2	SET-1 M3
P1	-0.028	0.049	-	-0.036	0.187	-
P2	-0.023	-0.012	-	-0.033	0.190	-

Table 4.167 EN-8 method-wise differences for SET-2

	EN M2-M _y			EN M3-M _x		
	Compared with M1			Compared with M1		
	SET-2 M1	SET-2 M2	SET-2 M3	SET-2 M1	SET-2 M2	SET-2 M3
P1	-	0.007	0.002	-	-0.033	-0.011
P2	-	0.007	-0.002	-	-0.024	-0.008

	Compared with M2			Compared with M2		
	SET-2 M1	SET-2 M2	SET-2 M3	SET-2 M1	SET-2 M2	SET-2 M3
	P1	-0.007	-	-0.005	0.034	-
P2	-0.007	-	-0.008	0.024	-	0.016

	Compared with M3			Compared with M3		
	SET-2 M1	SET-2 M2	SET-2 M3	SET-2 M1	SET-2 M2	SET-2 M3
	P1	-0.002	0.005	-	0.011	-0.022
P2	0.002	0.008	-	0.008	-0.016	-

Table 4.168 EN-8 method-wise differences for SET-3

	EN M2-M _y			EN M3-M _x		
	Compared with M1			Compared with M1		
	SET-3 M1	SET-3 M2	SET-3 M3	SET-3 M1	SET-3 M2	SET-3 M3
P1	-	-0.014	-0.032	-	-0.030	-0.058
P2	-	-0.042	-0.041	-	-0.029	-0.055

	Compared with M2			Compared with M2		
	SET-3 M1	SET-3 M2	SET-3 M3	SET-3 M1	SET-3 M2	SET-3 M3
	P1	0.014	-	-0.018	0.031	-
P2	0.044	-	0.001	0.030	-	-0.027

	Compared with M3			Compared with M3		
	SET-3 M1	SET-3 M2	SET-3 M3	SET-3 M1	SET-3 M2	SET-3 M3
	P1	0.033	0.019	-	0.061	0.029
P2	0.043	-0.001	-	0.058	0.027	-

As can be seen from Figure 4.47 and 4.48, for *TDY-2020* design spectrum scaling, there is a consistency between the methods. In other words the maximum M_x and M_y moment values that are not varying in a vast scale among the scaling methods like those in AASHTO LRFD and EN-8.

For the bridge transverse (M_y) and longitudinal direction (M_x), when the three ground motion sets applied for each method are compared, SET-2 gives the maximum values for all of the three scaling methods. However, the sorting of the other sets are not certain because they change according to method and pier column like those in EN-8.

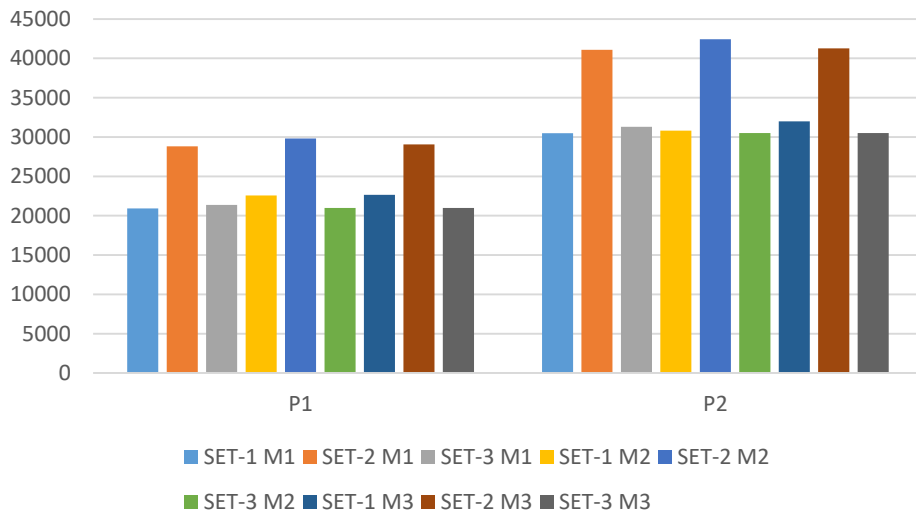


Figure 4.47. M_y values of all of the pier columns for three scaling methods applied according to TDY 2020 (kN.m)

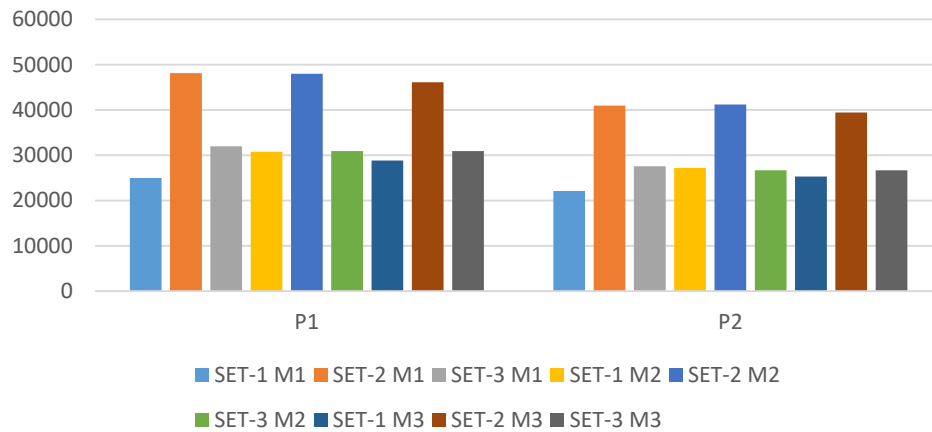


Figure 4.48. M_x values of all of the pier columns for three scaling methods applied according to TDY 2020 (kN.m)

It can be said that by following the TDY specification for the design, there is a consistency between the methods. Method-wise percentage differences can be seen in the Tables 169-171. Thus each method can be chosen for the time history analysis. In the case of the selection of ground motion sets, SET-2 gives the maximum moments. Thus, SET-2 and any of the methods should be employed in the design to obtain reliable results.

Table 4.169 TDY 2020 method-wise differences for SET-1

	TDY M2-M _y			TDY M3-M _x		
	Compared with M1			Compared with M1		
	SET-1 M1	SET-1 M2	SET-1 M3	SET-1 M1	SET-1 M2	SET-1 M3
P1	-	0.079	0.083	-	0.232	0.154
P2	-	0.011	0.050	-	0.230	0.144

	Compared with M2			Compared with M2		
	SET-1 M1	SET-1 M2	SET-1 M3	SET-1 M1	SET-1 M2	SET-1 M3
	P1	-0.073	-	0.004	-0.188	-
P2	-0.011	-	0.038	-0.187	-	-0.070

	Compared with M3			Compared with M3		
	SET-1 M1	SET-1 M2	SET-1 M3	SET-1 M1	SET-1 M2	SET-1 M3
	P1	-0.077	-0.004	-	-0.133	0.068
P2	-0.047	-0.037	-	-0.126	0.075	-

Table 4.170 TDY 2020 method-wise differences for SET-2

	TDY M2-M _y			TDY M3-M _x		
	Compared with M1			Compared with M1		
	SET-2 M1	SET-2 M2	SET-2 M3	SET-2 M1	SET-2 M2	SET-2 M3
P1	-	0.035	0.008	-	-0.003	-0.042
P2	-	0.033	0.005	-	0.005	-0.037

	Compared with M2			Compared with M2		
	SET-2 M1	SET-2 M2	SET-2 M3	SET-2 M1	SET-2 M2	SET-2 M3
	P1	-0.034	-	-0.025	0.003	-
P2	-0.032	-	-0.027	-0.005	-	-0.042

	Compared with M3			Compared with M3		
	SET-2 M1	SET-2 M2	SET-2 M3	SET-2 M1	SET-2 M2	SET-2 M3
	P1	-0.008	0.026	-	0.044	0.041
P2	-0.005	0.028	-	0.039	0.044	-

Table 4.171 TDY 2020 method-wise differences for SET-3

	TDY M2-M _y			TDY M3-M _x		
	Compared with M1			Compared with M1		
	SET-3 M1	SET-3 M2	SET-3 M3	SET-3 M1	SET-3 M2	SET-3 M3
P1	-	-0.019	-0.019	-	-0.034	-0.034
P2	-	-0.026	-0.026	-	-0.032	-0.032

	Compared with M2			Compared with M2		
	SET-3 M1	SET-3 M2	SET-3 M3	SET-3 M1	SET-3 M2	SET-3 M3
	P1	0.019	-	0.000	0.035	-
P2	0.027	-	0.000	0.033	-	0.000

	Compared with M3			Compared with M3		
	SET-3 M1	SET-3 M2	SET-3 M3	SET-3 M1	SET-3 M2	SET-3 M3
	P1	0.019	0.000	-	0.035	0.000
P2	0.027	0.000	-	0.033	0.000	-

It appears that in all cases any of the three methods can be chosen because the moment values are close to each other between each method, in other words there is a consistency between methods. Besides, in both directions, SET-2 gives the maximum values with Method-2. Thus, SET-2 and any of the methods can be employed in the seismic design of bridges having fundamental periods smaller than 1 ($T_n < 1$) to obtain reliable and accurate results.

CHAPTER 5

CONCLUSIONS AND FUTURE WORK

In this study, ground motion scaling methods and scaling criteria for highway bridges are investigated. It can be stated that ground motion selection, forming of ground motion sets and choosing an appropriate method are important to conduct a time history analysis.

In this thesis, three bridges are selected to understand the role of the fundamental period of a structure in different scaling methods and ground motion sets. Three scaling methods are compared between each other to understand the effects of the scaling methods. Also, three ground motion sets are compared to see the importance of the ground motion selection. These comparisons are done by following different specifications because they have similar but different criteria.

Results show that there is no consistency between neither scaling methods nor ground motion sets among different bridges with different fundamental periods and even among a bridge's piers columns. While in one column one of the methods under a ground motion gives the maximum values, in another column different cases lead to maximum values. Thus, to set a straightforward scaling rule for time history analysis cannot be justified considering the results here. This can lead to an over- or under-designed, poorly constructed bridges.

Pier column moment and displacement results show that the most critical values were determined in scaling according to the Eurocode-8 design spectrum for 3 different scaling methods with 3 different sets. Also, TDY scaling methods shows that the least moment and displacement values are obtained when compared to the other methods. For example, in V03 Bridge M_y values are sorted as EN-8 > AASHTO LRFD > TDY 2020 with the values of 92641>75157>63133 kNm for Method-1 employing SET-1.

The difference between the moments is generally smaller when the period of structure is smaller. In other words, the structure with the longest period, V03 Bridge, shows mostly the greatest difference in method-wise comparison both for specifications and ground motion sets. In the lowest period structure, V14 Bridge, the difference between values of different methods is closer. For example, for AASHTO LRFD scaling, sorting of the percentage differences between the methods for ground motion set SET-2 is $V03 > V08 > V14$ with the values of $46\% > 19\% > 13\%$ in the transverse direction, M_y .

It is resulted that the most critical values of moments and displacements do not always occur in the same column and in the same ground motion set for V03 Bridge having fundamental period of greater than 1 ($T_n > 1$). Sorting of the ground motion sets for displacement values are much different than the sorting of the sets for moments. For example, in V03 Bridge scaling according to the AASHTO LRFD, sorting of the maximum M_y values are $SET-3 > SET-2 > SET-1$ in Method-1, while the sorting of the maximum u_y values are $SET-3 > SET-1 > SET-2$. However, sorting of the ground motion sets for displacement values become less different than the sorting of the sets for moments for the V08 Bridge having fundamental period equal to 1 ($T_n = 1$). This sorting difference is closed and become the same in V14 Bridge having fundamental period less than 1 ($T_n < 1$). For example, in V14 Bridge scaling according to the AASHTO LRFD, sorting of the maximum M_y values are $SET-3 > SET-2 > SET-1$ in Method-1, while the sorting of the maximum u_y values are $SET-3 > SET-2 > SET-1$.

For the V03 Bridge having fundamental periods greater than 1 ($T_n > 1$), it appears that in all cases Method-2 gives the largest values for M_y in transverse direction. This can be explained by having no upper limit for scaling. However, for M_x in longitudinal direction it cannot be decided that which method give the maximum values. Also, in both directions, it seems to be not clear that which ground motion set should be used. Thus, different ground motion sets and methods should be employed in the seismic design of bridges having fundamental periods greater than 1 ($T_n > 1$) to obtain reliable and accurate results for each bridge design specification.

For the V08 Bridge having fundamental period equal to 1 ($T_n=1$), it is resulted that in all cases Method-2 gives the largest moment values of M_x and M_y for AASHTO LRFD and TDY 2020. Besides, in both directions, SET-2 gives the maximum values with Method-2. Unlikely, for Eurocode-8, there is an uncertainty about which method and set to be used. Thus, different ground motion sets and methods should be employed in the seismic design of bridges having fundamental periods equal to 1 ($T_n=1$) to obtain reliable and accurate results for Eurocode-8 bridge design specification, while for AASHTO LRFD and TDY Method-2 and SET-2 can be accepted.

For the V14 Bridge having fundamental period less than 1 ($T_n<1$), in all cases any of the three methods can be chosen because the moment values are close to each other between each method, in other words there is a consistence between methods. Besides, in both directions, SET-2 gives the maximum values with Method-2. Thus, SET-2 and any of the methods can be employed in the seismic design of bridges having fundamental periods smaller than 1 ($T_n<1$) to obtain reliable and accurate results.

One reason behind the difference in the moment and displacement values can be stated as the fundamental period of the bridge. Because as fundamental period of the bridge gets smaller, the consistency between the results of scaling methods and ground motion sets gets similar.

Another reason for the moment and displacement differences between sets is based on the spectral shapes of the selected earthquakes. At the fundamental period, these 3 sets produce different pseudo-spectral acceleration values. Therefore, it is reasonable to acquire different moment values for different sets. It is suggested that the spectral shape of a calculated mean spectrum values should be similar to target spectrum.

Each structure has their own characteristics and natures. Ground motions should be selected not only with the magnitudes and rupture distances but also with considering all of their aspects. In other words earthquake records should be carefully selected to meet the necessities of the bridges to be designed. In the light of this study, it can be suggested that, to successfully conduct a time history analysis, different methods and different ground motion sets should be participated in the analysis.

In the future study;

- Different soil types can be investigated.
- Deeper research on earthquake parameters like PGV and PGD can be compared to make a relation with the earthquake sets and the results.
- The spectral shape of the selected ground motions can be selected in terms of being similar to the target spectrum.
- The near field effects can be considered.
- Frequency content of motions may lead differences in the seismic demand parameters. Frequency content search may be included in the design procedure.
- Nonlinear time history analysis can be employed.

REFERENCES

- AAASHTO LRFD. (2012). Bridge Design Specifications, 6th Edition. In American Association of State Highway and Transportation Officials, Washington, DC.
- Computers & Structures Inc. (2016). CSI ETABS v.2015. SAP2000 Reference Manual, (July), 556.
- Chopra, K., Kalkan, E. (2010). Practical Guidelines to Select and Scale Earthquake Records for Nonlinear Response History Analysis of Structures.
- Erdik, M., Demircioglu, M., Şeşeyatan, K. (2017). Seismic Hazard Assessment of Bridges and Viaducts on the Marmara Motorway. Bogazici University Kandilli Observatory and Earthquake Research Institute. (2017).
- Eurocode 8. (2003). Design of Structures for Earthquake Resistance.
- Katsanos, I. E., Sextos, G. A., Manolis, D.G. (2009). Selection of Earthquake Ground Motion Records: A State of the Art Review from a Structural Engineering Perspective.
- Lancieri, M., Bazzurro, P., Scotti, O., (2018). Spectral Matching in Time Domain: A Seismological and Engineering Analysis, Bulletin of the Seismological Society of America (2018), Vol.108, No. 4: 1972–1994
- Liang, X., Mosalam, K. (2017). Evaluation of Ground Motion Selection and Modification Methods on Reinforced Concrete Highway Bridges. Conference Paper.
- O'Donnell, A. P., Kurama, Y.C., Kalkan, E., Taflanidis, A. (2016). Experimental Evaluation of Four Ground-motion Scaling Methods for Dynamic Response-history Analysis of Nonlinear Structures.

PEER, (2010). User's Manual for the PEER Ground Motion Database Web Application Beta Version-October 1, 2010.

SeismoSignal Version 2021: SeismoSoft.

Turkish Seismic Code. (2020). Provisions for Highway and Railway Bridges and Viaducts under the Seismic Effects.

APPENDICES

A. Accelerograms of Selected Earthquakes

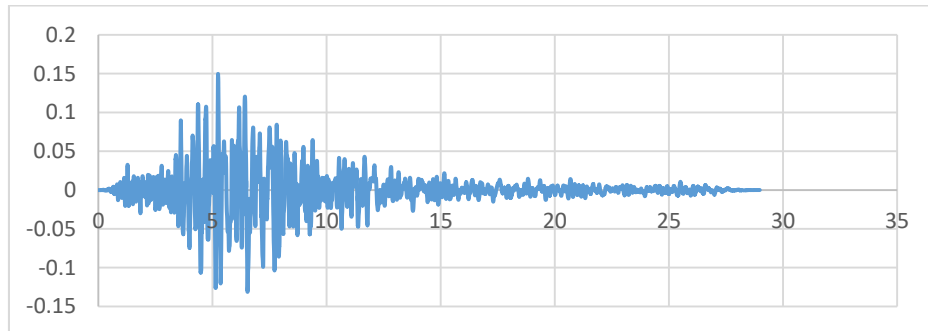


Figure A.1. Accelerogram of Basso Tirreno earthquake in x-direction (SET-1)

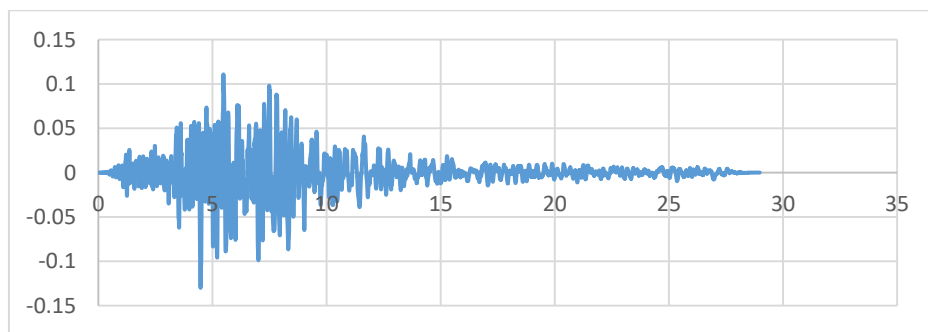


Figure A.2. Accelerogram of Basso Tirreno earthquake in y-direction (SET-1)

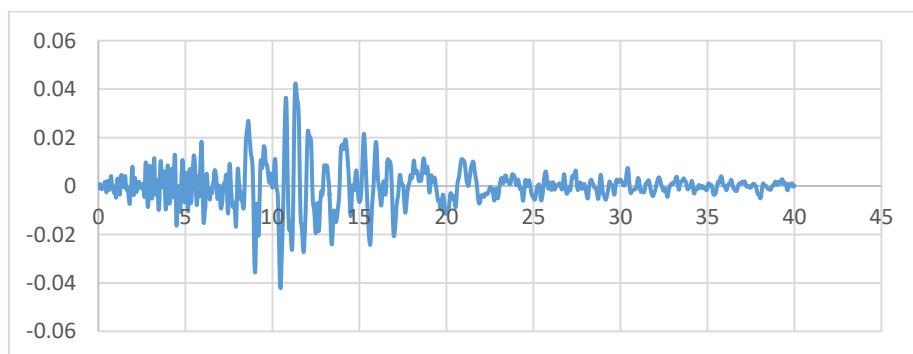


Figure A.3. Accelerogram of Chi Chi_2871 earthquake in x-direction (SET-1)

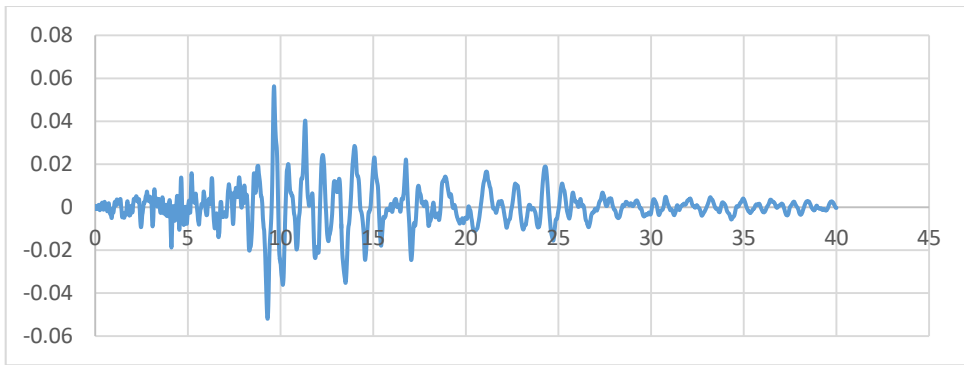


Figure A.4. Accelerogram of Chi Chi_2871 earthquake in y-direction (SET-1)

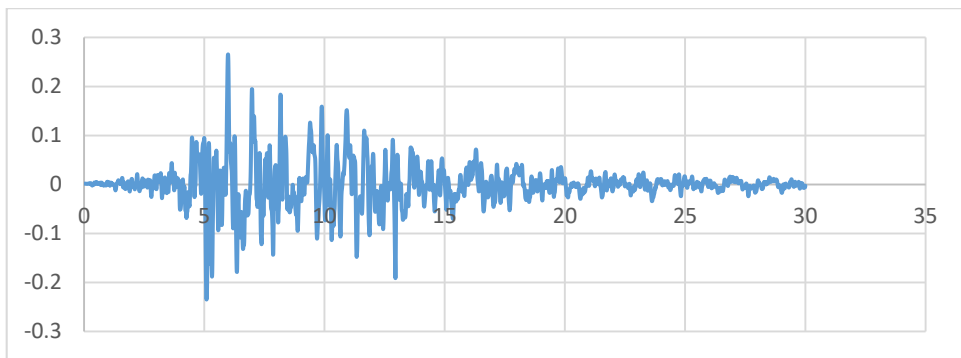


Figure A.5. Accelerogram of Hector earthquake in x-direction (SET-1)

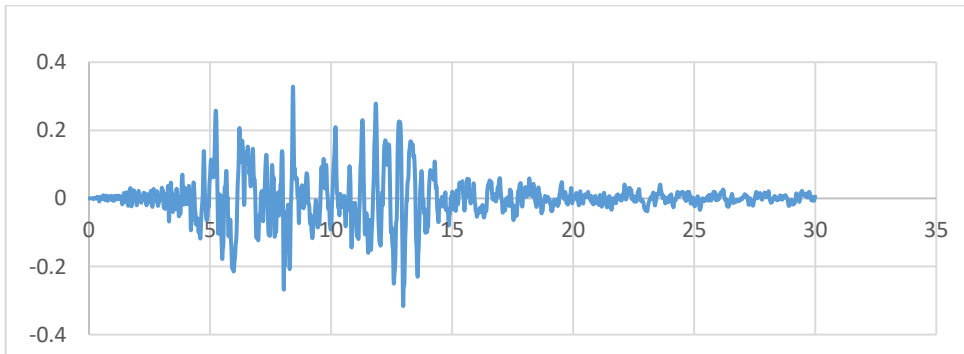


Figure A.6. Accelerogram of Hector earthquake in y-direction (SET-1)

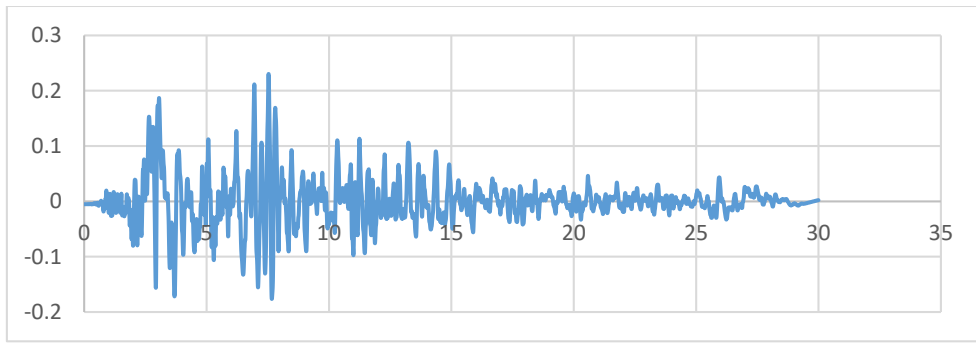


Figure A.7. Accelerogram of Kocaeli_1165 earthquake in x-direction (SET-1)

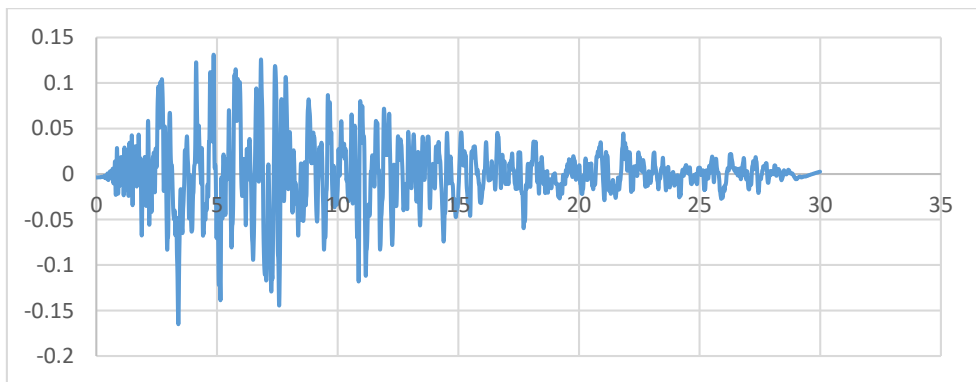


Figure A.8. Accelerogram of Kocaeli_1165 earthquake in y-direction (SET-1)

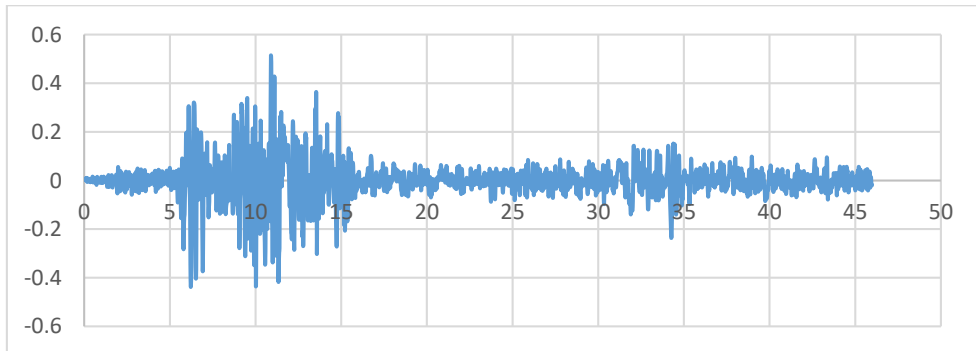


Figure A.9. Accelerogram of Manjil Abbar earthquake in x-direction (SET-1)

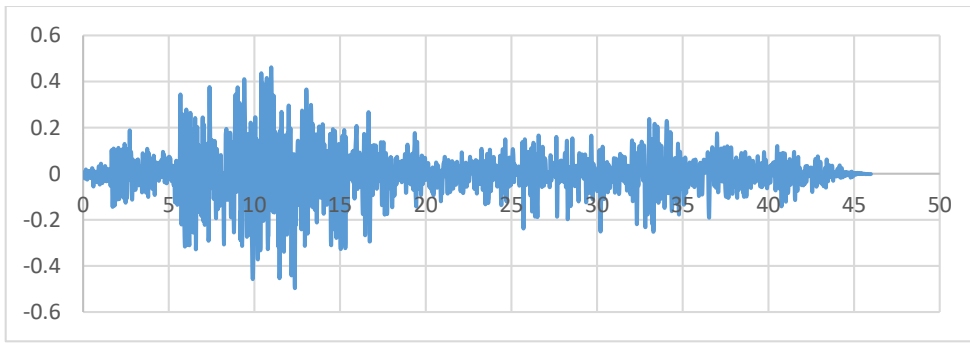


Figure A.10. Accelerogram of Manjil Abbar earthquake in y-direction (SET-1)

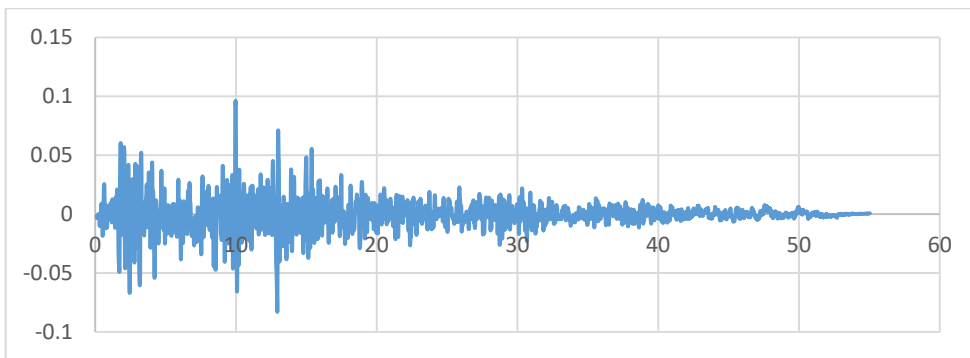


Figure A.11. Accelerogram of Sitka earthquake in x-direction (SET-1)

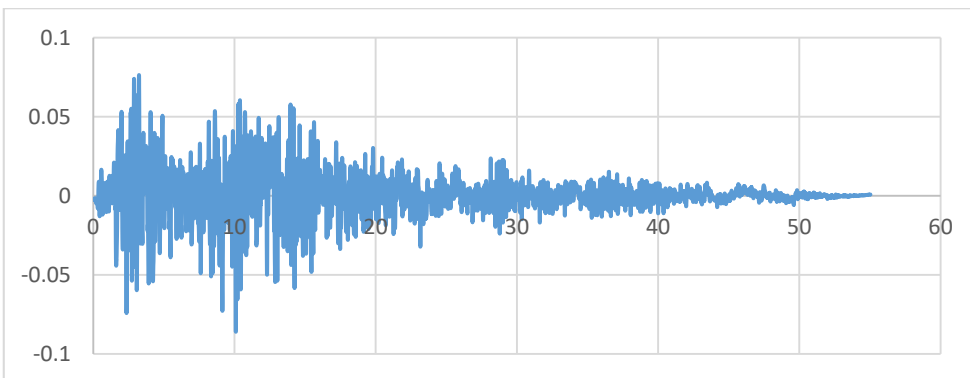


Figure A.12. Accelerogram of Sitka earthquake in y-direction (SET-1)

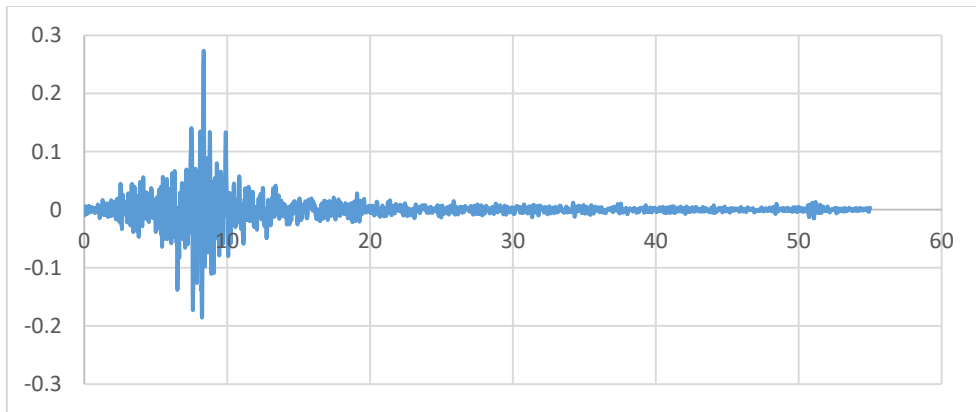


Figure A.13. Accelerogram of Tottori-3 earthquake in x-direction (SET-1)

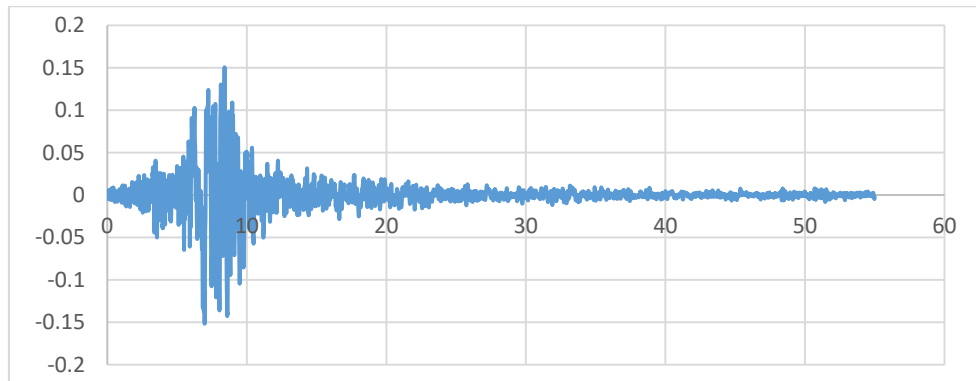


Figure A.14. Accelerogram of Tottori-3 earthquake in y-direction (SET-1)

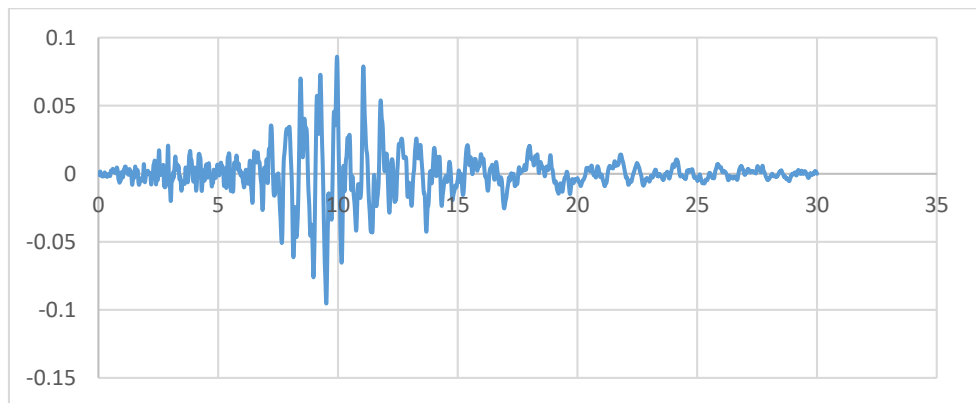


Figure A.15. Accelerogram of Chi Chi_2712 earthquake in x-direction (SET-2)

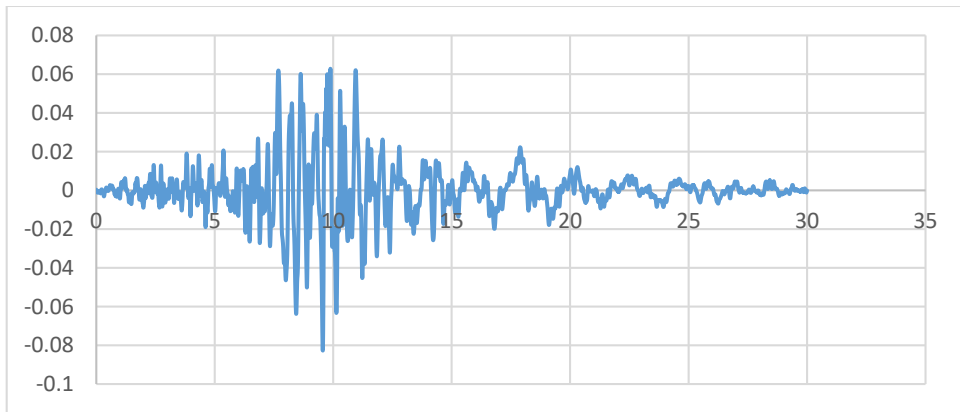


Figure A.16. Accelerogram of Chi Chi_2712 earthquake in y-direction (SET-2)

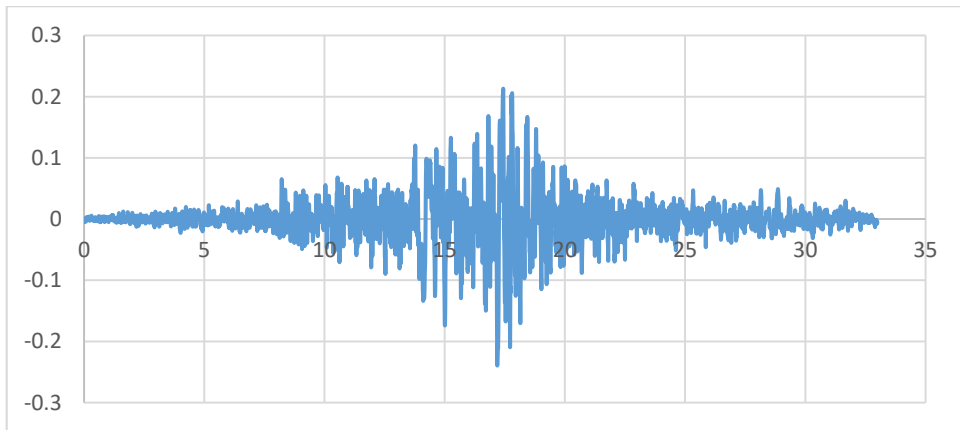


Figure A.17. Accelerogram of Darfield earthquake in x-direction (SET-2)

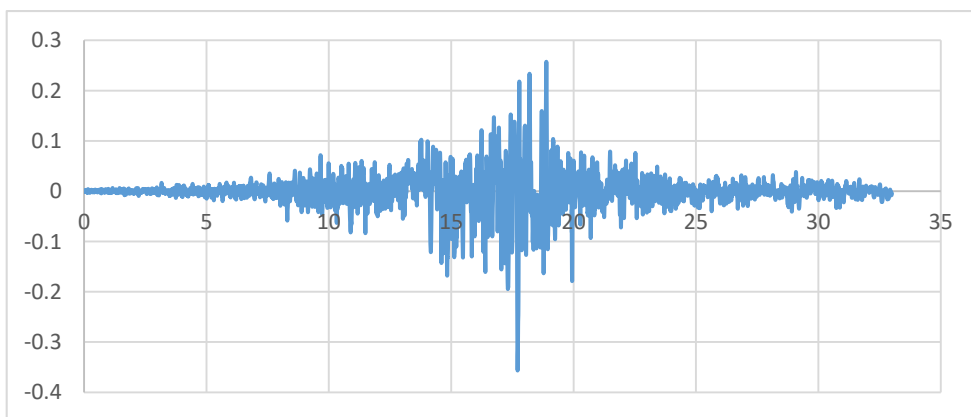


Figure A.18. Accelerogram of Darfield earthquake in y-direction (SET-2)

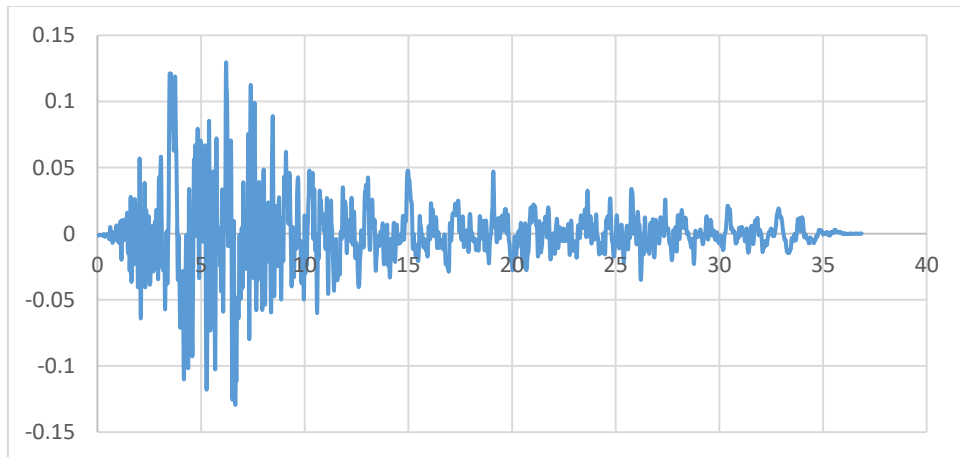


Figure A.19. Accelerogram of Irpiana285 earthquake in x-direction (SET-2)

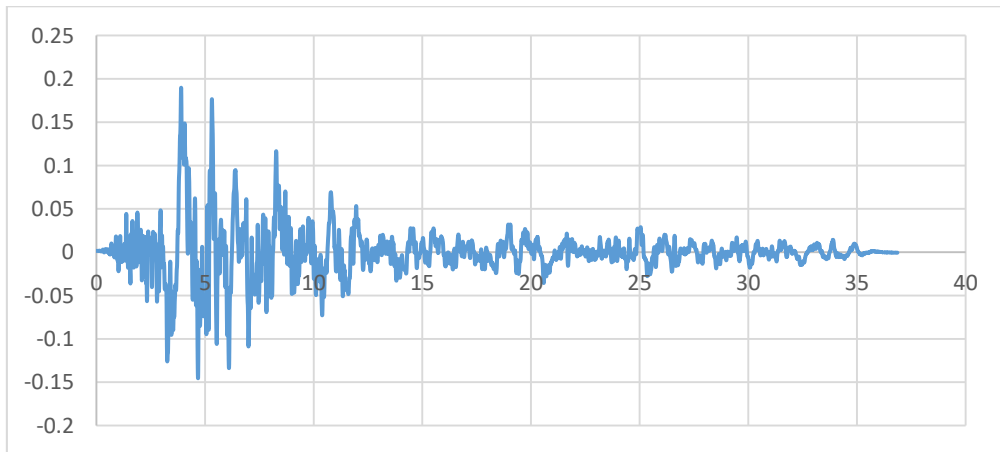


Figure A.20. Accelerogram of Irpiana285 earthquake in y-direction (SET-2)

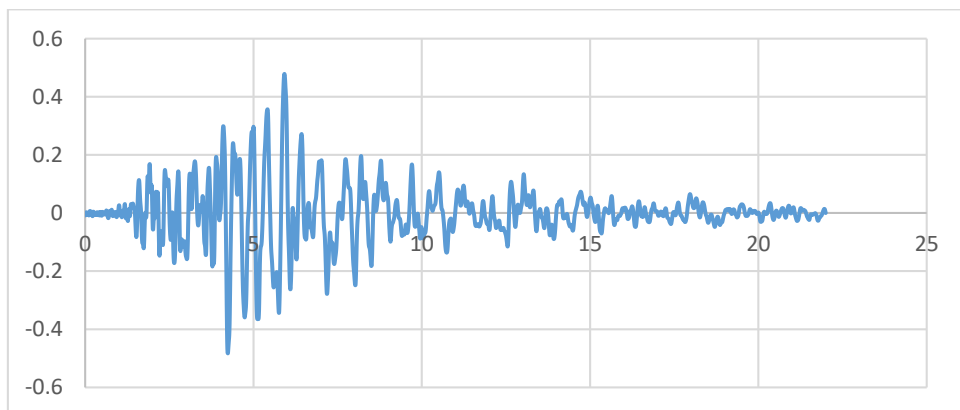


Figure A.21. Accelerogram of Kobe earthquake in x-direction (SET-2)

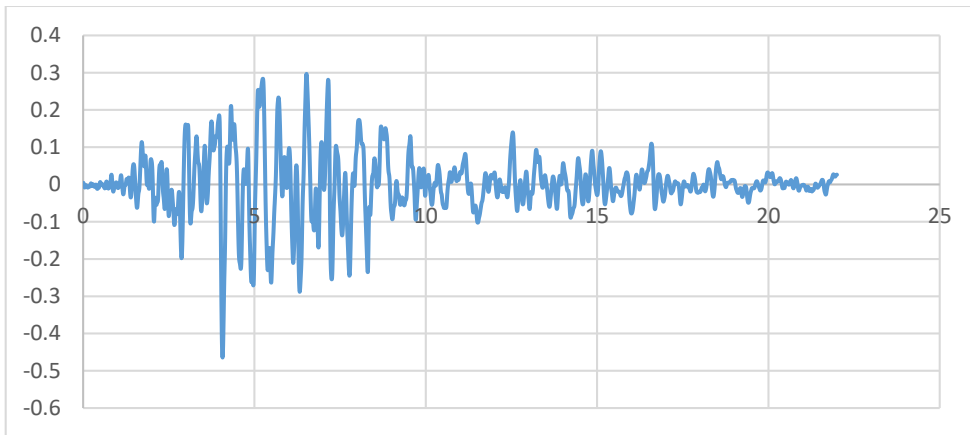


Figure A.22. Accelerogram of Kobe earthquake in y-direction (SET-2)

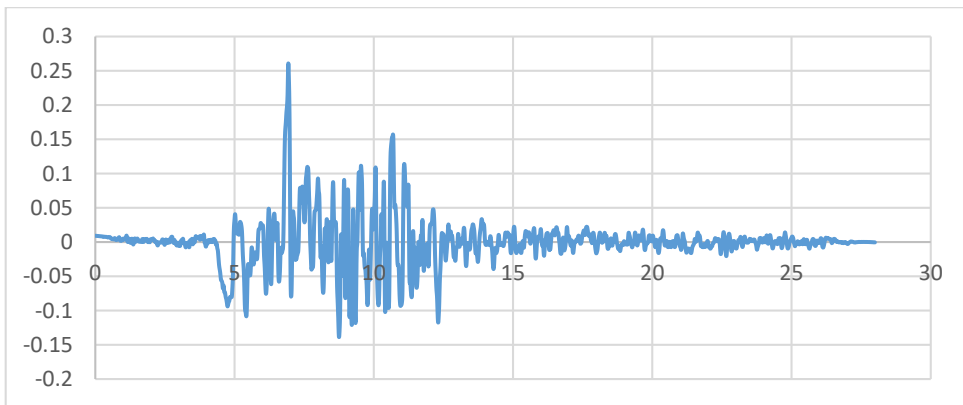


Figure A.23. Accelerogram of Kocaeli_1161 earthquake in x-direction (SET-2)

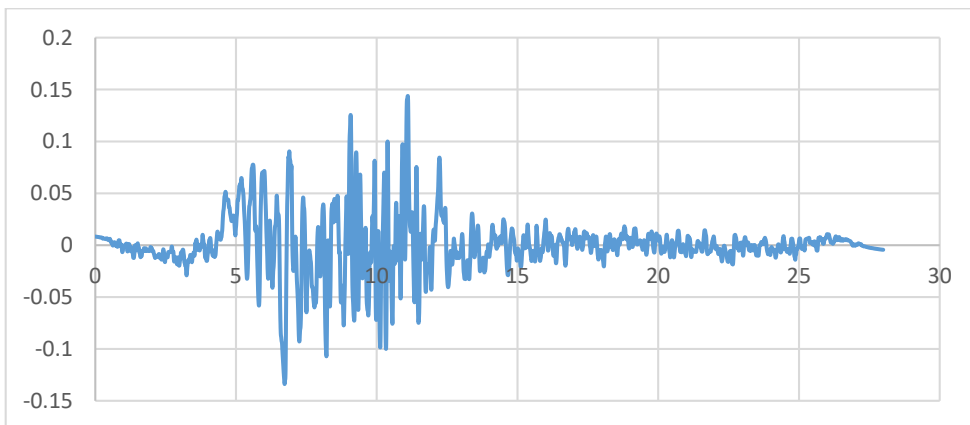


Figure A.24. Accelerogram of Kocaeli_1161 earthquake in y-direction (SET-2)

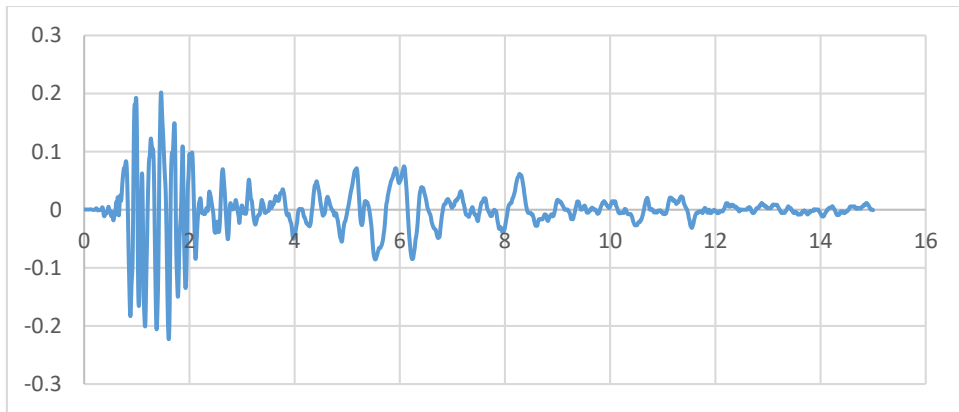


Figure A.25. Accelerogram of Morgan Hill-2 earthquake in x-direction (SET-2)

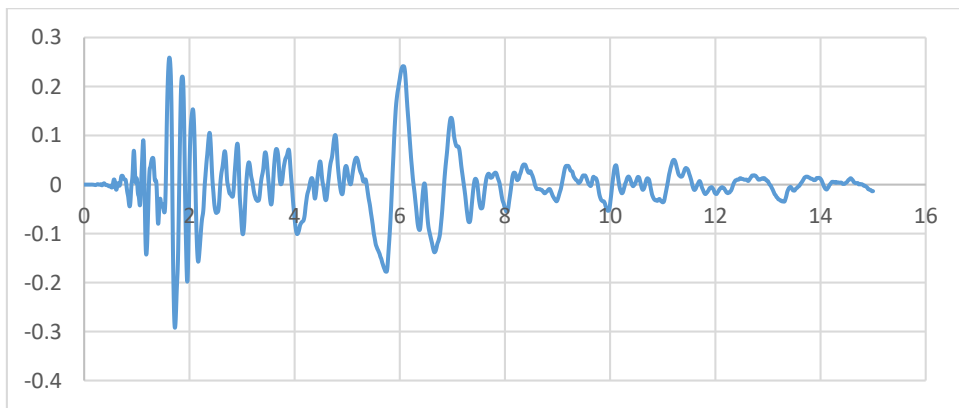


Figure A.26. Accelerogram of Morgan Hill-2 earthquake in y-direction (SET-2)

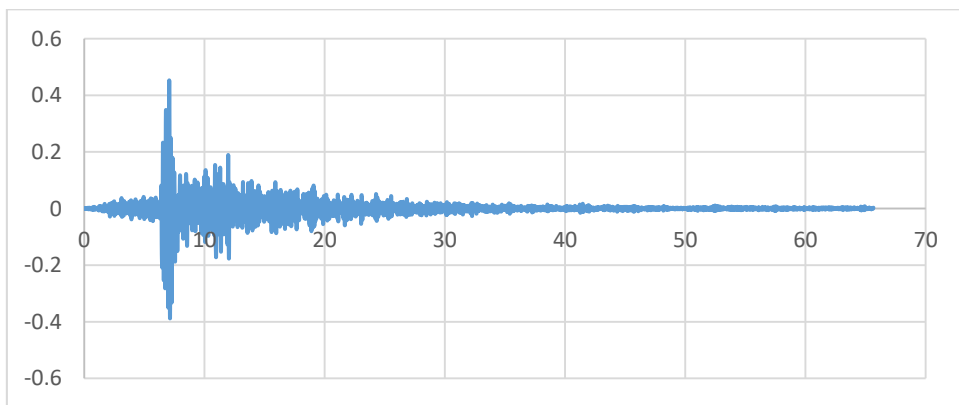


Figure A.27. Accelerogram of Tottori-2 earthquake in x-direction (SET-2)

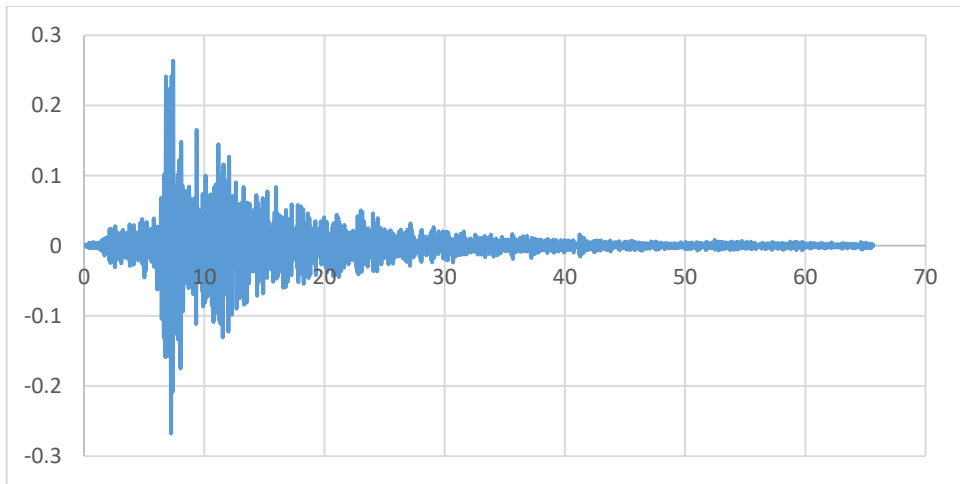


Figure A.28. Accelerogram of Tottori-2 earthquake in y-direction (SET-2)

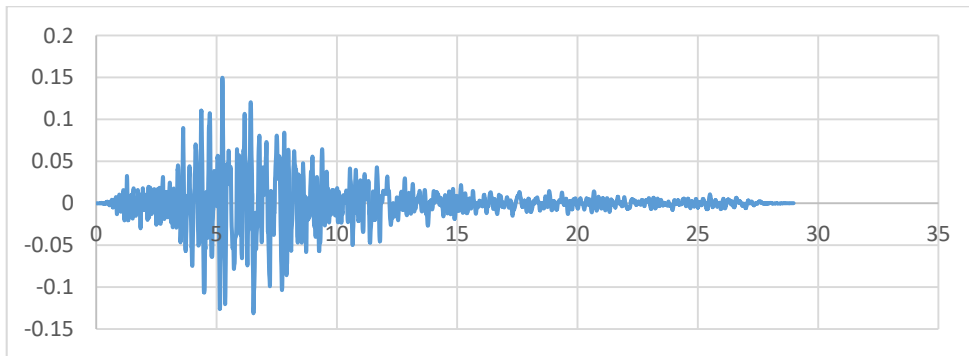


Figure A.29. Accelerogram of Basso Tirreno earthquake in x-direction (SET-3)

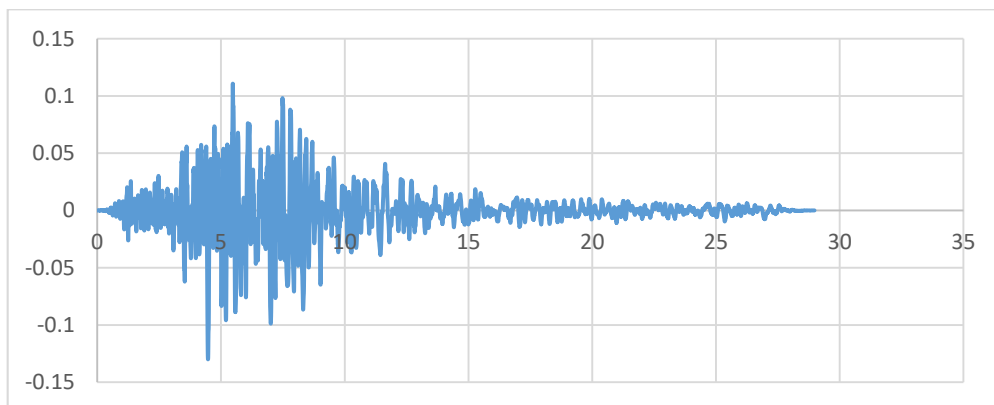


Figure A.30. Accelerogram of Basso Tirreno earthquake in y-direction (SET-3)

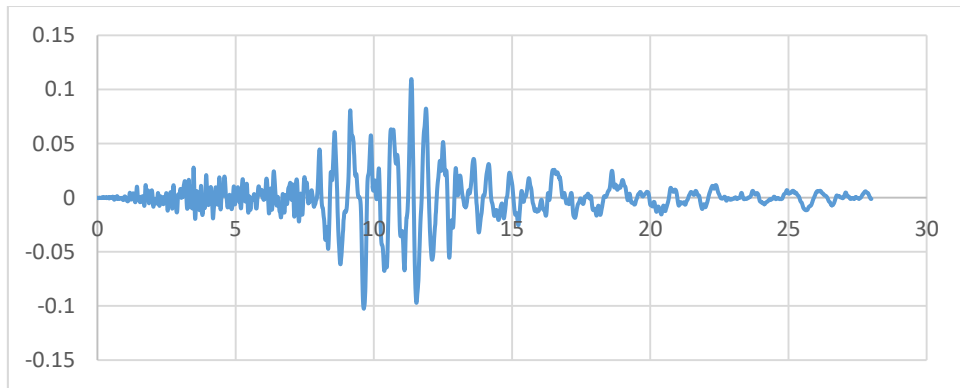


Figure A.31. Accelerogram of Chi Chi_2742 earthquake in x-direction (SET-3)

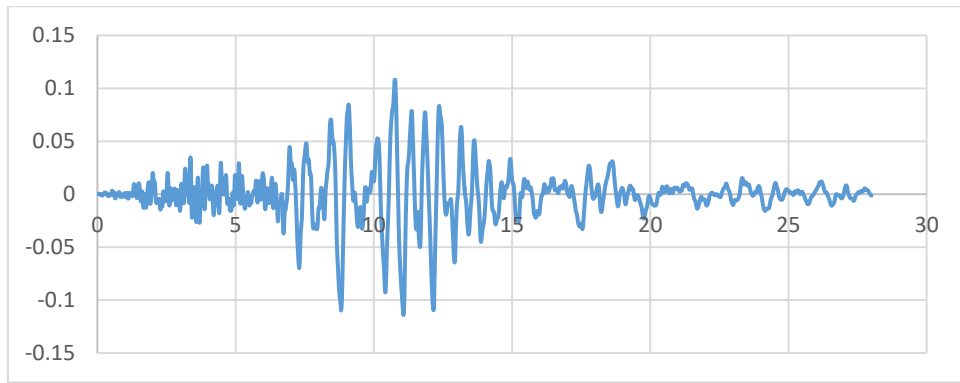


Figure A.32. Accelerogram of Chi Chi_2742 earthquake in y-direction (SET-3)

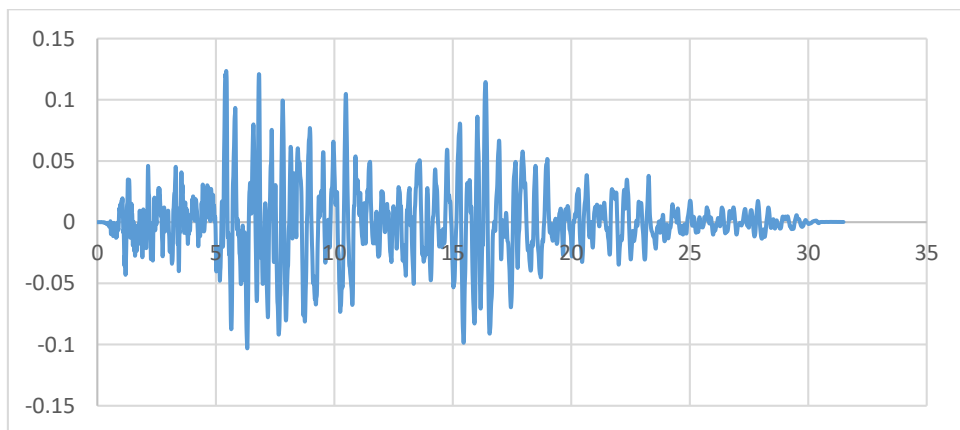


Figure A.33. Accelerogram of Düzce_1618 earthquake in x-direction (SET-3)

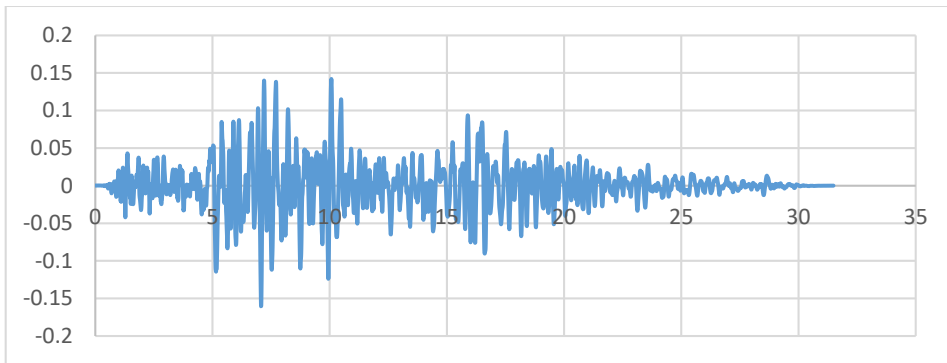


Figure A.34. Accelerogram of Düzce_1618 earthquake in y-direction (SET-3)

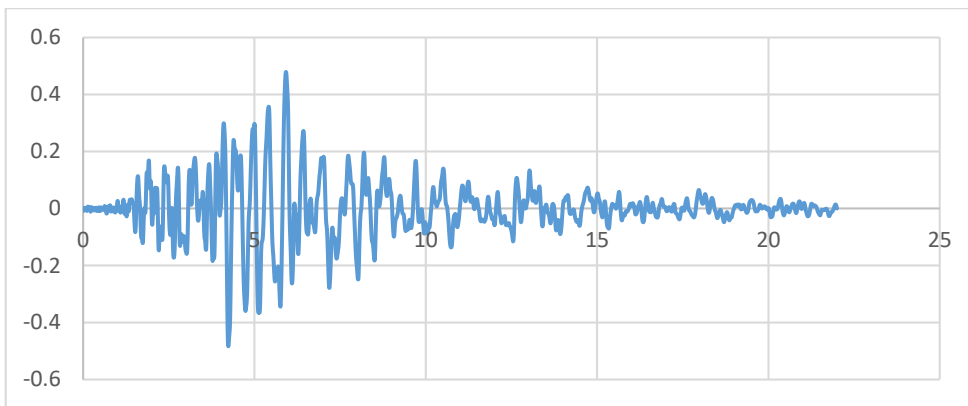


Figure A.35. Accelerogram of Kobe earthquake in x-direction (SET-3)

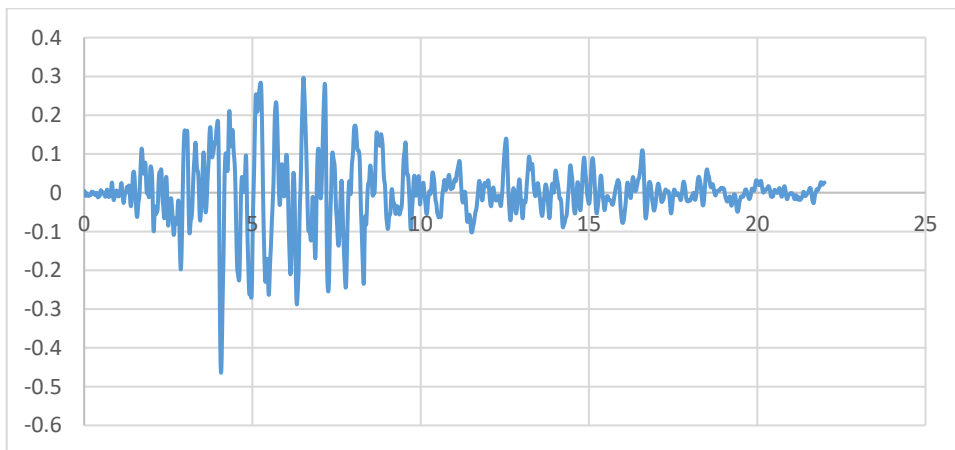


Figure A.36. Accelerogram of Kobe earthquake in y-direction (SET-3)

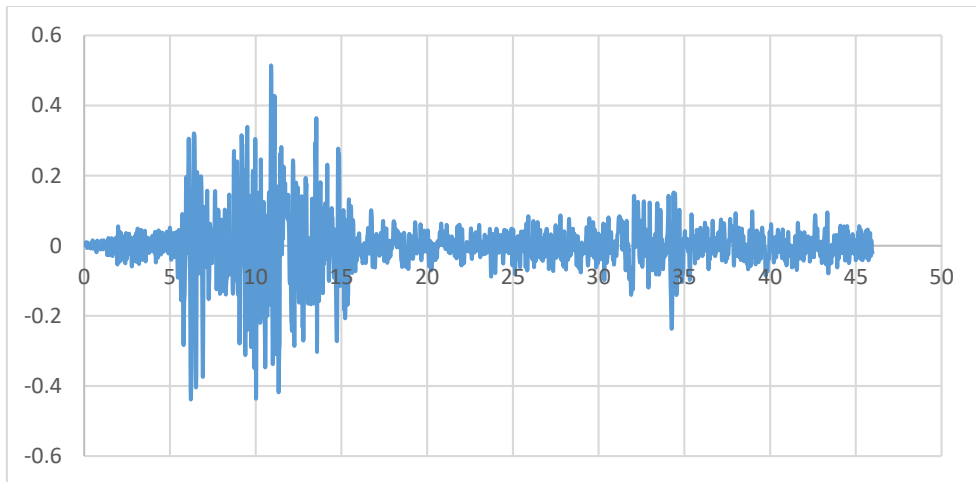


Figure A.37. Accelerogram of Manjil Abbar earthquake in x-direction (SET-3)

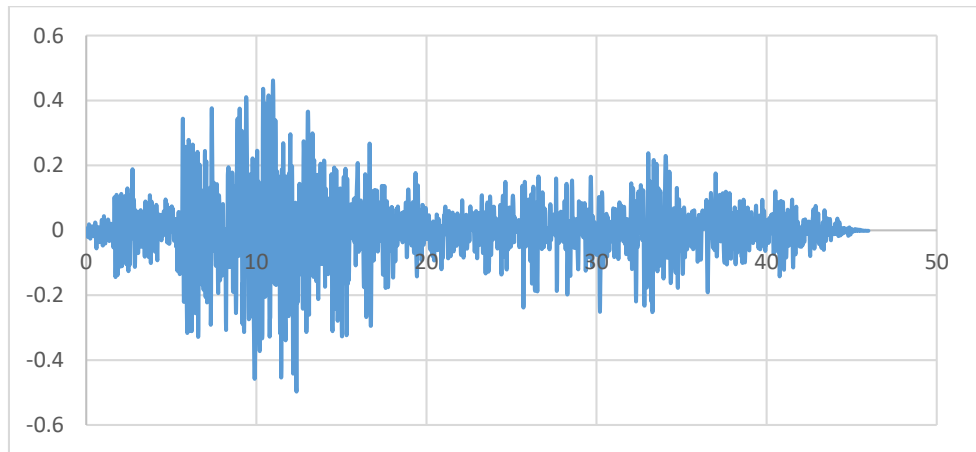


Figure A.38. Accelerogram of Manjil Abbar earthquake in y-direction (SET-3)

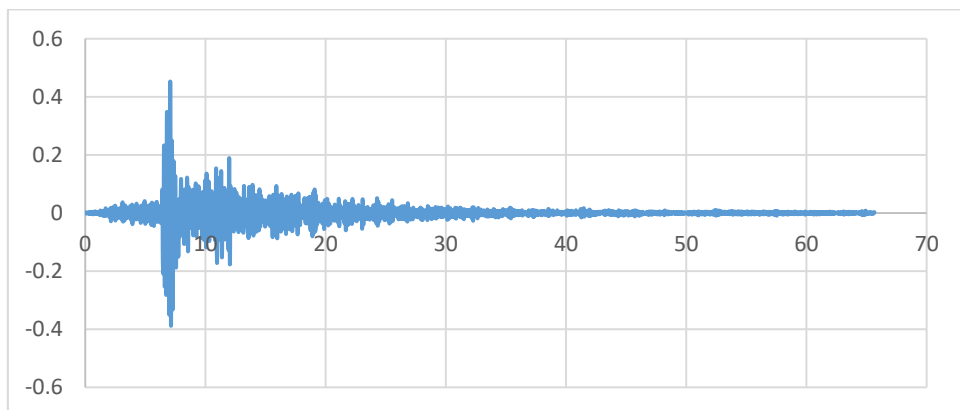


Figure A.39. Accelerogram of Tottori-2 earthquake in x-direction (SET-3)

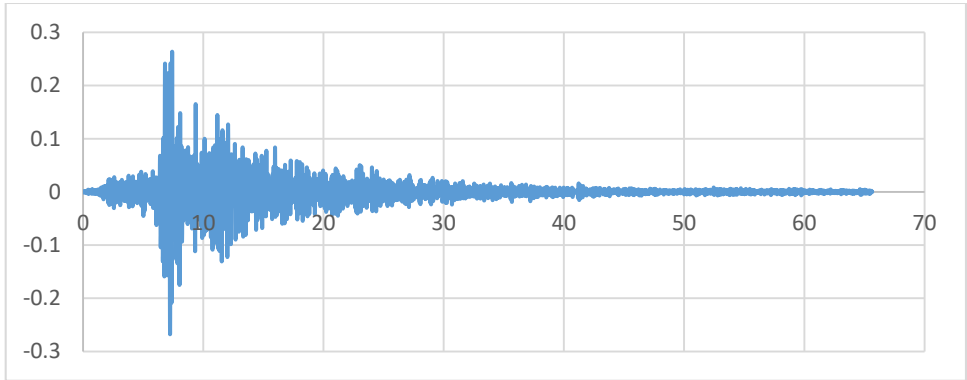


Figure A.40. Accelerogram of Tottori-2 earthquake in y-direction (SET-3)

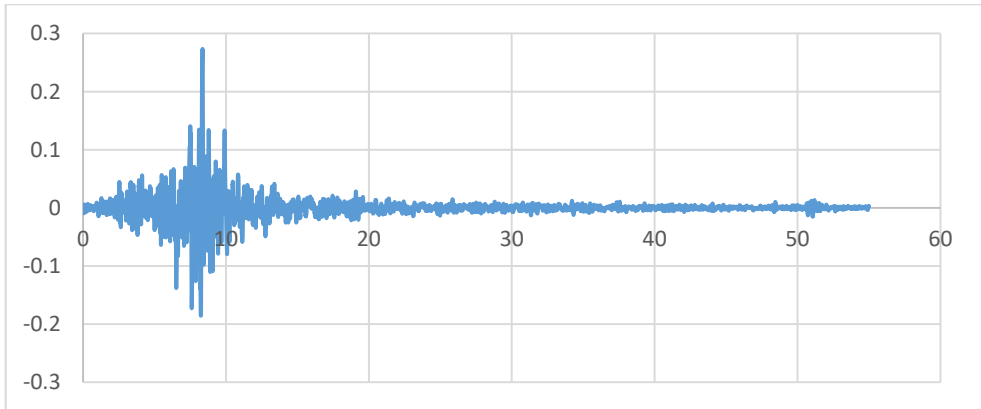


Figure A.41. Accelerogram of Tottori-3 earthquake in x-direction (SET-3)

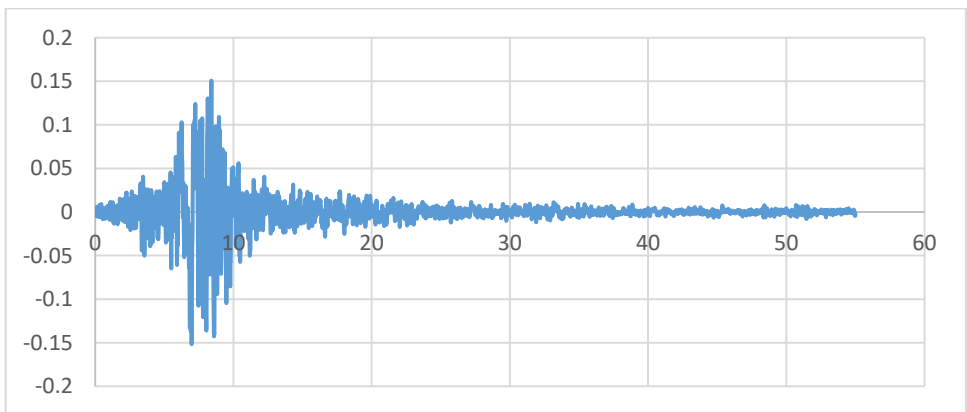


Figure A.42. Accelerogram of Tottori-3 earthquake in y-direction (SET-3)

B. Response Spectra of Unscaled and Scaled Time Histories

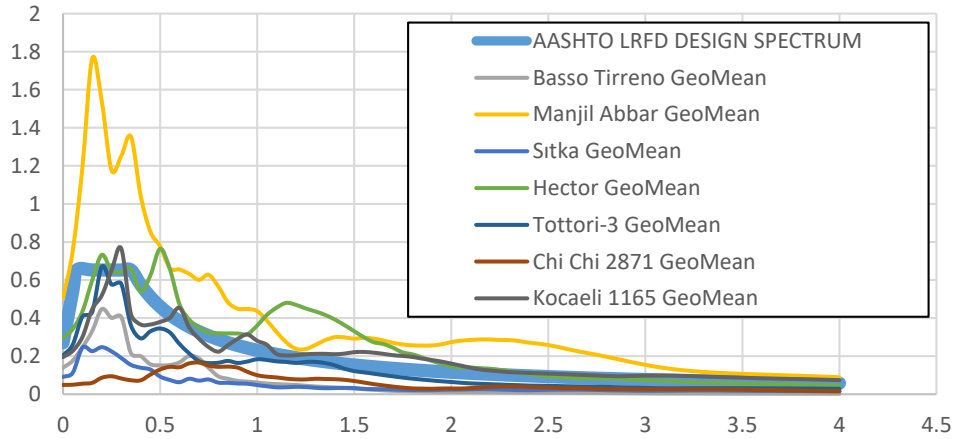


Figure B.1. AASHTO LRFD design spectrum and response spectrum of unscaled time histories for ground motion SET-1 and scaling method M1 of V03 Bridge

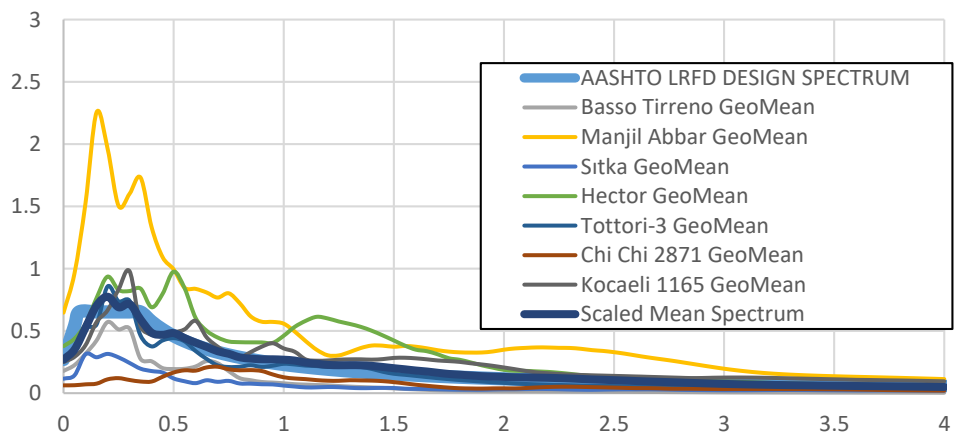


Figure B.2. AASHTO LRFD design spectrum and response spectrum of scaled time histories for ground motion SET-1 and scaling method M1 of V03 Bridge

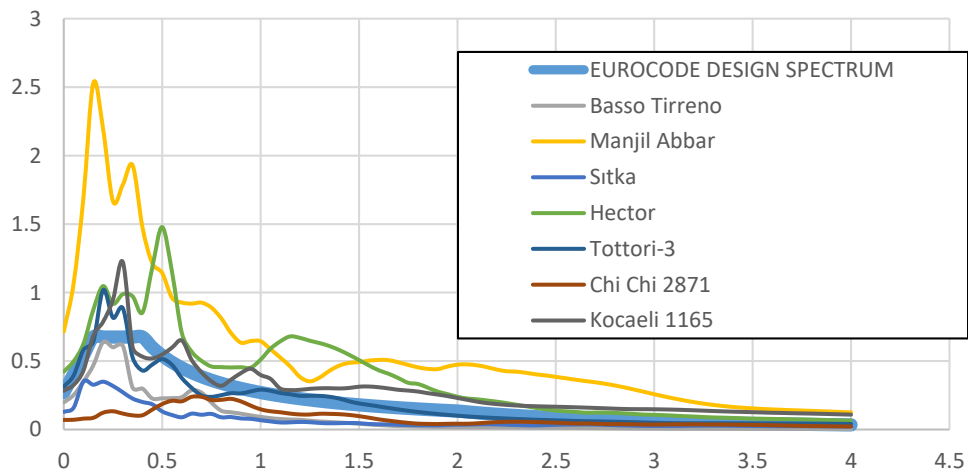


Figure B.3. EN-8 design spectrum and response spectrum of unscaled time histories for ground motion SET-1 and scaling method M1 of V03 Bridge

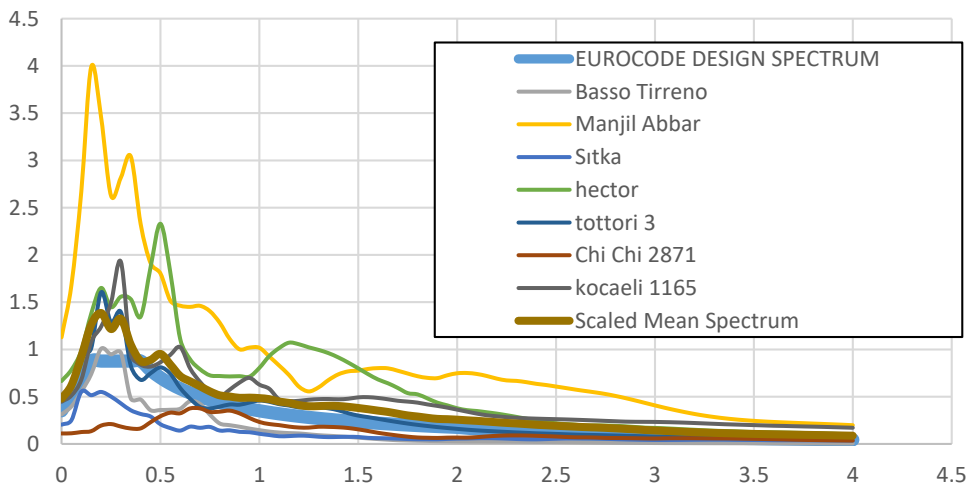


Figure B.43. EN-8 design spectrum and response spectrum of scaled time histories for ground motion SET-1 and scaling method M1 of V03 Bridge

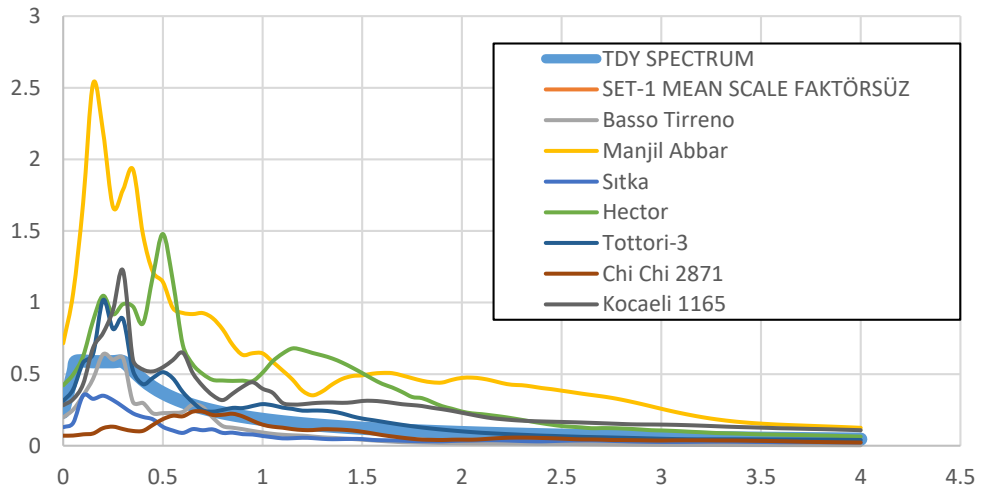


Figure B.5. TDY 2020 design spectrum and response spectrum of unscaled time histories for ground motion SET-1 and scaling method M1 of V03 Bridge

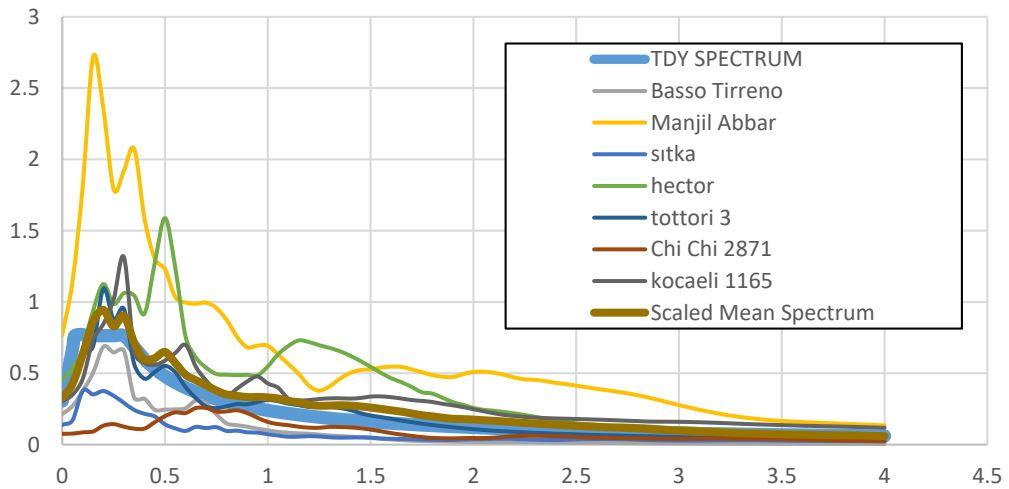


Figure B.6. TDY 2020 design spectrum and response spectrum of scaled time histories for ground motion SET-1 and scaling method M1 of V03 Bridge

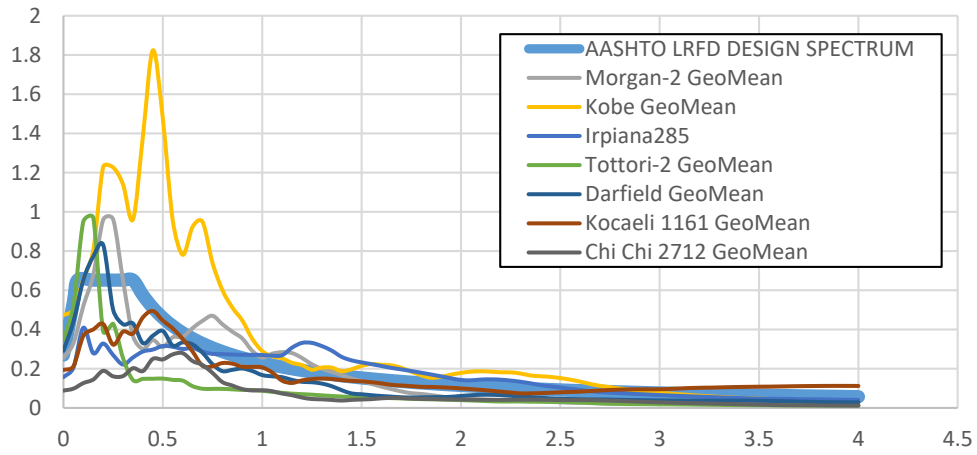


Figure B.7. AASHTO LRFD design spectrum and response spectrum of unscaled time histories for ground motion SET-2 and scaling method M1 of V03 Bridge

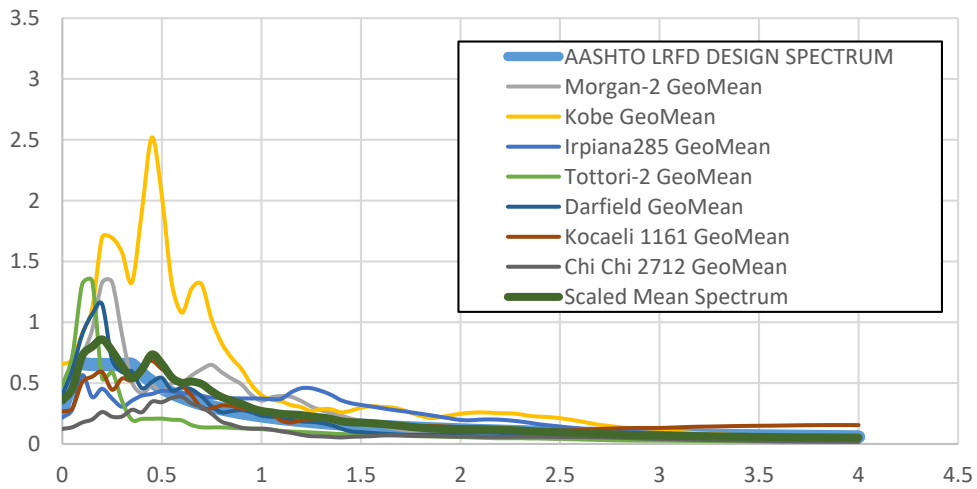


Figure B.8. AASHTO LRFD design spectrum and response spectrum of scaled time histories for ground motion SET-2 and scaling method M1 of V03 Bridge

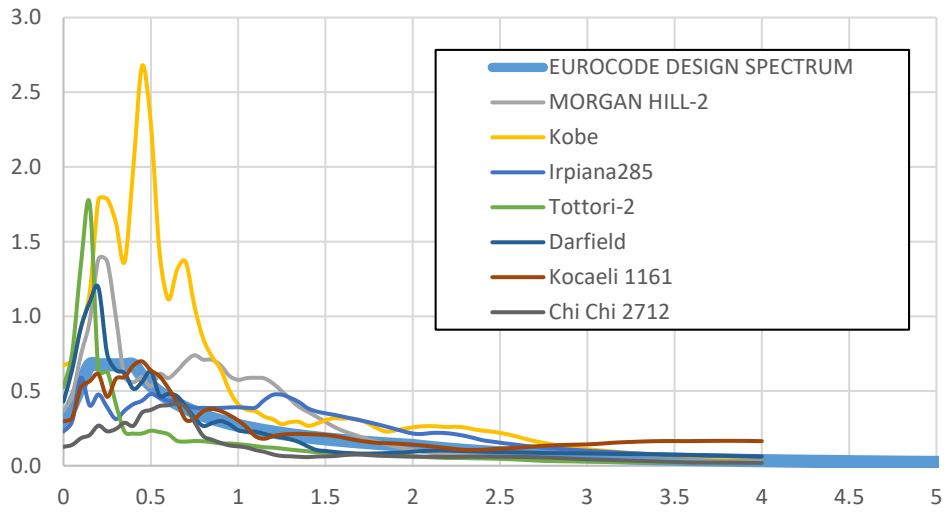


Figure B.9. EN-8 design spectrum and response spectrum of unscaled time histories for ground motion SET-2 and scaling method M1 of V03 Bridge

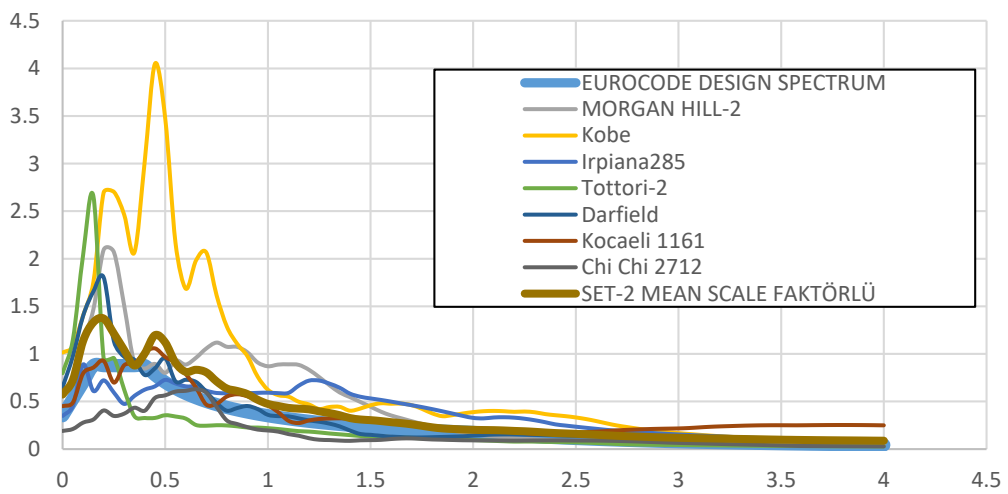


Figure B.10. EN-8 design spectrum and response spectrum of scaled time histories for ground motion SET-2 and scaling method M1 of V03 Bridge

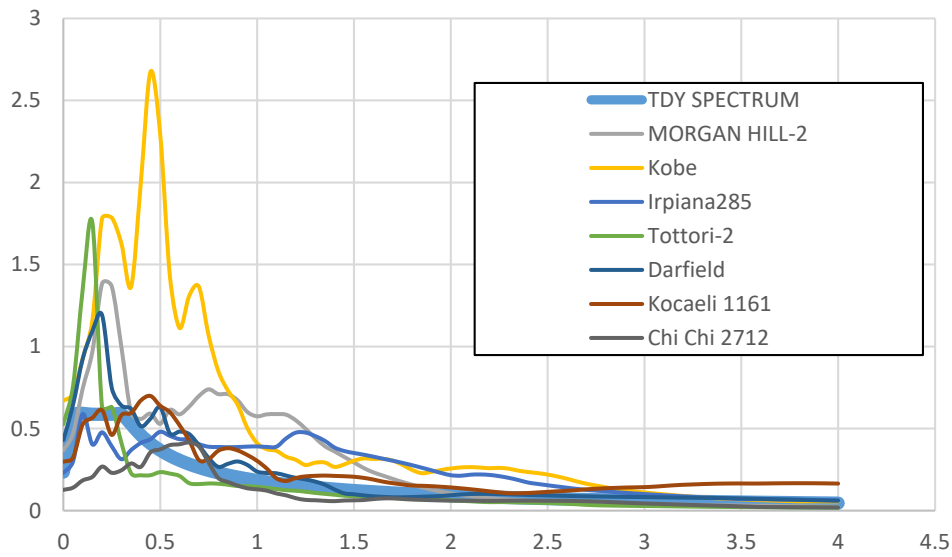


Figure B.11. TDY 2020 design spectrum and response spectrum of unscaled time histories for ground motion SET-2 and scaling method M1 of V03 Bridge

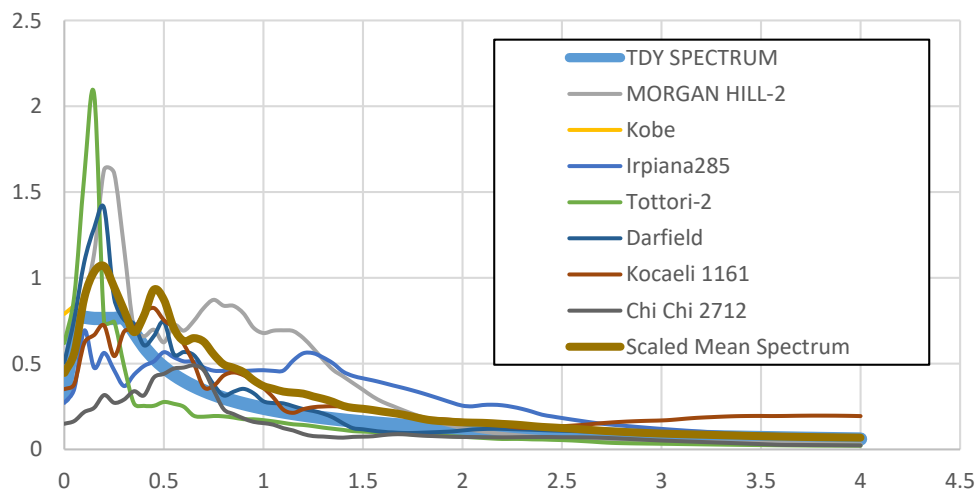


Figure B.12. TDY 2020 design spectrum and response spectrum of scaled time histories for ground motion SET-2 and scaling method M1 of V03 Bridge

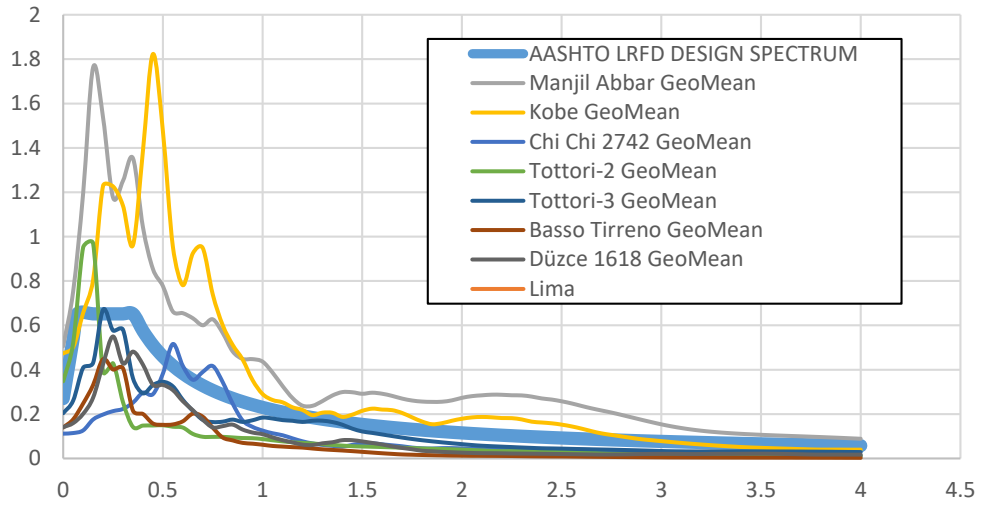


Figure B.13. AASHTO LRFD design spectrum and response spectrum of unscaled time histories for ground motion SET-3 and scaling method M1 of V03 Bridge

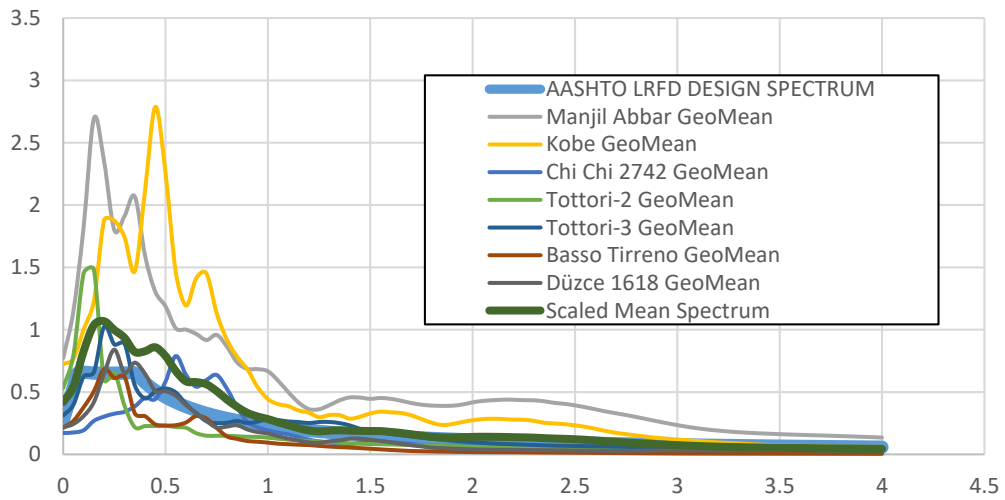


Figure B.14. AASHTO LRFD design spectrum and response spectrum of scaled time histories for ground motion SET-3 and scaling method M1 of V03 Bridge

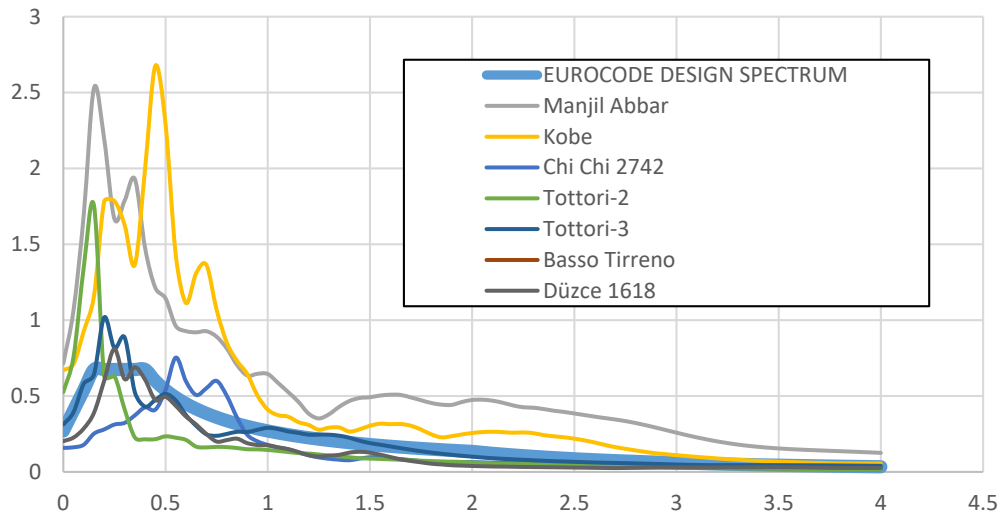


Figure B.15. EN-8 design spectrum and response spectrum of unscaled time histories for ground motion SET-3 and scaling method M1 of V03 Bridge

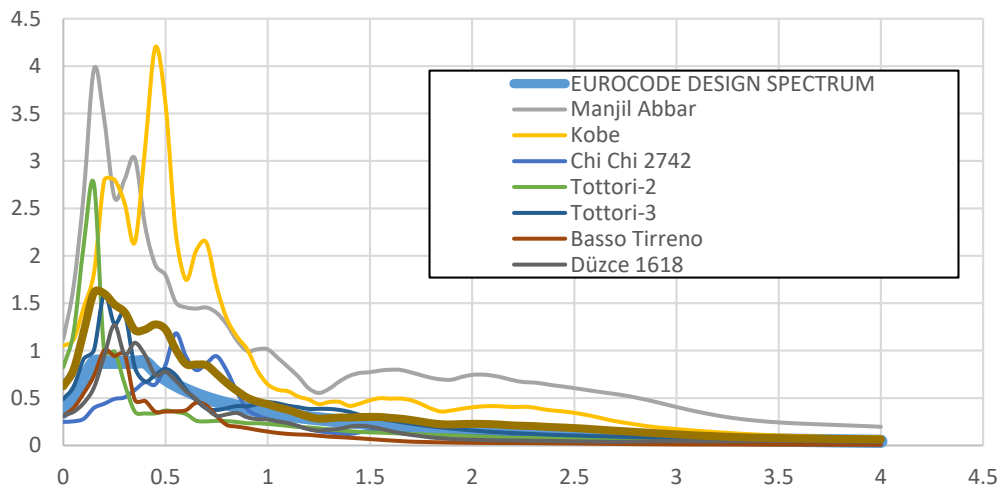


Figure B.16. EN-8 design spectrum and response spectrum of scaled time histories for ground motion SET-3 and scaling method M1 of V03 Bridge

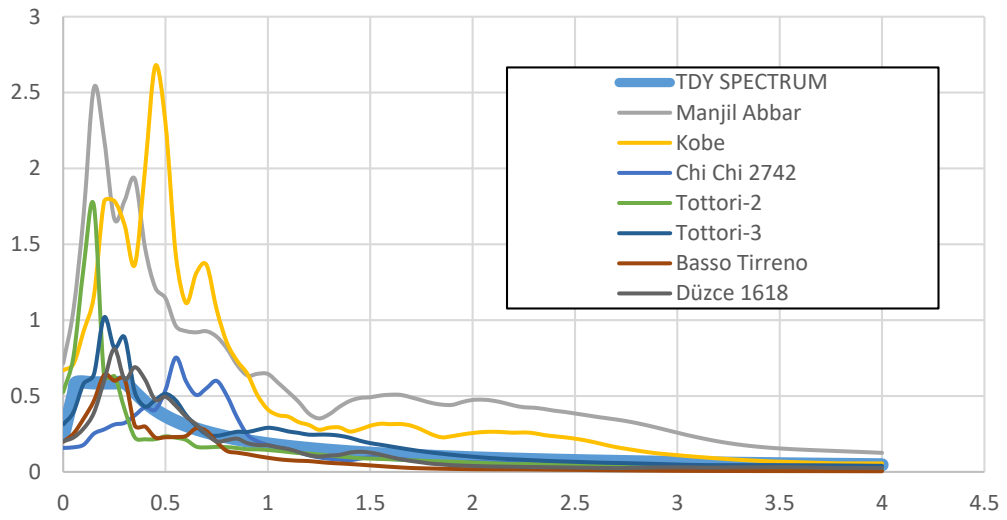


Figure B.17. TDY 2020 design spectrum and response spectrum of unscaled time histories for ground motion SET-3 and scaling method M1 of V03 Bridge

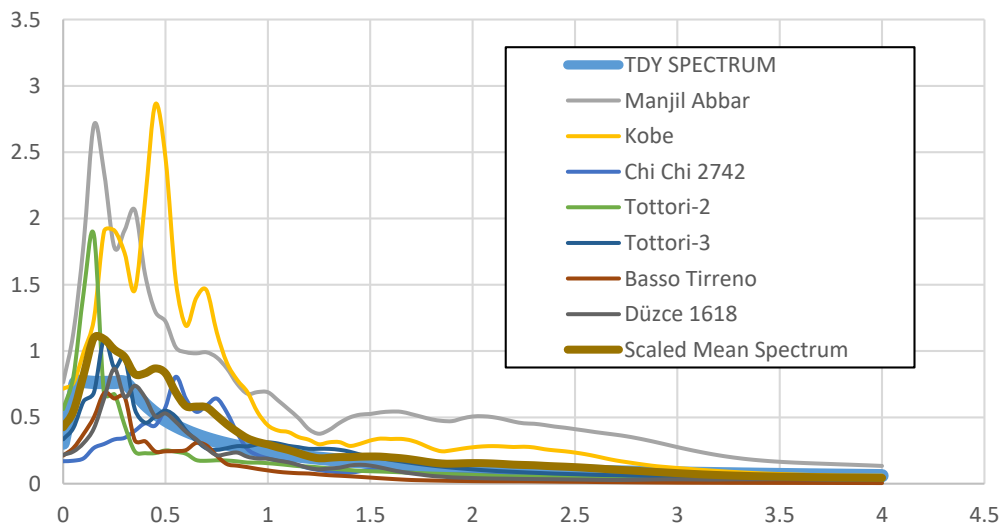


Figure B.18. TDY 2020 design spectrum and response spectrum of scaled time histories for ground motion SET-3 and scaling method M1 of V03 Bridge

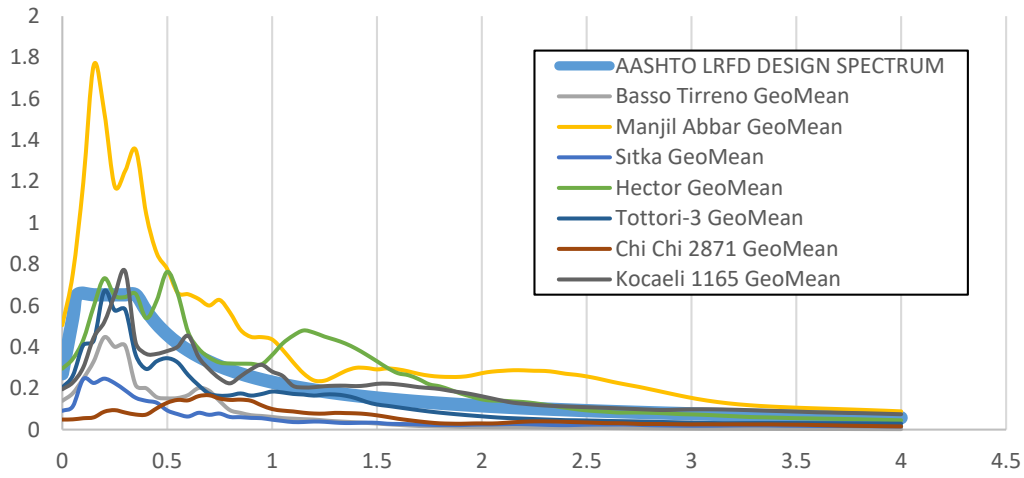


Figure B.19. AASHTO LRFD design spectrum and response spectrum of unscaled time histories for ground motion SET-1 and scaling method M2 of V03 Bridge

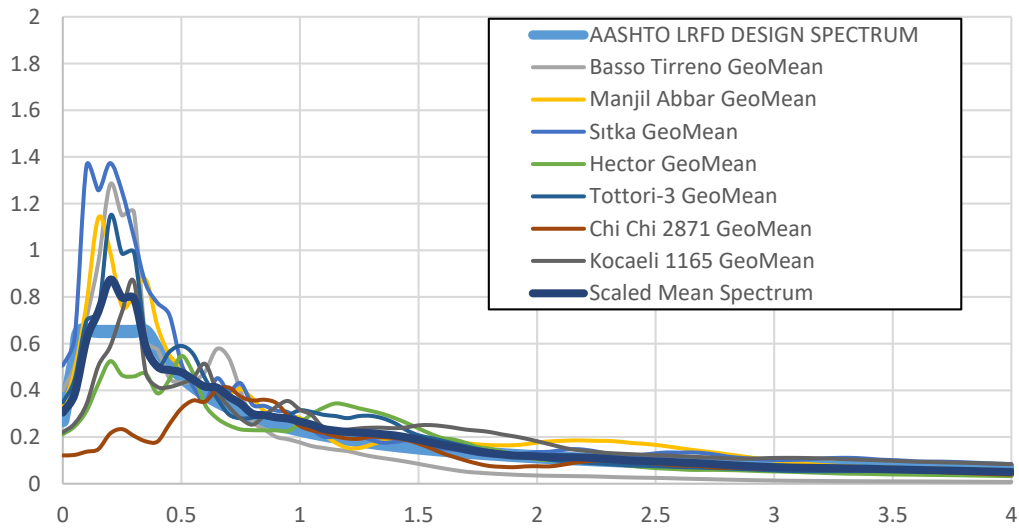


Figure B.20. AASHTO LRFD design spectrum and response spectrum of scaled time histories for ground motion SET-1 and scaling method M2 of V03 Bridge

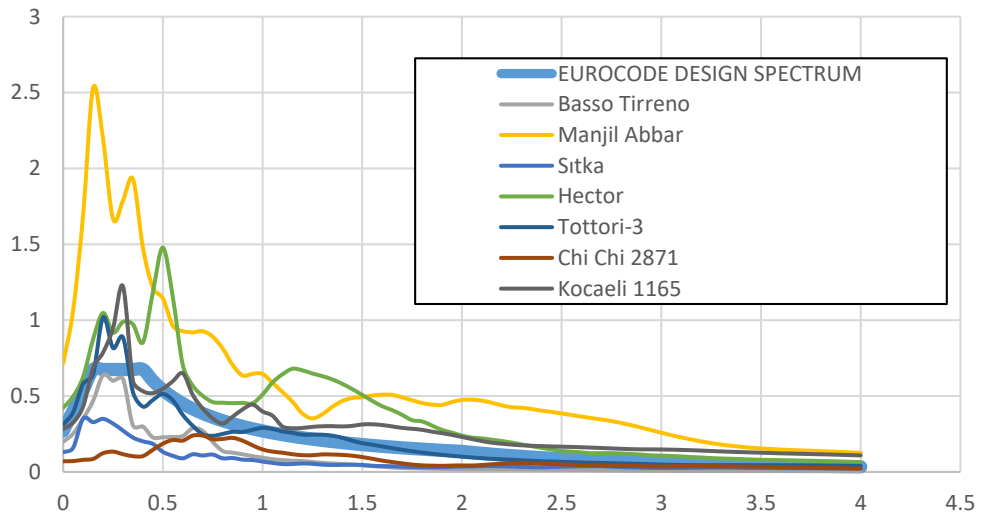


Figure B.21. EN-8 design spectrum and response spectrum of unscaled time histories for ground motion SET-1 and scaling method M2 of V03 Bridge

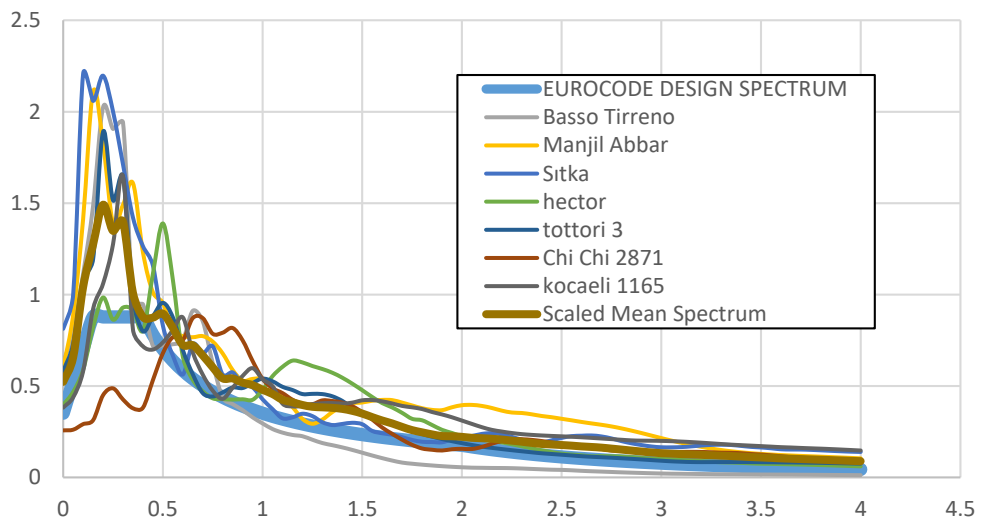


Figure B.22. EN-8 design spectrum and response spectrum of scaled time histories for ground motion SET-1 and scaling method M2 of V03 Bridge

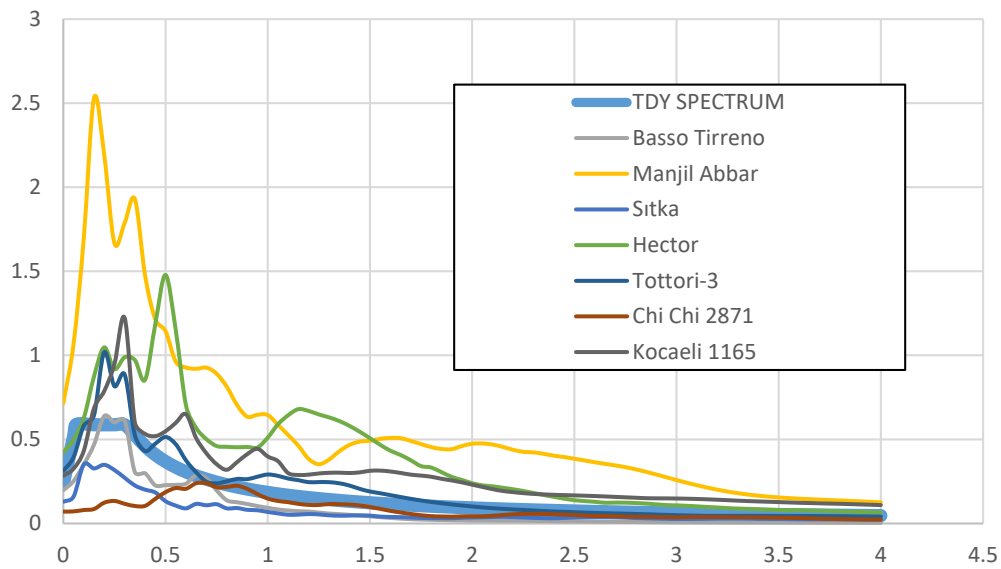


Figure B.23. TDY 2020 design spectrum and response spectrum of unscaled time histories for ground motion SET-1 and scaling method M2 of V03 Bridge

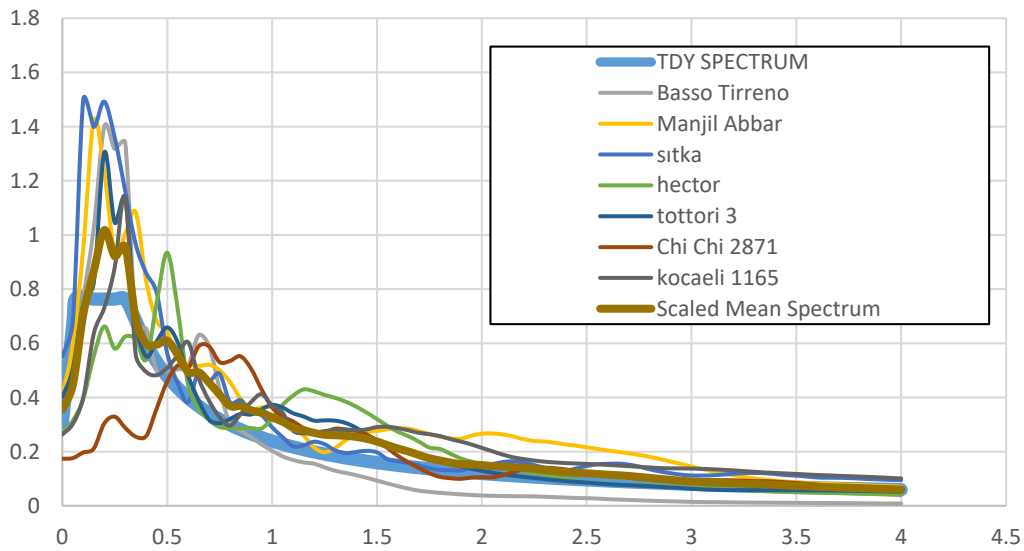


Figure B.24. TDY 2020 design spectrum and response spectrum of scaled time histories for ground motion SET-1 and scaling method M2 of V03 Bridge

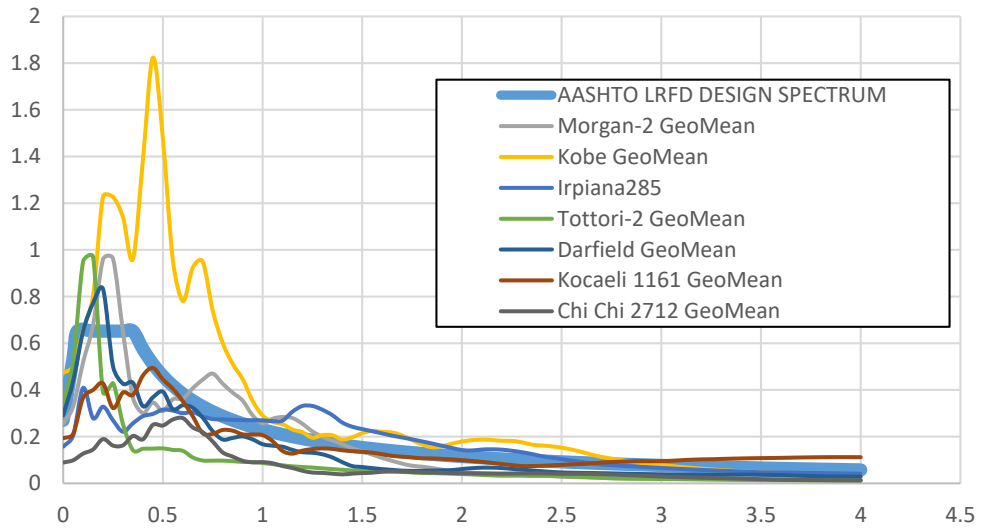


Figure B.25. AASHTO LRFD design spectrum and response spectrum of unscaled time histories for ground motion SET-2 and scaling method M2 of V03 Bridge

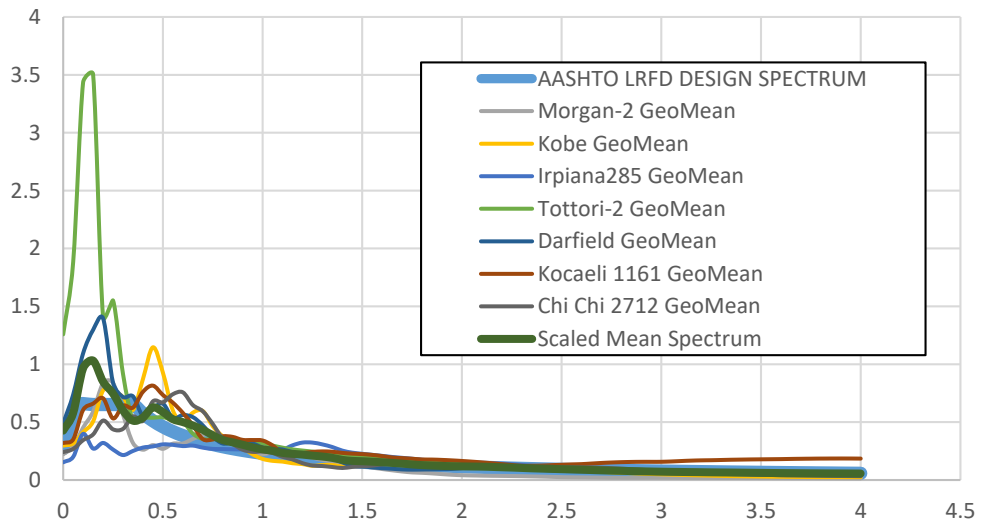


Figure B.26. AASHTO LRFD design spectrum and response spectrum of scaled time histories for ground motion SET-2 and scaling method M2 of V03 Bridge

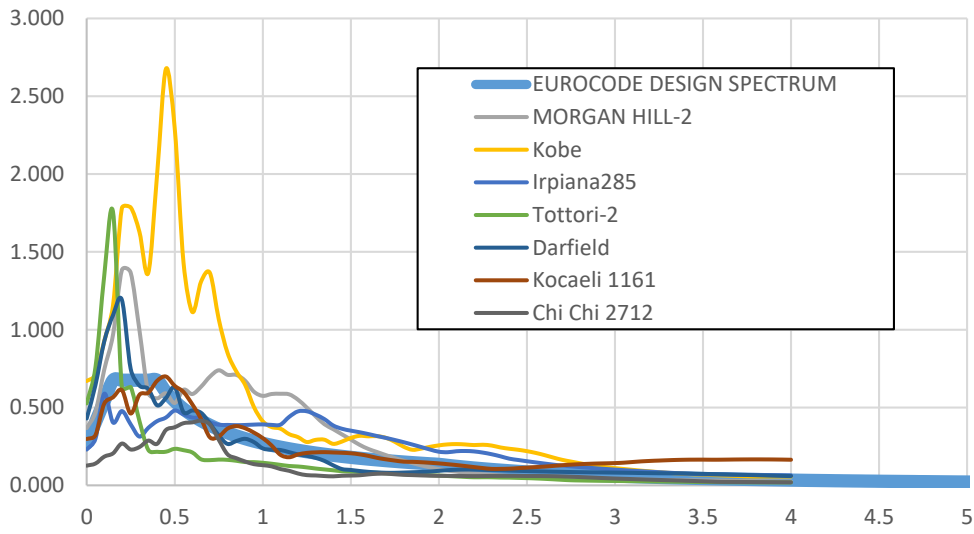


Figure B.27. EN-8 design spectrum and response spectrum of unscaled time histories for ground motion SET-2 and scaling method M2 of V03 Bridge

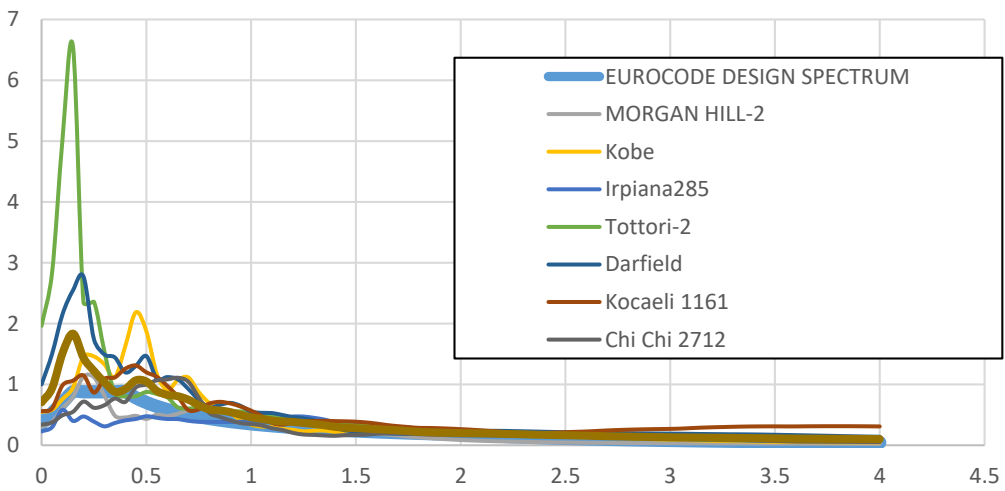


Figure B.28. EN-8 design spectrum and response spectrum of scaled time histories for ground motion SET-2 and scaling method M2 of V03 Bridge

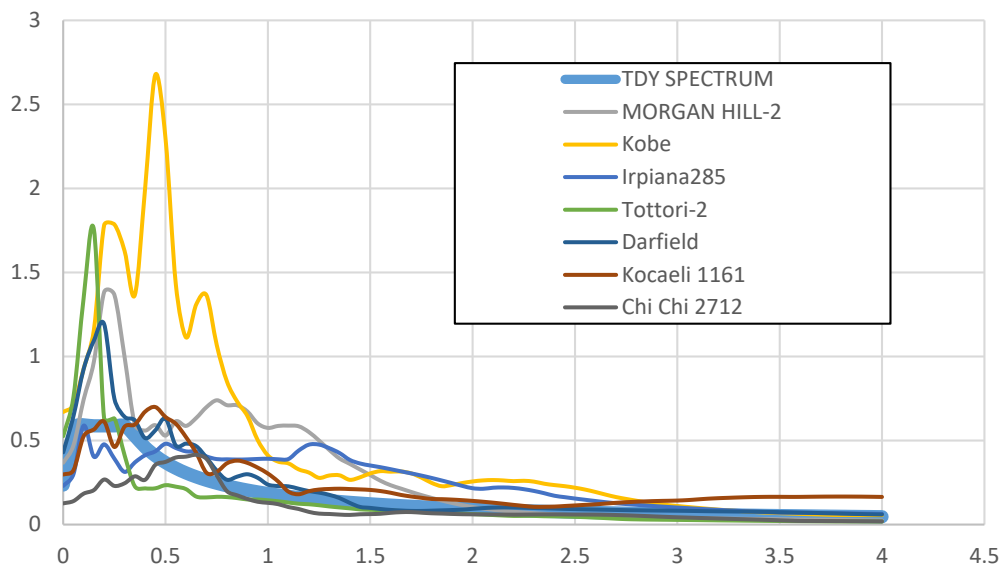


Figure B.29. TDY 2020 design spectrum and response spectrum of unscaled time histories for ground motion SET-2 and scaling method M2 of V03 Bridge

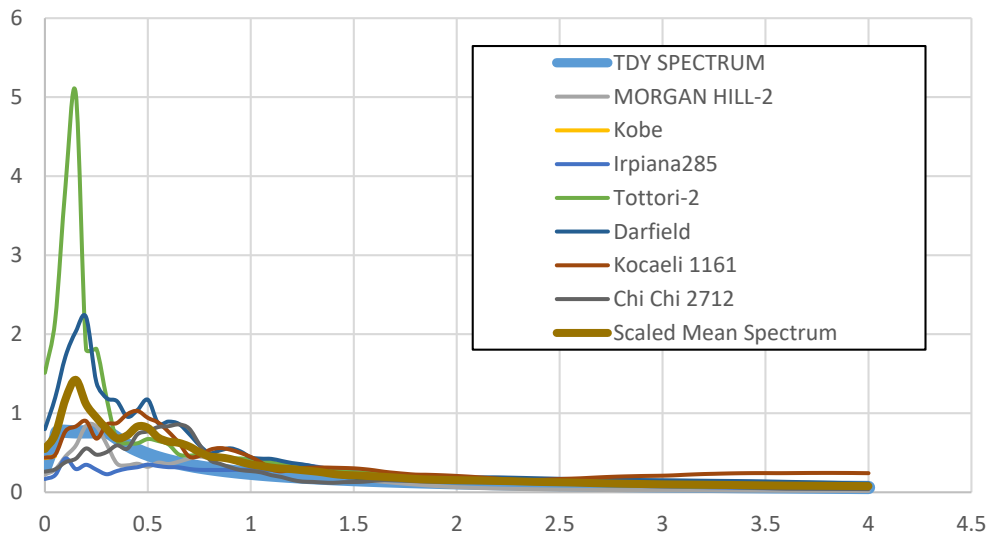


Figure B.30. TDY 2020 design spectrum and response spectrum of scaled time histories for ground motion SET-2 and scaling method M2 of V03 Bridge

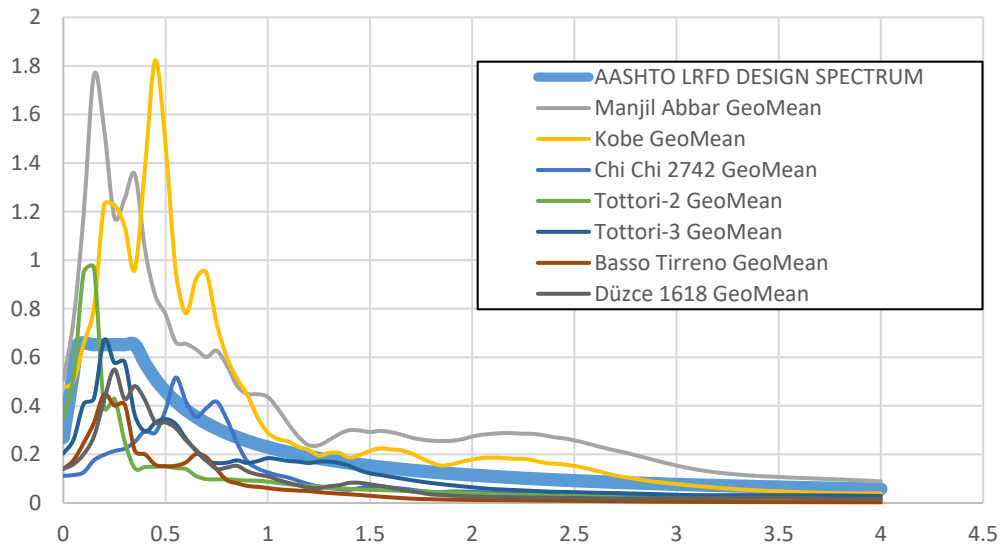


Figure B.31. AASHTO LRFD design spectrum and response spectrum of unscaled time histories for ground motion SET-3 and scaling method M2 of V03 Bridge

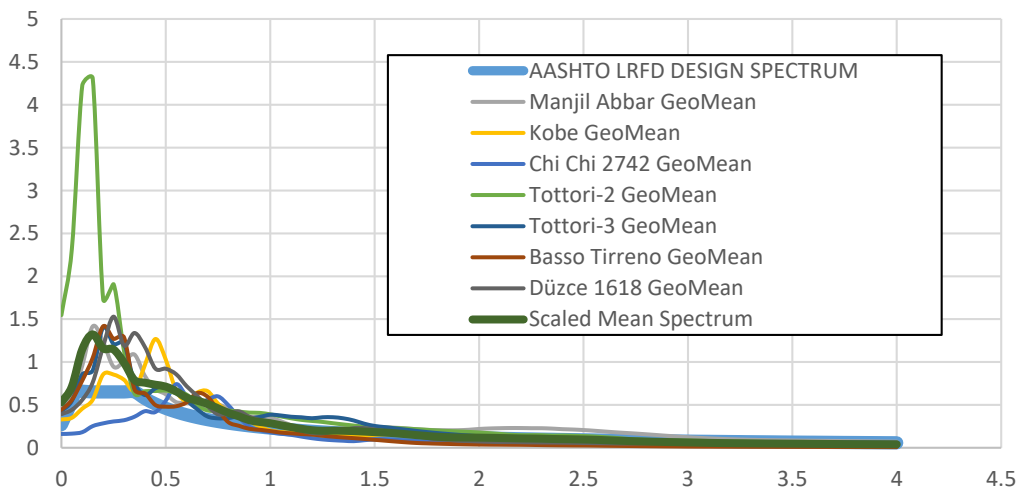


Figure B.32. AASHTO LRFD design spectrum and response spectrum of scaled time histories for ground motion SET-3 and scaling method M2 of V03 Bridge

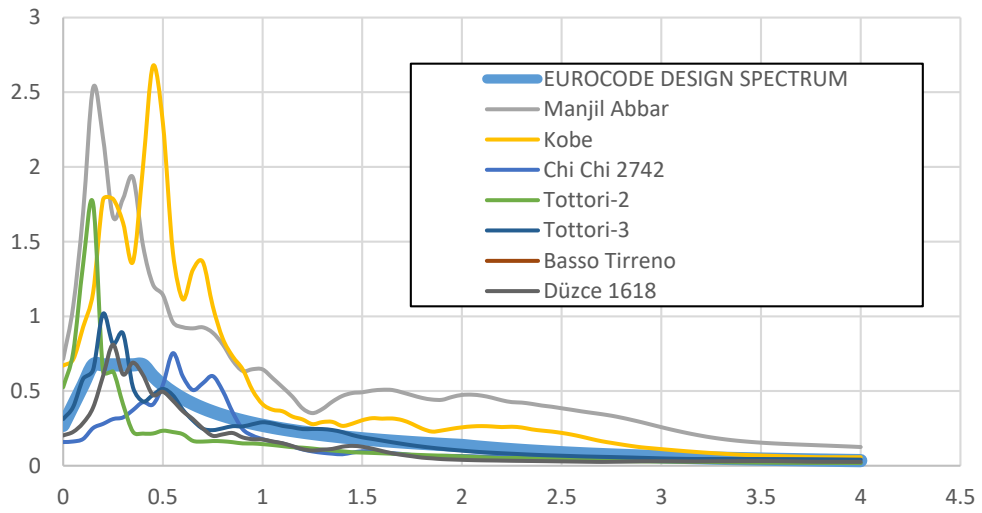


Figure B.33. EN-8 design spectrum and response spectrum of unscaled time histories for ground motion SET-3 and scaling method M2 of V03 Bridge

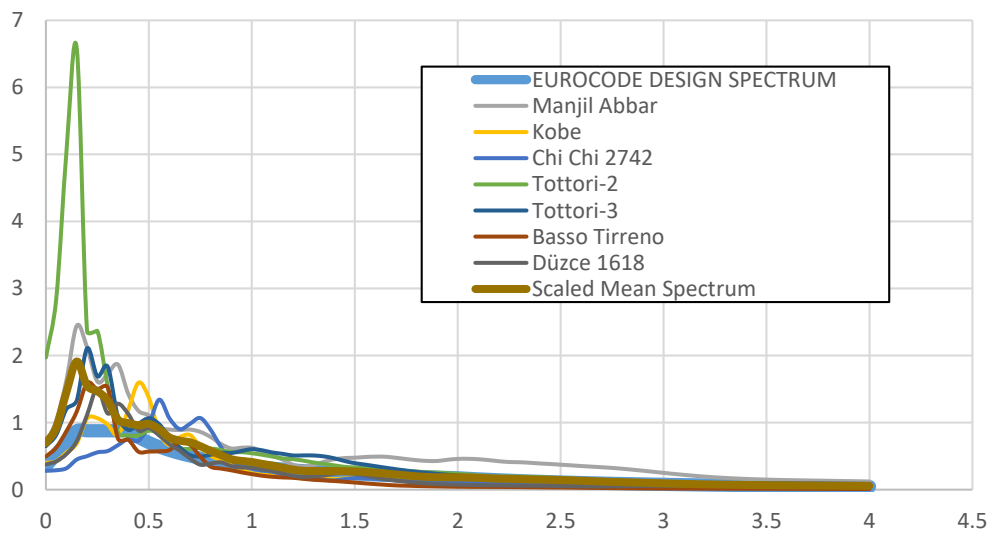


Figure B.34. EN-8 design spectrum and response spectrum of scaled time histories for ground motion SET-3 and scaling method M2 of V03 Bridge

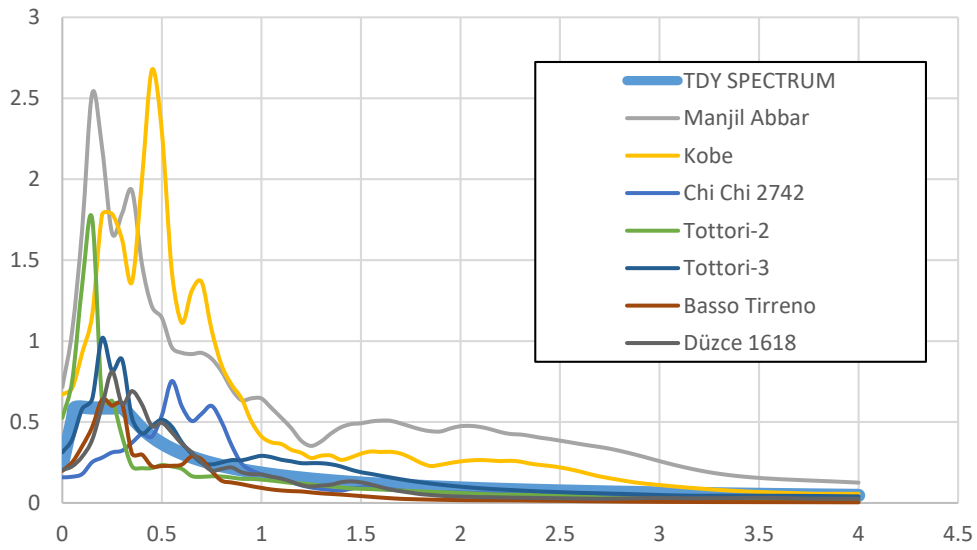


Figure B.35. TDY 2020 design spectrum and response spectrum of unscaled time histories for ground motion SET-3 and scaling method M2 of V03 Bridge

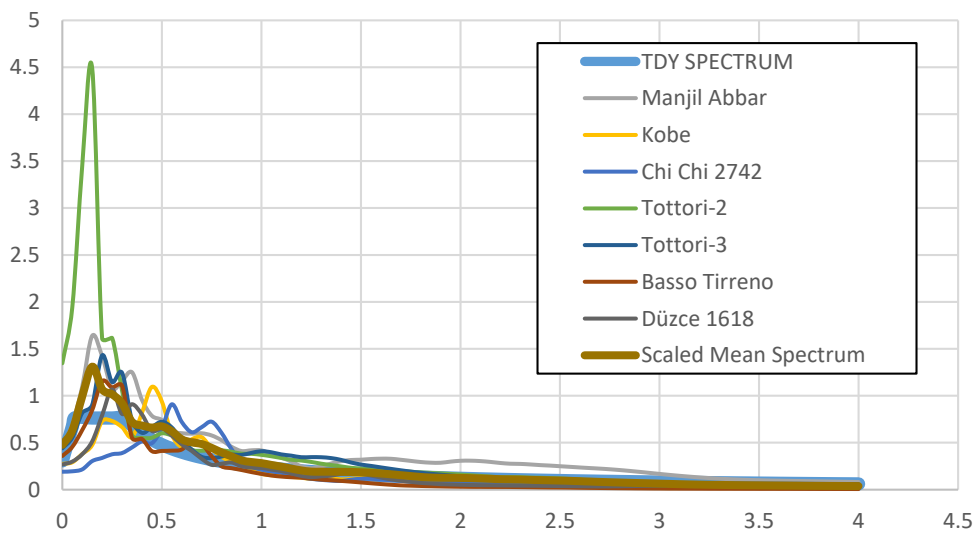


Figure B.36. TDY 2020 design spectrum and response spectrum of scaled time histories for ground motion SET-3 and scaling method M2 of V03 Bridge

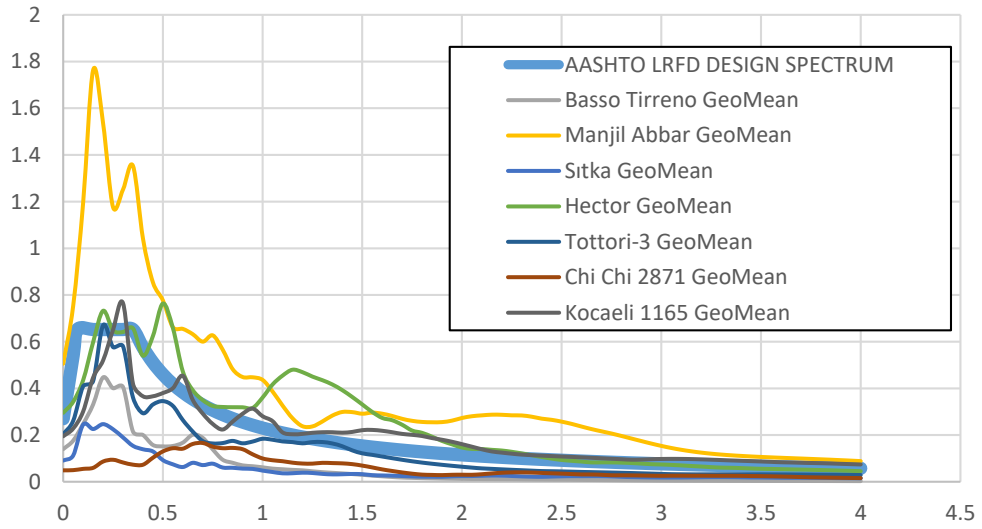


Figure B.37. AASHTO LRFD design spectrum and response spectrum of unscaled time histories for ground motion SET-1 and scaling method M3 of V03 Bridge

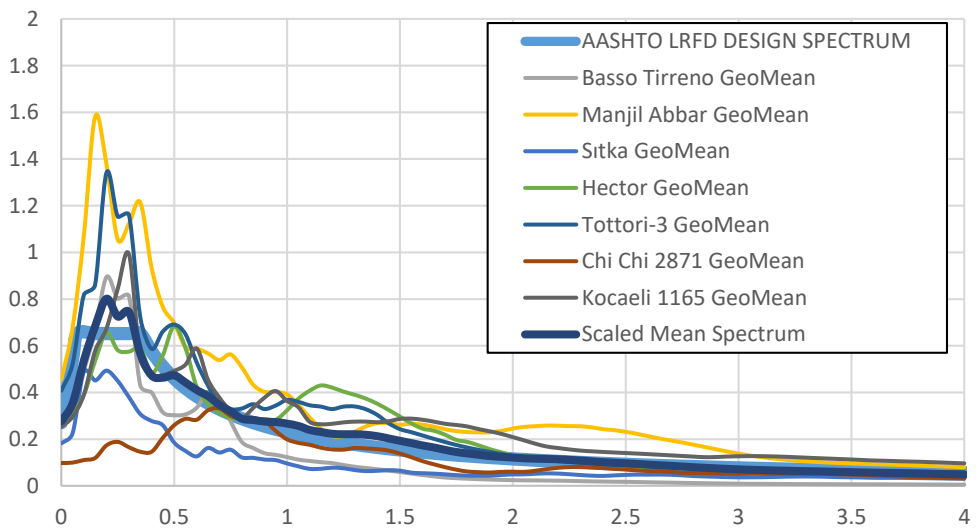


Figure B.38. AASHTO LRFD design spectrum and response spectrum of scaled time histories for ground motion SET-1 and scaling method M3 of V03 Bridge

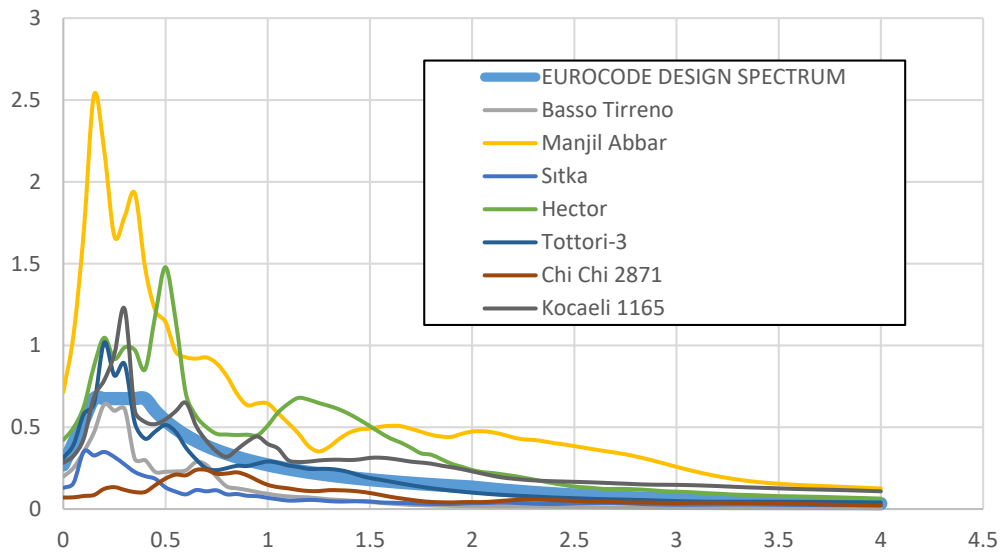


Figure B.39. EN-8 design spectrum and response spectrum of unscaled time histories for ground motion SET-1 and scaling method M3 of V03 Bridge

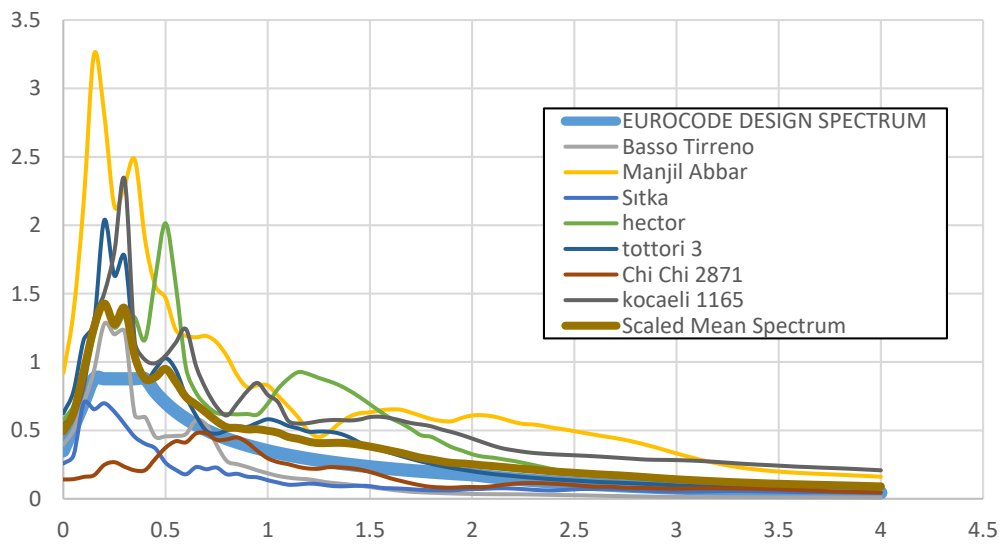


Figure B.40. EN-8 design spectrum and response spectrum of scaled time histories for ground motion SET-1 and scaling method M3 of V03 Bridge

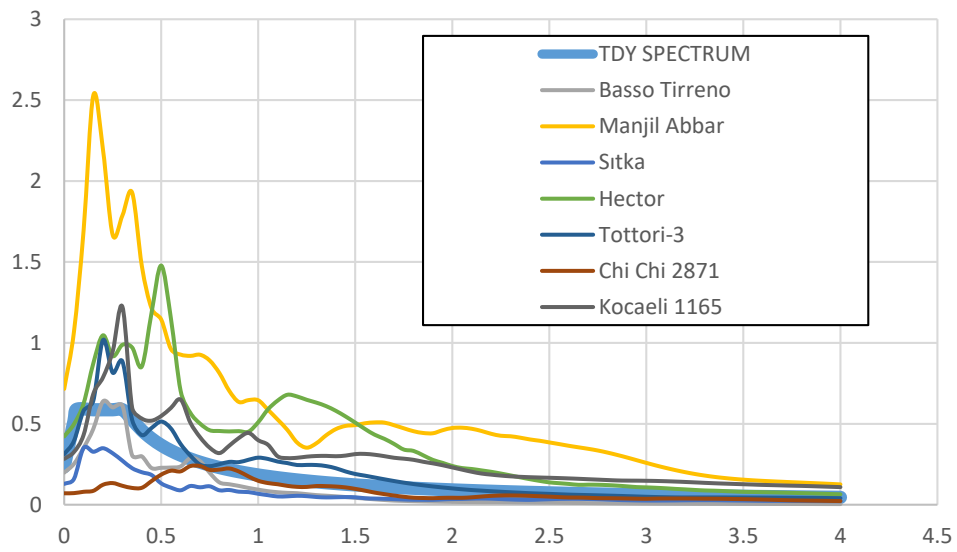


Figure B.41. TDY 2020 design spectrum and response spectrum of unscaled time histories for ground motion SET-1 and scaling method M3 of V03 Bridge

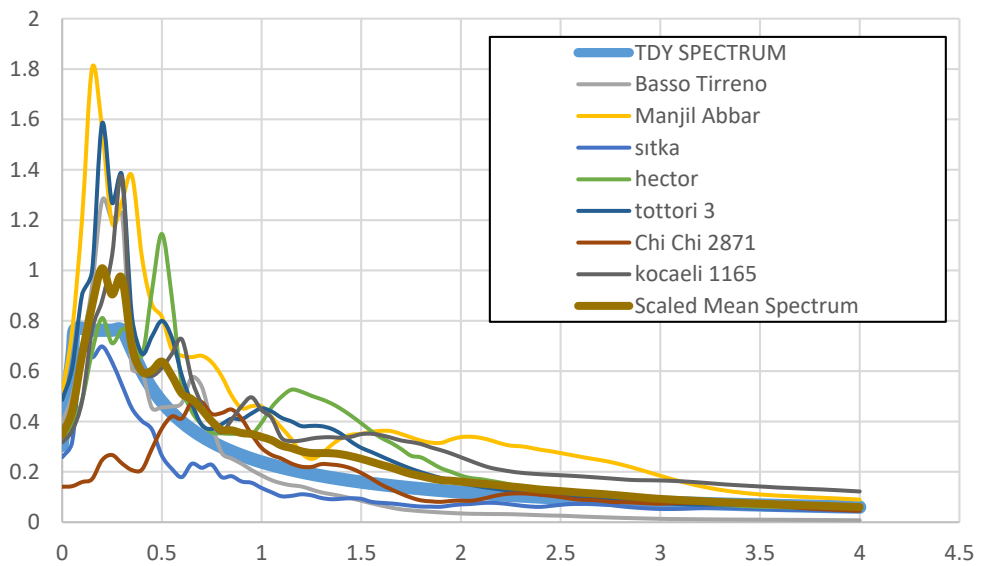


Figure B.42. TDY 2020 design spectrum and response spectrum of scaled time histories for ground motion SET-1 and scaling method M3 of V03 Bridge

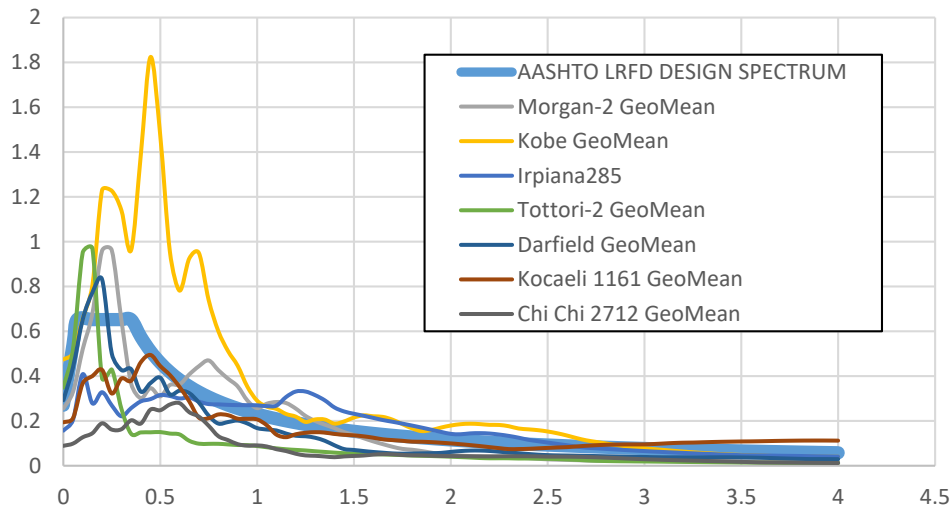


Figure B.43. AASHTO LRFD design spectrum and response spectrum of unscaled time histories for ground motion SET-2 and scaling method M3 of V03 Bridge

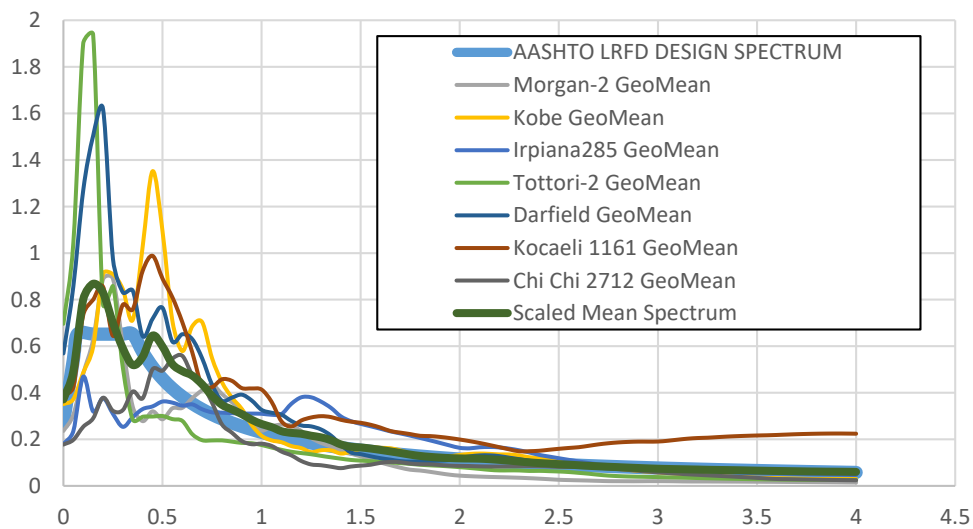


Figure B.44. AASHTO LRFD design spectrum and response spectrum of scaled time histories for ground motion SET-2 and scaling method M3 of V03 Bridge

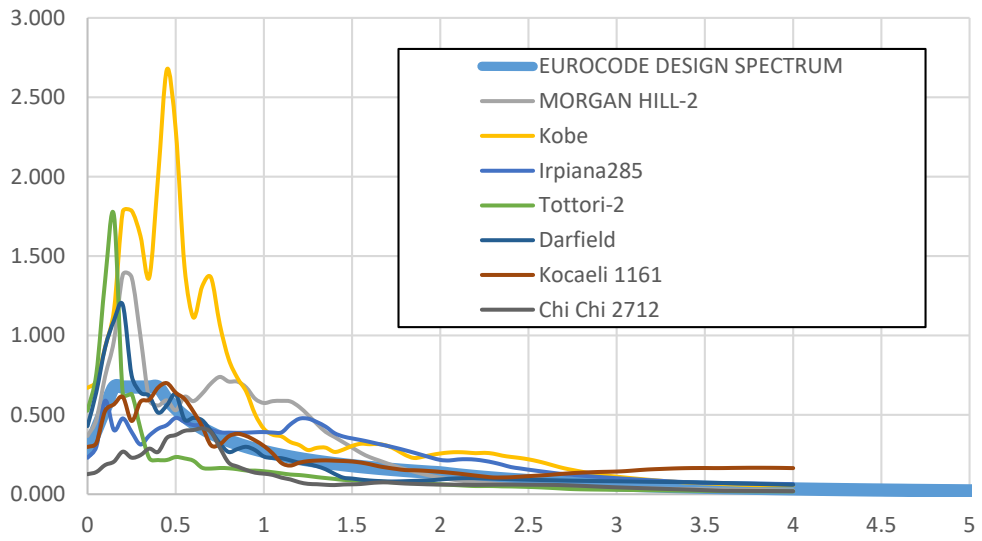


Figure B.45. EN-8 design spectrum and response spectrum of unscaled time histories for ground motion SET-2 and scaling method M3 of V03 Bridge

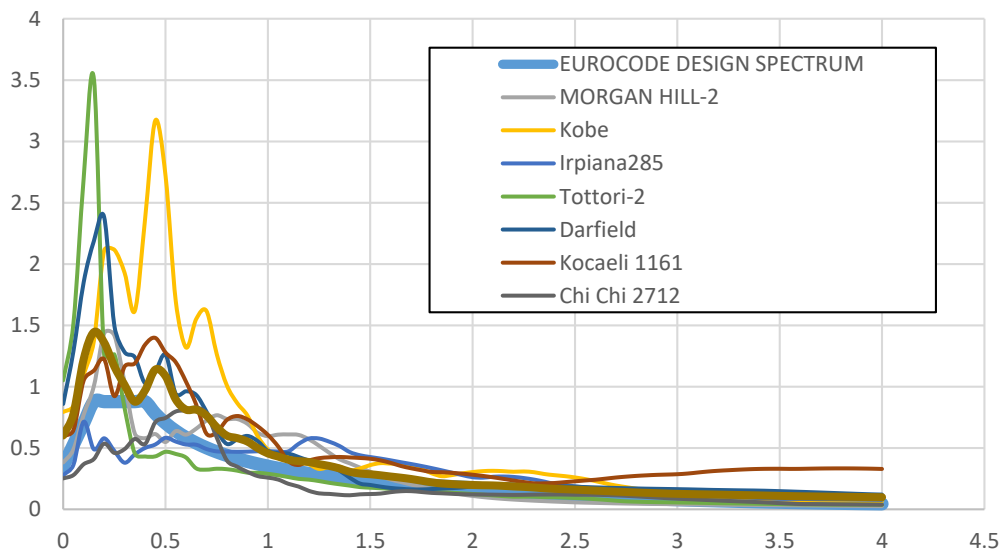


Figure B.46. EN-8 design spectrum and response spectrum of scaled time histories for ground motion SET-2 and scaling method M3 of V03 Bridge

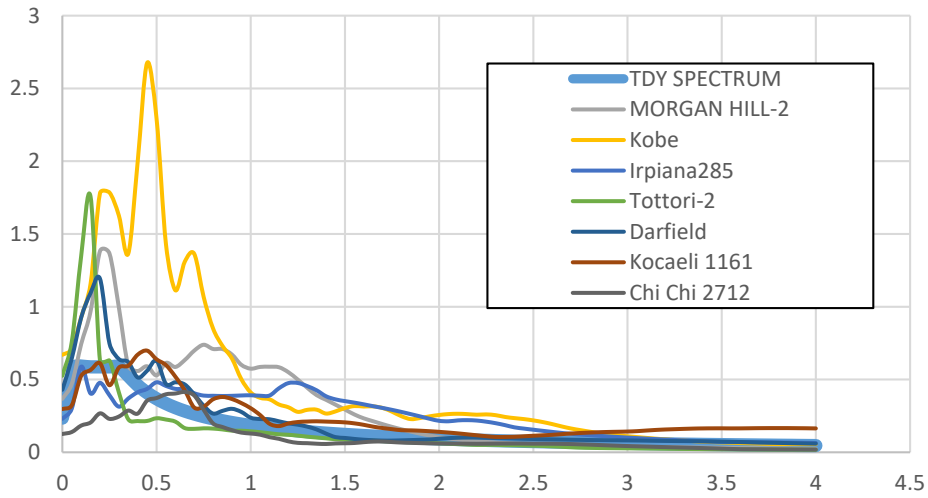


Figure B.47. TDY 2020 design spectrum and response spectrum of unscaled time histories for ground motion SET-2 and scaling method M3 of V03 Bridge

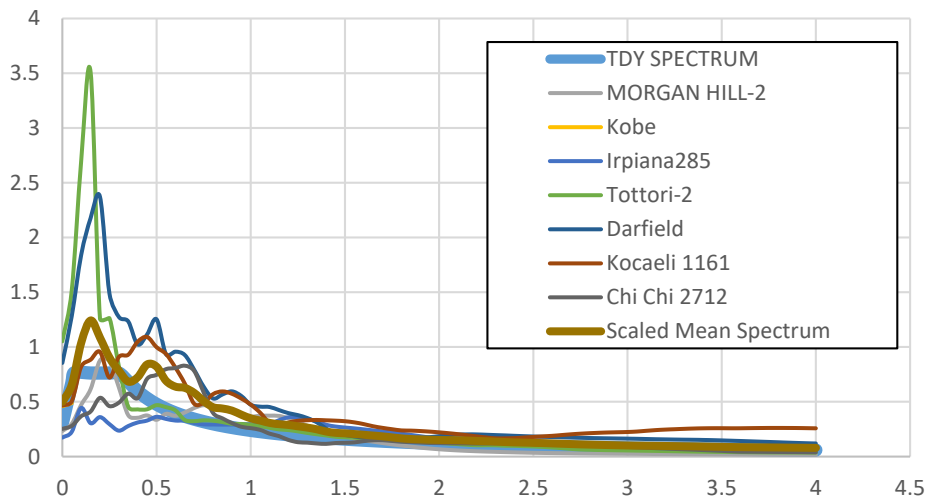


Figure B.48. TDY 2020 design spectrum and response spectrum of scaled time histories for ground motion SET-2 and scaling method M3 of V03 Bridge

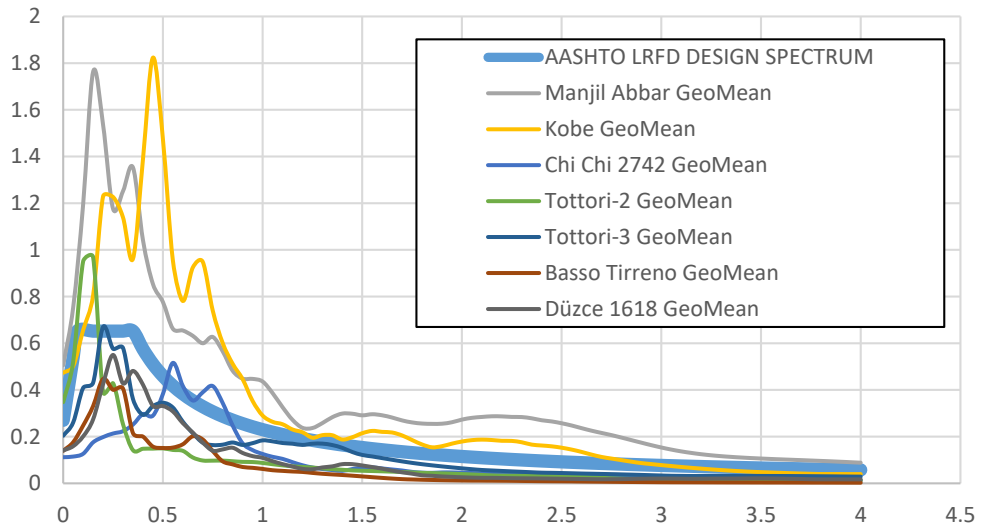


Figure B.49. AASHTO LRFD design spectrum and response spectrum of unscaled time histories for ground motion SET-3 and scaling method M3 of V03 Bridge

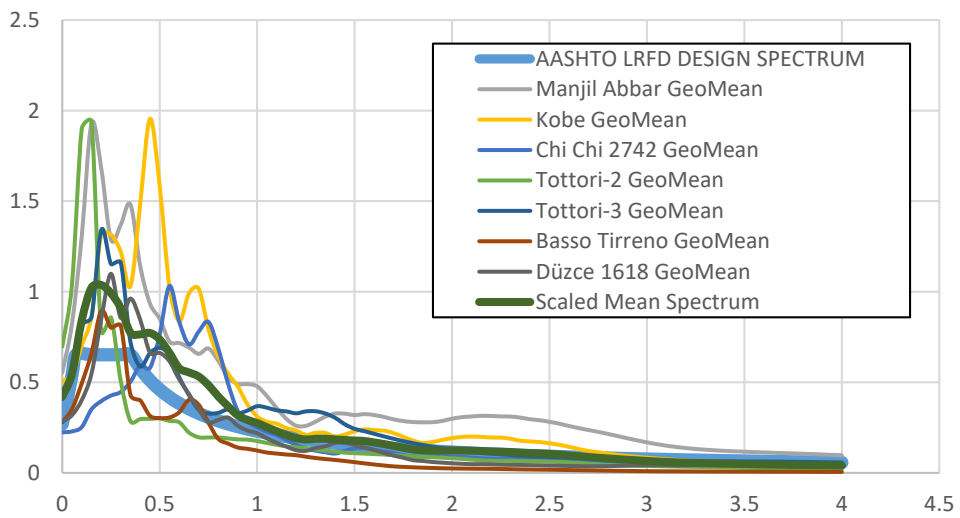


Figure B.50. AASHTO LRFD design spectrum and response spectrum of scaled time histories for ground motion SET-3 and scaling method M3 of V03 Bridge

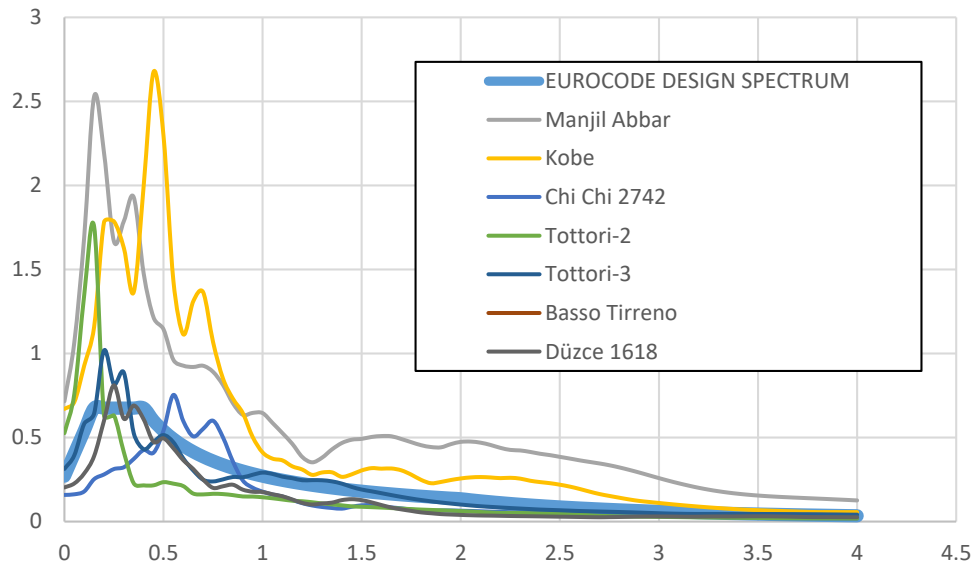


Figure B.51. EN-8 design spectrum and response spectrum of unscaled time histories for ground motion SET-3 and scaling method M3 of V03 Bridge

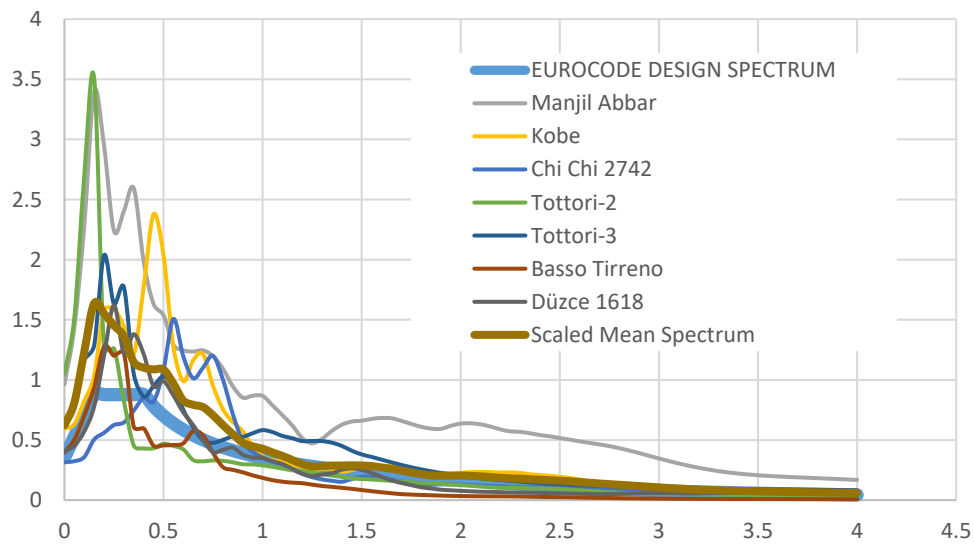


Figure B.52. EN-8 design spectrum and response spectrum of scaled time histories for ground motion SET-3 and scaling method M3 of V03 Bridge

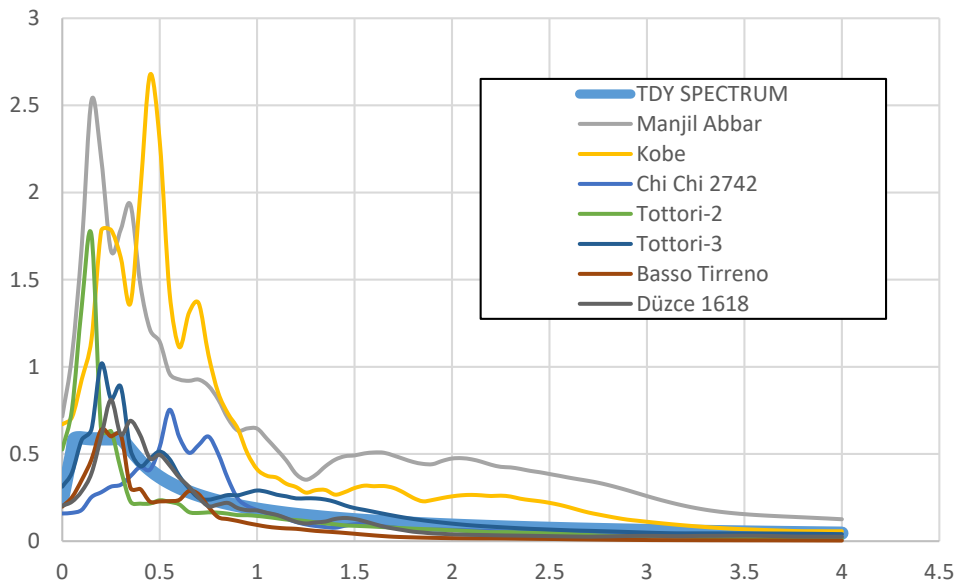


Figure B.53. TDY 2020 design spectrum and response spectrum of unscaled time histories for ground motion SET-3 and scaling method M3 of V03 Bridge

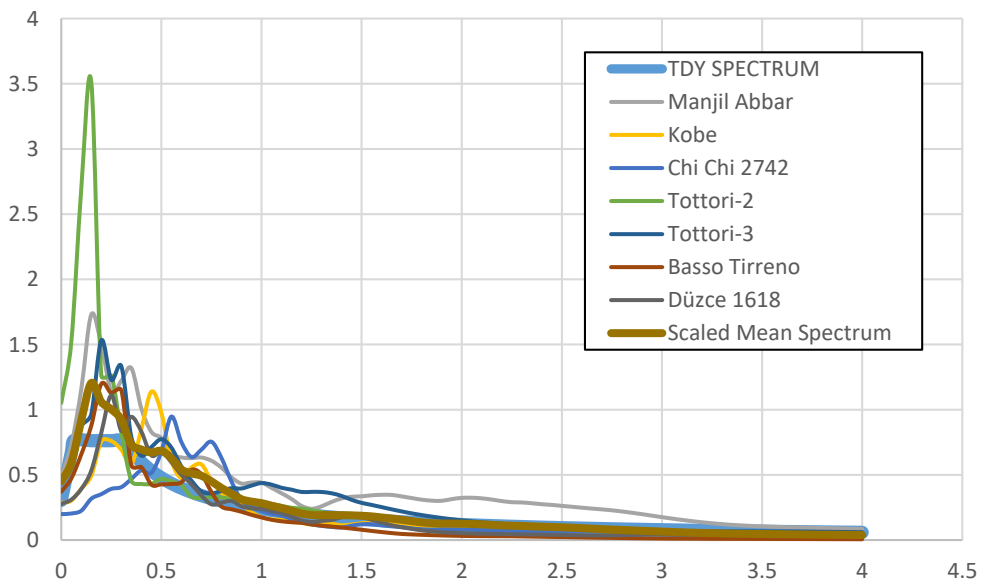


Figure B.54. TDY 2020 design spectrum and response spectrum of scaled time histories for ground motion SET-3 and scaling method M3 of V03 Bridge

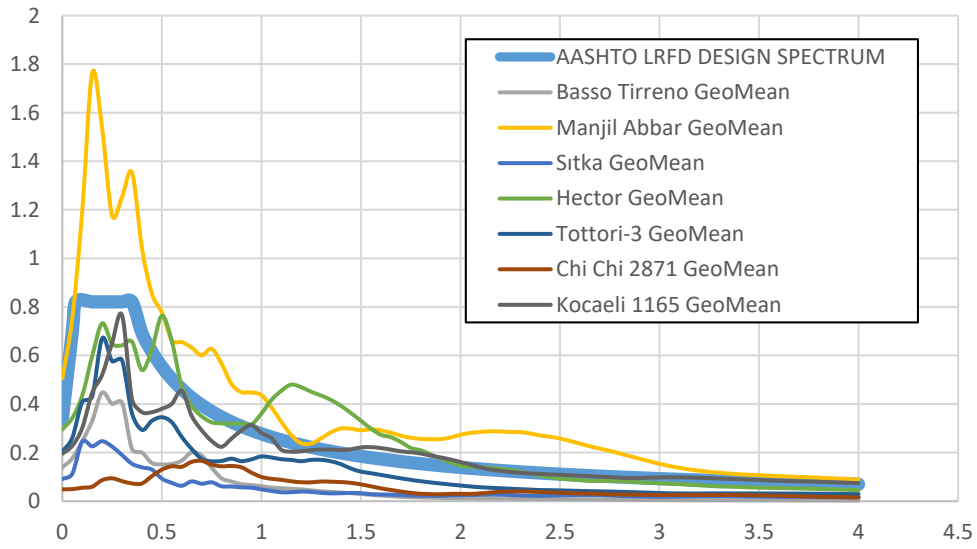


Figure B.55. AASHTO LRFD design spectrum and response spectrum of unscaled time histories for ground motion SET-1 and scaling method M1 of V08 Bridge

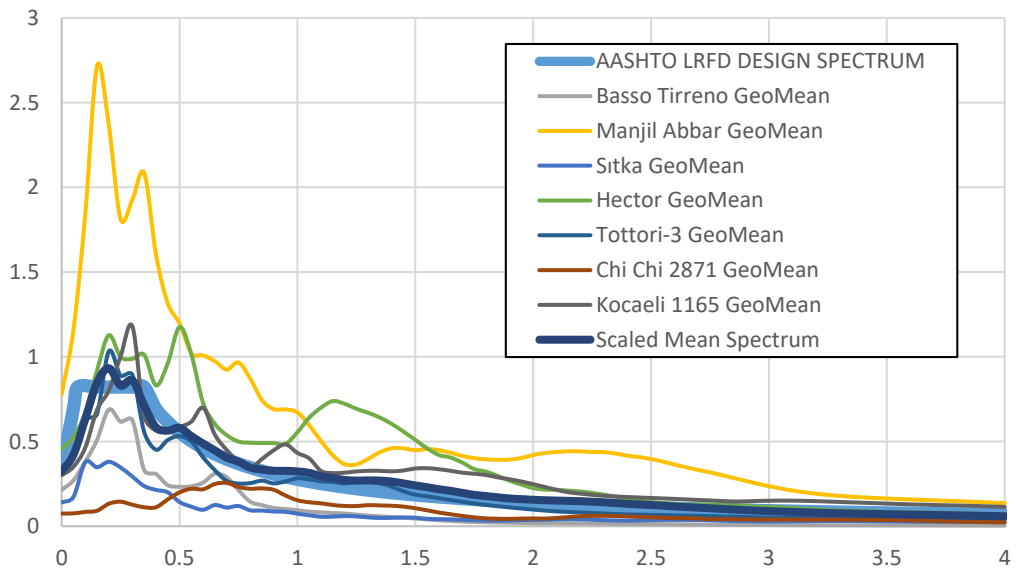


Figure B.56. AASHTO LRFD design spectrum and response spectrum of scaled time histories for ground motion SET-1 and scaling method M1 of V08 Bridge

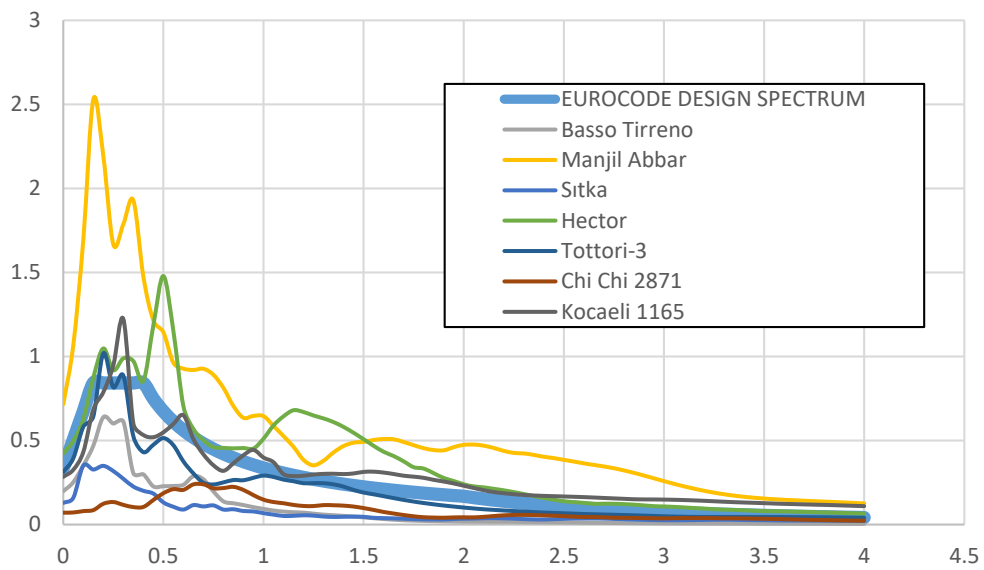


Figure B.57. EN-8 design spectrum and response spectrum of unscaled time histories for ground motion SET-1 and scaling method M1 of V08 Bridge

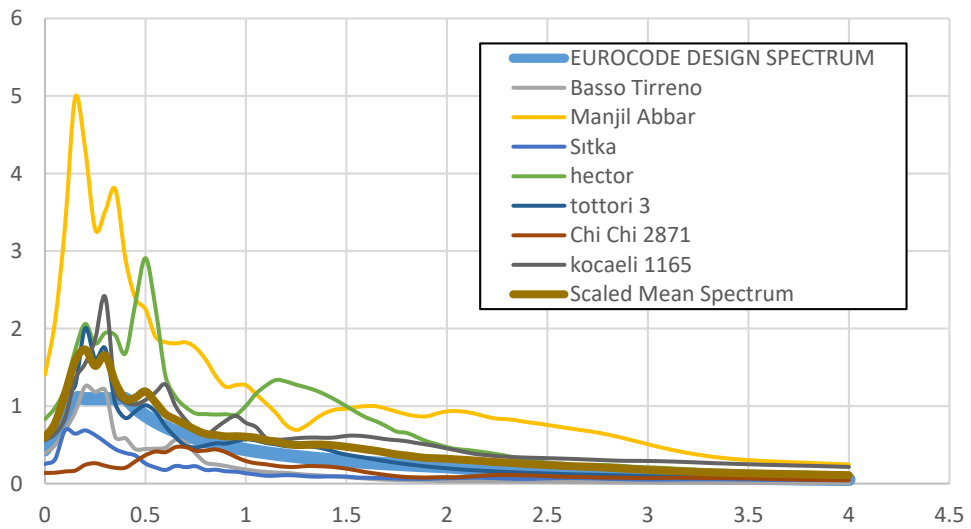


Figure B.58. EN-8 design spectrum and response spectrum of scaled time histories for ground motion SET-1 and scaling method M1 of V08 Bridge

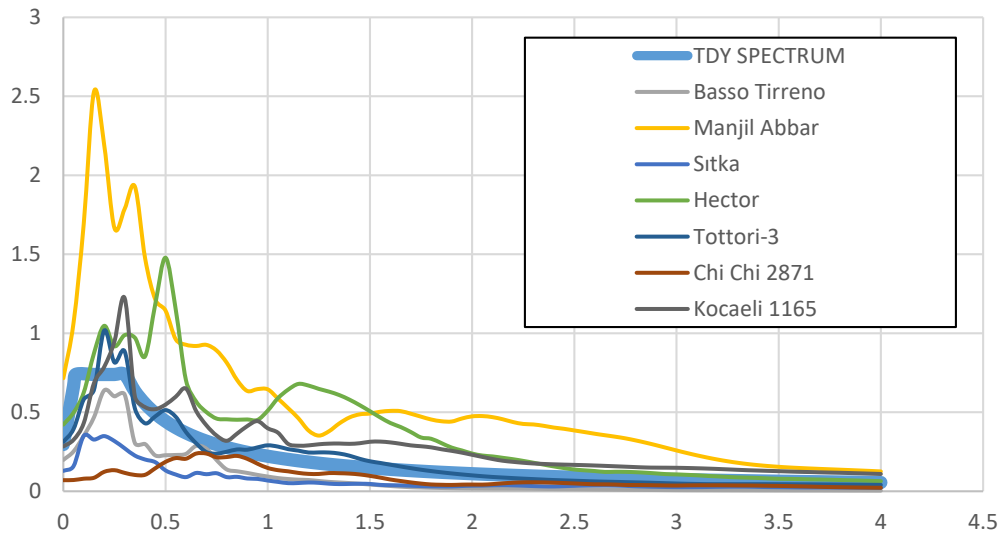


Figure B.59. TDY 2020 design spectrum and response spectrum of unscaled time histories for ground motion SET-1 and scaling method M1 of V08 Bridge

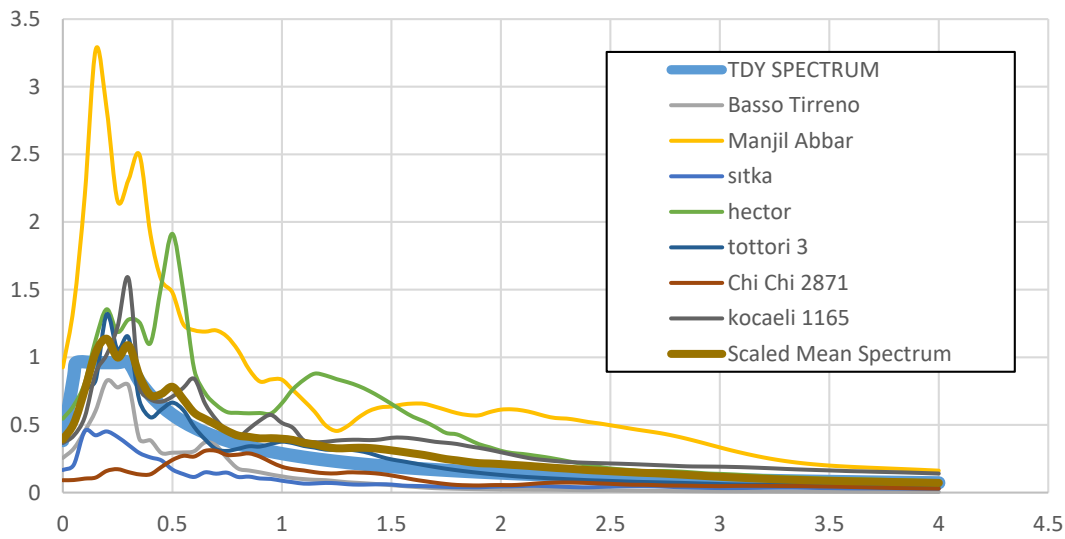


Figure B.60. TDY 2020 design spectrum and response spectrum of scaled time histories for ground motion SET-1 and scaling method M1 of V08 Bridge

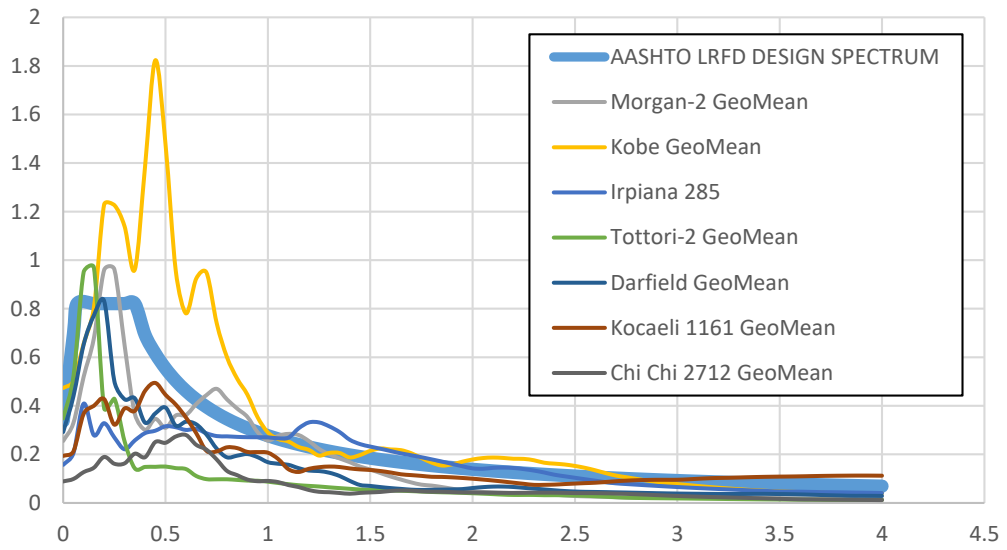


Figure B.61. AASHTO LRFD design spectrum and response spectrum of unscaled time histories for ground motion SET-2 and scaling method M1 of V08 Bridge

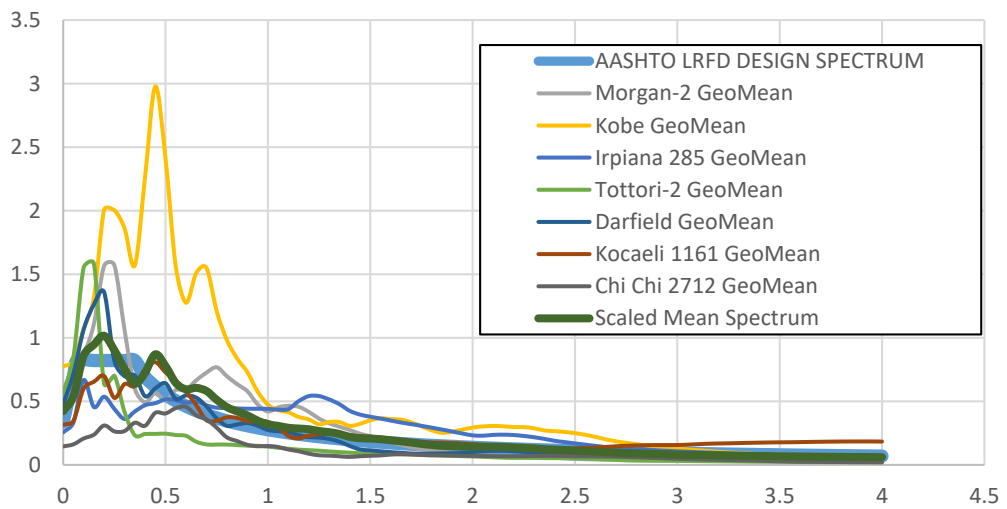


Figure B.62. AASHTO LRFD design spectrum and response spectrum of scaled time histories for ground motion SET-2 and scaling method M1 of V08 Bridge

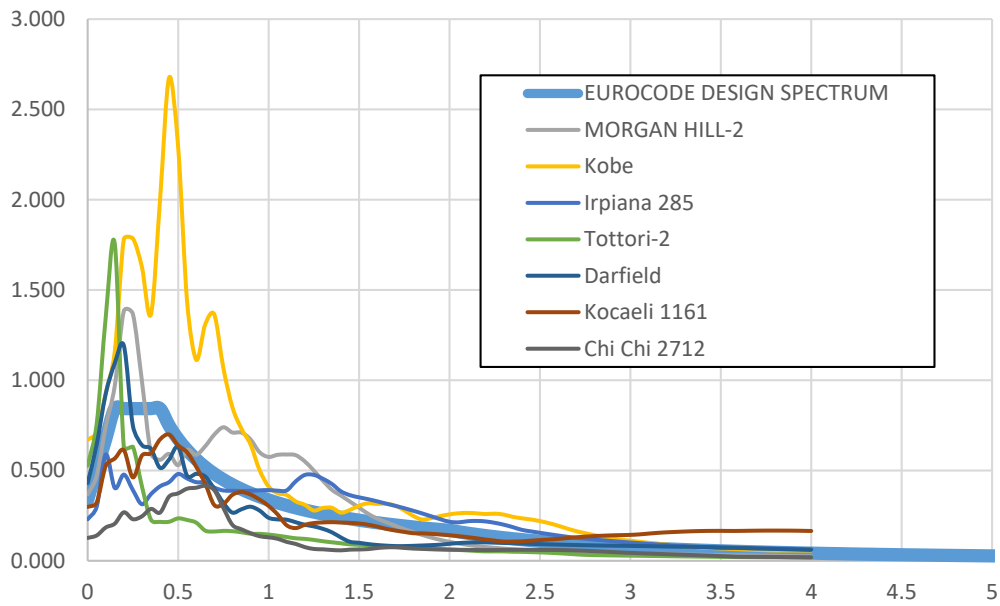


Figure B.63. EN-8 design spectrum and response spectrum of unscaled time histories for ground motion SET-2 and scaling method M1 of V08 Bridge

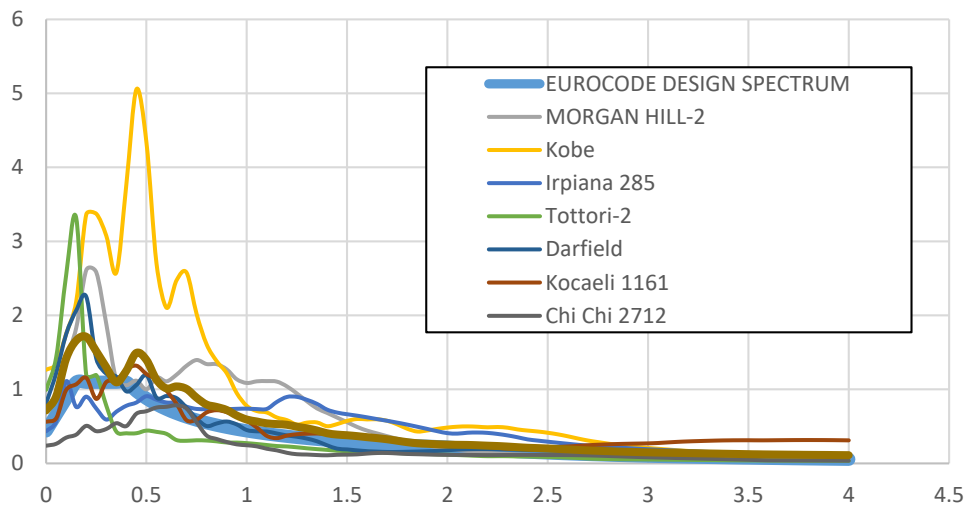


Figure B.64. EN-8 design spectrum and response spectrum of scaled time histories for ground motion SET-2 and scaling method M1 of V08 Bridge

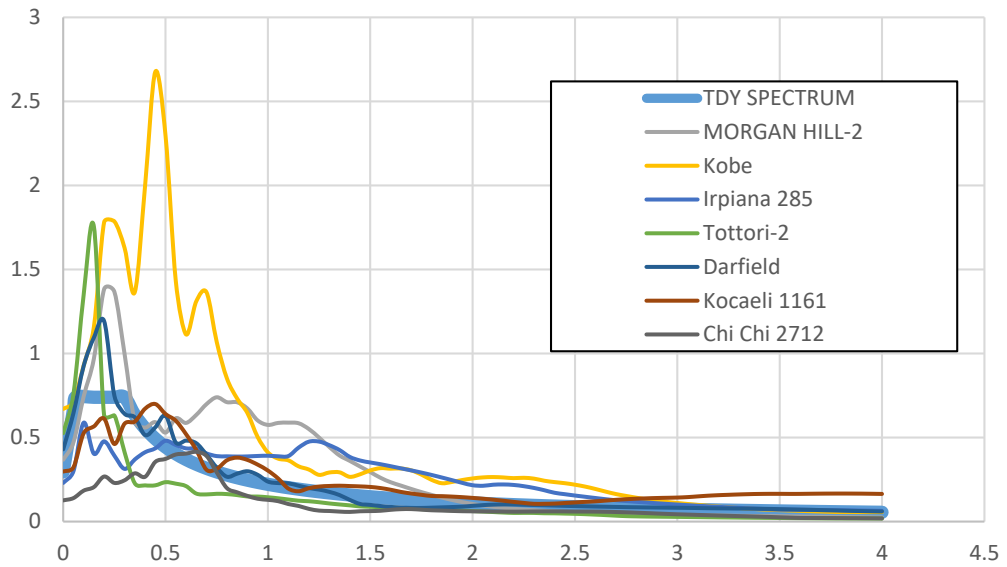


Figure B.65. TDY 2020 design spectrum and response spectrum of unscaled time histories for ground motion SET-2 and scaling method M1 of V08 Bridge

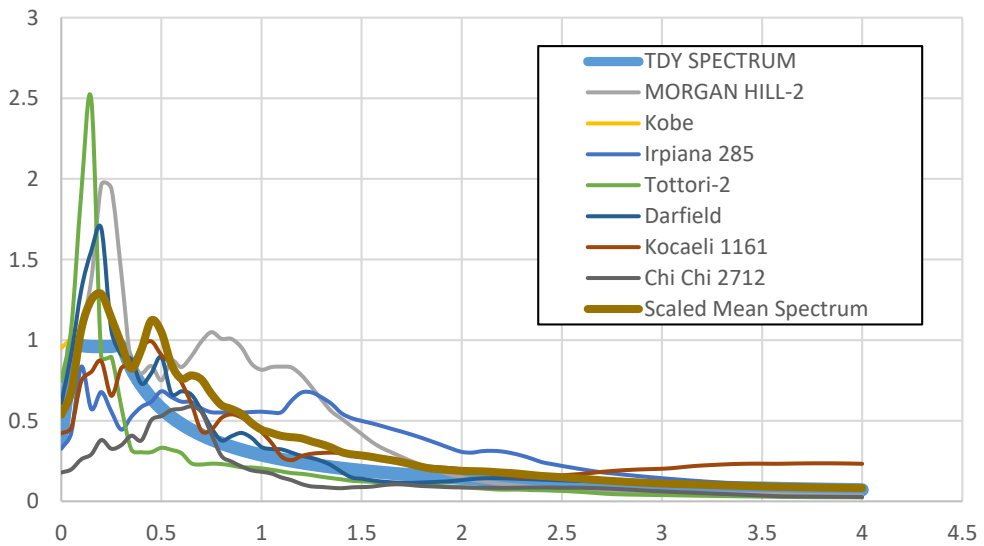


Figure B.66. TDY 2020 design spectrum and response spectrum of scaled time histories for ground motion SET-2 and scaling method M1 of V08 Bridge

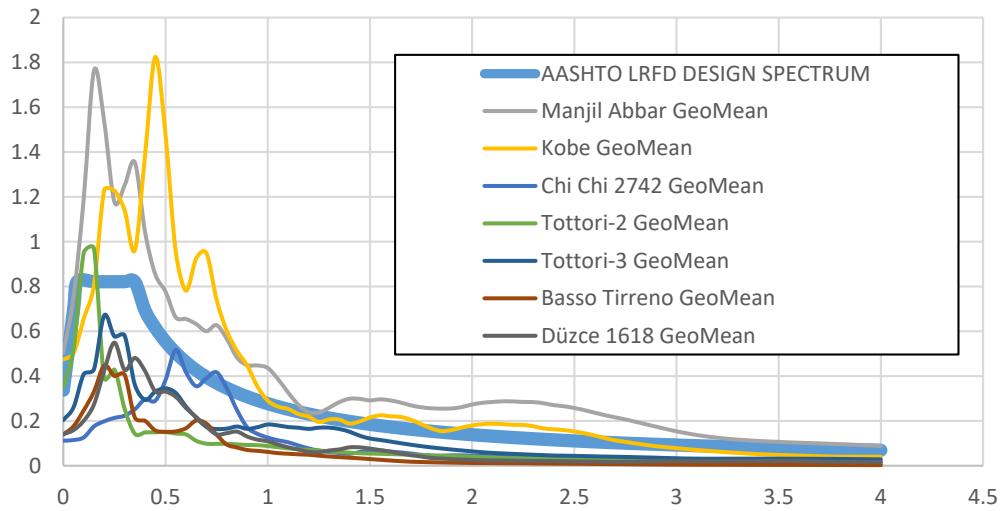


Figure B.67. AASHTO LRFD design spectrum and response spectrum of unscaled time histories for ground motion SET-3 and scaling method M1 of V08 Bridge

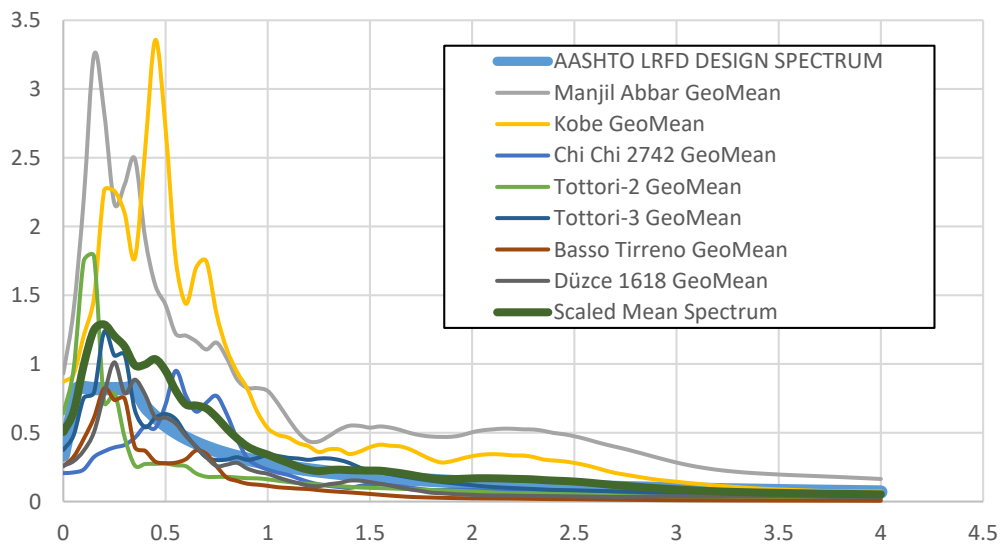


Figure B.68. AASHTO LRFD design spectrum and response spectrum of scaled time histories for ground motion SET-3 and scaling method M1 of V08 Bridge

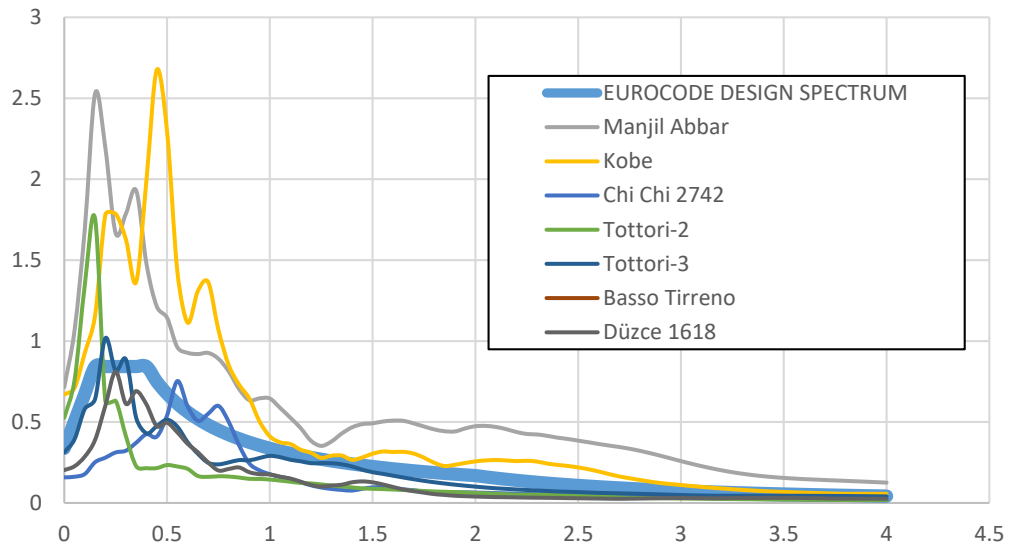


Figure B.69. EN-8 design spectrum and response spectrum of unscaled time histories for ground motion SET-3 and scaling method M1 of V08 Bridge

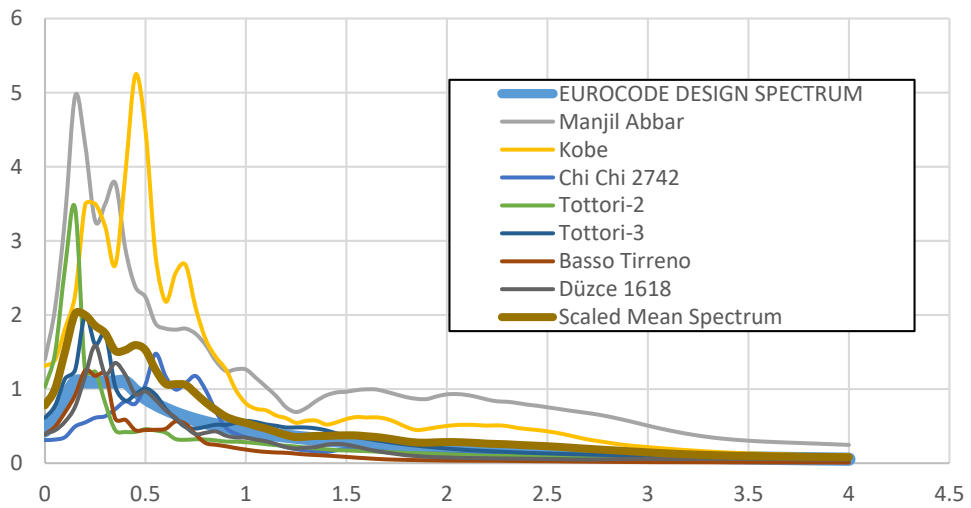


Figure B.70. EN-8 design spectrum and response spectrum of scaled time histories for ground motion SET-3 and scaling method M1 of V08 Bridge

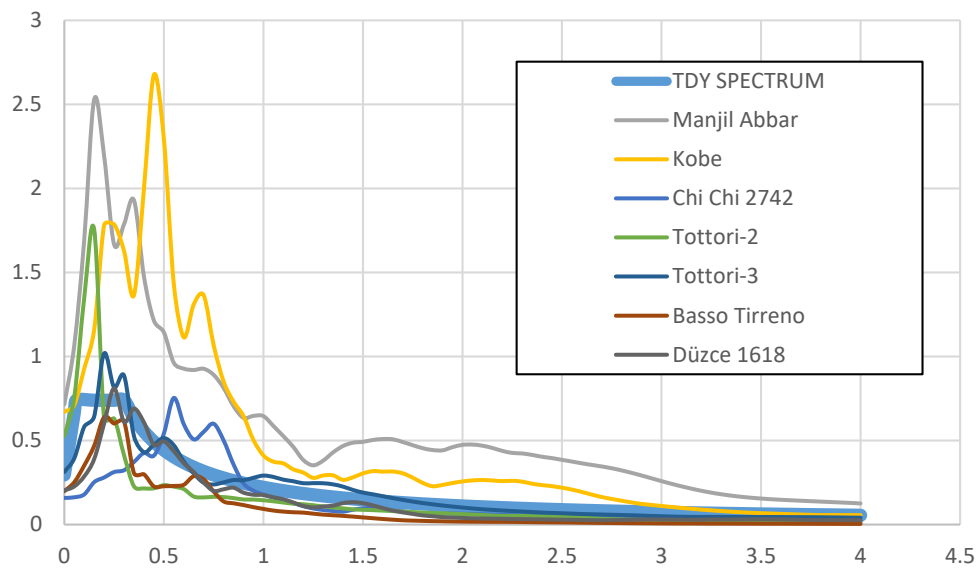


Figure B.71. TDY 2020 design spectrum and response spectrum of unscaled time histories for ground motion SET-3 and scaling method M1 of V08 Bridge

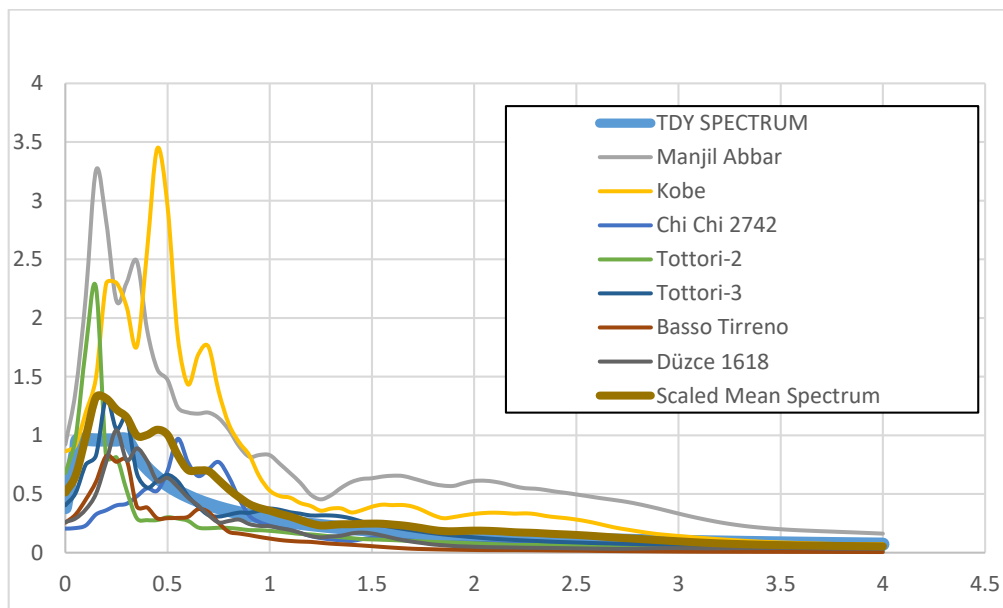


Figure B.72. TDY 2020 design spectrum and response spectrum of scaled time histories for ground motion SET-3 and scaling method M1 of V08 Bridge

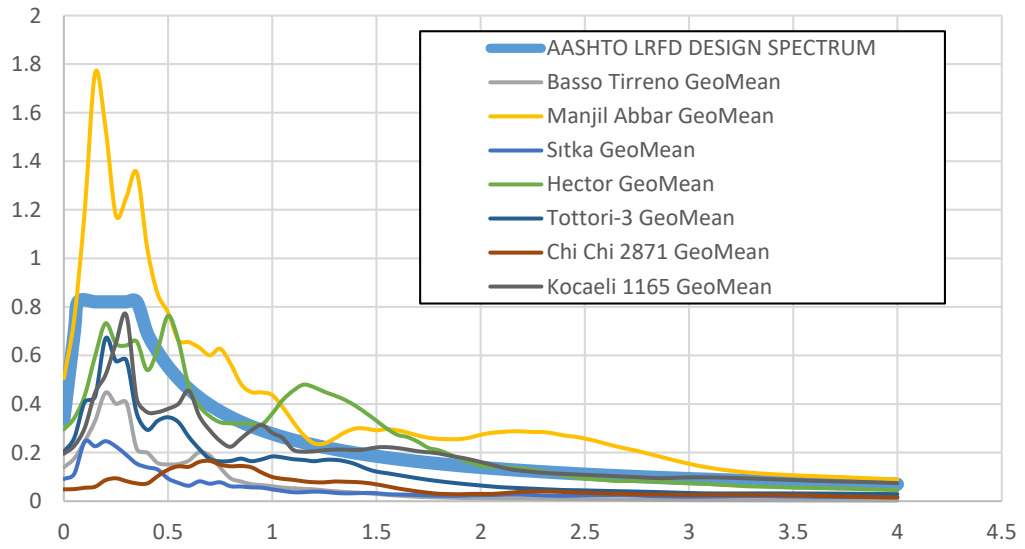


Figure B.73. AASHTO LRFD design spectrum and response spectrum of unscaled time histories for ground motion SET-1 and scaling method M2 of V08 Bridge

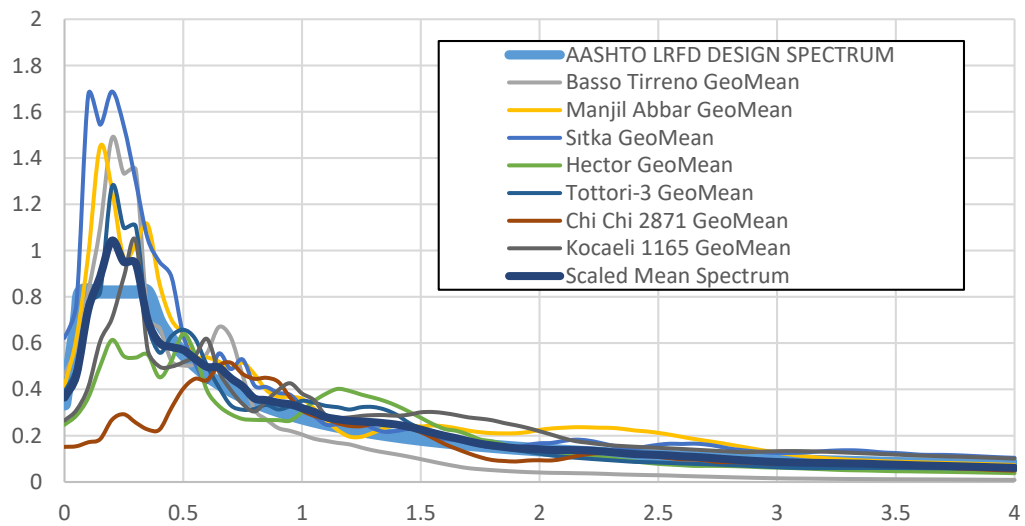


Figure B.74. AASHTO LRFD design spectrum and response spectrum of scaled time histories for ground motion SET-1 and scaling method M2 of V08 Bridge

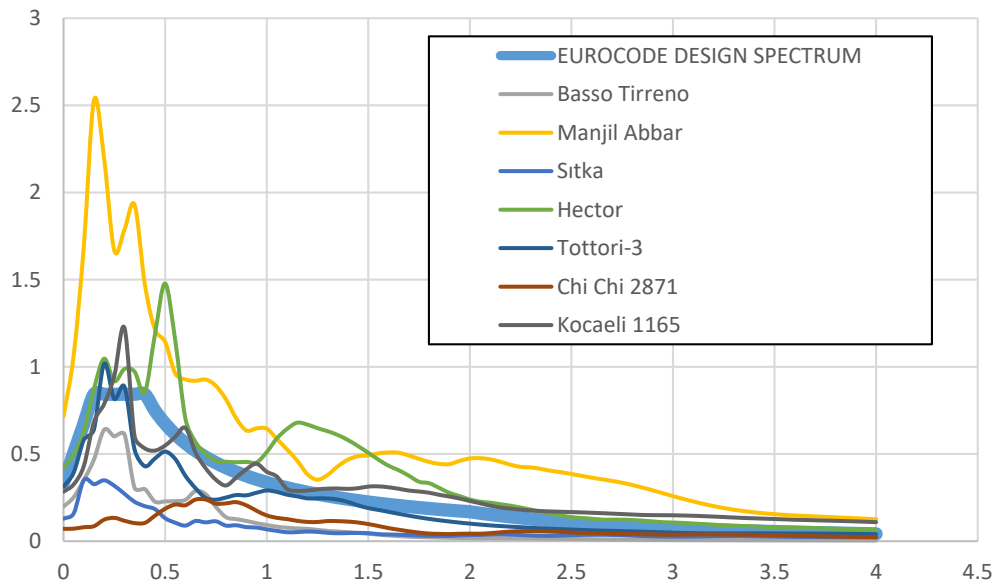


Figure B.75. EN-8 design spectrum and response spectrum of unscaled time histories for ground motion SET-1 and scaling method M2 of V08 Bridge

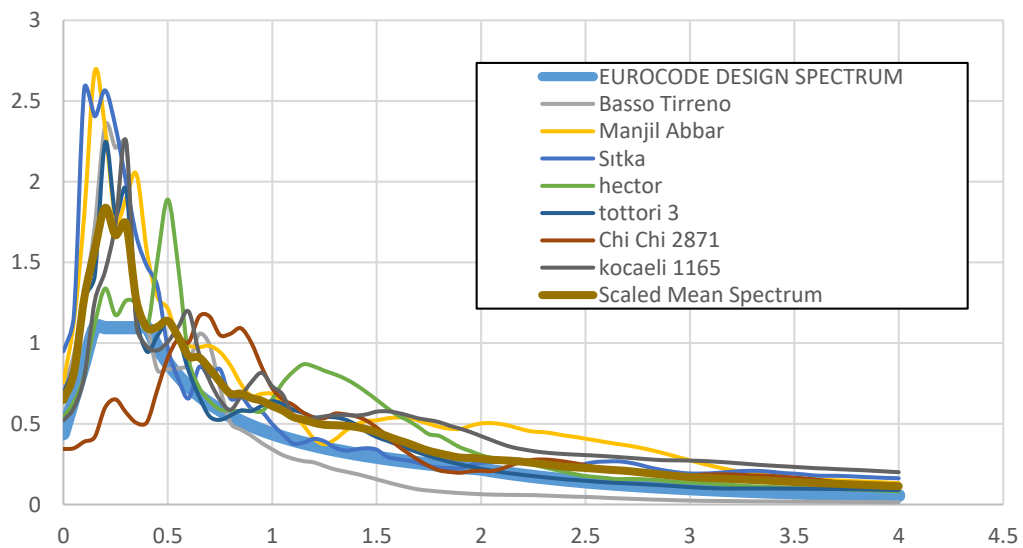


Figure B.76. EN-8 design spectrum and response spectrum of scaled time histories for ground motion SET-1 and scaling method M2 of V08 Bridge

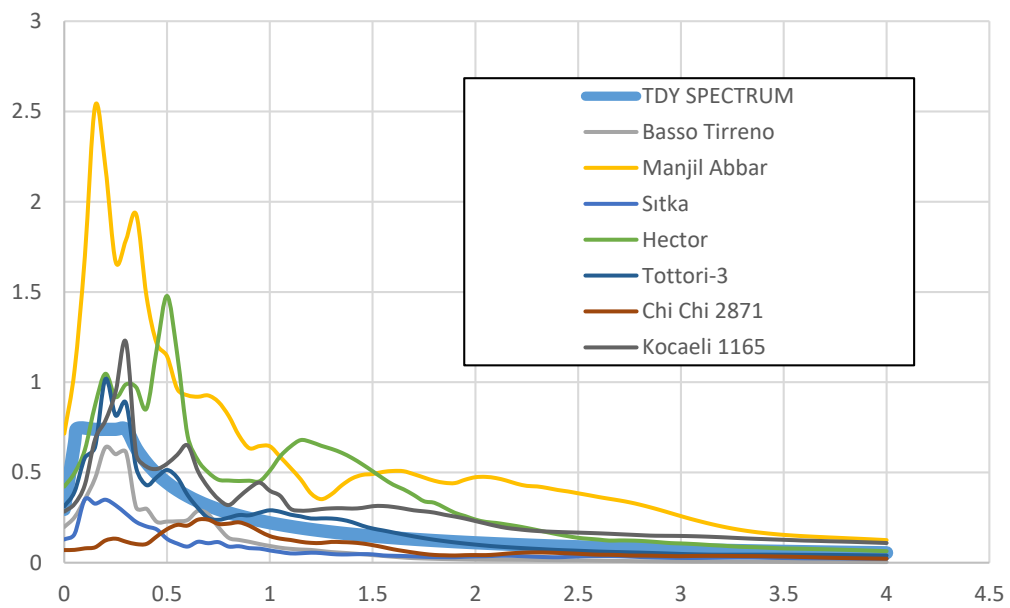


Figure B.77. TDY 2020 design spectrum and response spectrum of unscaled time histories for ground motion SET-1 and scaling method M2 of V08 Bridge

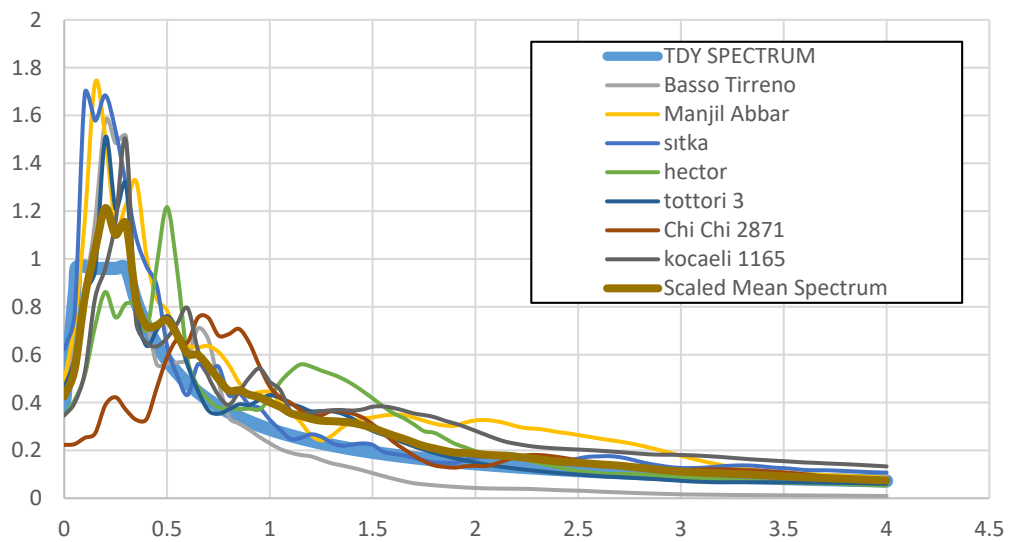


Figure B.78. TDY 2020 design spectrum and response spectrum of scaled time histories for ground motion SET-1 and scaling method M2 of V08 Bridge

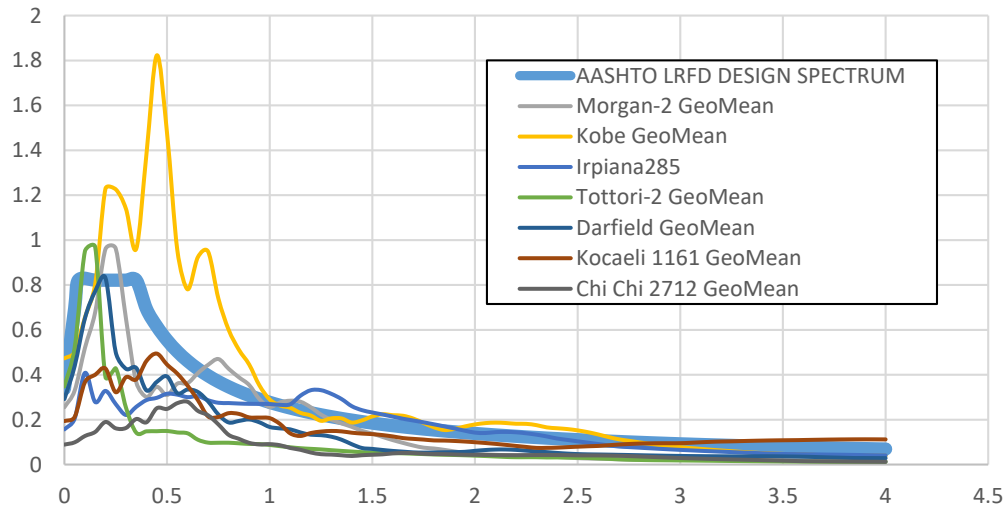


Figure B.79. AASHTO LRFD design spectrum and response spectrum of unscaled time histories for ground motion SET-2 and scaling method M2 of V08 Bridge

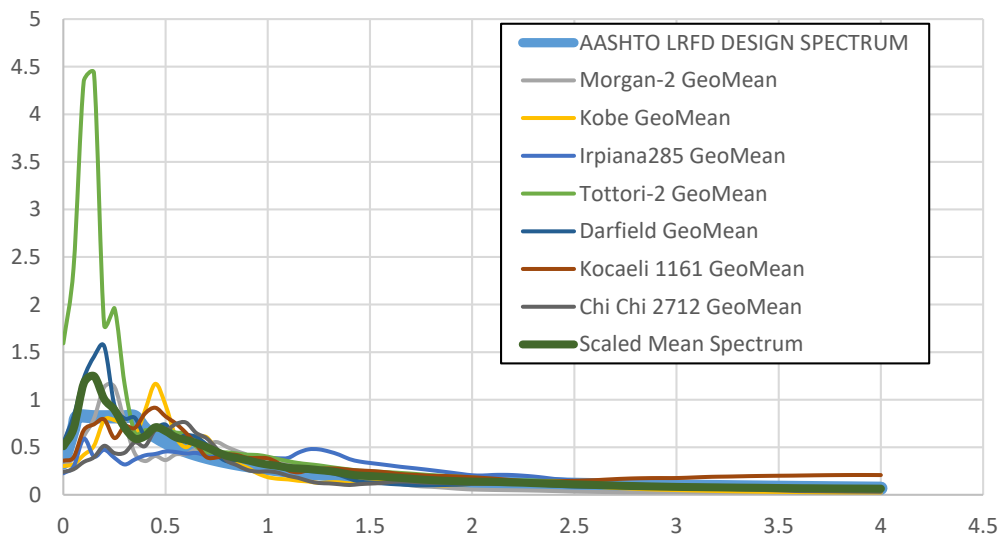


Figure B.80. AASHTO LRFD design spectrum and response spectrum of scaled time histories for ground motion SET-2 and scaling method M2 of V08 Bridge

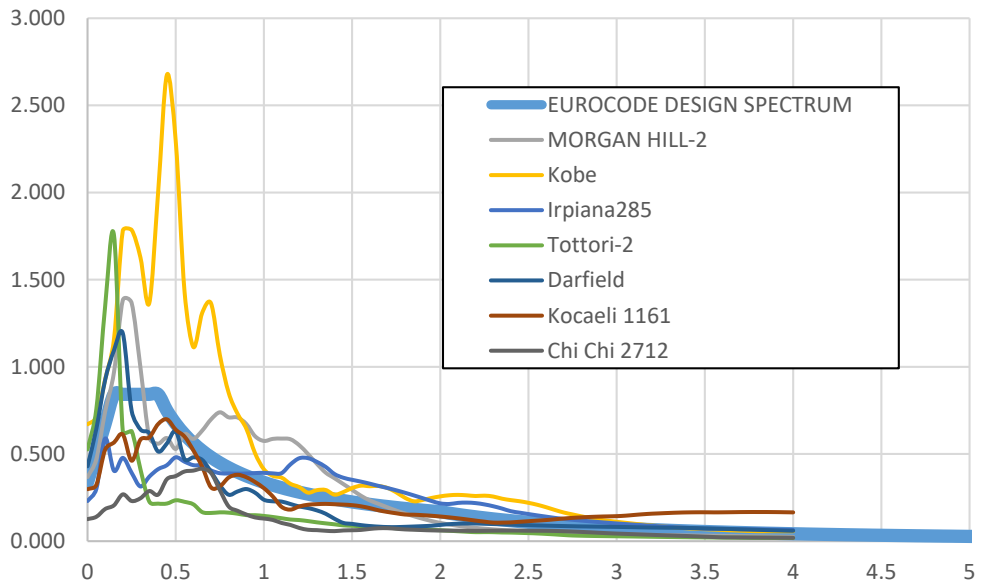


Figure B.81. EN-8 design spectrum and response spectrum of unscaled time histories for ground motion SET-2 and scaling method M2 of V08 Bridge

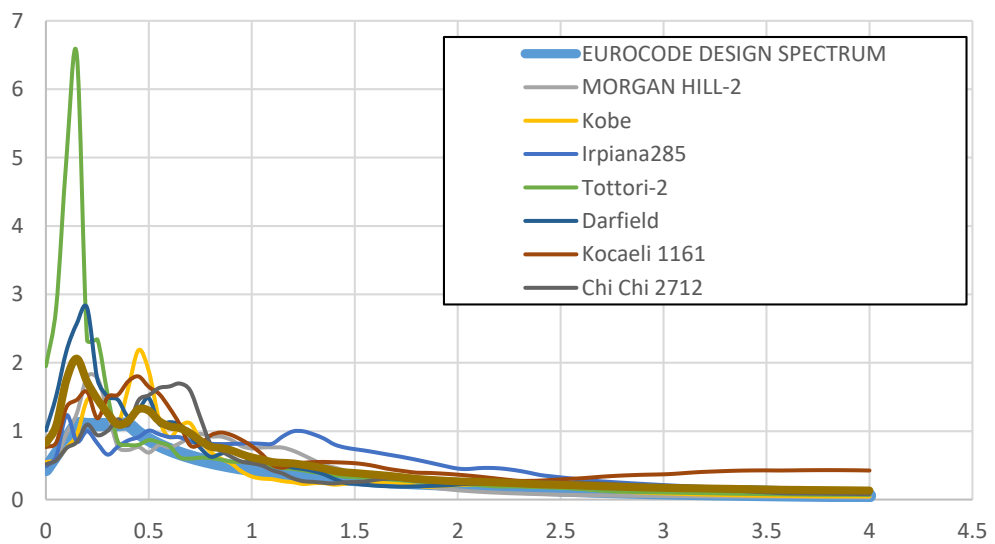


Figure B.82. EN-8 design spectrum and response spectrum of scaled time histories for ground motion SET-2 and scaling method M2 of V08 Bridge

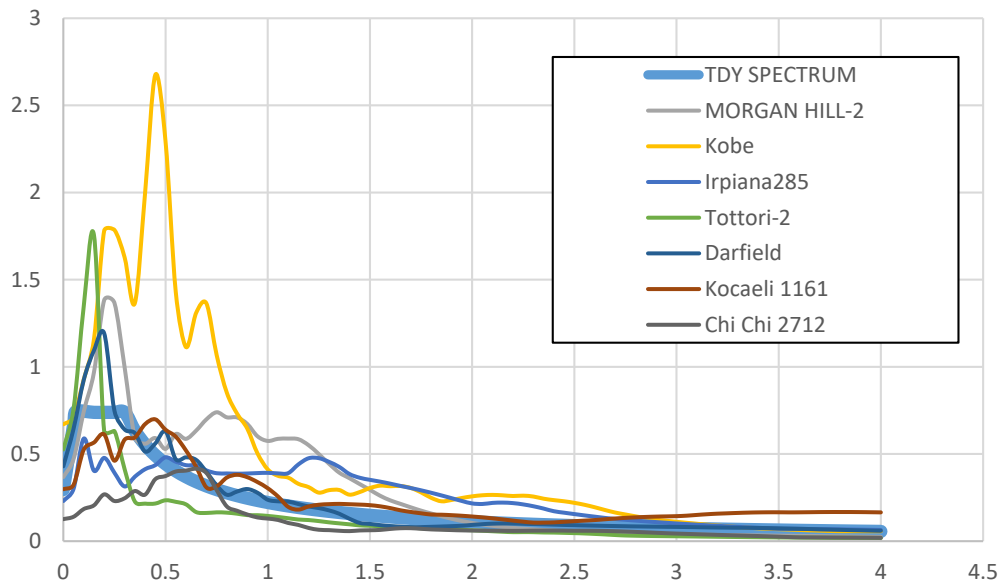


Figure B.83. TDY 2020 design spectrum and response spectrum of unscaled time histories for ground motion SET-2 and scaling method M2 of V08 Bridge

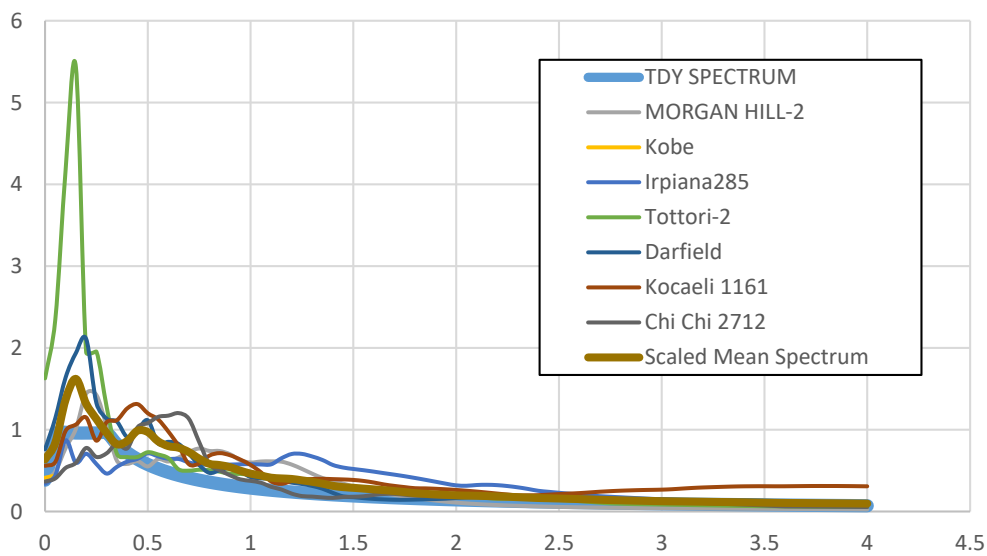


Figure B.84. TDY 2020 design spectrum and response spectrum of scaled time histories for ground motion SET-2 and scaling method M2 of V08 Bridge

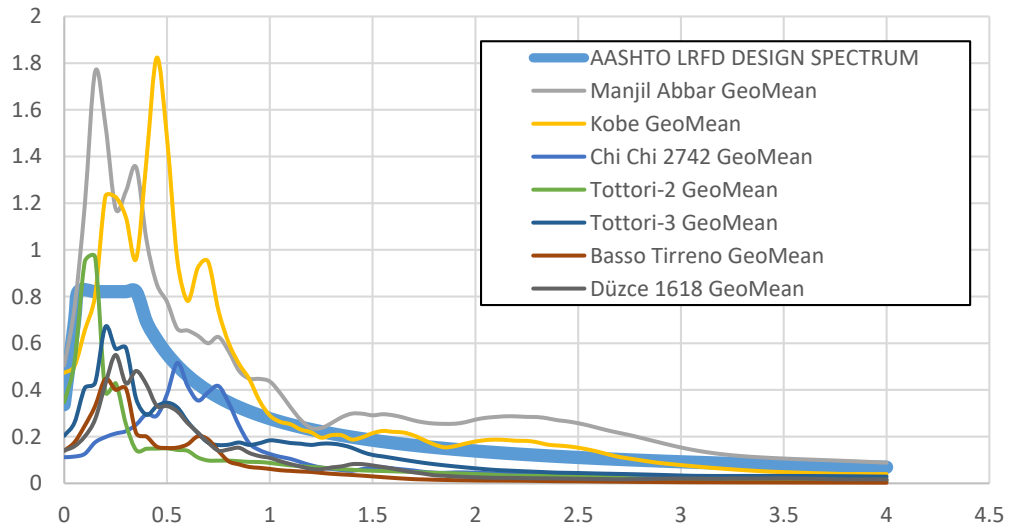


Figure B.85. AASHTO LRFD design spectrum and response spectrum of unscaled time histories for ground motion SET-3 and scaling method M2 of V08 Bridge

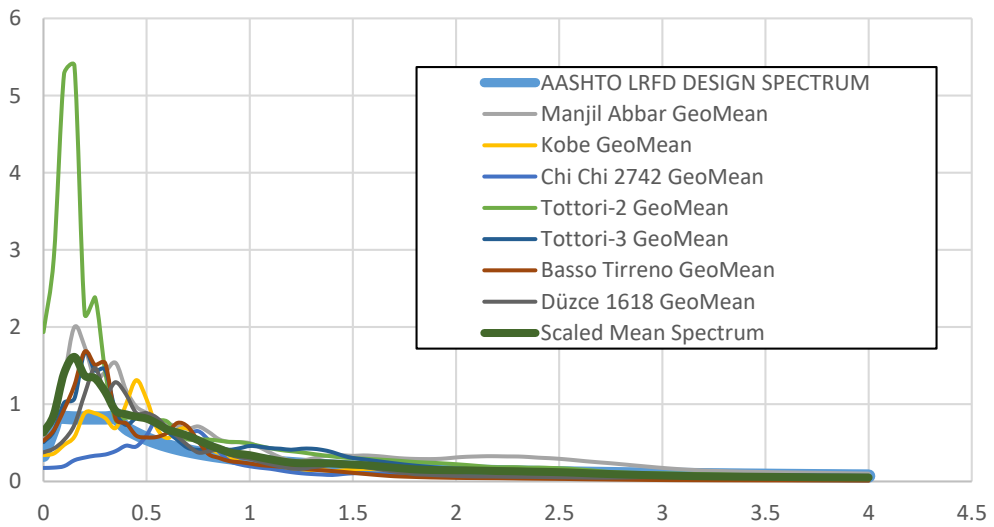


Figure B.86. AASHTO LRFD design spectrum and response spectrum of scaled time histories for ground motion SET-3 and scaling method M2 of V08 Bridge

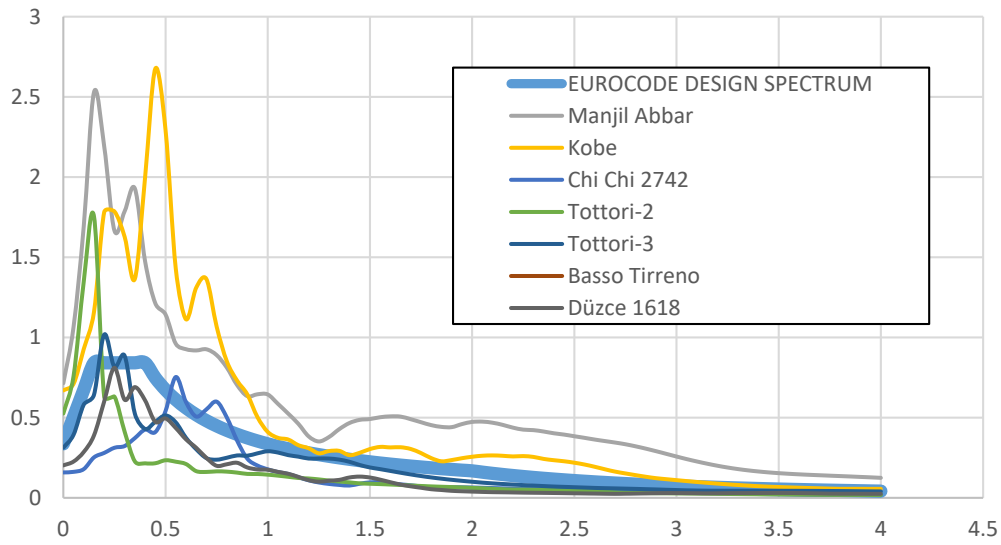


Figure B.87. EN-8 design spectrum and response spectrum of unscaled time histories for ground motion SET-3 and scaling method M2 of V08 Bridge

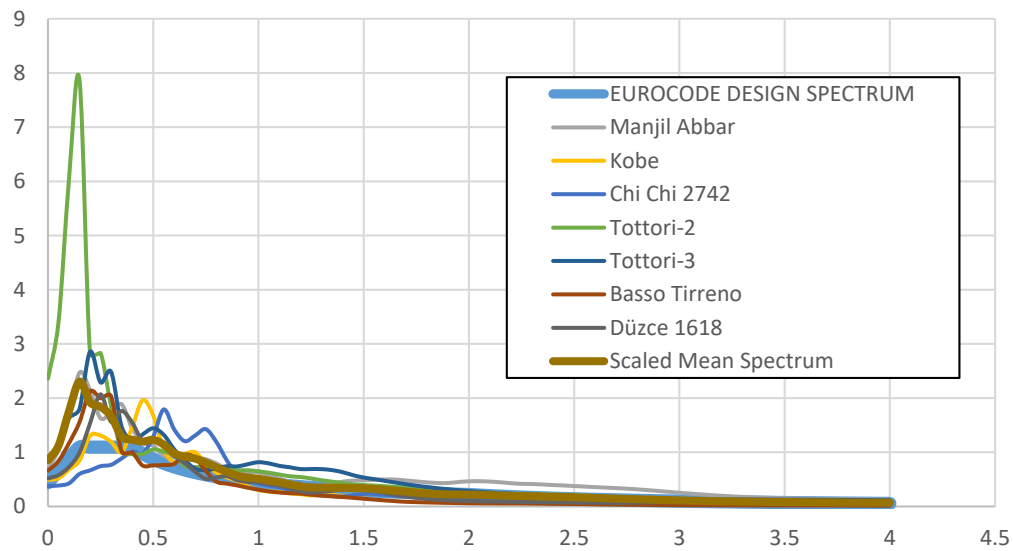


Figure B.88. EN-8 design spectrum and response spectrum of scaled time histories for ground motion SET-3 and scaling method M2 of V08 Bridge

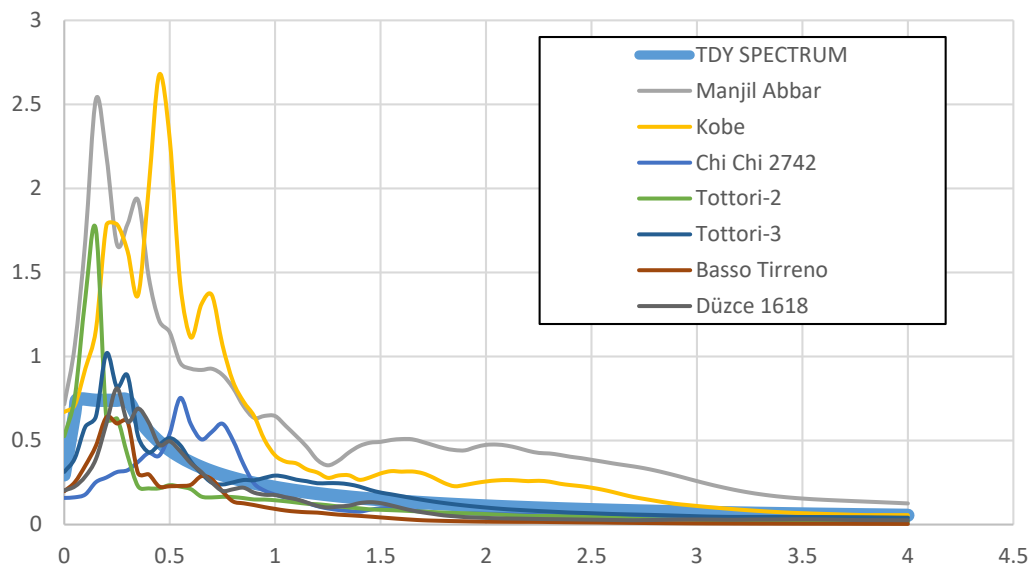


Figure B.89. TDY 2020 design spectrum and response spectrum of unscaled time histories for ground motion SET-3 and scaling method M2 of V08 Bridge

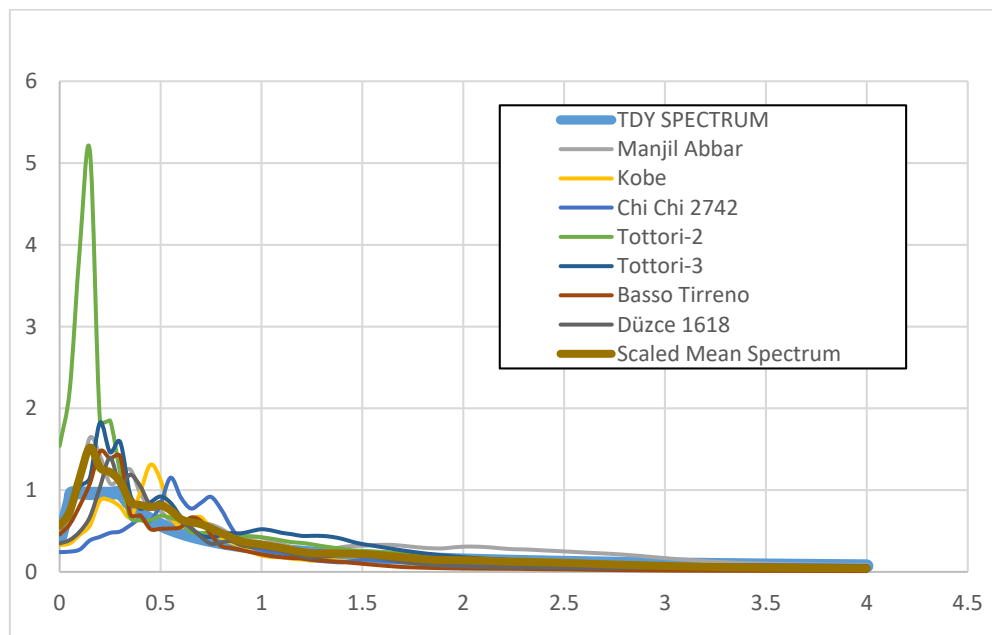


Figure B.90. TDY 2020 design spectrum and response spectrum of scaled time histories for ground motion SET-3 and scaling method M2 of V08 Bridge

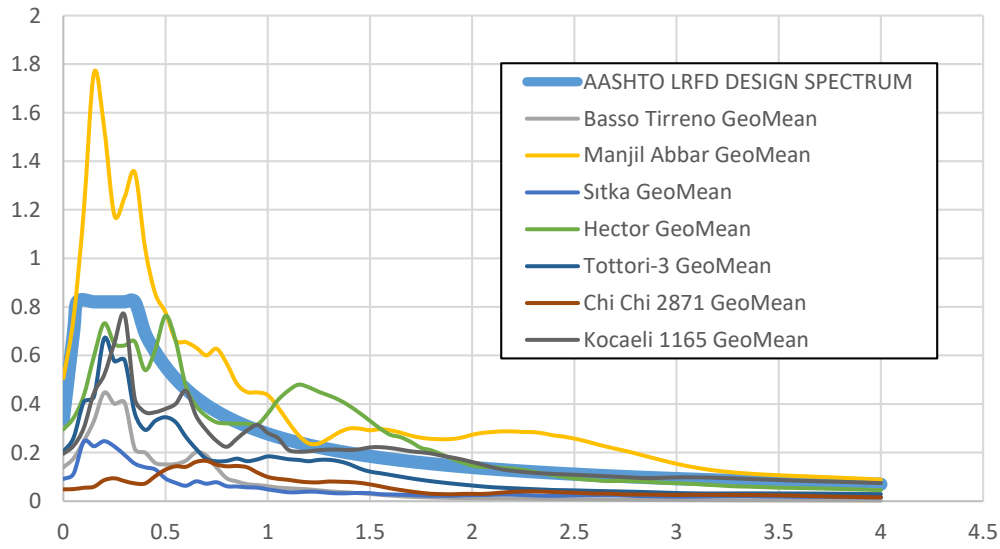


Figure B.91. AASHTO LRFD design spectrum and response spectrum of unscaled time histories for ground motion SET-1 and scaling method M3 of V08 Bridge

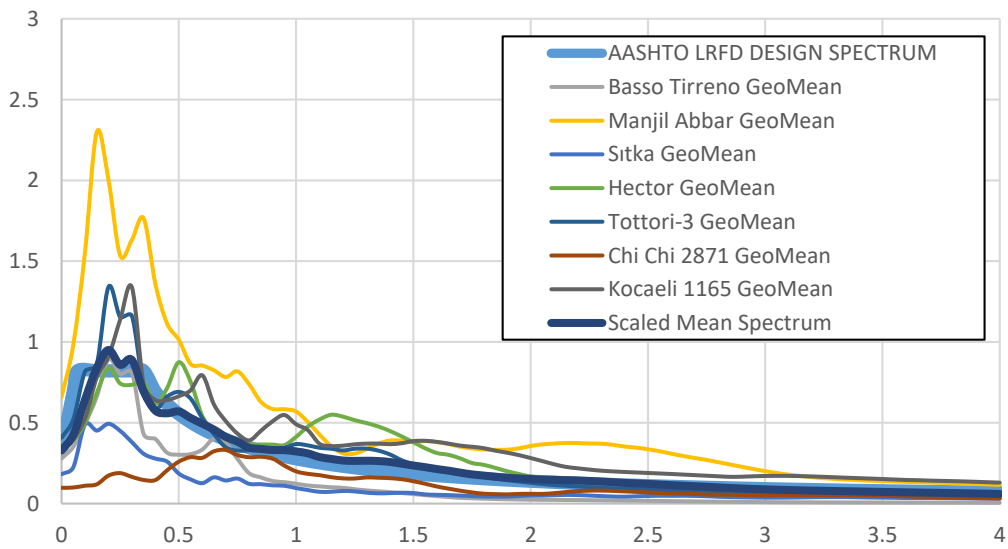


Figure B.92. AASHTO LRFD design spectrum and response spectrum of scaled time histories for ground motion SET-1 and scaling method M3 of V08 Bridge

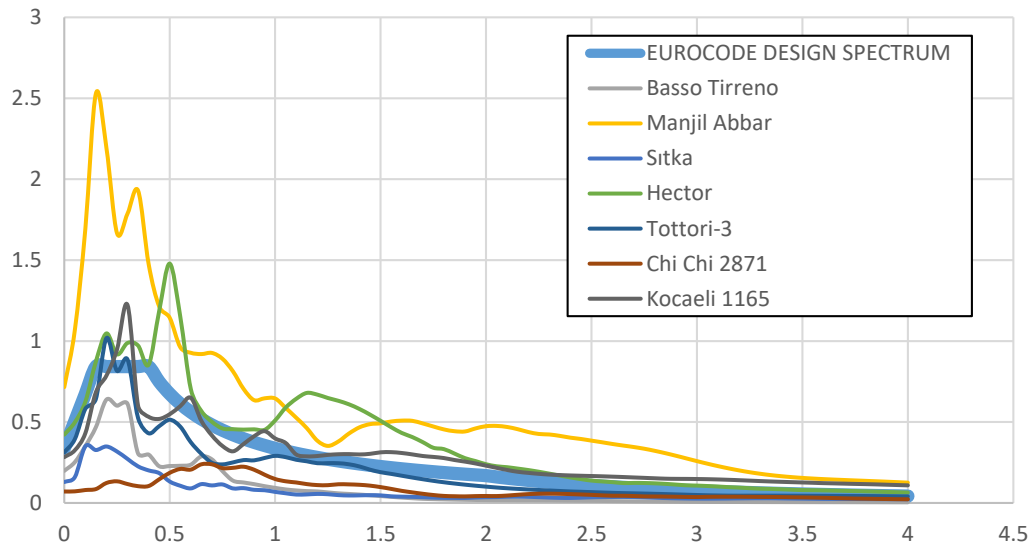


Figure B.93. EN-8 design spectrum and response spectrum of unscaled time histories for ground motion SET-1 and scaling method M3 of V08 Bridge

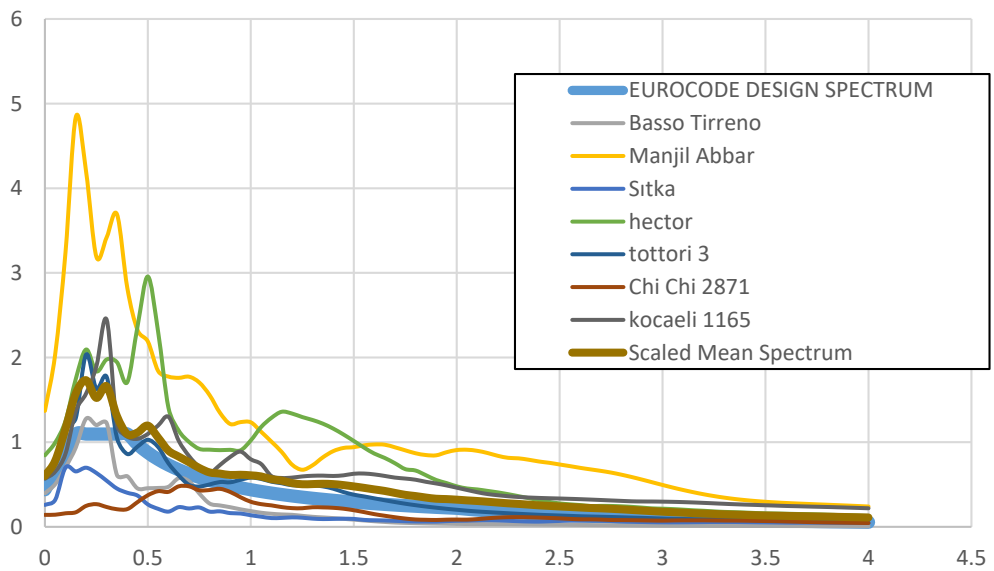


Figure B.94. EN-8 design spectrum and response spectrum of scaled time histories for ground motion SET-1 and scaling method M3 of V08 Bridge

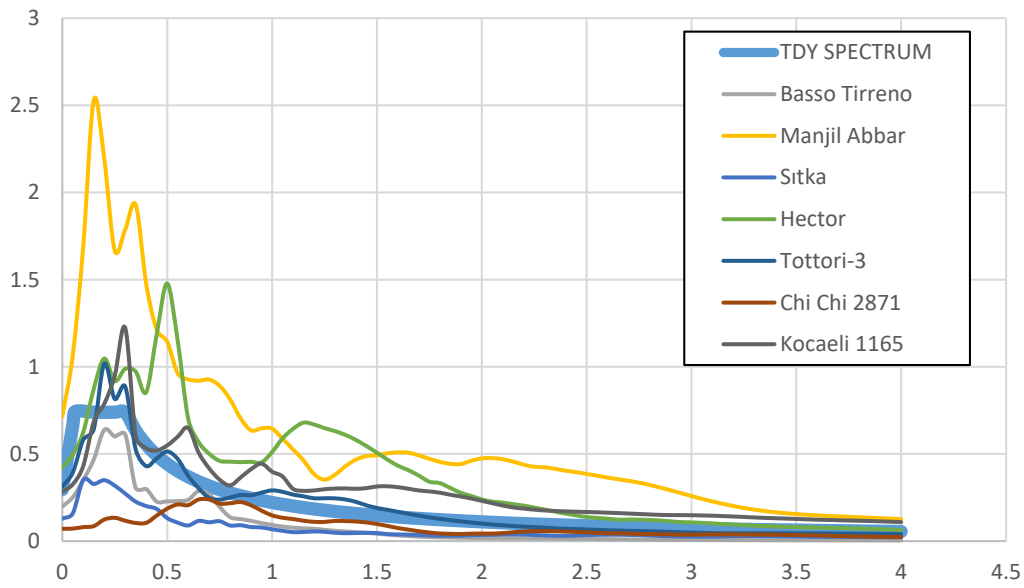


Figure B.95. TDY 2020 design spectrum and response spectrum of unscaled time histories for ground motion SET-1 and scaling method M3 of V08 Bridge

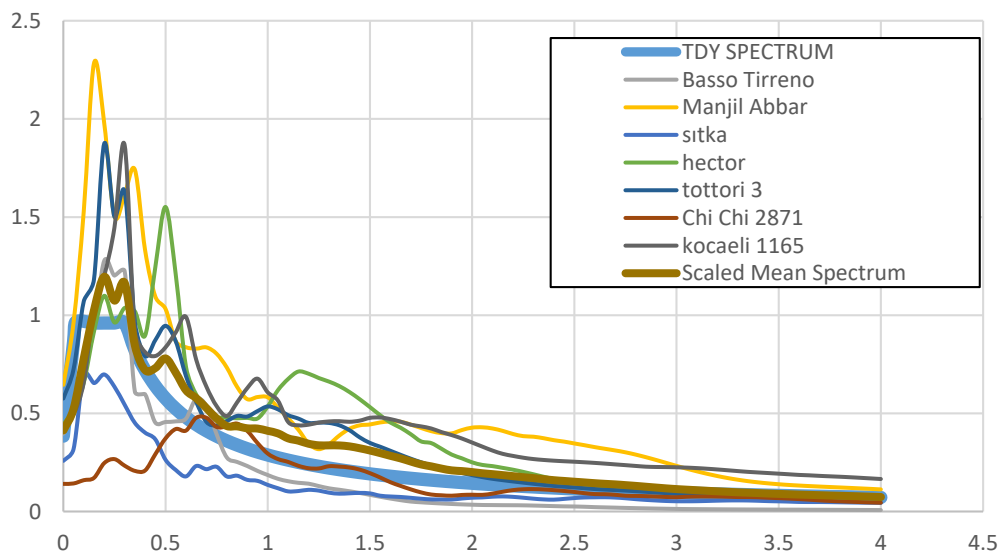


Figure B.96. TDY 2020 design spectrum and response spectrum of scaled time histories for ground motion SET-1 and scaling method M3 of V08 Bridge

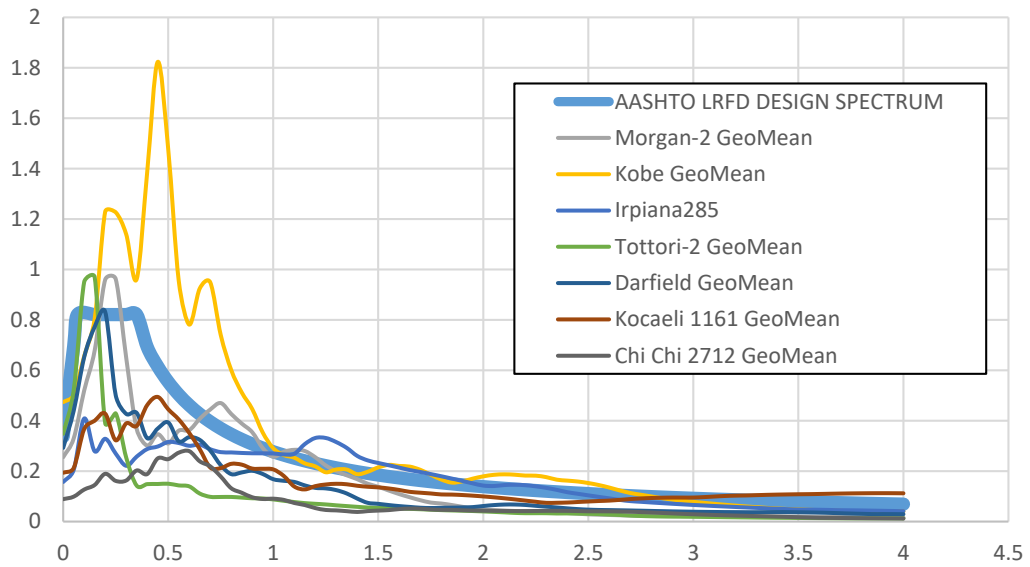


Figure B.97. AASHTO LRFD design spectrum and response spectrum of unscaled time histories for ground motion SET-2 and scaling method M3 of V08 Bridge

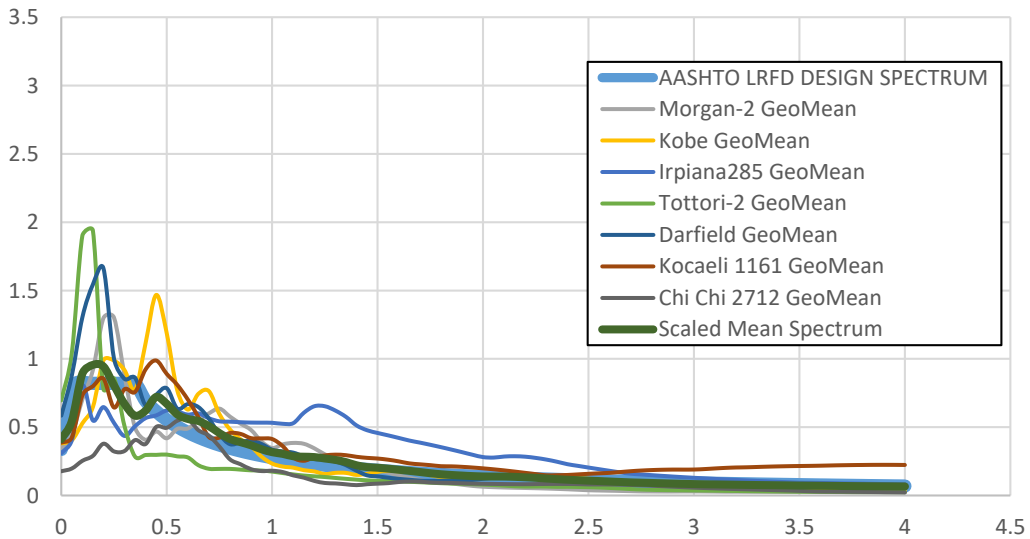


Figure B.98. AASHTO LRFD design spectrum and response spectrum of scaled time histories for ground motion SET-2 and scaling method M3 of V08 Bridge

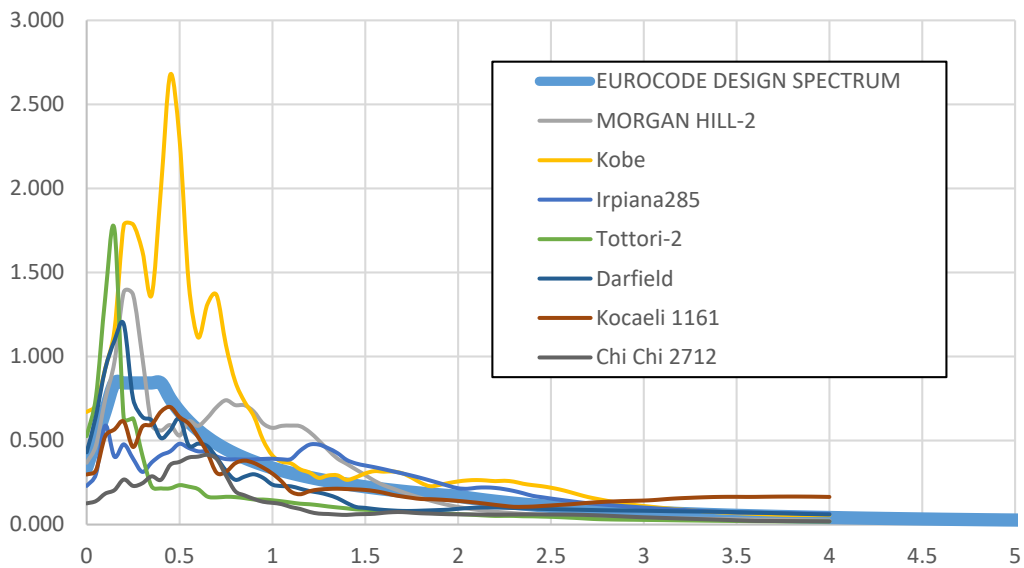


Figure B.99. EN-8 design spectrum and response spectrum of unscaled time histories for ground motion SET-2 and scaling method M3 of V03 Bridge

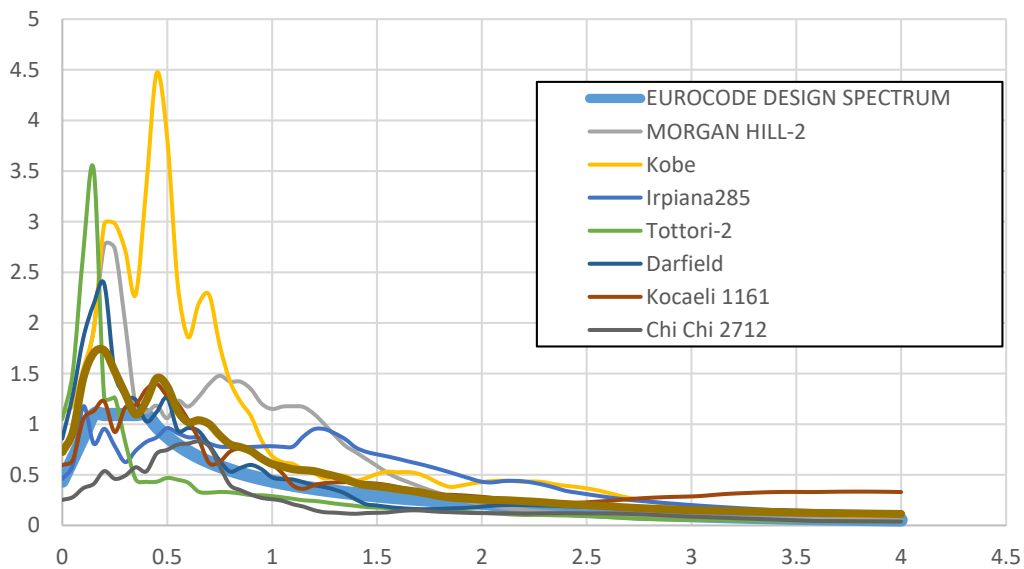


Figure B.100. EN-8 design spectrum and response spectrum of scaled time histories for ground motion SET-2 and scaling method M3 of V03 Bridge

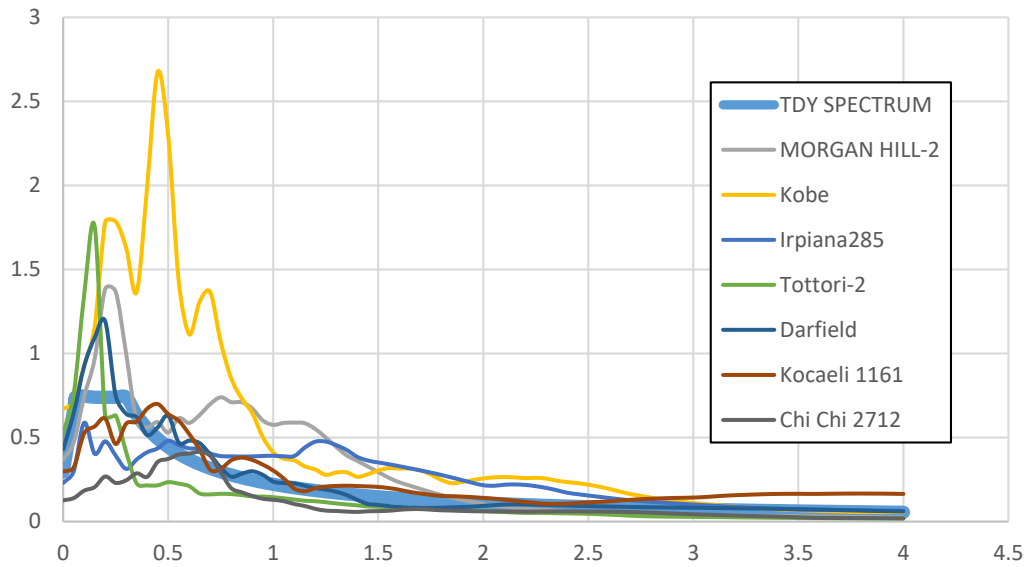


Figure B.101. TDY 2020 design spectrum and response spectrum of unscaled time histories for ground motion SET-2 and scaling method M3 of V03 Bridge

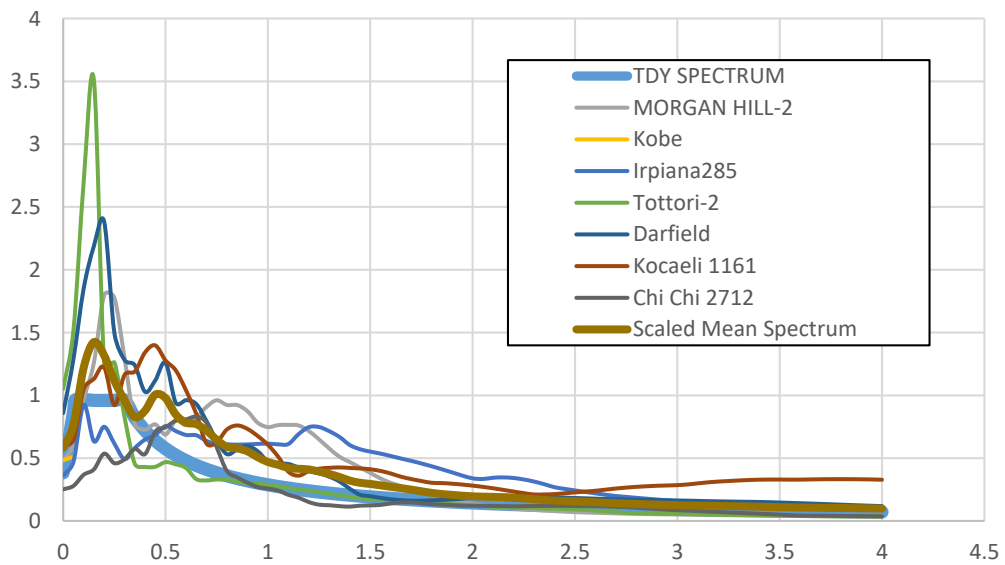


Figure B.102. TDY 2020 design spectrum and response spectrum of scaled time histories for ground motion SET-2 and scaling method M3 of V08 Bridge

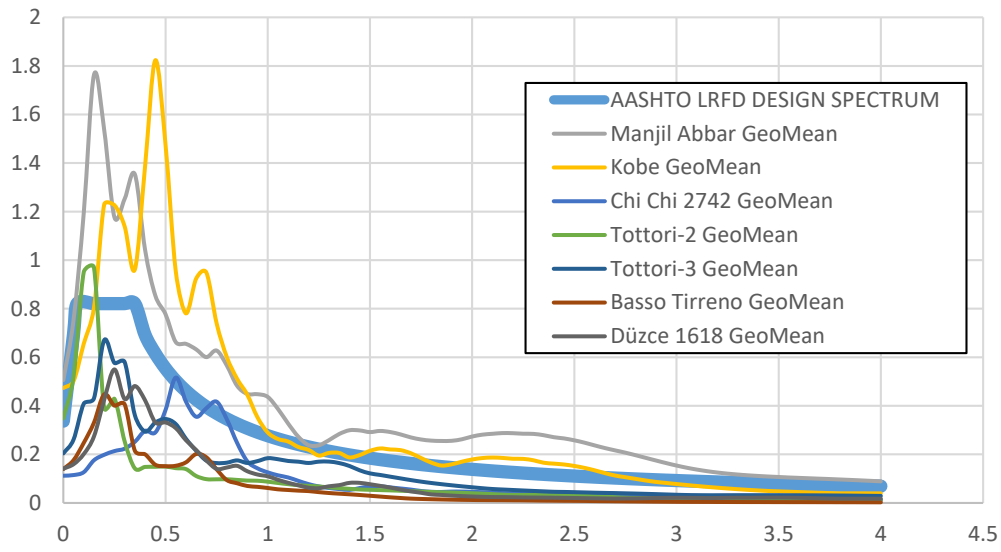


Figure B.103. AASHTO LRFD design spectrum and response spectrum of unscaled time histories for ground motion SET-3 and scaling method M3 of V08 Bridge

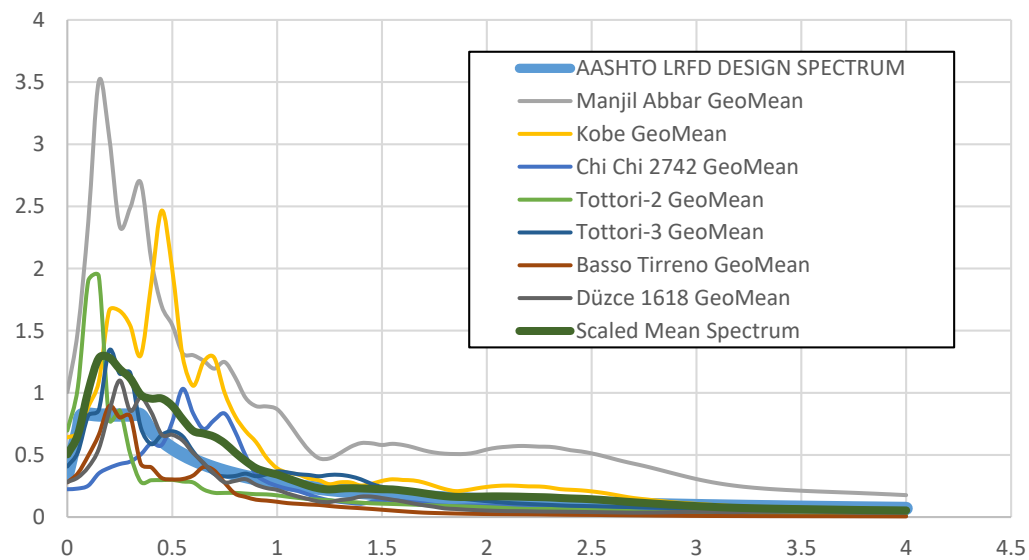


Figure B.104. AASHTO LRFD design spectrum and response spectrum of scaled time histories for ground motion SET-3 and scaling method M3 of V08 Bridge

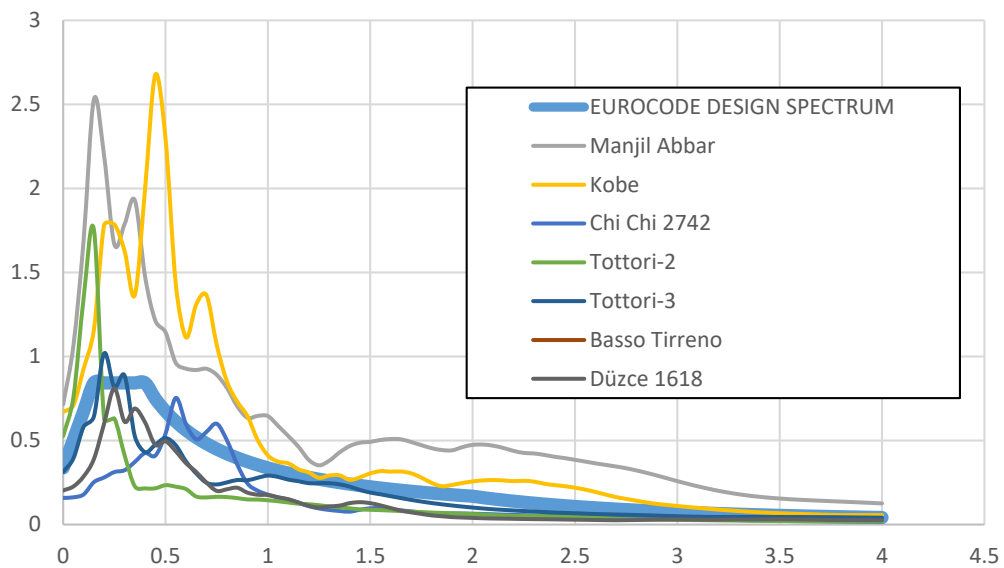


Figure B.105. EN-8 design spectrum and response spectrum of unscaled time histories for ground motion SET-3 and scaling method M3 of V03 Bridge

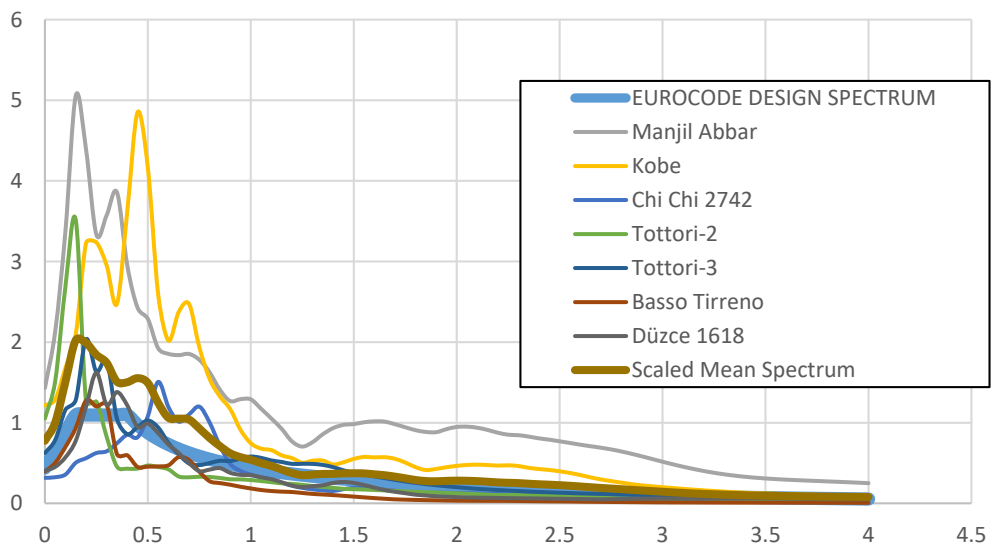


Figure B.4406. EN-8 design spectrum and response spectrum of scaled time histories for ground motion SET-3 and scaling method M3 of V03 Bridge

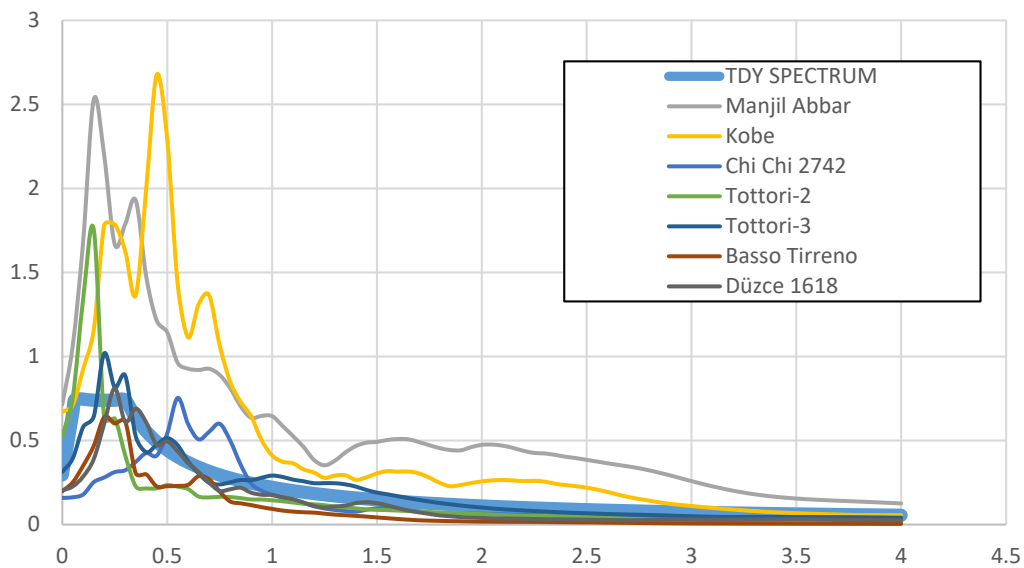


Figure B.107. TDY 2020 design spectrum and response spectrum of unscaled time histories for ground motion SET-3 and scaling method M3 of V03 Bridge

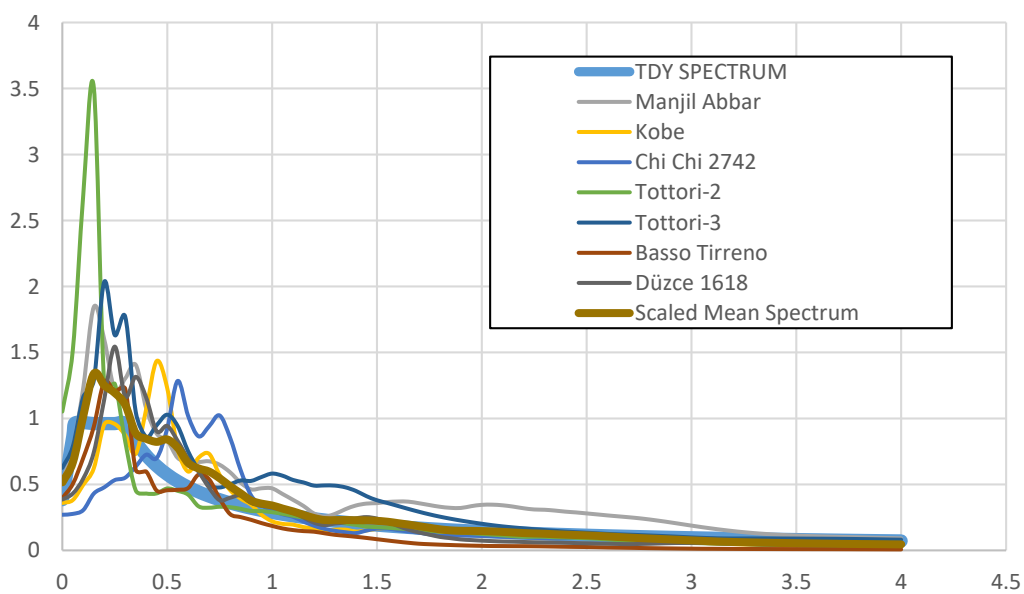


Figure B.108. TDY 2020 design spectrum and response spectrum of scaled time histories for ground motion SET-3 and scaling method M3 of V03 Bridge

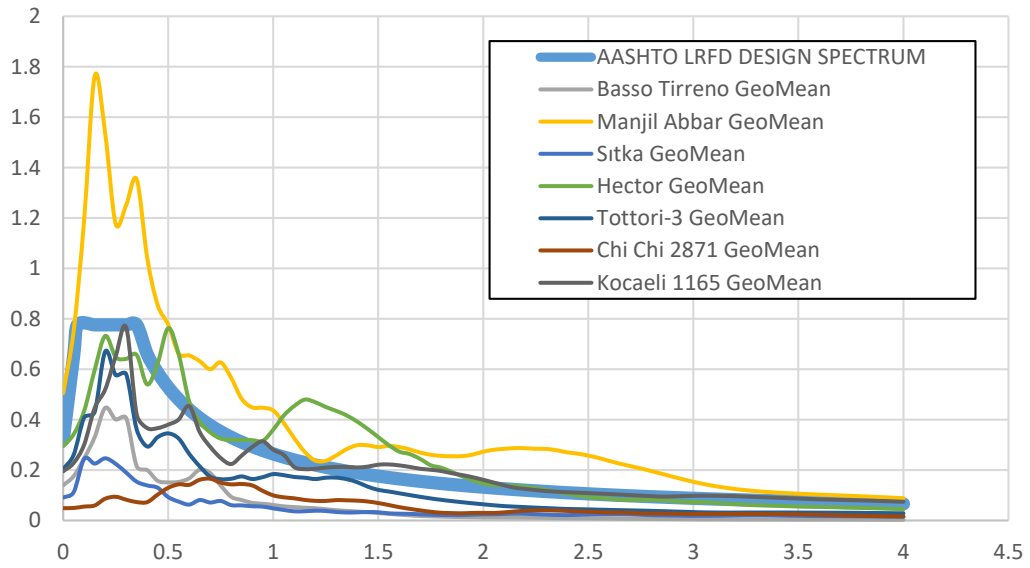


Figure B.4509. AASHTO LRFD design spectrum and response spectrum of unscaled time histories for ground motion SET-1 and scaling method M1 of V14 Bridge

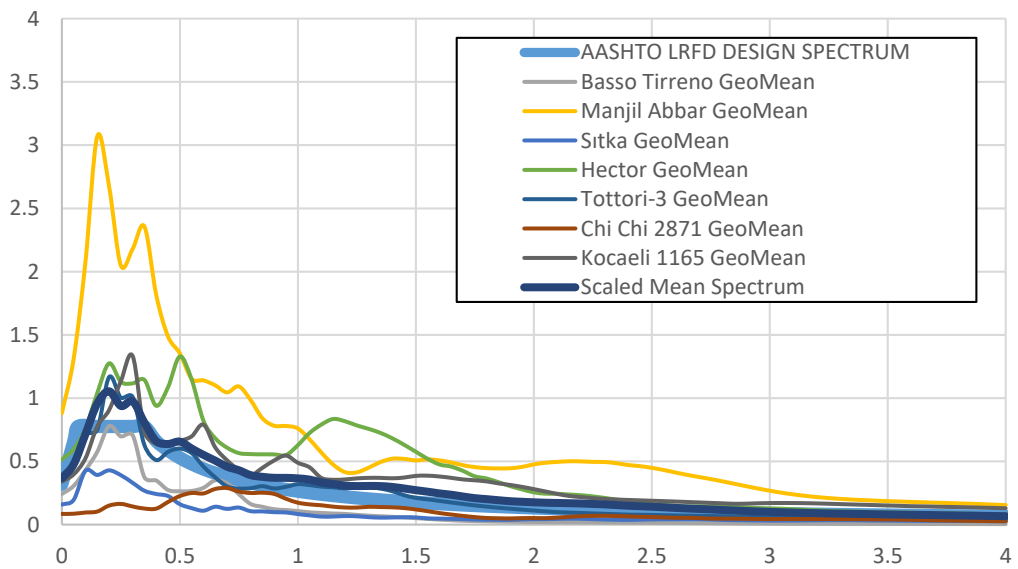


Figure B.4610. AASHTO LRFD design spectrum and response spectrum of scaled time histories for ground motion SET-1 and scaling method M1 of V14 Bridge

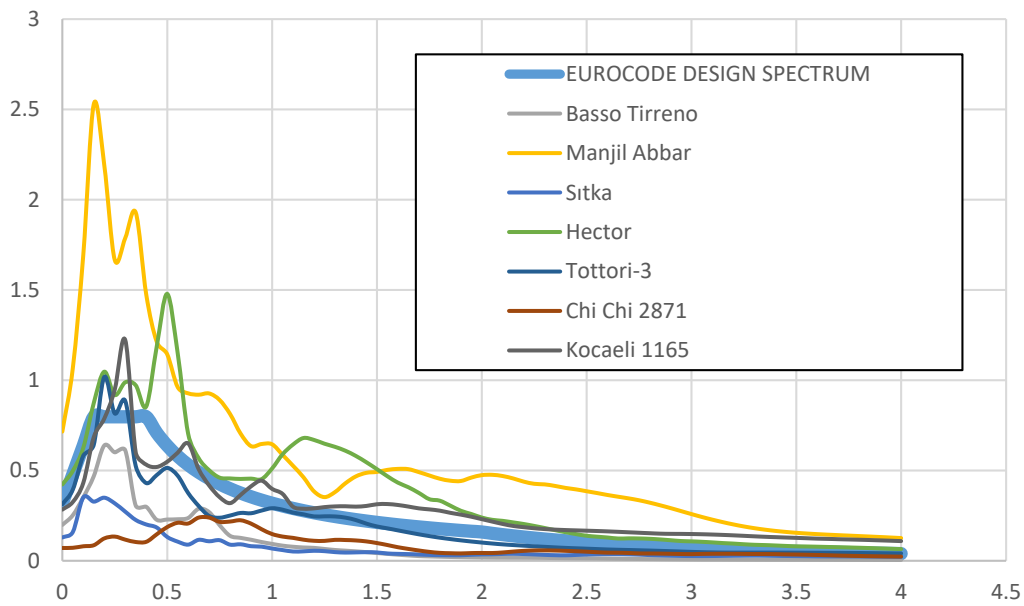


Figure B.4711. EN-8 design spectrum and response spectrum of unscaled time histories for ground motion SET-1 and scaling method M1 of V14 Bridge

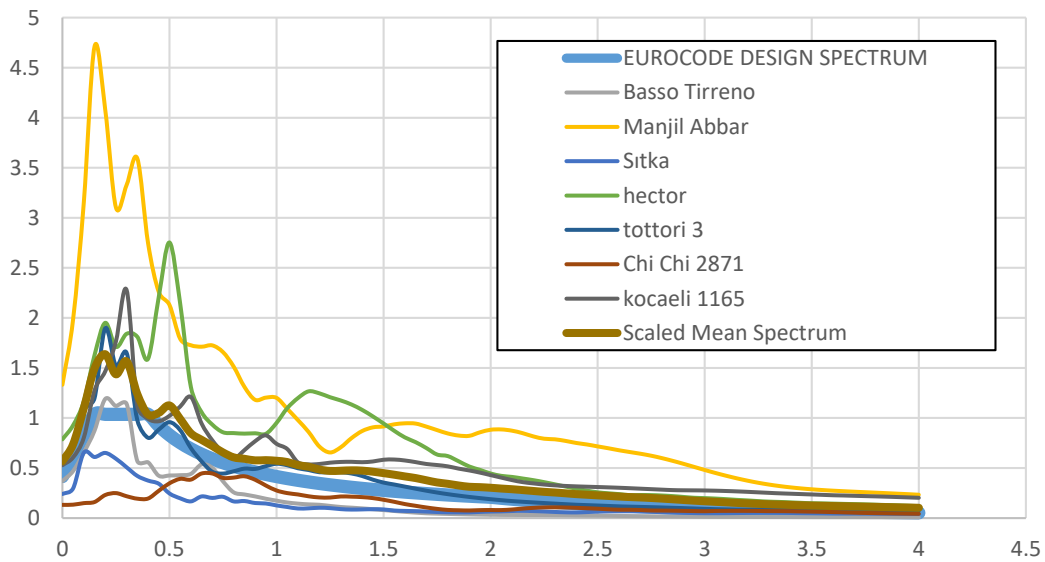


Figure B.4812. EN-8 design spectrum and response spectrum of scaled time histories for ground motion SET-1 and scaling method M1 of V14 Bridge

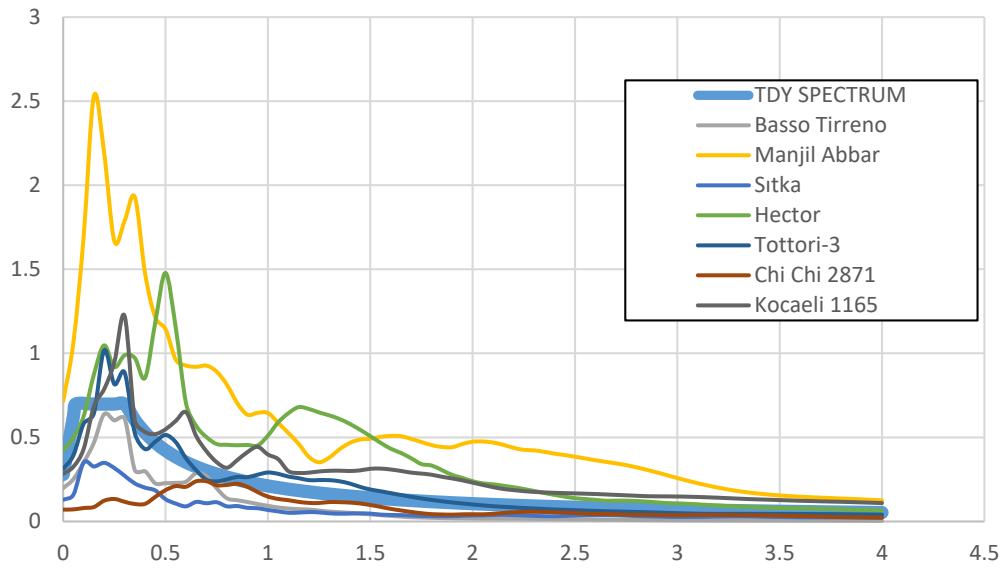


Figure B.4913. TDY 2020 design spectrum and response spectrum of unscaled time histories for ground motion SET-1 and scaling method M1 of V14 Bridge

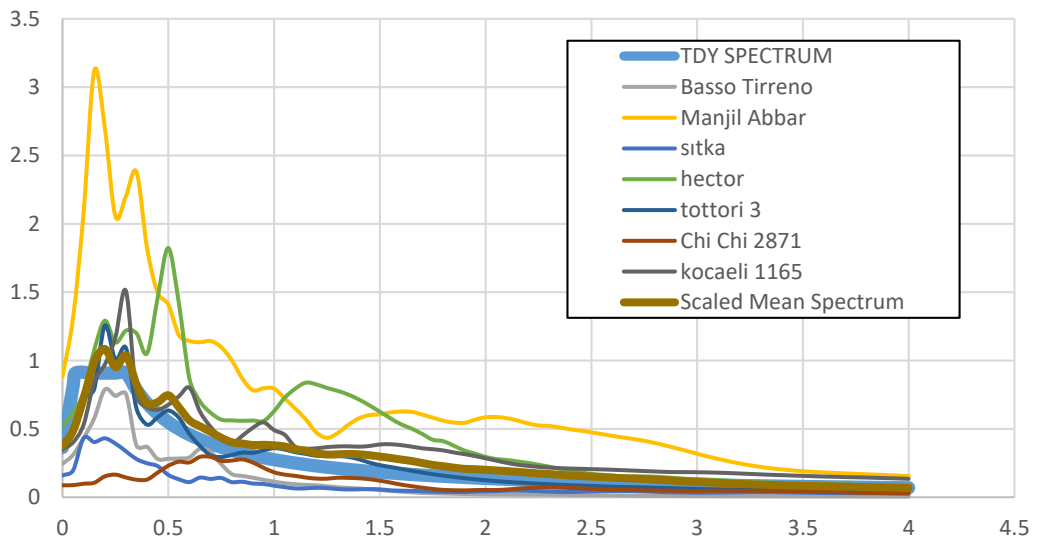


Figure B.5014. TDY 2020 design spectrum and response spectrum of scaled time histories for ground motion SET-1 and scaling method M1 of V14 Bridge

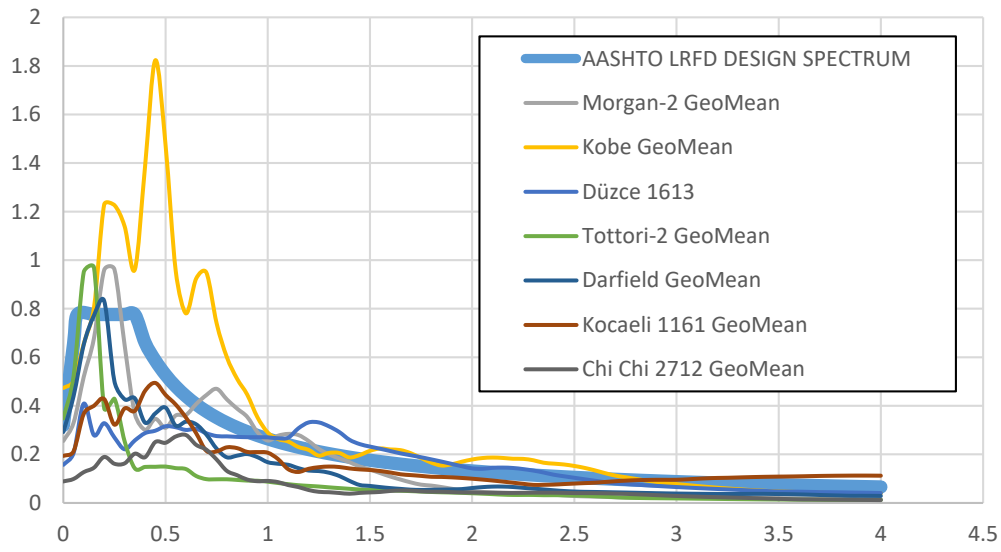


Figure B.5115. AASHTO LRFD design spectrum and response spectrum of unscaled time histories for ground motion SET-2 and scaling method M1 of V14 Bridge

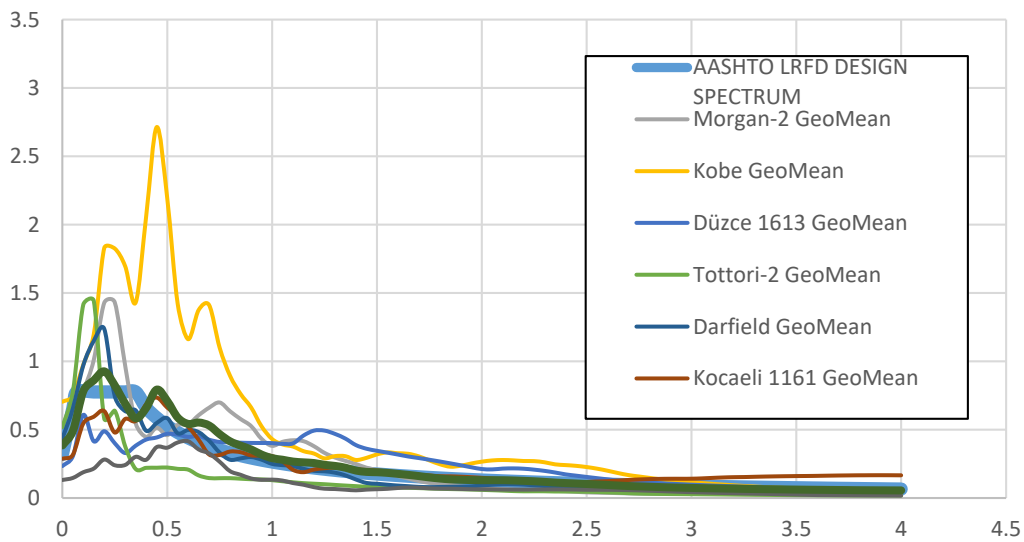


Figure B.5216. AASHTO LRFD design spectrum and response spectrum of scaled time histories for ground motion SET-2 and scaling method M1 of V14 Bridge

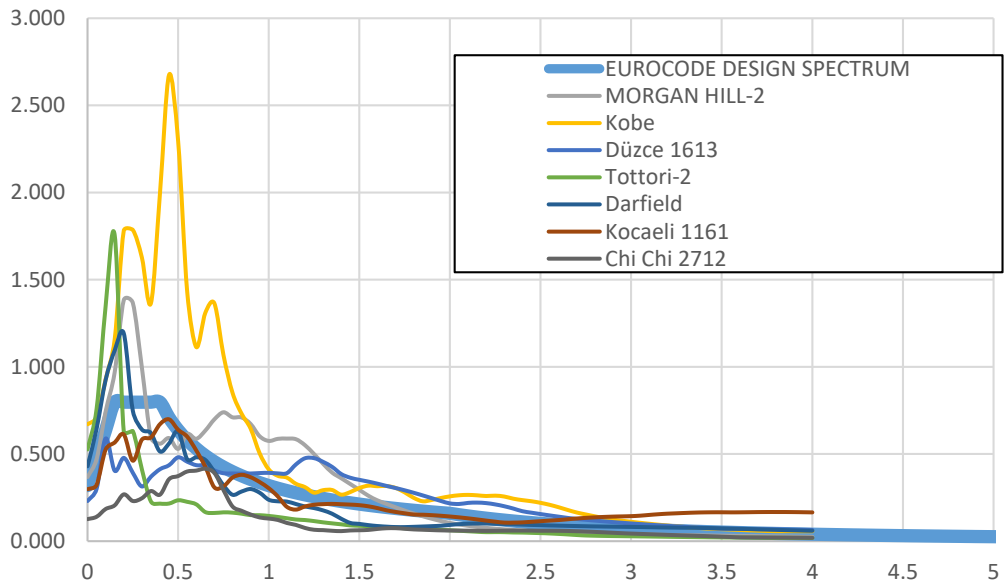


Figure B.117. EN-8 design spectrum and response spectrum of unscaled time histories for ground motion SET-2 and scaling method M1 of V14 Bridge

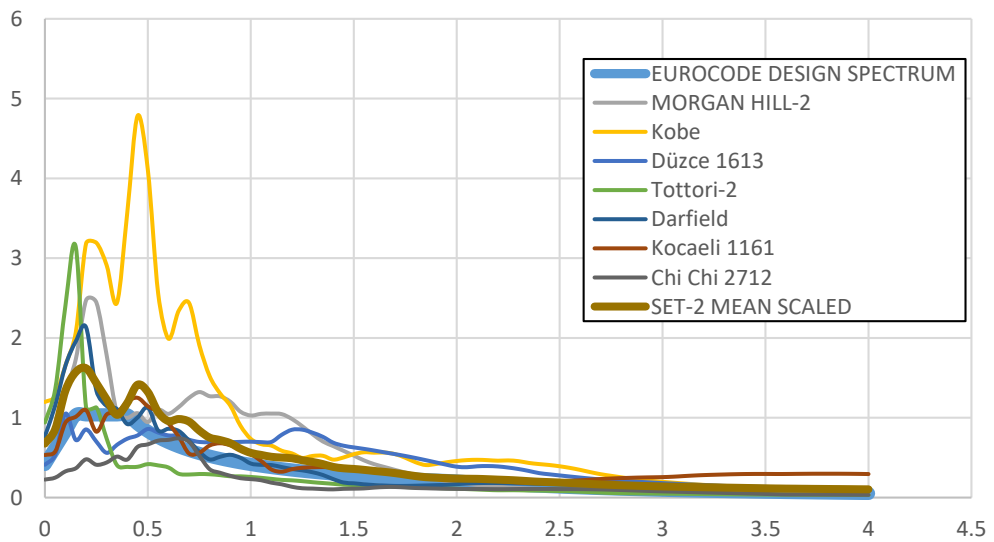


Figure B.118. EN-8 design spectrum and response spectrum of scaled time histories for ground motion SET-2 and scaling method M1 of V14 Bridge

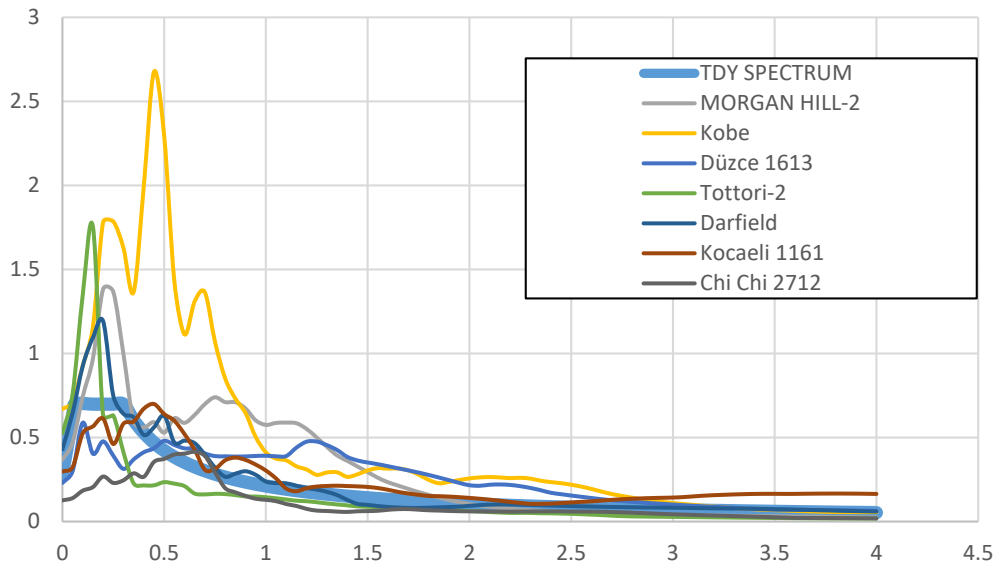


Figure B.5319. TDY 2020 design spectrum and response spectrum of unscaled time histories for ground motion SET-2 and scaling method M1 of V14 Bridge

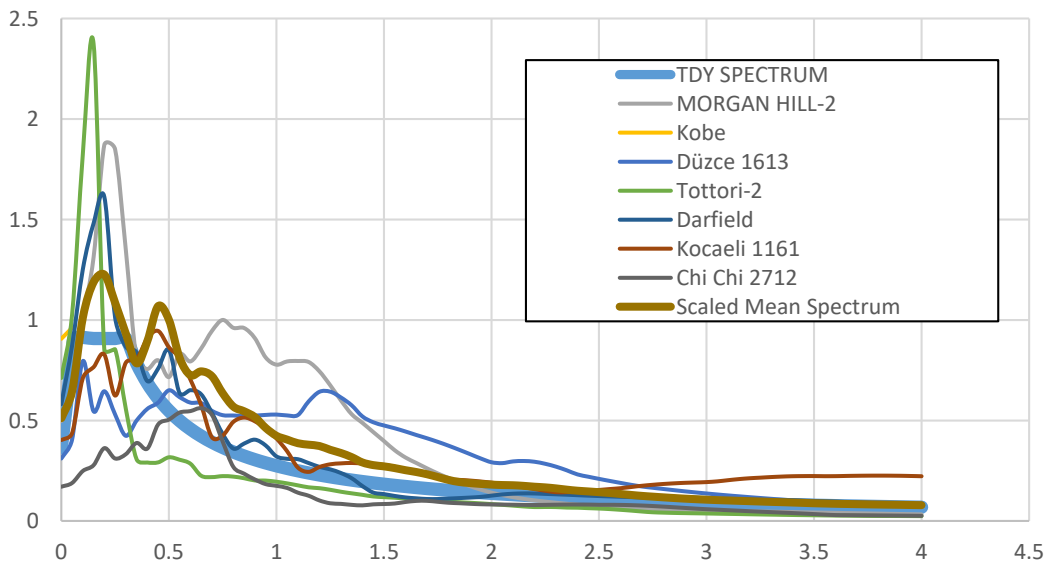


Figure B.5420. TDY 2020 design spectrum and response spectrum of scaled time histories for ground motion SET-2 and scaling method M1 of V14 Bridge

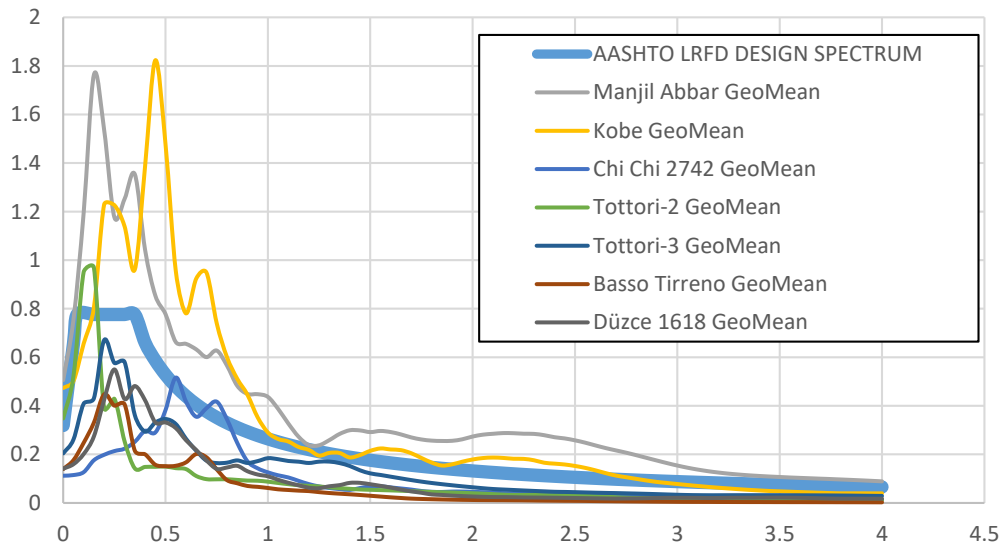


Figure B.5521. AASHTO LRFD design spectrum and response spectrum of unscaled time histories for ground motion SET-3 and scaling method M1 of V14 Bridge

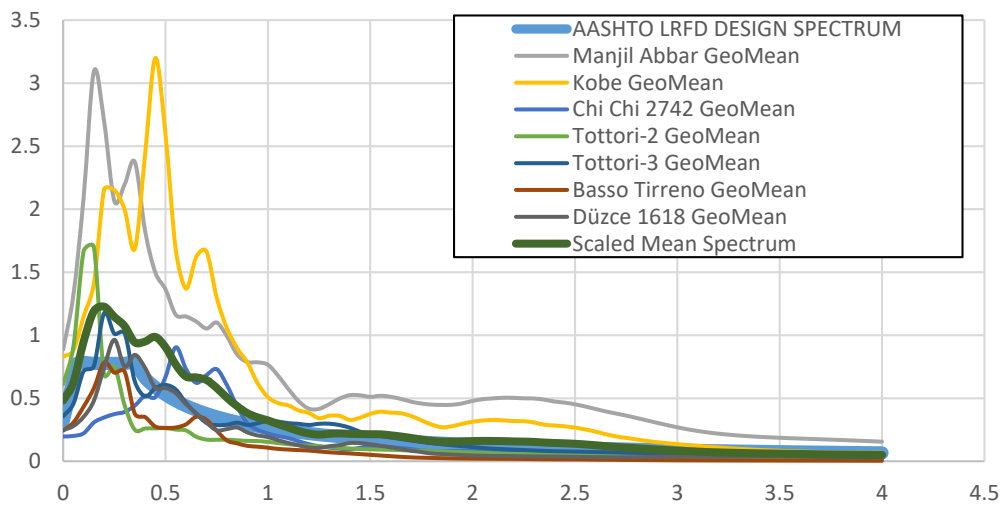


Figure B.5622. AASHTO LRFD design spectrum and response spectrum of scaled time histories for ground motion SET-3 and scaling method M1 of V14 Bridge

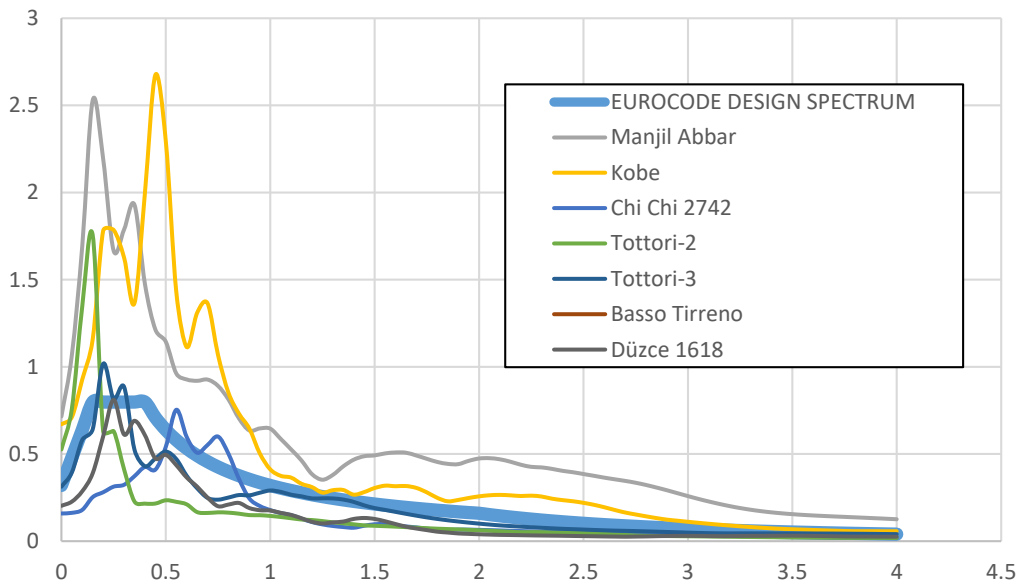


Figure B.5723. EN-8 design spectrum and response spectrum of unscaled time histories for ground motion SET-3 and scaling method M1 of V14 Bridge

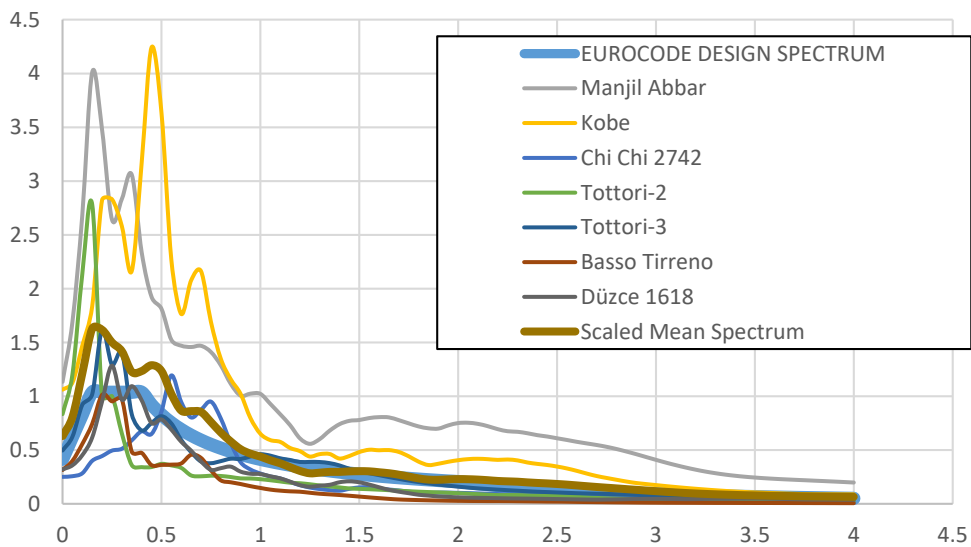


Figure B.5824. EN-8 design spectrum and response spectrum of scaled time histories for ground motion SET-3 and scaling method M1 of V14 Bridge

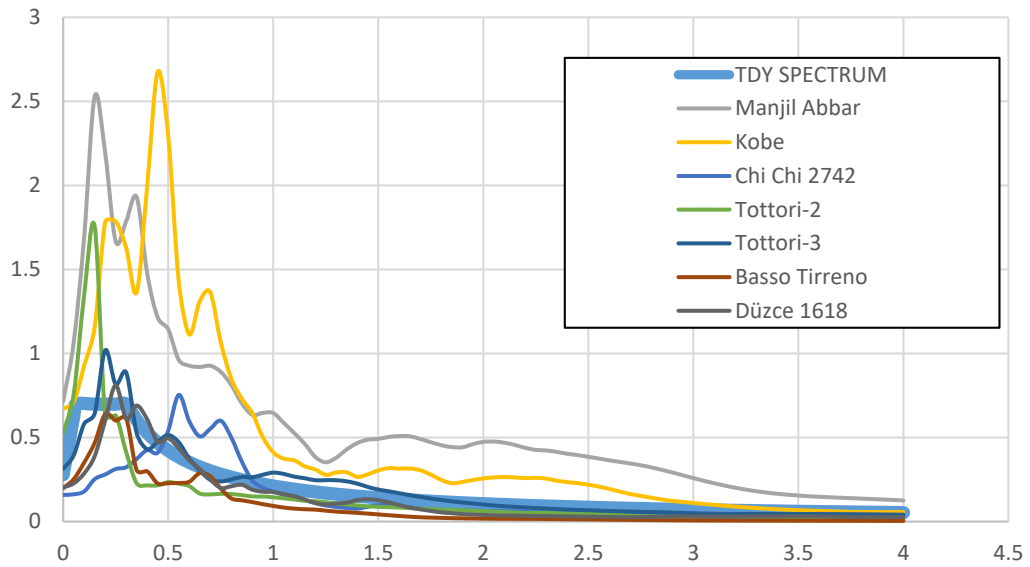


Figure B.5925. TDY 2020 design spectrum and response spectrum of unscaled time histories for ground motion SET-3 and scaling method M1 of V14 Bridge

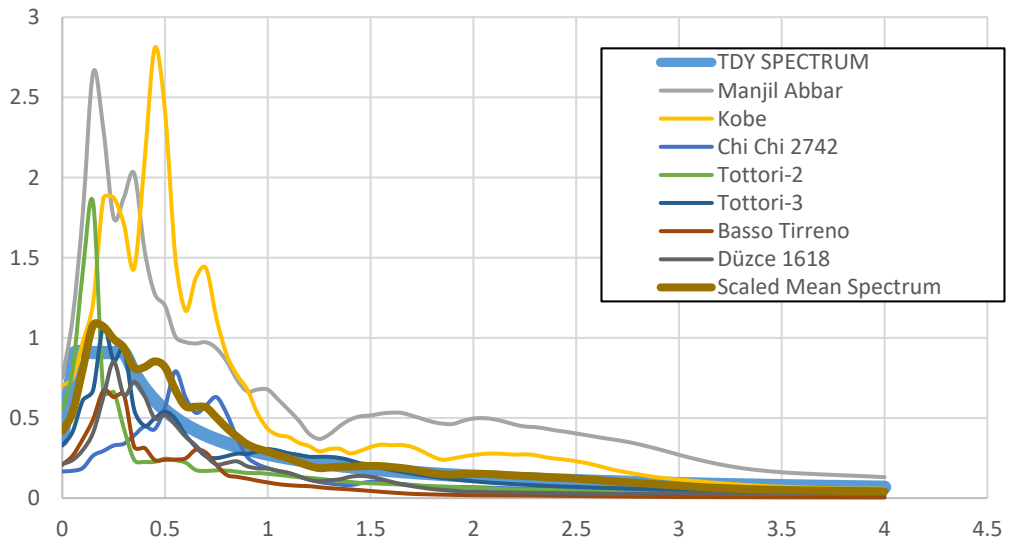


Figure B.6026. TDY 2020 design spectrum and response spectrum of scaled time histories for ground motion SET-3 and scaling method M1 of V14 Bridge

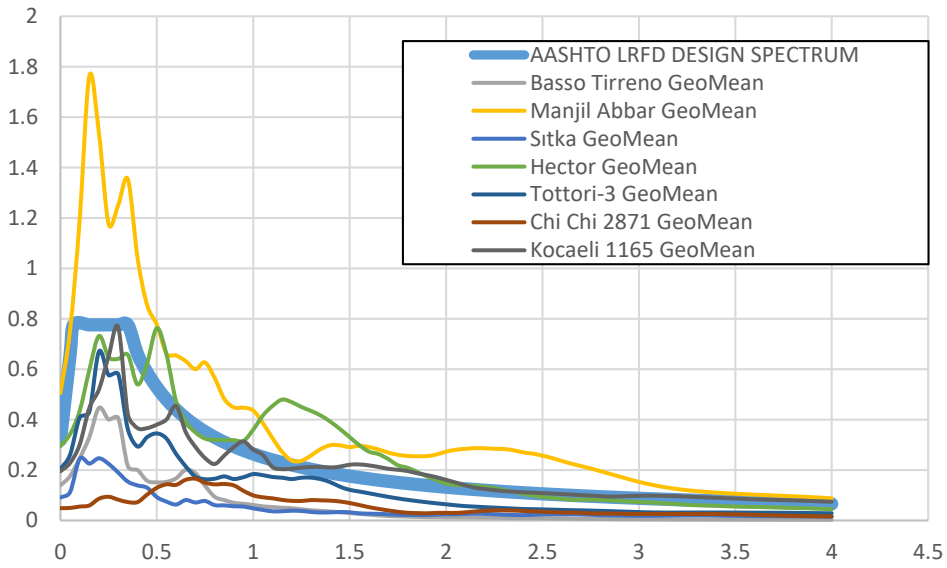


Figure B.6127. AASHTO LRFD design spectrum and response spectrum of unscaled time histories for ground motion SET-1 and scaling method M2 of V14 Bridge

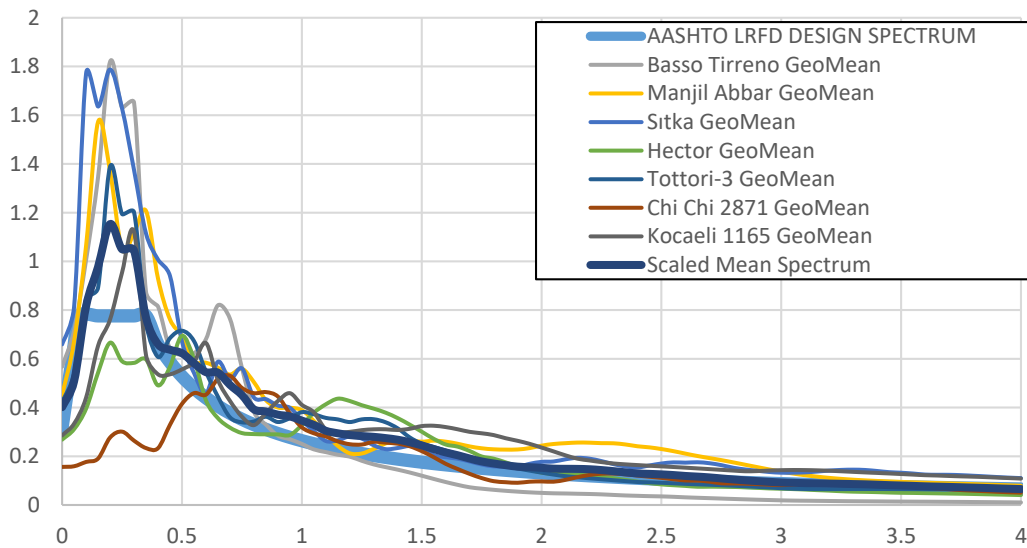


Figure B.6228. AASHTO LRFD design spectrum and response spectrum of scaled time histories for ground motion SET-1 and scaling method M2 of V14 Bridge

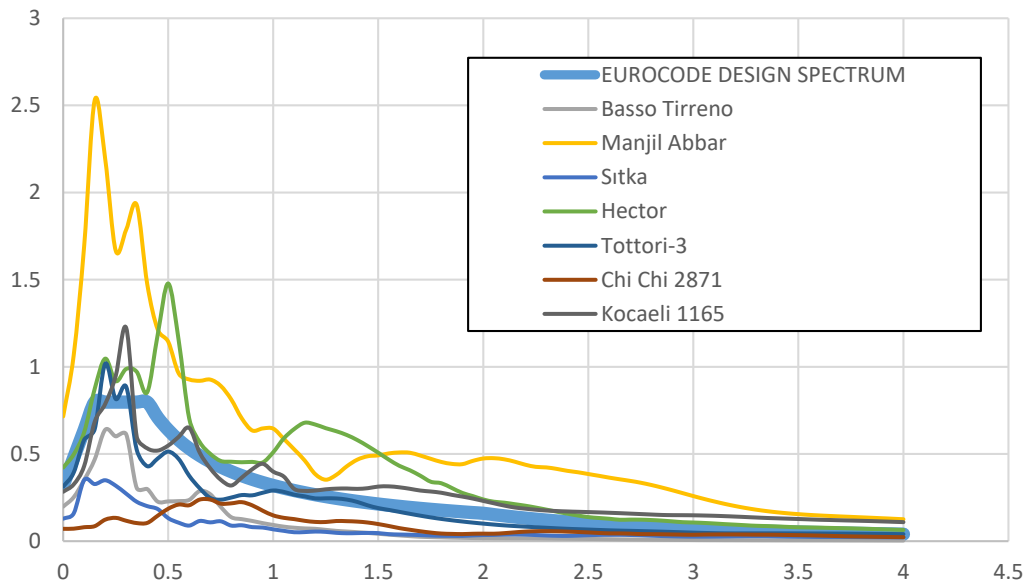


Figure B.129. EN-8 design spectrum and response spectrum of unscaled time histories for ground motion SET-1 and scaling method M2 of V14 Bridge

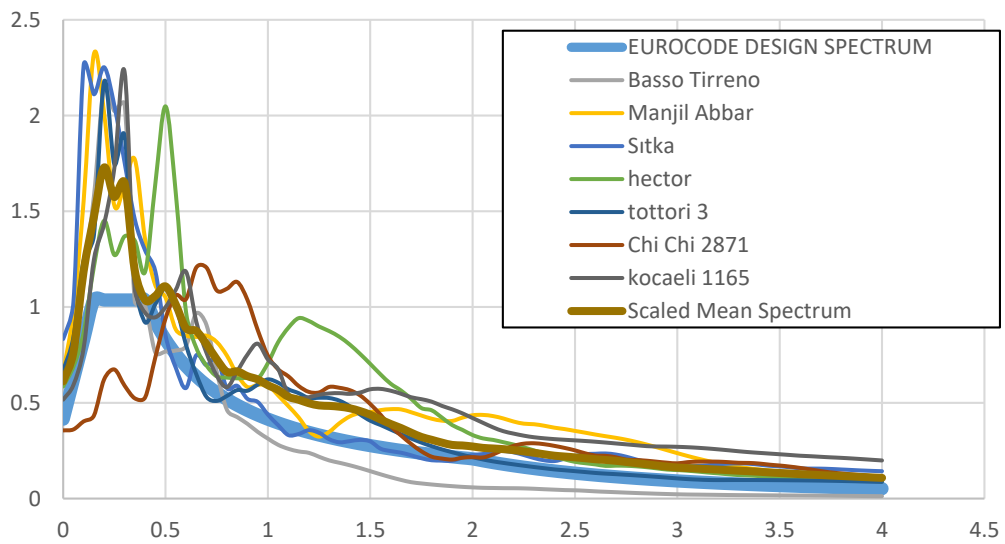


Figure B.130. EN-8 design spectrum and response spectrum of scaled time histories for ground motion SET-1 and scaling method M2 of V14 Bridge

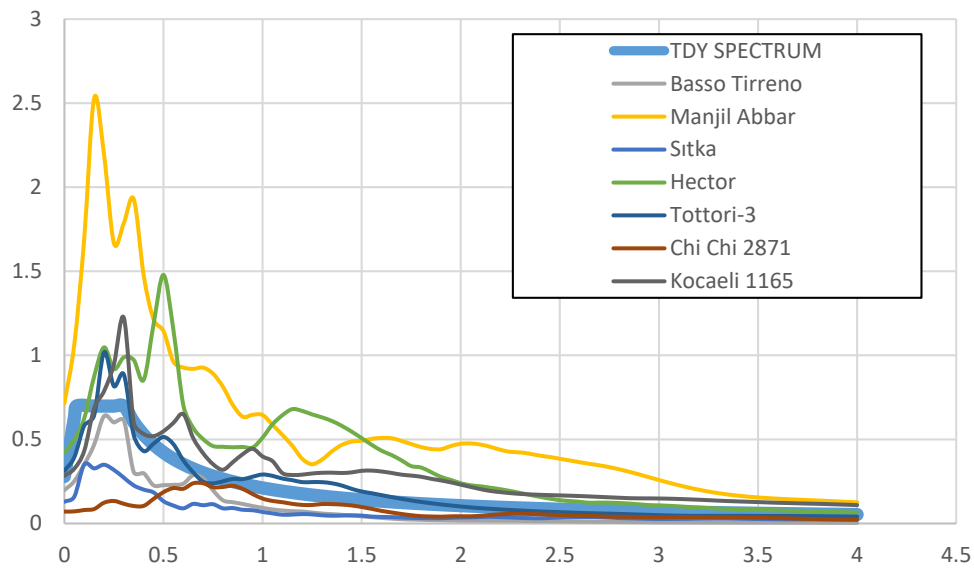


Figure B.131. TDY 2020 design spectrum and response spectrum of unscaled time histories for ground motion SET-1 and scaling method M2 of V14 Bridge

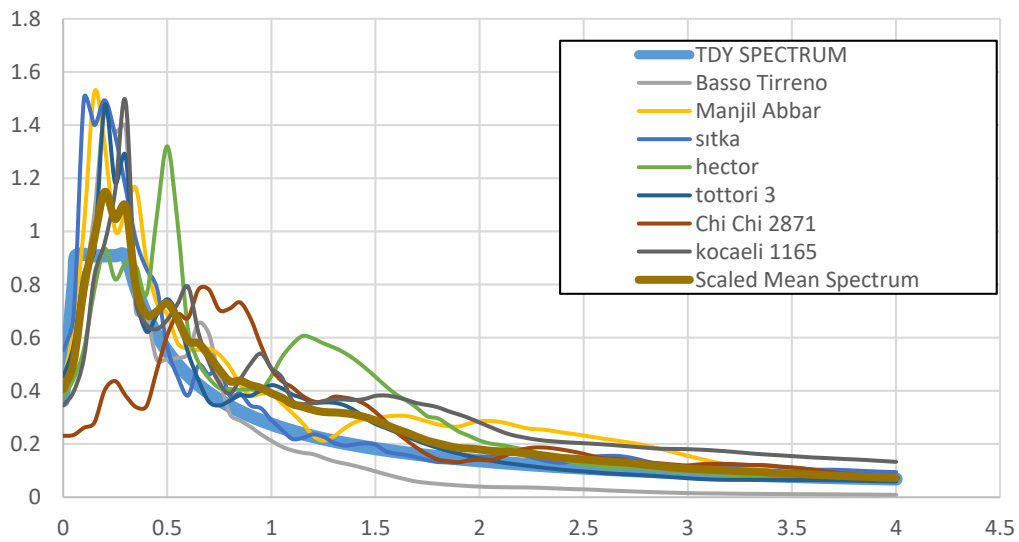


Figure B.6332. TDY 2020 design spectrum and response spectrum of scaled time histories for ground motion SET-1 and scaling method M2 of V14 Bridge

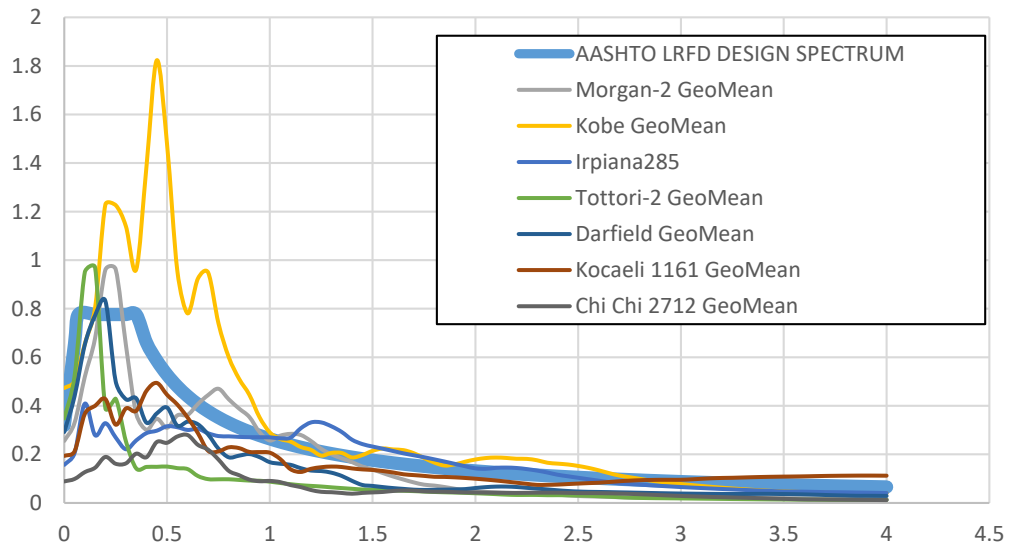


Figure B.6433. AASHTO LRFD design spectrum and response spectrum of unscaled time histories for ground motion SET-2 and scaling method M2 of V14 Bridge

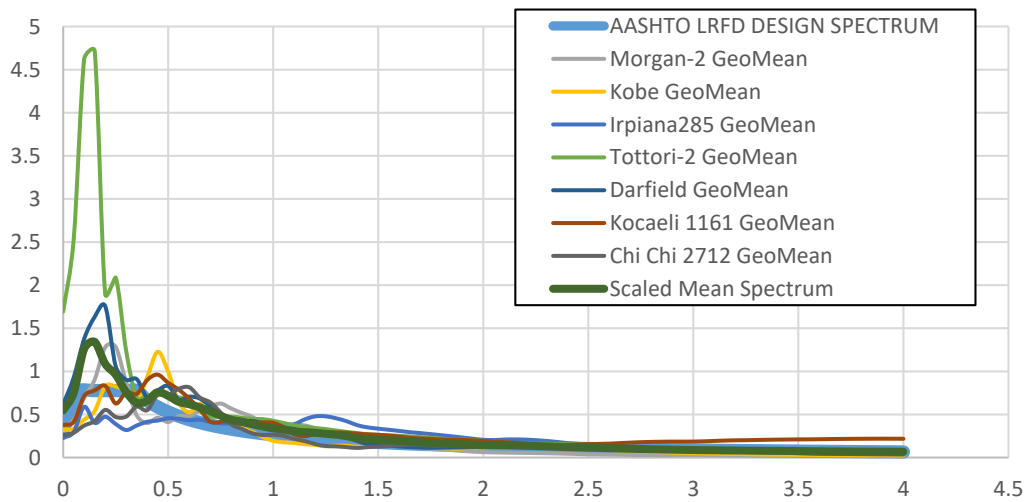


Figure B.6534. AASHTO LRFD design spectrum and response spectrum of scaled time histories for ground motion SET-2 and scaling method M2 of V14 Bridge

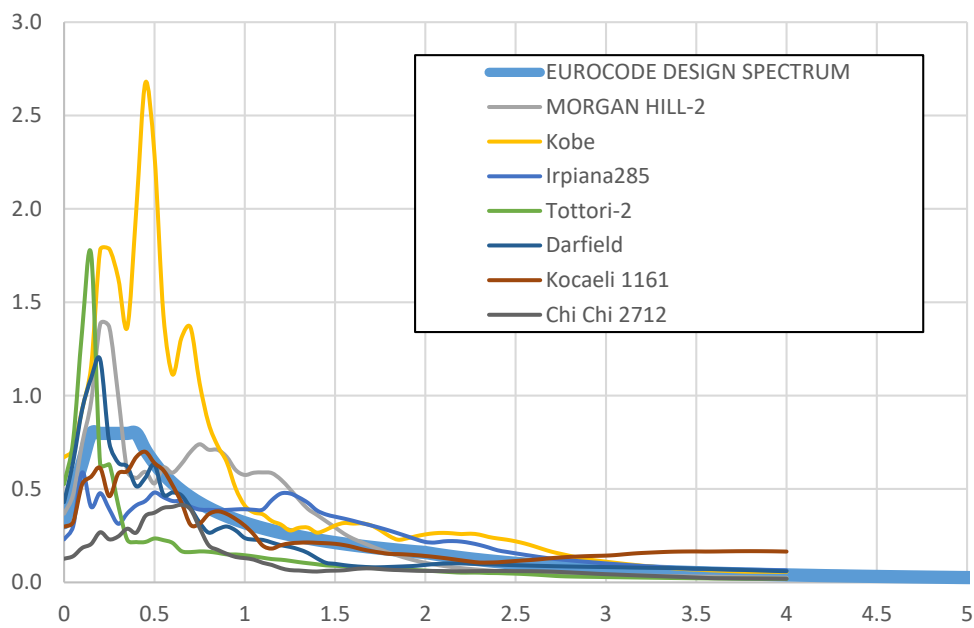


Figure B.6635. EN-8 design spectrum and response spectrum of unscaled time histories for ground motion SET-2 and scaling method M2 of V14 Bridge

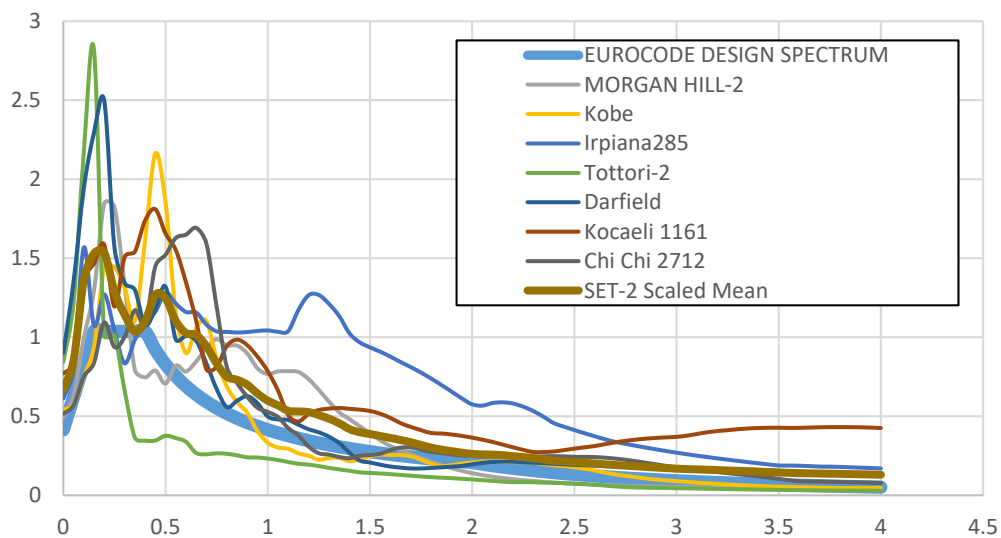


Figure B.6736. EN-8 design spectrum and response spectrum of scaled time histories for ground motion SET-2 and scaling method M2 of V14 Bridge

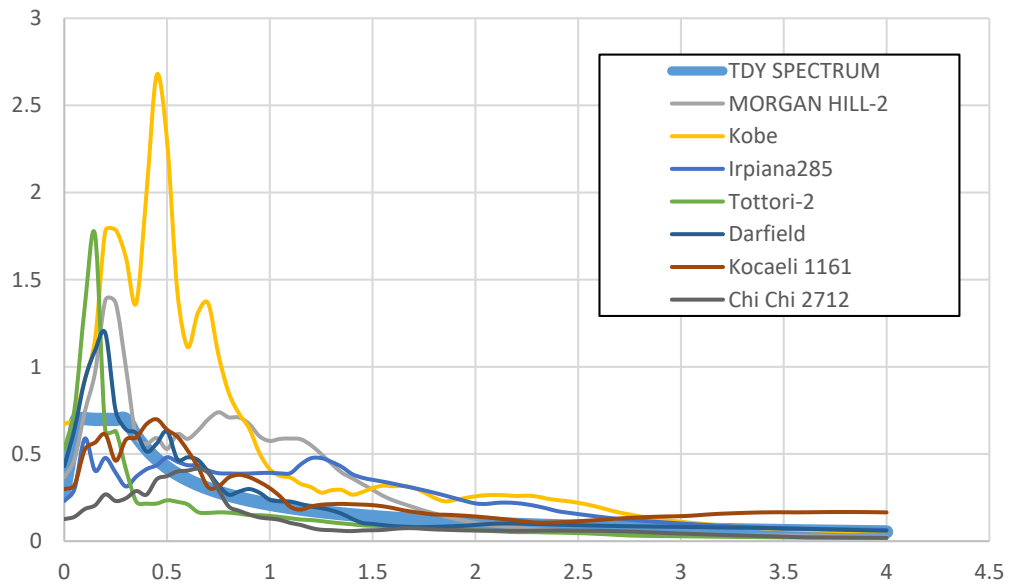


Figure B.6837. TDY 2020 design spectrum and response spectrum of unscaled time histories for ground motion SET-2 and scaling method M2 of V14 Bridge

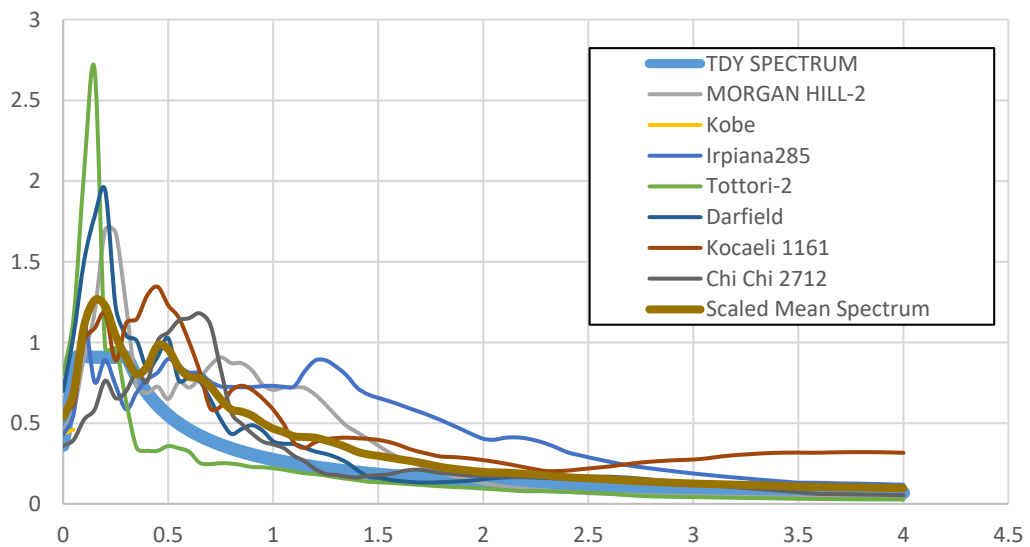


Figure B.6938. TDY 2020 design spectrum and response spectrum of scaled time histories for ground motion SET-2 and scaling method M2 of V14 Bridge

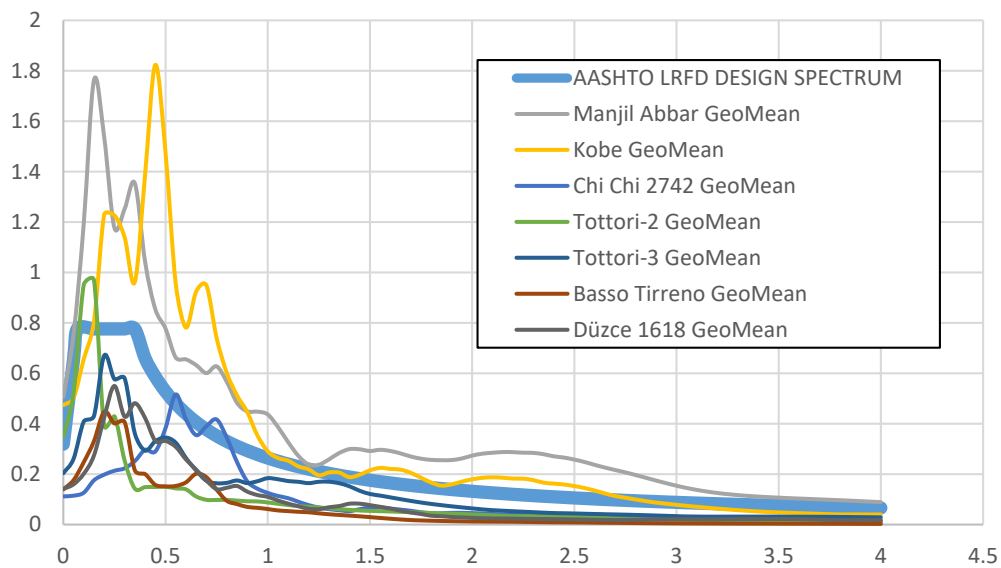


Figure B.7039. AASHTO LRFD design spectrum and response spectrum of unscaled time histories for ground motion SET-3 and scaling method M2 of V14 Bridge

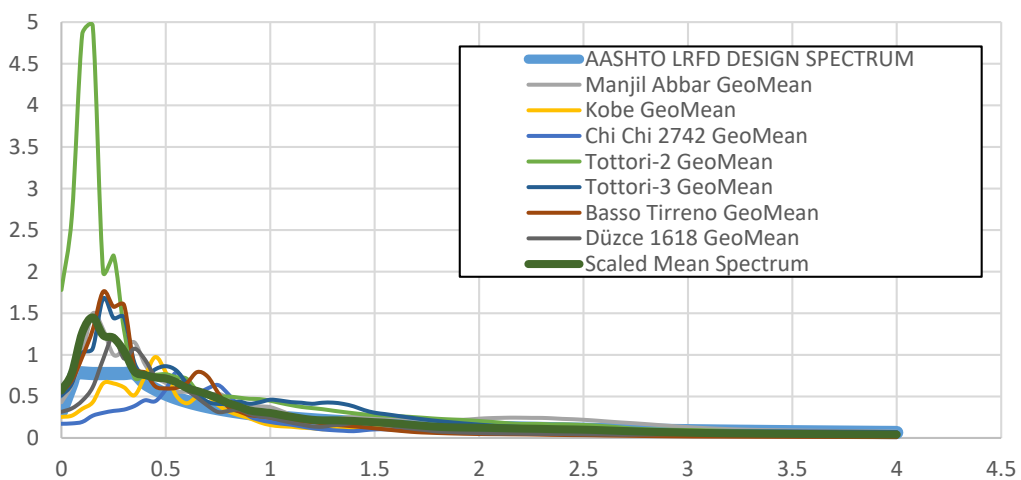


Figure B.7140. AASHTO LRFD design spectrum and response spectrum of scaled time histories for ground motion SET-3 and scaling method M2 of V14 Bridge

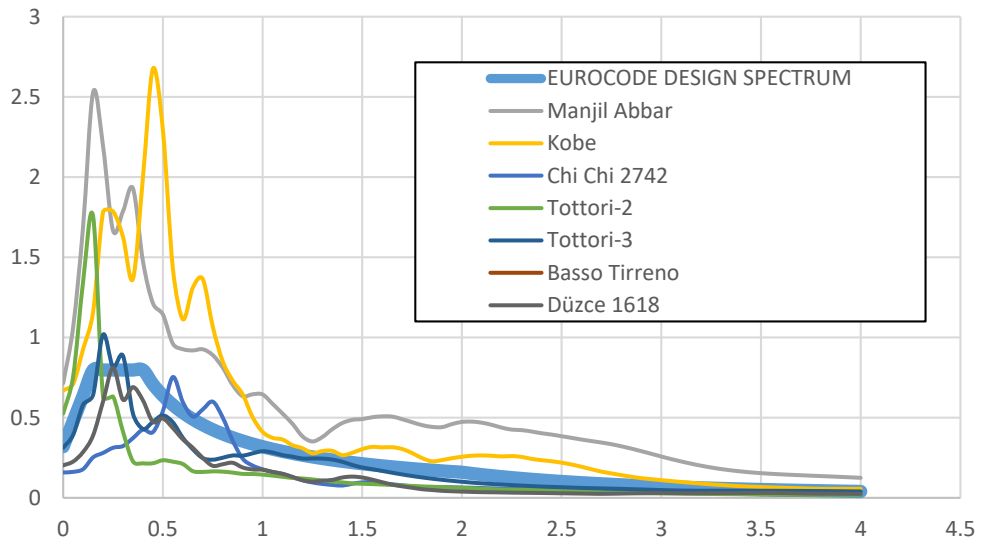


Figure B.7241. EN-8 design spectrum and response spectrum of unscaled time histories for ground motion SET-3 and scaling method M2 of V14 Bridge

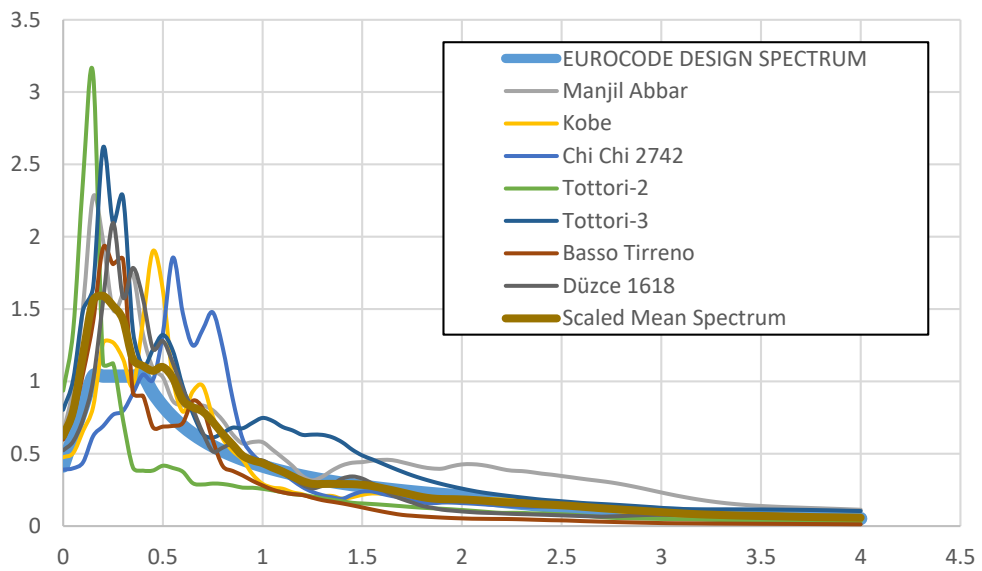


Figure B.142. EN-8 design spectrum and response spectrum of scaled time histories for ground motion SET-3 and scaling method M2 of V14 Bridge

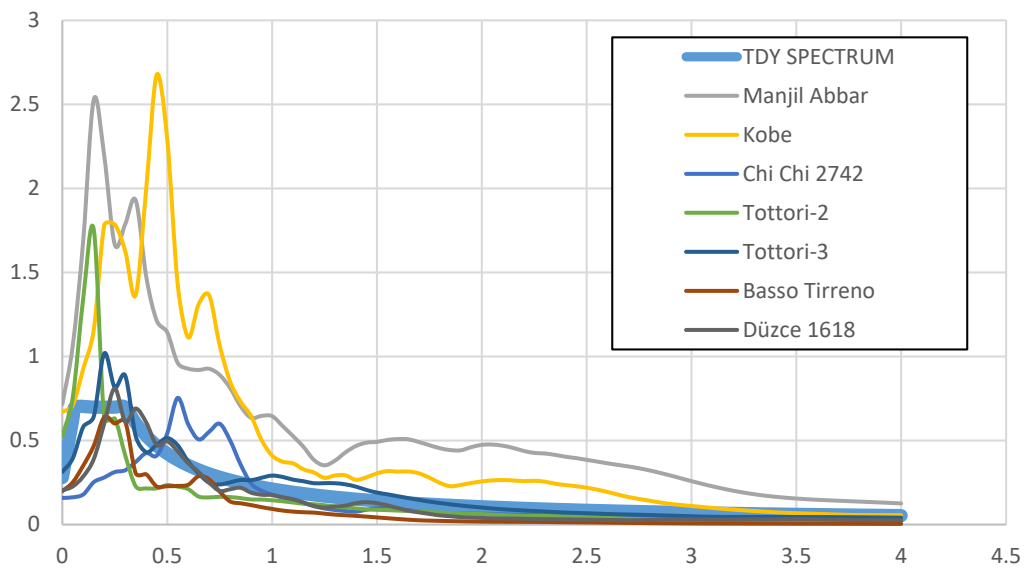


Figure B.7343. TDY 2020 design spectrum and response spectrum of unscaled time histories for ground motion SET-3 and scaling method M2 of V14 Bridge

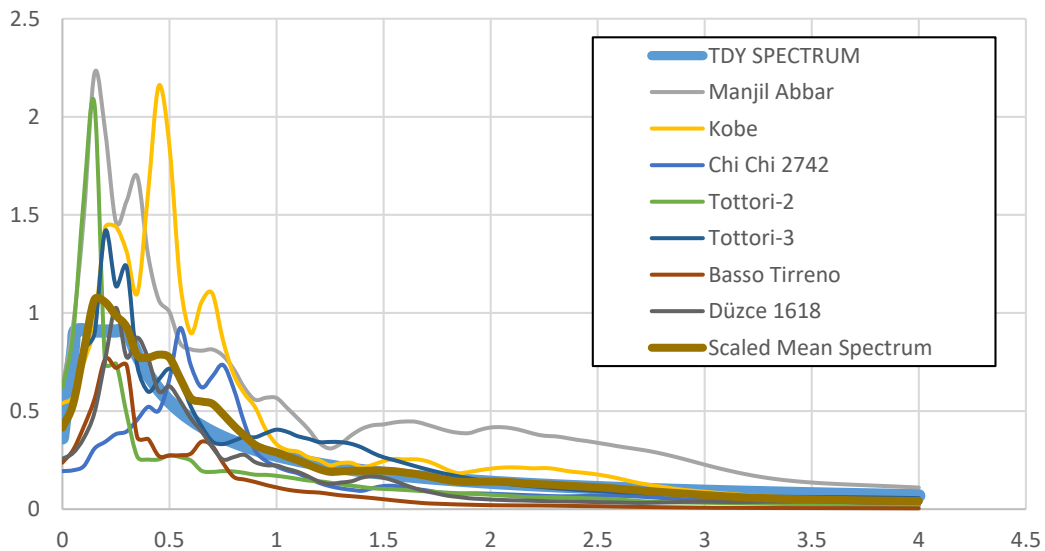


Figure B.7444. TDY 2020 design spectrum and response spectrum of scaled time histories for ground motion SET-3 and scaling method M2 of V14 Bridge

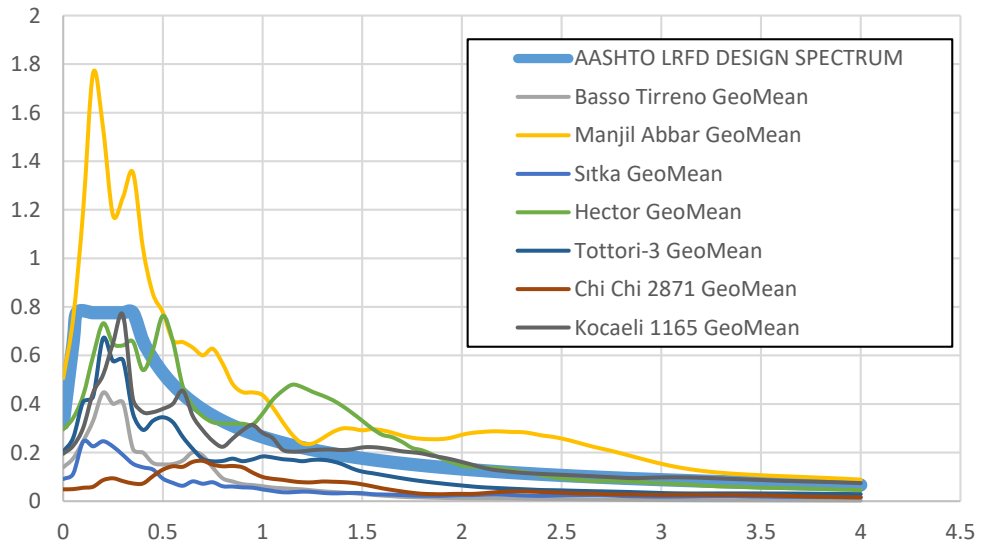


Figure B.7545. AASHTO LRFD design spectrum and response spectrum of unscaled time histories for ground motion SET-1 and scaling method M3 of V14 Bridge

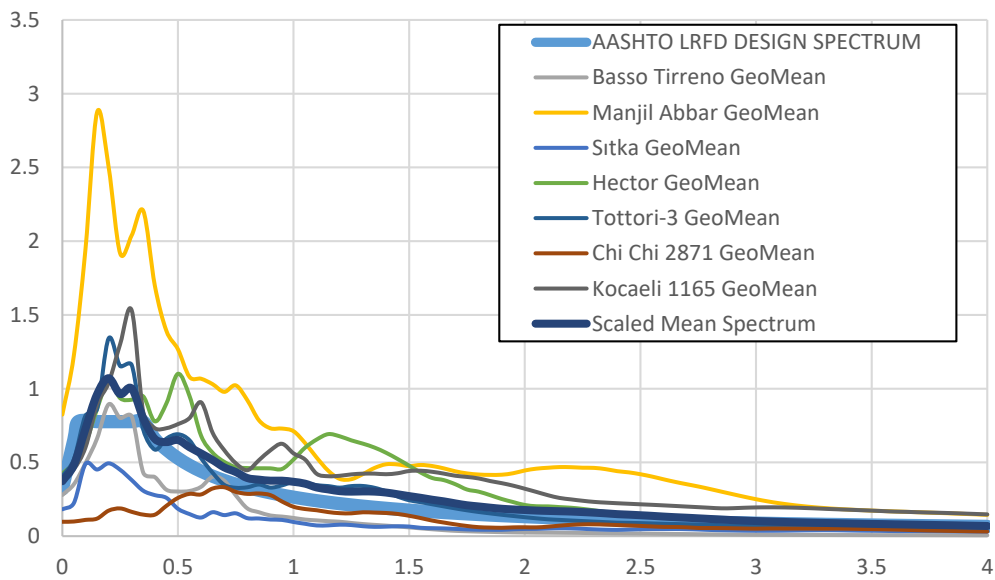


Figure B.7646. AASHTO LRFD design spectrum and response spectrum of scaled time histories for ground motion SET-1 and scaling method M3 of V14 Bridge

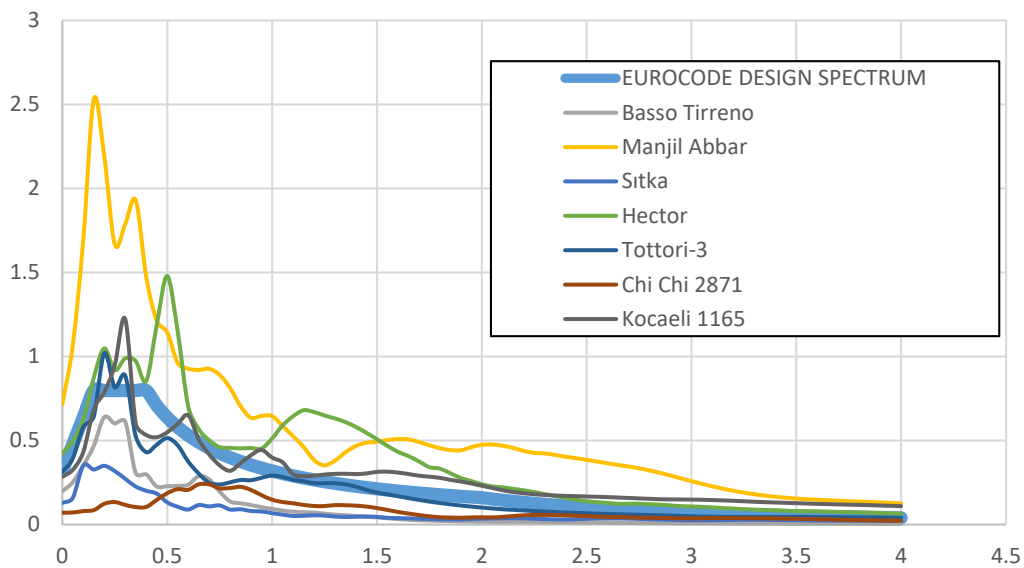


Figure B.7747. EN-8 design spectrum and response spectrum of unscaled time histories for ground motion SET-1 and scaling method M3 of V14 Bridge

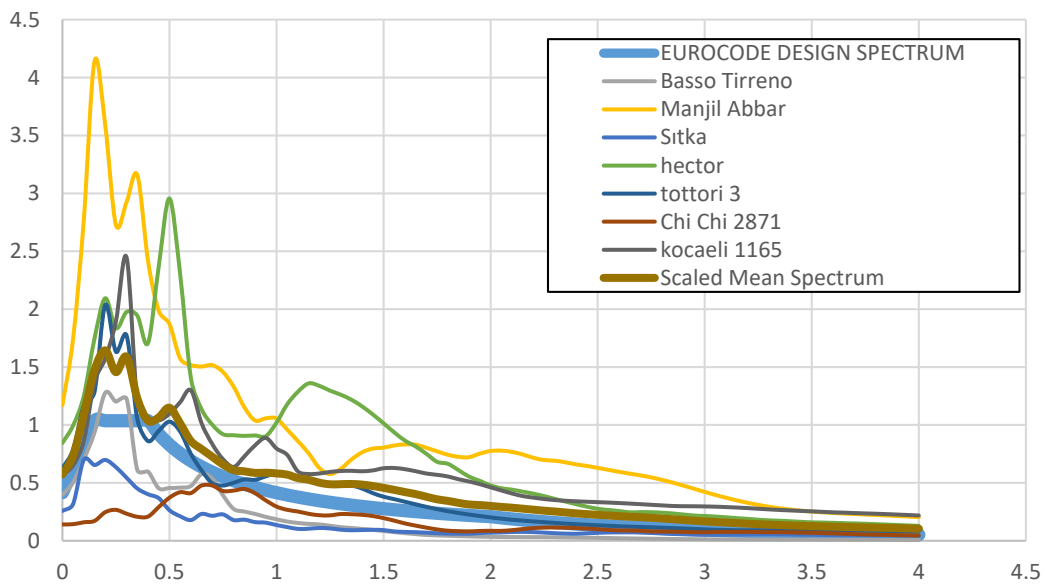


Figure B.7848. EN-8 design spectrum and response spectrum of scaled time histories for ground motion SET-1 and scaling method M3 of V14 Bridge

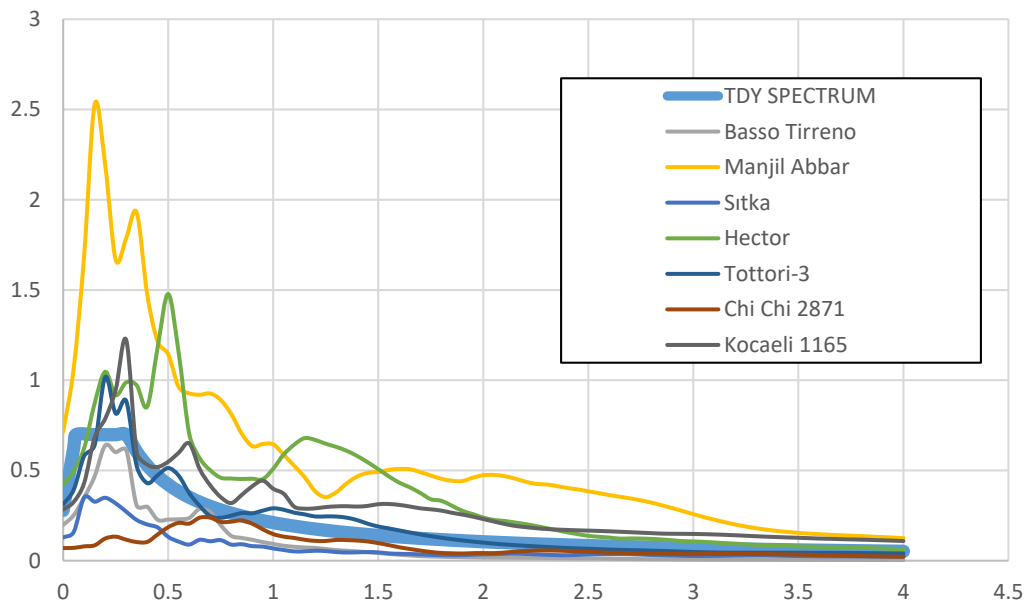


Figure B.7949. TDY 2020 design spectrum and response spectrum of unscaled time histories for ground motion SET-1 and scaling method M3 of V14 Bridge

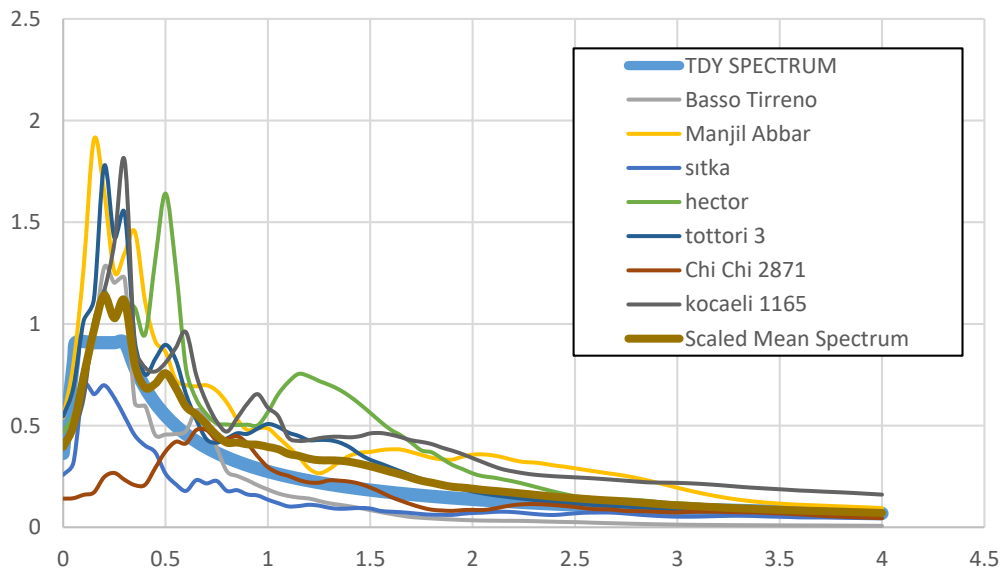


Figure B.8050. TDY 2020 design spectrum and response spectrum of scaled time histories for ground motion SET-1 and scaling method M3 of V14 Bridge

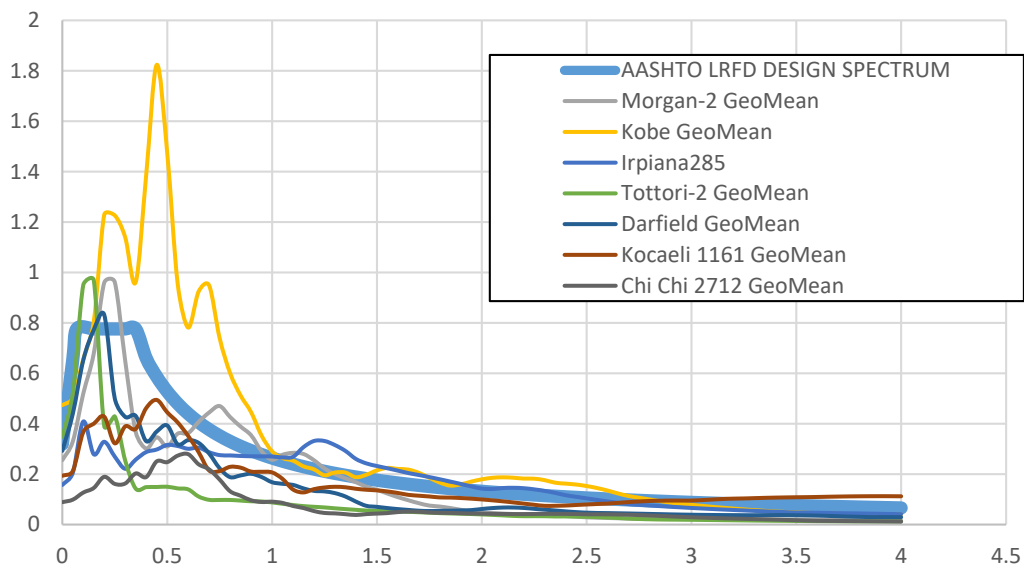


Figure B.8151. AASHTO LRFD design spectrum and response spectrum of unscaled time histories for ground motion SET-2 and scaling method M3 of V14 Bridge

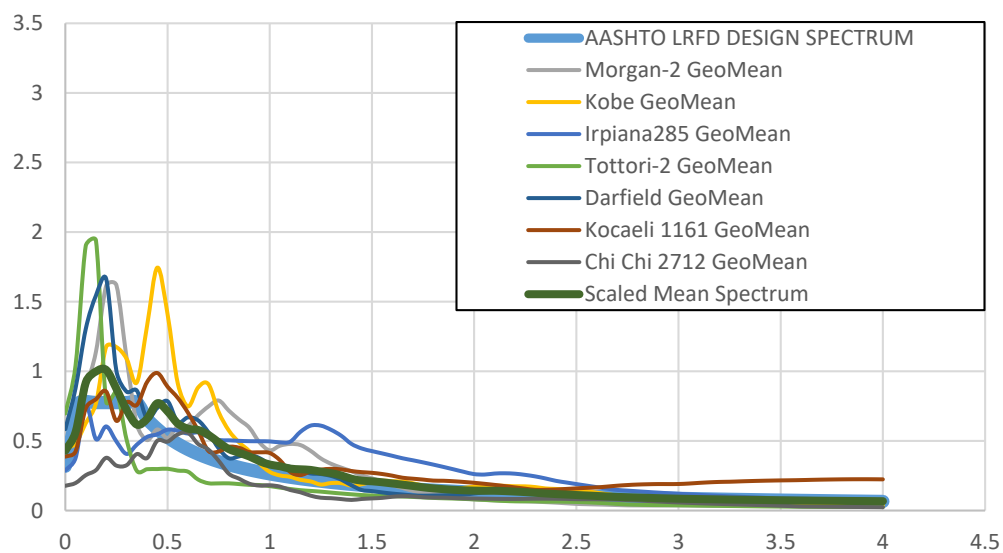


Figure B.8252. AASHTO LRFD design spectrum and response spectrum of scaled time histories for ground motion SET-2 and scaling method M3 of V14 Bridge

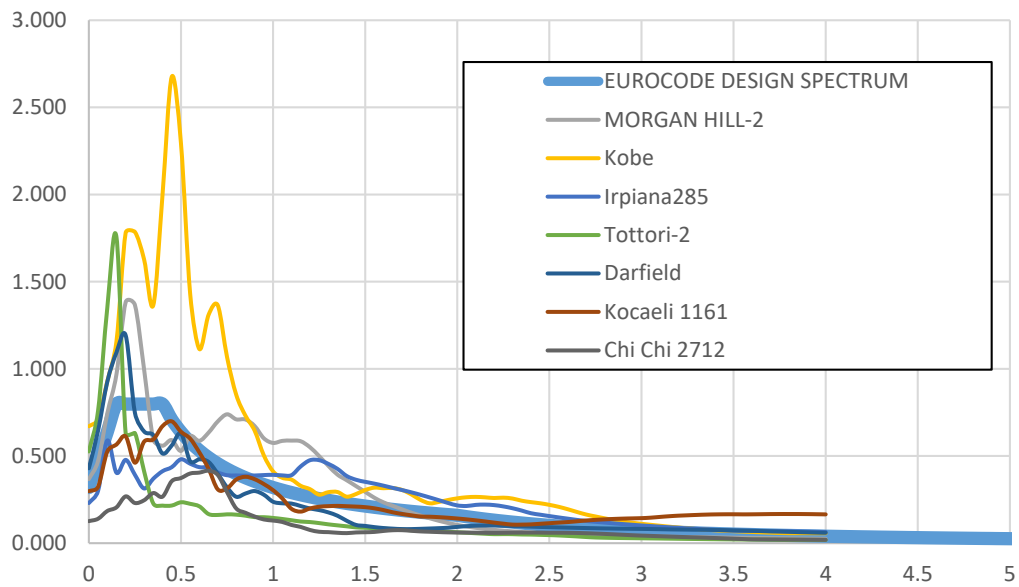


Figure B.8353. EN-8 design spectrum and response spectrum of unscaled time histories for ground motion SET-2 and scaling method M3 of V14 Bridge

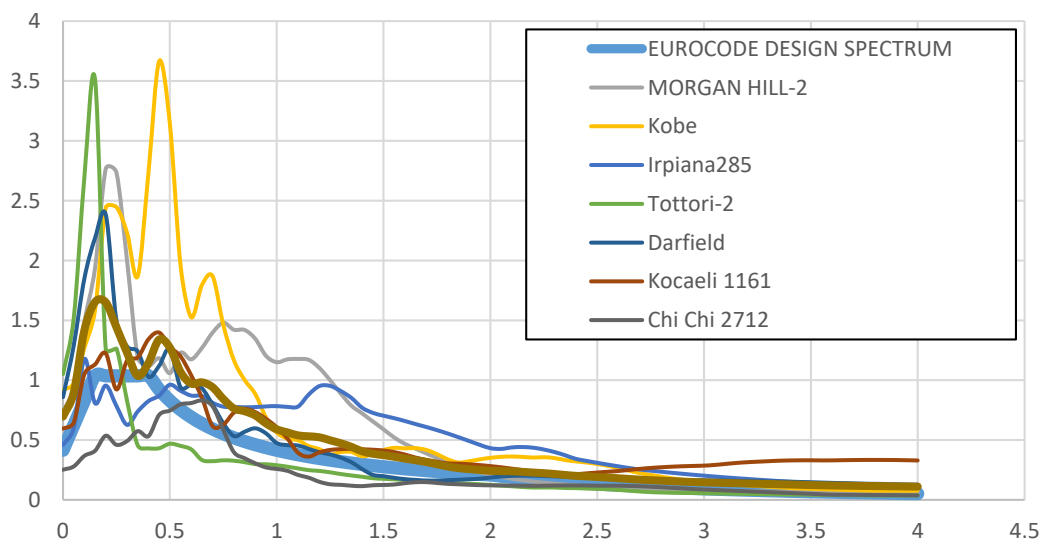


Figure B.8454. EN-8 design spectrum and response spectrum of scaled time histories for ground motion SET-2 and scaling method M3 of V14 Bridge

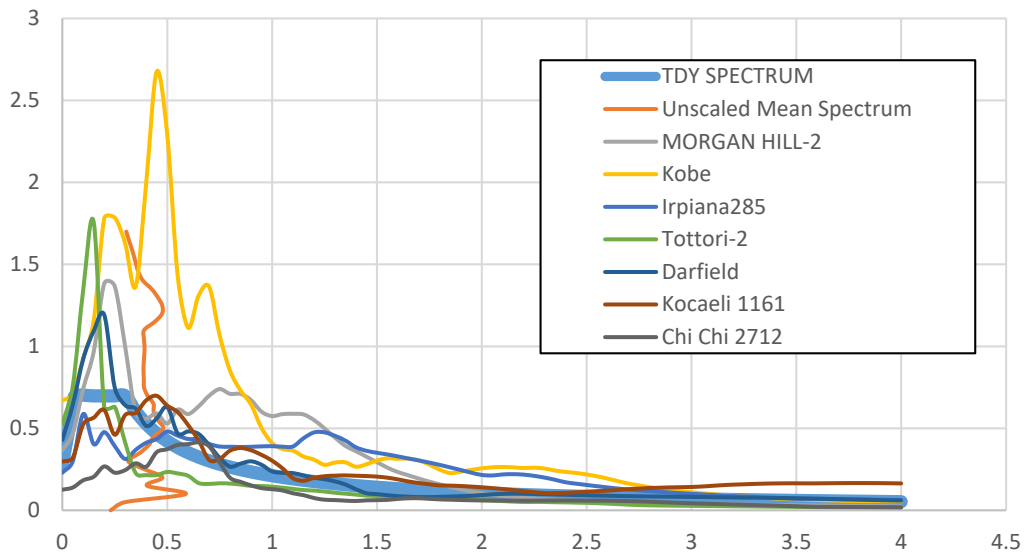


Figure B.8555. TDY 2020 design spectrum and response spectrum of unscaled time histories for ground motion SET-2 and scaling method M3 of V14 Bridge

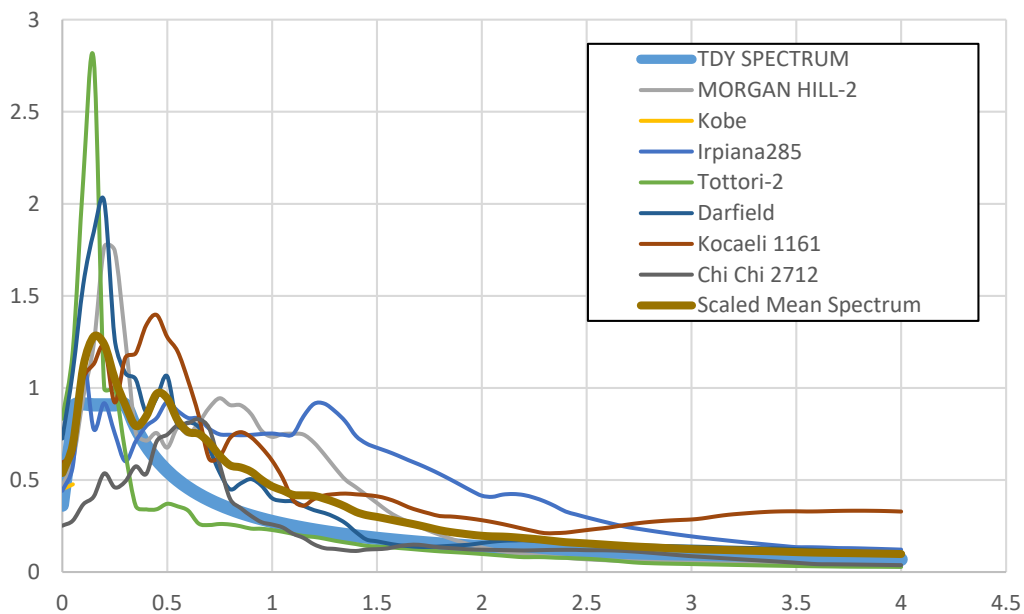


Figure B.8656. TDY 2020 design spectrum and response spectrum of scaled time histories for ground motion SET-2 and scaling method M3 of V14 Bridge

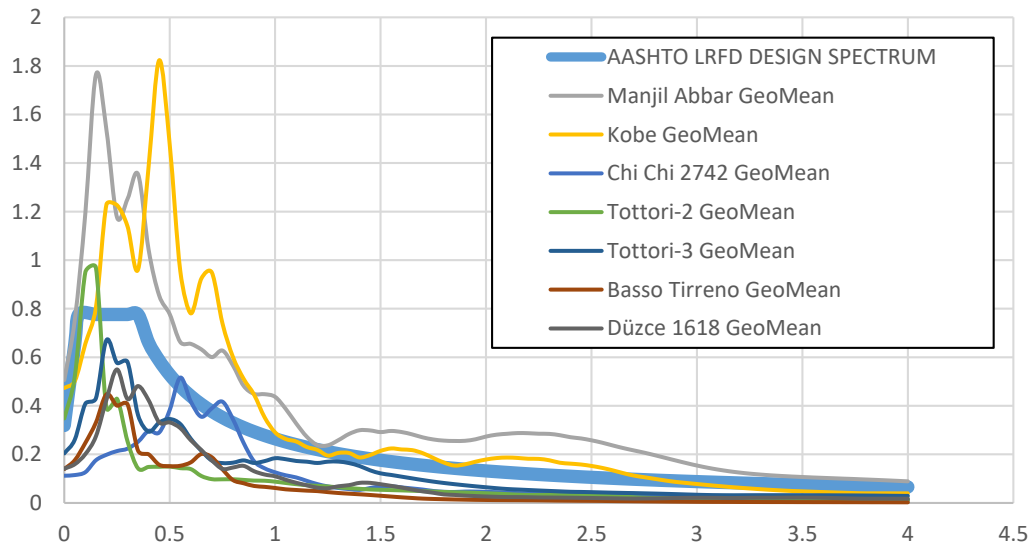


Figure B.8757. AASHTO LRFD design spectrum and response spectrum of unscaled time histories for ground motion SET-3 and scaling method M3 of V14 Bridge

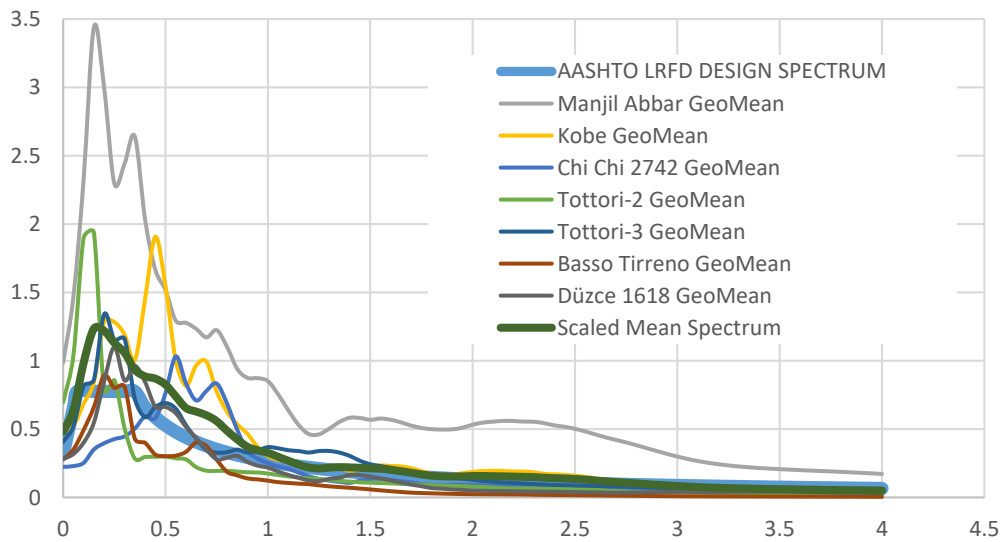


Figure B.158. AASHTO LRFD design spectrum and response spectrum of scaled time histories for ground motion SET-3 and scaling method M3 of V14 Bridge

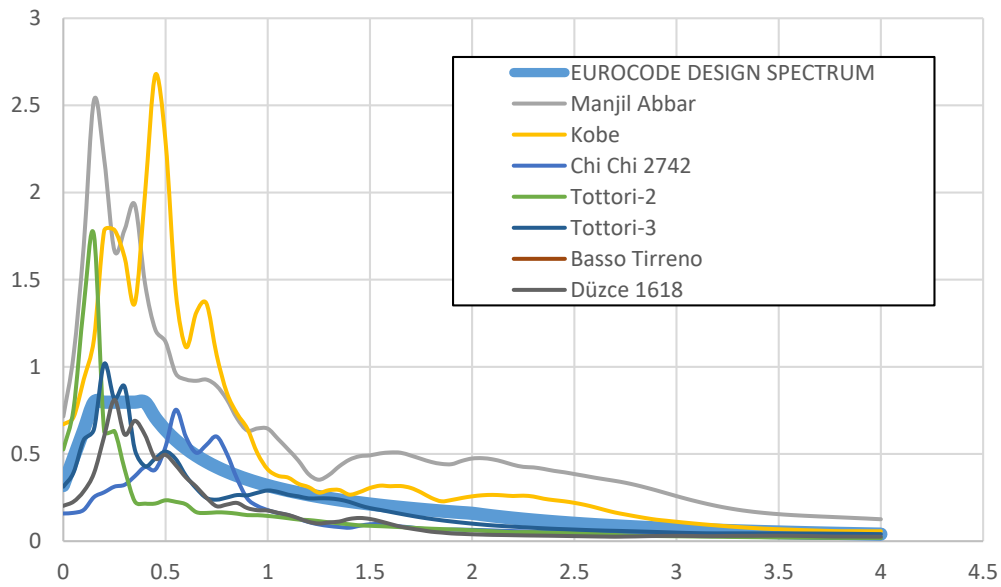


Figure B.159. EN-8 design spectrum and response spectrum of unscaled time histories for ground motion SET-3 and scaling method M3 of V14 Bridge

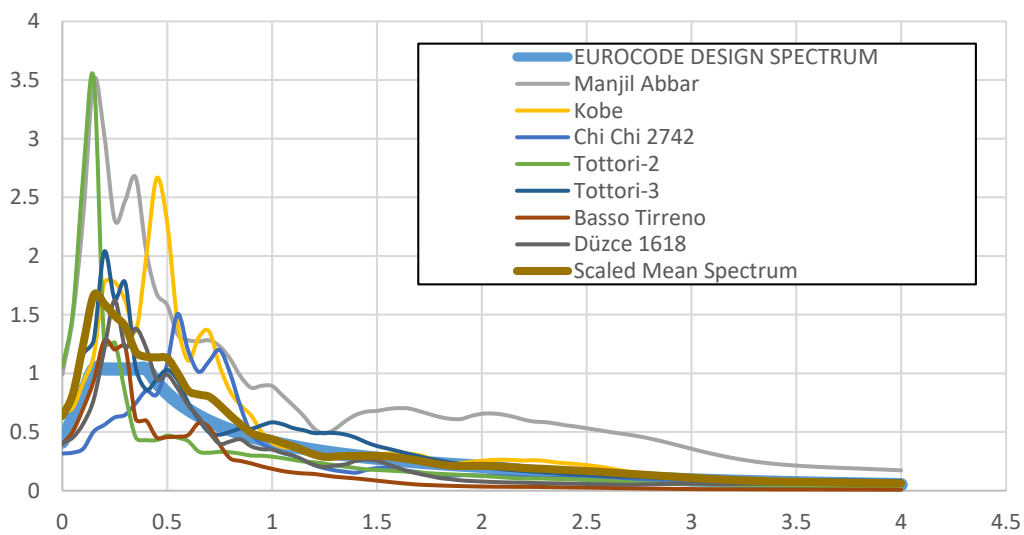


Figure B.160. EN-8 design spectrum and response spectrum of scaled time histories for ground motion SET-3 and scaling method M3 of V14 Bridge

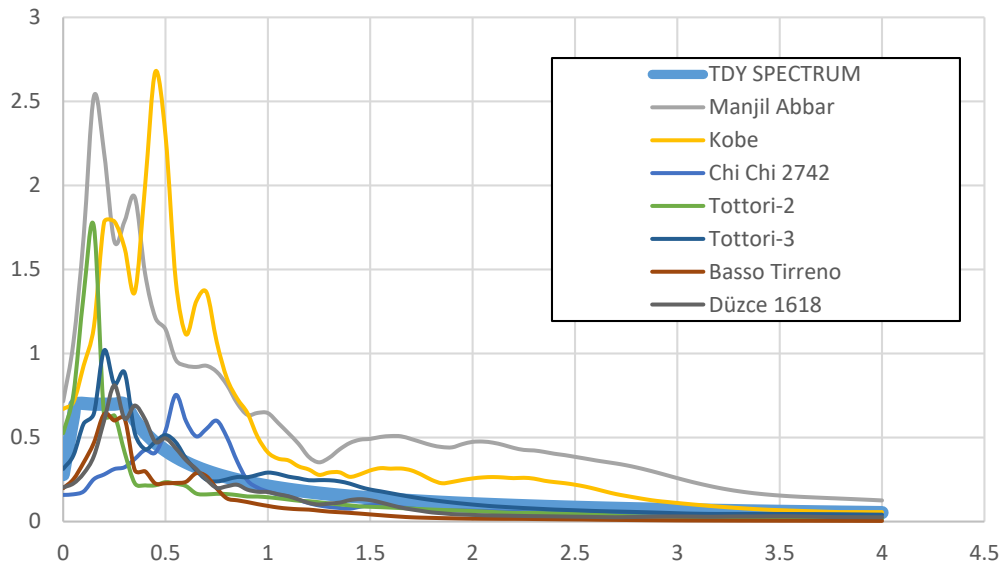


Figure B.161. TDY 2020 design spectrum and response spectrum of unscaled time histories for ground motion SET-3 and scaling method M3 of V14 Bridge

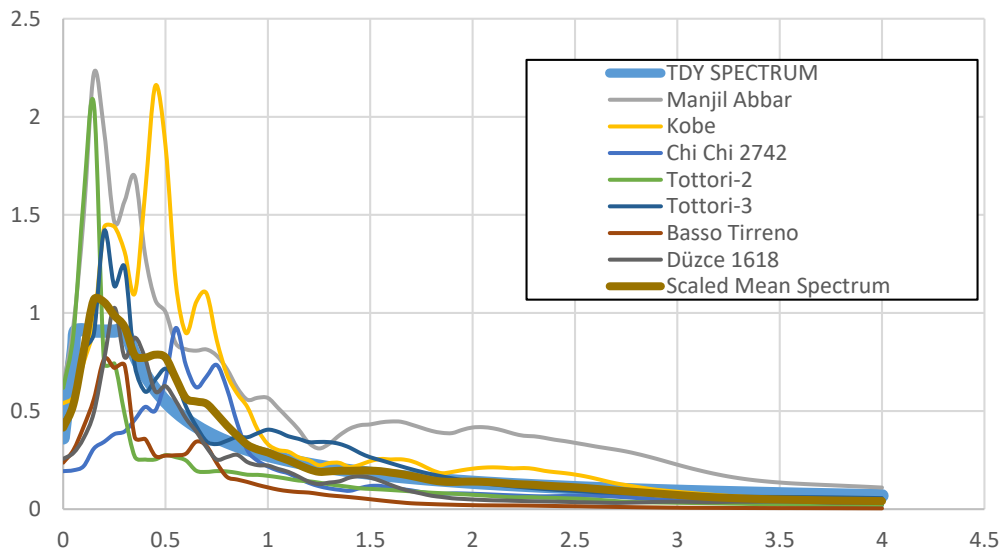


Figure B.162. TDY 2020 design spectrum and response spectrum of scaled time histories for ground motion SET-3 and scaling method M3 of V14 Bridge